Nutrient limitation in *Clostridium autoethanogenum* and characterisation of its carbonic anhydrase

by

Bart Pander, MSc

Thesis submitted to the University of Nottingham

for the degree of Doctor of Philosophy

September 2017

University of Nottingham

UK | CHINA | MALAYSIA

Declaration

Unless otherwise acknowledged, the work presented in this thesis is my own. No part has been submitted for another degree at any institute of learning.

Bart Pander

September 2017

Abstract

Clostridium autoethanogenum is an anaerobic, facultative autotrophic bacterium that was isolated from rabbit faces in the last decennium of the twentieth century. It is used to convert carbon monoxide rich waste gas in to compounds such as acetate, ethanol, 2,3-butanediol and lactate.

Carbon dioxide reacts with water to form carbonic acid and bicarbonate. This reaction is catalysed by enzymes called carbonic anhydrases. It was unknown if these enzymes were present in *C. autoethanogenum.* Genes encoding putative carbonic anhydrases were cloned and heterologous expressed. One gene encoded an active enzyme of a novel sub-clade of β-carbonic anhydrases. This gene was disrupted in the genome of *C. autoethanogenum*. The mutant was unable to grow at low pH and low carbon dioxide concentrations.

Production of ethanol and 2,3-butanediol by WT *C. autoethanogenum* in carbon monoxide fed chemostat cultures was improved by employing phosphate limitation. A pilot study on the effect of phosphate limitation on rhamnose based growth showed 1,2-propanol and 1-propanol as native products of *C. autoethanogenum*.

Acetolactate is the metabolic branch point for both branched chain amino acid and 2,3-butanediol production. An acetolactate synthase gene was deleted. The resulting mutant shows a subtle growth difference in media containing amino acids.

Finally the strength of a series of heterologous promoters was determined in *C. autoethanogenum*.

The research presented in this thesis improves our knowledge on *C. autoethanogenum'*s metabolism and offers tools to optimise it for product formation. This will enable improved exploitation of this organism for a carbon neutral future.

Acknowledgements

The work presented in this thesis would not have happened without the help of a great many people. First and foremost I want to extend my gratitude to my first supervisor Anne Meint Henstra. You gave me advice when I asked, guidance when I needed it, and the freedom to become an independent researcher. Klaus Winzer, I appreciated our conversations over tea time and your friendly questions during the supervisor meetings. Nigel Minton, your group has grown to one of the largest in microbiology in the UK. I admire that you managed to do that while maintaining regular supervisor meetings and close contact with me and all the other students in your group. Thanks for the supervision.

Thank you: Tom, Ola, Jon, John, Dave, Katrin, Sarah, Ying, Michelle, Ben, Lilli, Patrick, Nial, Sam, Christian, Rob, Ryan, Jennifer, Chris, Zeenat, Bashir, James, Vinod, Magda, Andy, Erik, Jacqueline & Kati.

Special thanks to my B60 lab buddies. Louise Sewel for teaching me how to build and maintain the bioreactors and being my lab neighbour. Pawel Piatek, 'baie dankie' for being my bench buddy. Florence J. Annan, it was a pleasure keeping those bioreactor cultures running for record breaking times together with you. Chris Humphreys, Erik Liew, James Millard, Rob Mansfield, Jon Baker, Craig Woods, Samantha Mclean Philippa Strong you all helped me out in many awesome ways. Ronja Breitkopf, you supplied me with all the stash needed for Strep-tag purification and musical shows, danke schön. Pete Rowe, thanks for being such great babysitters for my daughters when we needed it and for organising Clostridia Touch Rugby. The CO2 office and touch rugby crew; Andrew, Alex, Patrick, Ollie, Hymke Emily, Mickey, Lorna, Gareth thanks for being awesome people. Rupert Norman I hope my results will help your genome scale model of *C. autoethanogenum* just as much as your model was insightful to me. Laudina Safo, you introduced me to LC-MS which turned to be a much bigger part of my thesis than I expected, thanks.

Thomas Millat thanks for your advice and your Matlab scripts, but most of all thank you for your question in the last hour before we would be off for Christmas 2013: "Do you know if there are any carbonic anhydrases in *C. autoethanogenum*?" You can read your answer in chapter 3 and 4.

I would like to aknowledge the people at Lanzatech for their advice, support and their kind welcome when I visited them. Gemma Harrison, Stephen Carr, Megan Cox and David Scott thank you for your efforts in elucidating the structural properties of Caut-bCA. Denise McLean, thanks for teaching me electron microscopy. David Onion & Veeren Chauhan, our work did not end up in this thesis but thanks for the cross-disciplinary collaboration. Alex Grosse-Honebrink, Zak Bean, David Kirk thanks for your laughs and your useful comments on some chapters of this thesis. James Gilbert, Jamie Twycross thanks for the support with running the phylogenetic software that would have fried my laptop. Matt Abbot many thanks for keeping the HPLC and GC running and for your efforts, together with David Tooth, to identify some of the unknown peaks.

Victor Tudorica my gratitude you can't read anymore but you're in my thoughts. It was a pleasure to assist you in the *Oligotropha carboxidovorans* project.

Carl Winfield, Carol White, Tullia Randal, Shelly Alsop, Slawomir Bianketti cheers for keeping the building safe and organised.

Hans en Marijke, thanks for being supportive in our chosen career path. Bianca, Ymkje & Kor my sister and parents, thanks for all your visits while we are living abroad. Your love and support were a great help in writing this thesis.

I thought becoming a PhD student in the UK would change my life but that was nothing compared to the change of becoming father of Hanna Yfke and Freya Nynke. Thank you my dear daughters for reminding me of what is truly important. Finally, Jolanda van Munster, this thesis would not have existed without you. Thank you for being my best friend, a fantastic mother to our children, my primary scientific advisor and my love.

Table of Contents

List of figures

List of tables

List of abbreviations

AOR	Aldehyde ferredoxin oxidoreductase
CA	Carbonic Anhydrase
CAA	Cas Amino Acids
Fd_{red}	Reduced Ferredoxin
FPKM	Fragments Per Kilobase of transcript per Million mapped reads
GC	Gas Chromotography
GHG	Green House Gases
HPLC	High Pressure Liquid Chromotography
LB	Lysogeny Broth
LC-MS	Liquid Chromotography Mass Spectrometry
MES	2-(N-morpholino)ethanesulfonic acid
Nfn	ferredoxin-dependent transhydrogenase
OPLS-DA	Orthogonal Projections to Latent Structures Discriminant Analysis
PAGE	Polyacrylamide gel electrophoresis
PCA	Principal Component Analysis
PFOR	pyruvate:ferredoxin oxidoreductase
PHB	Poly-3-hydroxybutyrate
PLS-DA	Partialy Least Squares Discriminant Analysis
PMF	Proton Motive Force
PPP	Pentose Phosphate Pathway
RBS	Ribosome Binding Site
Rnf	Rhodobacter Nitrogen Fixation (Proton translocating NADH oxidoreductase)
SDS	Sodium Dodecyl Sulphate
SLP	Substrate Level Phosphorylation
TCA	Tricarboxylic acid
WLP	Woods-Ljungdahl Pathway
YE	Yeast Extract
YTF	Yeast Tryptone Fructose (medium)

Chapter 1:

Introduction

"Life is nothing but an electron looking for a place to rest"

Albert Szent-Györgyi, discoverer of vitamin C and aspects of the citric acid cycle (1)

"If the quantity of carbonic acid in the air should sink to one-half its present percentage, the temperature would fall by about 4°C; a diminution to one-quarter would reduce the temperature by 8 °C. On the other hand, any doubling of the percentage of carbon dioxide in the air would raise the temperature of the earth's surface by 4°C; and if the carbon dioxide were increased fourfold, the temperature would rise by 8 °C."

Svante Arrhenius, discoverer of dissociation of salts, acids and bases. The quote is the first quantitative prediction of the effects of carbon dioxide on global temperature in 1906 (2)

1 Introduction

Bacteria that use gases such as carbon monoxide (CO) or carbon dioxide (CO_2), and hydrogen (H_2), as their energy and carbon source have long fascinated microbiologists (3–6). The metabolic properties of these bacteria give insight into the earliest forms of life (7–9) and they play an important role in the global carbon cycle (3, 10–12). Recently, research in these organisms has intensified due to their potential to help us solve the major crises faced by humanity: the combination of global warming (figure 1.1), increased use of resources by a growing population and the need to decrease use of fossil resources. This PhD thesis describes research into the ability of *Clostridium autoethanogenum,* a bacterium first isolated from rabbit droppings (13), to convert industrial waste gas into acetate, ethanol, 2,3-butanediol and other non-native products (14–17).

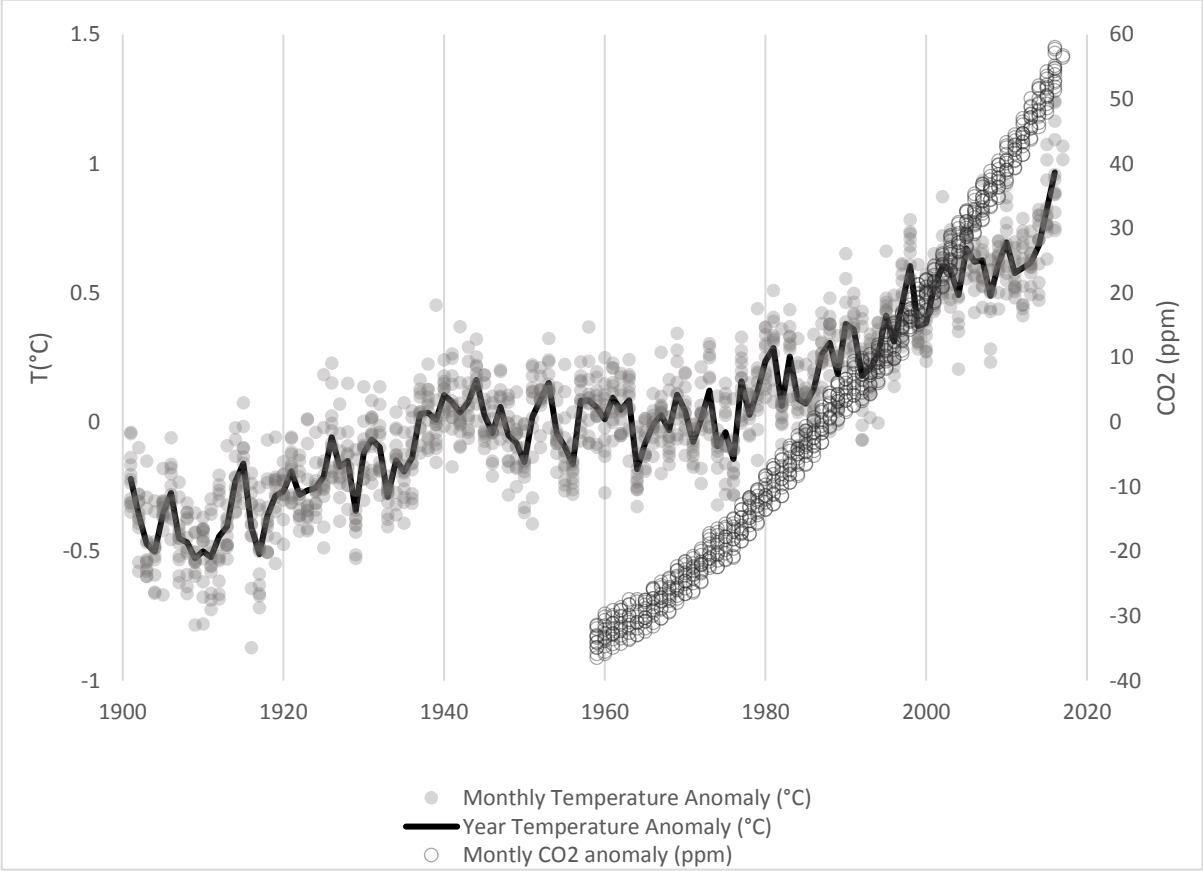

Figure 1-1 Global Temperature and CO_2 anomaly.

This graph shows the rise of both CO_2 and global temperature. The graph combines global temperature data from the Berkeley global temperature data set (http://berkeleyearth.org/data/) and CO_2 anomaly calculated from data from National Oceanic and Atmospheric Administration (NOAA) Mauna Loa (https://www.esrl.noaa.gov/gmd/ccgg/trends/data.html). Anomaly of the temperature is calculated with base period 1951-1980. Anomaly of CO_2 was calculated with mean of whole dataset (1959-2016)

1.1 The global carbon and energy crisis

Five out of the last seventeen years broke the global temperature record, and we experienced 16 of the 17 warmest years on record since in this century (18) (figure 1-1)). Global warming is likely to have catastrophic effects on coastal, arctic and dry areas. A main cause of this warming is the accumulation of greenhouse gasses (GHG) present in the atmosphere through release of previously fossilised carbon as CO_2 and, to a lesser extent, methane (19).

Modern society is almost unimaginable without the use of fossilised carbon. Not only do we burn fossil carbon (oil, gas, coal) to meet more than 80% of our global energy demand (20) we also use fossilised carbon sources as the basis of many of the organic chemicals we use to support our daily lives. A modern cityscape is unthinkable without reinforced concrete; production of its components, steel and concrete inherently releases large amounts of CO_2 (21).

The impact of GHG release is global, and gave rise to global initiatives to mitigate its effects. The latest agreement to limit global warming has been signed by 195 countries in Paris in 2015 (22) but the issue has been on the global policy agenda since the 1980's (23). Considering the changes to our society and economy that are needed it is unsurprising that earlier agreements such as the Tokyo agreement (24) did not achieve their full ambitions and GHG emissions are still on the rise. Some of the most important reasons for this slow improvement are political and economical and are outside of the remit of this thesis.

The global problem is defined here:

1. The global temperature is rising due to the release of gaseous carbon compounds of which the carbon atoms were previously fixed as fossil deposits (19).
2. The population is rising (25) and expects a living standard that now depends mostly on the use of fossil resources.
3. There is no direct replacement available for the full set of fossil resources we use for the current standard of living.

It is generally agreed that we need many approaches to solve this problem, one of the approaches is a bio-based economy where our resources are from biological origin.

Replacing fossil resources with biological production of chemicals goes beyond merely lowering GHG emissions. The use and mining for fossil resources is both environmental unfriendly and dangerous to the miners and users (26). Our current dependency on fossil resources also means being dependent on, and enriching, governments who do not share our core values of humanism.

The success of biological approaches to solving this global problem depends on the synergy with other tactics, such as, sustainable chemistry and sustainable engineering. For example, the vast majority of transportation fuels, are fossil derived (20). Promising alternatives for aviation fuel are biofuels (27), while electrical powered vehicles might be the better alternative for personal transportation (28), providing the electricity is produced in sustainable fashion.

1.2 Biology based industrial chemistry

For most of the existence of humanity we have had a bio-based economy; our food, energy and most of our luxury products were derived from biological sources. The fossil based economy we have now is likely a short, but destructive, transient period. However, the historical bio-based economy had to sustain a dramatically smaller population, at much lower levels of health and luxury than our current standard. It is almost impossible to contemplate the effects of stopping the use of fossil resources and returning to using only biological based production as it was done before Ca. 1750 (29). A highly technological and modern approach to bio based production is therefore needed to fulfil the needs of the population.

Biofuels are compounds derived from biomass that can be combusted to release energy stored in chemical bonds. Many of these chemicals have uses other than just burning and can be used as chemical building blocks. Although this introduction uses the term biofuel, almost all that will be discussed is also applicable to other bio based chemicals. The development of biofuels has received much attention in the recent decade, resulting in a range of products.

In literature biofuels are commonly classed in four generations. The first generation of biofuels are derived from feedstocks that are fit for human consumption. Ethanol is produced by fermenting mono- and disaccharide rich plant material, mostly sugar cane and maize. Discussion about the favourability of this type of biofuel is ongoing. since there are important drawbacks (30, 31). First, the strong relation between food and fuel prizes is undesirable. Second, the inherent carbon inefficiency of using only a small proportion of a plant, i.e. the part that contains the easy to ferment sugars such as starch, sucrose, glucose and fructose.

Second generation biofuels are those that are made from non-food plant materials. The main reason that we cannot use those plant materials for food are because of the high, hard to digest, lignocellulose content and low digestible (poly)saccharide content. The indigestible nature of high lignocellulose plant materials makes it more difficult to use as resource for bioethanol and other biofuels. These second-generation biofuels therefore are less well developed and are still a focus of intensive research. The definition of third and fourth generation biofuels are less clear but generally third are those biofuels that are made by using algae. The fourth generation biofuels are all other types of biofuel that are mostly still in development such as the conversion of industrial waste gas into fuels, the techniques that are the focus of this thesis (32, 33).

1.3 Autotrophic prokaryotes in biofuel production

Autotrophic organisms build their organic material from inorganic, one carbon atom (C1) compounds while heterotrophs need to consume organic material. Both first and second generation biofuels utilise heterotrophs to transform organic material derived from mostly plants into biofuels. This inherently leads to energy and mass inefficiencies and releasing GHGs in the process. Using autotrophs directly for biofuel production is, hypothetically, intrinsically more efficient. There is a range of biologically relevant C1-compounds, of which methane, CO and CO_2 are currently pursued as substrates for biofuel production.

1.3.1 Methanotrophs

Autotrophy is defined as reduction of the highly oxidised CO_2 to more reduced forms of carbon compounds in biomass (34). From this viewpoint methanotrophs are not autotrophs. While recognising this semantic issue I will review them shortly since they are candidates for industrial biotechnological production from c1-feedstocks.

Whereas CO_2 is the most oxidised carbon compound, methane is the most reduced. Methanotrophs oxidise methane for energy conservation and biomass formation. Classical methanotrophs are proteobacteria that use oxygen as the terminal electron acceptor (35). The aerobic methanotrophs gained popularity in the 1960's as source of protein but interest has waned, mostly due to economic reasons. Companies like Calysta have redeveloped the idea, and produce fish food from methane (36). The methane used for the process currently is from non-renewable sources, and thus the process seems at first not to help much in the way of reducing GHG emission however the CO_2 released by the end consumers contributes less to the greenhouse effect than the methane. Anaerobic methanotrophy also exist, as a process in which methane oxidation in archaea is coupled to nitrate, nitrite or sulphate reduction by a bacterial partner (35, 37, 38). Currently, this anaerobic methanotrophy appears to have little direct biotechnological use except in waste water treatment (39). However, the potentially high carbon efficiency (compared to the aerobic version) makes it an attractive process to potentially drive biologic gas-to-liquid fuel conversion (38).

1.3.2 Carbon dioxide reducers

Other types of C1-gas consuming prokaryotes are clear autotrophs as they reduce CO_2 to biomass. Based on origin of the reducing electrons and the products formed these organisms are classified into different groups that are discussed in more detail below.

There are at least six different metabolic pathways known by which autotrophic organisms can fix CO_2 to biomass (40, 41). The only non-cyclic pathway is the reductive acetyl-CoA pathway or Wood-Ljungdahll pathway (WLP). Despite the diverse nature of the pathways some generalisation is possible (17, 34). The pathways use a small set of redox carriers that are common in nature. NADH, NADPH and ferredoxin are carrying the reductive power derived from an electron donor to metabolic steps that gradually reduce CO_2 to organic compounds. Besides these main carbon fixation pathways there are other parts of the metabolic network where additional CO_2 is fixed in carboxylation reactions.

1.3.2.1 Photosynthetic bacteria

The reducing power in photosynthetic bacteria is supplied by light. This energises a photosensitive reaction centre in which electrons get excited and subsequently bind to redox intermediates that can be used to reduce the CO_2 derived carbon.

The most important photosynthetic prokaryotes from a biotechnological perspective are cyanobacteria such as *Synechococcus elongatus* that can be used to produce a range of products such as ethanol, butanol and lactic acid (42). From an energetic perspective, photosynthetic prokaryotes appear ideal as sunlight is without cost, however, it is not permanently available and it is not a simple task to scale and optimise a bioreactor for mass transfer of CO_2 and for light transfer (43).

1.3.2.2 Knallgas bacteria

Some bacteria can use the energy of the knallgas reaction, the explosive reaction between H_2 and O_2, to fix CO_2. For biotechnology *Cupriavidus necator* (previously *Ralstonia eutropha*) is one of the most promising knallgas bacteria. It uses O_2 tolerant hydrogenases to reduce electron carriers that supply the Calvin-Benson-Bassham cycle. The wild type organism already produces poly-3-hydroxybutyrate (PHB), which can be used as a basis for biopolymers (44). *C. necator* is genetically tractable and has been modified to produce many useful compounds such as isobutanol, 3-methyl-1-butanol and methyl ketones (45, 46). The thermophile *Aquifex aeolicus* is a knallgas bacterium that is less explored for biotechnological use. It is the evolutionary deepest branching bacterium, harbours one of the smallest genomes of any autotroph, and uses the reductive TCA cycle for carbon fixating. It has one of the highest optimum growth temperatures among bacteria which has biotechnological advantages; substrate cooling needs are lower and removal of products as volatile solvents would be effortless.

1.3.2.3 Methanogens

Hydrogenotrophic methanogens are Archaea that can use H_2 for the reduction of CO_2 in the WLP, forming methane as the major product (47). The biological origin of methane was stipulated in 1776 by Volta who noted that the amount of explosive marsh gas was dependent on incidence of rotting plant material. In 1909 Söhngen isolated the first methanogens and noted their ability to grow on CO_2 and H_2 amongst other substrates (6). It were also the methanogens of which Woese first found the 16sRNA to be so different from Bacteria that he had to propose the three domain classification of life (48).

Anaerobic digestion is a common method to produce methane as a biofuel from plant waste. The process is performed by a complex ecosystem of microorganisms in which methanogens are responsible for the end product formation (49). Methanogens are explored for biotechnological purposes by at least two companies: Trelys (50) focuses on amino acid production from H_2 and CO_2 and Electrochaea (51) on biogas production from electricity and CO_2.

1.3.2.4 Acetogens

Acetogens are prokaryotes (mostly bacteria) that can reduce CO_2 in the WLP towards Acetyl-CoA (52). The name derives from the fact that most of them produce acetate. The first acetogen, *Clostridium aceticum* was isolated by Wieringa in 1933 from soil that was incubated with CO_2 and H_2 (4). Electron donors other than H_2 can be used. Many acetogens can use CO as the sole carbon and energy source (carboxydotropy). In that case, half of the CO is oxidised to CO_2 to release the reductive potential to produce biomass acetate and other products. In the field of biofuel production acetogens have a promising role that is explored by multiple companies. Since *C. autoethanogenum,* the organism that the work in this thesis focusses on, is an acetogen this group will be discussed in more detail below.

1.3.2.5 Other carboxydotrophs

The utilisation of CO (carboxydotrophy) by bacteria first was reported by Beijerinck *et al*. in 1903 (5). In addition to CO utilising acetogens there is a range of other bacteria and archaea that can use CO. Although the autotrophy of methanogens is mostly studied with CO_2 and H_2 as substrates, some can grow utilising CO. The methanogenic archaea *Methanosarcina acetivorans* can, due to a lack of hydrogenases, not grow on CO_2 and H_2 but shows acetogenesis when grown on CO as substrate (53, 54). Two other modes of anaerobic CO utilisation are sulphate reduction and H_2 formation. These modes of redox metabolism can often be just one of several options for an organism. The archaeon *Archeoglobus fulgidus* was studied as a sulphate reducing carboxydotroph but it was shown CO can be used as its single carbon and energy source without sulphate (55). In fact, like *M. acetivorans*, *A. fulgidus* is an Archeal acetogen.

H_2 forming carboxydotrophs rely on the energy of the water-gas-shift reaction. The best studied species of this type are *Rhodospirillum rubrum* (56) and *Carboxydothermus hydrogenoformans* (57). *R. rubrum* can be used to produce β-hydroxybutyrate and β-hydroxyvalerate from CO (58) and *C. hydrogenoformans* is proposed for biological H_2 production (59). In both organisms, hydrogenic carboxydotrophy is just one mode of metabolism. *R. rubrum* has a much more diverse metabolism, including photosynthesis, than *C. hydrogenoformans* (59). It should be noted that some H_2 production from CO is also found in acetogens (60).

1.3.2.6 Aerobic carboxydotrophs

Aerobic carboxydotrophs are not always capable of fixing carbon. Of those that can, *Oligotropha carboxidovorans* is best studied. The aerobic oxidation of CO yields more energy than the anaerobic version and thus, *O. carboxidovorans* could be used to make compounds that require more energy in their production (61). However, neither this organism, nor any other aerobic carboxydotroph has to date been developed for biotechnological use.

1.3.3 Mixed cultures

Many biofuel production methods employ single strain cultures, especially when genetic optimisation of a strain is employed. Multi species systems are more complex, and therefore, less straightforward to engineer. However, it is generally known that ecosystems can be robust and mixed culture approaches may have many advantages. There are broadly two approaches to mixed culture biofuel production, one is using undefined or semi-defined multispecies microbiota, the other is mixing two or a small set of defined strains. The first approach is common in anaerobic digestion where a complex microbial ecosystem of Eukaryotes, Bacteria and Archaea first degrades lignocellulose to shorter oligo and monosaccharides (by eukaryotes and bacteria) which are then transformed to acetate (by acetogenic bacteria) and finally to methane by the acetoclastic methanogens. The microbial ecosystem is often derived from ruminant excrement and the species living in soil and on the plants that are fed to the anaerobic digester (49). The second approach of well-defined small sets of strains has been applied with some promising results. The previously mentioned two species syntrophic consortium in anaerobic methane oxidation is a natural phenomenon, but artificial small consortia can also be applied. A mixed culture of the closely related *C. autoethanogenum* and *Clostridium kluyveri* converted CO and syngas to butyrate, caproate and the alcohols butanol and hexanol (62, 63). Accidental cocultures can lead to surprising positive results and start exiting further investigation. An example is the finding that a mixture of *Alkalibaculum bacchi* and *Clostridium propionicum* forms longer chain alcohols such as n-propanol and n-butanol from syngas (64, 65)

Combining the power of multiple species does not necessarily need to be done in a mixed culture, but can be done in multiple stage bioreactors. *Yarrowia lipolytica* converts acetate to lipids that can be used as biodiesel. The economic value of the acetate produced by acetogens is low. By combining syngas fermentation by *Moorella thermoacetica* with the lipid production of *Y. lipolytica* the economic value of the products of syngas fermentation can be increased (66). Finally, when the previously mentioned combination *C. autoethanogenum* and C.*kluyveri* is used in two separate stages, the control of growth parameters is likely more straightforward (67).

1.3.4 Mixotrophy and carbon efficiency

CO_2 is a major waste product in the production of most biological based chemicals and biofuels as a natural consequence of the metabolism of most organisms. The ability of acetogens to use the WLP for reuptake of the CO_2 formed in other metabolic processes is promising in the light of carbon efficiency. Most of the research on *C. autoethanogenum* and other above mentioned facultative autotrophs focuses on the C1-feedstocks, but much of what we have learnt is useful for using feedstock with multiple carbon atoms. Next to the carbon efficiency, substrate flexibility is a major advantage of using acetogens in industry. Acetogens can utilise sugars and gaseous carbon sources at the same time (mixotrophy) which increases the feedstock flexibility and carbon efficiency (68, 69). Next to this true mixotrophy some acetogens can reduce short-chain carboxylic acids to their respective alcohols which is an attractive way to increase the value of these compounds (70).

1.3.5 Choice of organism

In the pursuit of a more sustainable economy there are many routes to take. The discussion above was limited to some uses of autotrophic prokaryotes but even with that limitation the plethora of possibilities is staggering. Acetogens are among the most promising organisms for turning waste into valuable products, especially since they have high product to biomass yields and are already biotechnologically and industrially developed.

1.4 History of acetogens in microbiology

1.4.1 Early days

In 1936, Wieringa provided strong evidence for the hypothesis that organisms that consume CO_2 and H_2 where responsible for formation of acetate in soil by isolation of *Clostridium aceticum* (4, 6, 71). Wieringa's culture was considered lost until 1980 when some of Wieringa's original spore stocks were found and revived (72).It was therefore the second isolated acetogen that became the best studied, and the model organism to study acetogenesis. *Clostridium thermoaceticum,* later renamed *Moorella thermoacetica,* was isolated in 1940 from horse dung (73). In their paper describing the isolation and characterisation, Fontaine *et al*. report of an unusual fermentation of glucose. The ratio of acetate/glucose was measured at 2.5 while the then known metabolic models did not permit a ratio above 2.0. This sparked research into the metabolism of *M. thermoacetica,* which in turn contributed to our understanding of most of the unusual metabolism of the acetogens (3).

The metabolism of *M. thermoacetica* turned out to be quite unlike that of most organisms described at that time. Its defining feature, and that of all other acetogens, is the central role of a non-cyclical carbon capturing pathway; the acetyl-CoA pathway also named the Wood-Ljungdahll pathway (WLP), after the two researchers who supervised the bulk of the work elucidating the pathway (3, 74–76) The unusual acetate/glucose ration was found to be caused by the reuptake of CO_2 in the then unnamed Wood-Ljungdahl pathway.

The unique properties of the metabolism of *Moorella thermoacetica* were not immediately fully realized. It only later became clear that the organism was similar to Wieringa's culture in a crucial way; it can grow autotrophically on diverse mixtures of the gasses CO_2, H_2 or CO (77). The long interval between first isolation of an organism and its classification as an acetogen capable of autotrophic growth, is a recurring theme in acetogen microbiology. Three years before Wieringa's isolation of *C. aceticum*, Weinberg & Ginsbourg isolated*, Clostridium scatologenes* as a "dung smell" producing bacterium. It was shown to be able to use CO_2/H_2 or CO/CO_2 as carbon and energy source while producing acetate in 2000 (78). Recently also *Clostridium difficile,* a bacterium known as a troublesome pathogen since 1935, was identified as an acetogenic autotroph (79).

1.4.2 New isolations, recent boom

Initially it was assumed that acetogens only form acetate as product, but it was found that members of the genus *Acetobacterium* could, under phosphate limiting conditions, form ethanol (80). At the same time in the late 1980's and early 1990's, it was shown that growth of acetogens on syngas was possible and multiple autotrophic acetogens were isolated that produced other products than acetate in significant amounts (81–84). *Eubacterium limosum*, *Clostridium drakei*, *Clostridium carboxidivorans* (85) produce acetate, ethanol, butyrate and butanol while acetate, ethanol and relatively small amounts of 2,3-butanediol and lactate are the products of *Clostridium ljungdahlii*, *Clostridium autoethanogenum*, *Clostridium coskatei* and *Clostridium ragsdalei* (86, 87). These products are of higher economic value than acetate, and industrial applications were proposed and started up quickly. The interest from industry and the money from investors and governements spurred an increase in research into these organisms of which this PhD is part of.

1.4.3 Phylogeny and evolution

Acetogenesis is not a monophyletic trait and is found in diverse branches of the bacteria such as spirochaeta and acidobacteria but is particular common in the Firmicutes, specifically, in the class of anaerobic firmicutes, the Clostridia. Within this class, the genera *Clostridium*, *Acetobacterium* and *Moorella* contain most of the best studied acetogens, indeed the three so called model acetogens are *M. termoaceticum*, *Acetobacterium woodii* and *C. ljungdahlii* (88, 89). These three species represent a range of different metabolic versions of acetogenesis and are evolutionary separated. They show that even within the order of Clostridiales many variations in acetogen metabolism exist. We should therefore be careful applying facts we learned from these models to other acetogens that could be equally worthy of the model status had they been studied in more detail, such as members of the *Blautia, Eubacterium* and *Sporomusa* genera (90, 91).

Some genera such as *Acetobacterium* and *Moorella* are monophyletic acetogenic but as Figure 1-2 illustrates, in the genus *Clostridium* the situation is more complex. Famous members of the genus *Clostridium* are pathogens such as *Clostridium tetani, Clostridium botulinum & Clostridium difficile* and non-pathogenic solventogenic species as *Clostridium acetobultylicum & Clostridium beijerinckii*. Although some phylogenetic grouping of acetogenic species occurs, the actogenic clades are interspersed with non-acetogens.

The ethanogenic acetogens *C. ljungdahlii, C. autoethanogenum, C. ragsdalei* and *C. coskatei* are closely related to *Clostridium kluyveri* and *Clostridium tyrobutyricum* (92, 93). This clade is most related to the

acetogen clade containing *Clostridium scatologenes* (85) and to the classic solventogenic and pathogenic clostridium species.

Wieringa's *Clostridium aceticum* is less closely related to these ethanologenic acetogens. Some aspects of its genome are very similar, such as the gene cluster coding for some enzymes in the WLP, but others are different. Unlike the *A. woodii, C. ljungdahlii* and *C. scatologenes* clades, *C. aceticum* harbours a cytochrome. This, according to some, makes it a 'genomic missing link' between the much studied *A. woodii* and industrial relevant acetogen *Clostridia* on one hand and the genus *Moorella* on the other (94).

C. ljungdahlii, *C. autoethanogenum*, *C. ragsdalei*, *C. coskatei* are so closely related that many of the genes on the genome are identical. *C. ljungdahlii* and *C. autoethanogenum* are the most closely related with 99.3% average nucleotide identity (86). In fact all four can be seen as strains of *C. ljungdahlii* which is the only name recognised on the list of prokaryotic names with standing in nomenclature (95). Considering the similarity, in this thesis I will generally assume that what is true for *C. ljungdahlii* is also true for *C. autoethanogenum,* unless the few genomic differences or differences found literature indicate otherwise. Beside these strong similarities there are some important differences of which the ones between *C. ljungdahlii* and *C. autoethanogenum* will be discussed further down.

Like for many bacterial clades, the clostridia taxonomy has changed the last twenty years based on their genetics. This led to name changes of some acetogens and the debate on the taxonomy of the group is not finished (96–98).

The non-monophyletic nature of acetogens makes the understanding of the evolution of acetogenesis not straightforward. An existing hypothesis on the origin of life stipulates that the common ancestor of Bacteria was using the WLP of the acetogen type , while the common ancestor of Archaea used the WLP of the methanogen type (8, 9, 99–101).

If true this could mean that all current acetogens descend from a line that did not lose this metabolic capability. However since at least 3.5 billion years have passed, and the majority of bacteria are not capable of acetogenesis it is likely at least some are more recent acquirements. It is likely that the common ancestor of the *Moorella* genus was acetogenic, but the case for the more complex genus of *Clostridia* is not so clear. Is acetogenesis easily lost and was the common ancestor an acetogen or is the WLP and acetogenesis easily gained? The latter is suggested by the singular nature of the acetogenic spirochete species such as *Treponema primitia,* which was isolated from the termite gut (102). There are non-acetogen *Clostridium* species, such as *C. pasteurianum,* that harbour functional genes such as CO dehydrogenase (CODH) and hydrogenase that are essential for acetogenic metabolism (103, 104). Many enzymes of the methyl branch (section 1.7.4) are not unique for the WLP but are found in most organisms where they act in methionine and purine synthesis and other C1-metabolisms (74). However, simply transferring the genes known to be essential for the WLP to closely related species as *Clostridium acetobutylicum* or even to the unrelated *E.coli* have not resulted in allowing autotrophic growth (105–107). Some acetogens, such as *C. statologenes*, readily lose the ability for autotrophic acetogenic growth (78). All these facts combined do not give a clear view of whether the common ancestor of *Clostridia* was an acetogen or was preadapted for acetogenic growth without being an acetogen.

1.4.4 Ecology

Clostridial acetogens are anaerobes. While some can tolerate oxygen, they can only be active in environments with little or no oxygen, such as; the early earth atmosphere, the deeper layers of the soil, deep ponds and lakes, animal guts etc. Acetogens have indeed been isolated from such diverse environments (3, 10, 108). The role of acetogens in the global carbon cycle has been estimated to be significant as they produce ~10^{13} kg $year^{-1}$acetate in nature (101).

In the gut ecosystem, the acetate generated can be a nutrient for the host and for other members of the microbiome. This is of importance since acetogens compete with methanogenic archaea for H_2 or interact syntrophically with acetoclastic methanogens. The methane produced by the methanogens is a major GHG and cannot be used by the host or most other members of the microbiome. Methanogens and acetogens serve as H_2 sinks that use the H_2 that is generated in anaerobic biodegradation of organic material. Without hydrogenotrophs, biodegradation gets inhibited by H_2 build-up. Methanogens form the majority of hydrogenotrophs in many of these environments because the conversion of CO_2 and H_2 to methane is more thermodynamically favourable than the conversion to acetate (74, 109). It is thought that because of this common interaction and competition between methanogens and acetogens, the latter evolved the broad range of metabolic traits giving them the advantage of utilising many different substrates (74).

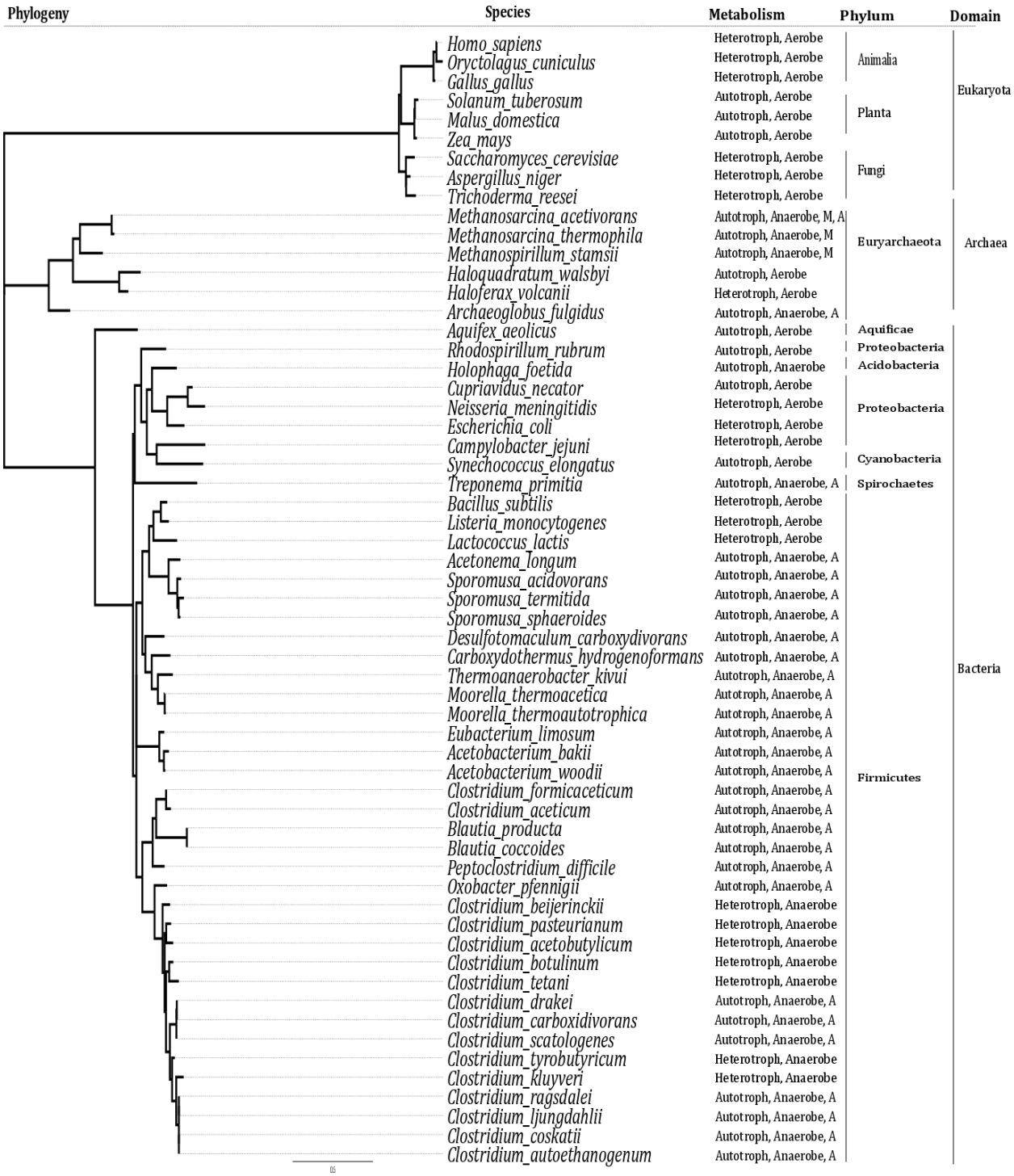

Figure 1-2 A 16s/18s rRNA phylogenetic tree created with ML-method in Mega7.0.

Selection of organisms is based on species of interest from the perspective of this thesis. The type of metabolism is based on the most defining feature. Thus the autotrophs in this list are almost all capable of hetrotrophic growth and thus facultative autotrophs. The bacteria and archaea defined as aerobes prefere aerobic enviroments but are mostly facultativly anaerobes. Acetogens are marked with an 'A' and methanogens with an 'M'. This diagram illustrates the non-monophyletic nature of of acetogeny in the *Clostridium* genus and the close relation of the *Clostridium ljungdahli* group to *Clostridium kluyveri.*

1.5 Industrial use of clostridial acetogens

Industrial use of species of *Clostridium* to produce solvents is now over a century old. In the early twentieth century Chaim Weizmann, Edward Strange, William Perkin Jr and others developed the so called ABE (Acetone, Butanol, Ethanol) fermentation which aided the allies in their effort to win the First World War (110). They spurred an industry that, using these anaerobic bacteria, produced much of the world's acetone and butanol until after the Second World War when petrochemical production took over. Weizmann gained considerable political influence through his contributions to the biotechnological process and went on to become one of the founders of the modern state of Israel and its first president. In recent years the ABE fermentation process is gaining popularity again as a way to produce biobutanol (110, 111). The knowledge on the industrial process of these heterotrophic *Clostridia* can now be used to great effect with the relatively new process of gas fermentation using the autotrophic gas fermentation process with *Clostridium autoethanogenum* and its relatives.

1.5.1 Companies

At the start of this PhD project in 2013, there were at least three companies, Lanzatech, Coskata and Ineos Bio, pursuing industrial use of autotrophic acetogenic clostridia (112). Coskata and Ineos Bio have not developed successfully. The Coskata team has recently restarted under a new name: Synata Bio, but, from the limited information available they now seem to be focusing on a methanotrophic process (113). The industrial plant with which Ineos Bio aimed to produce ethanol from lignocellulosic waste is for sale (114). Lanzatech is actively focused on developing the industrial use of acetogens with pilot and demonstration scale facilities utilising mainly steel mill off gas, but also syngas from waste as their feedstock. They partnered with ArcelorMittal, and Primetals Technologies to construct an industrial-scale facility in Ghent, Belgium (115). Other companies are in the process of developing products using acetogens, amongst them are multinationals like Invista and start-ups like Zuvasyntha.

1.6 Technological considerations

1.6.1 Gaseous feedstocks

The feedstocks of the discussed autotrophs are in the gaseous phase, an important difference compared to traditional biotechnological fermentation of carbohydrate substrates. CO and H_2 are poorly soluble, and the gas to liquid mass transfer is an important issue in any gas fed culture. The important factor for effective gas liquid mass transfer is the surface area between gas and liquid phase and the partial pressure of the gasses. Common lab scale solutions like shaking or stirring are energy intensive and therefore are not practical for industrial scale solutions (116). Since substrate inhibition is another important issue (see Chapter 5) regulation of the mass transfer should be integral to the design. Several scalable solutions have been proposed such as bubble column-, trickle bed- and hollow fibre-bioreactors (116).

1.6.2 Pyrolysis and Gasification of waste

Synthesis gas (Syngas) is a mixture of CO, CO_2 and H_2 which can be made by pyrolysing carbon rich substances as biomass, municipal waste or coal. This gas mixture has a history as a feedstock in chemical industry, as fuel for gaslights and as an alternative fuel in times of oil shortage (117, 118). The substrate, temperature and gas addition influence the specific product formation of pyrolysis and next to syngas, bio-oil and bio char are valuable potential products of this process(119). These process parameters also influence the composition of the produced syngas, which is important for downstream usage.

The Fischer-Tropsch process uses transition metal catalyst and high temperature to make hydrocarbon liquid fuels and commodity chemicals from syngas (120). This classical, thermochemical Fischer-Tropsch process is an energetically intensive, but a feasible method to create valuable products out of waste (121, 122) However its biological alternative, gas fermentation using acetogens has important advantages. The biological conversion from syngas to products require lower temperatures and pressures and thus lead to energy and cost savings. The less reversible nature and higher specificity of enzymes means that biological systems are more specific and can be used to create highly efficient, specific product yields (123, 124). And finally the biological Fischer-Tropsch process as performed by industrial acetogens is claimed to be less sensitive to feedstock gas composition than the classical Fischer-Tropsch process (15, 112, 125).

1.6.3 Composition of gas feedstock

The flexibility of the the gas feedstock composition is not unlimited. A relative high ratio of reducing gas (H_2, CO) to non-reducing gases (CO_2) and a low toxic compound level are most important parameters. The waste gas from steel mills is relatively high in CO and relatively low in gasses that would negatively affect the fermentation like oxygen and cyanide. It is no surprise that one of the most successful applications of gas fermenting organisms to date uses this waste gas as feedstock (15).

The syngas produced from biomass can be less suitable than the steel mill off gas to feed acetogens. The use of acetogens in a pre-commercial biomass derived syngas fed process has been hampered by cyanide in the syngas mixture (114). Whereas the bacteria are sensitive to oxygen and cyanide, the metal catalyst of the traditional Fischer-Tropsch is particular sensitive to sulphur gasses (H_2S, SO_2, COS) (126).

When syngas can be produced from municipal and biological waste, waste becomes a resource. This might be an important economic driver as acknowledged by for instance the Science and Technology Committee of the UK House of Lords in their report: 'Waste or resource? Stimulating a bioeconomy' (127). Municipal waste in Europe is now mostly incinerated or send to landfill. The potential use of municipal solid waste as a source of syngas for gas fermentation can be a good alternative to the other modes of disposal (127). There is not much literature exploring this possibility nor are there successful industrial applications. However recently the process has been demonstrated to be feasible in Japan by a collaboration of Lanzatech and Sekisui (128).

1.6.4 Microbial electro synthesis

Life can be seen as energetic electrons finding their terminal resting place (1). In most cases the energy of the electrons that drive the metabolism of an organism, is derived from energy rich molecules. However, some organisms can take their electrons directly from an electrode (129, 130). This 'electric biotech' could effectively use or store excesses of sustainably produced electricity that are generated in our electric grid when with peak production of renewable electricity does not coincide with peak consumption. Acetogens or methanogens are the best candidates to use in bioelectric production systems since they efficiently convert electrons to products (131). Furthermore, since modern photovoltaic cells are much more energy efficient than biological photosynthesis (132) combining photovoltaic cells with microbial electrosynthesis has the potential to become a more efficient photosynthesis process than the one evolved more than 2.5 billion years ago (132–134).

1.7 Metabolism of Clostridium autoethanogenum

The most promising use of acetogens like *C. autoethanogenum* in industry is autotrophic growth on gaseous carbon sources. On these substrates acetogenic metabolism is often considered to be 'on the thermodynamic limit of life' (89). This might conjure up an image of organisms that are struggling for energy, which is obviously not the case when enough substrate is present and in fact some authors say that the opposite from thermodynamically limited is true (135). Whichever view is true, it is clear the metabolic and process engineering of these organisms is bound by strict energetic constraints. Detailed knowledge of the metabolism is therefore essential for any engineering effort.

In much of the past research on metabolism, and to a lesser extend still this day, we consider bacteria mostly as a black box. We measure biomass growth, substrate uptake and product formation, creating a basic understanding of the organism. However, with modern techniques we can gain a clearer picture of the inner working of bacteria. Recent omics studies of *C. autoethanogenum* (136–140) and studies into key enzyme and metabolic pathways enlighten the black box to a grey box model. I will review the metabolism first from the black box perspective, describing substrates & products, and then delve in to the grey box of the internal working of the cells. Since *C. autoethanogenum* can grow on a wide variety of substrates (13), I will limit the discussion to those used in my research described in this thesis.

1.7.1 Substrates and Products

1.7.1.1 Carbon sources

In our lab we use fructose, xylose and CO as the main carbon sources. Also CO_2 (in combination with H_2), pyruvate, rhamnose, acetate, 1,2 propanediol and fumarate were used in experiments. The gas CO is toxic to most organisms since it binds to many metal containing co-factors in proteins such as haemoglobin and hydrogenases. Despite this toxicity it is used by many organisms, not only as a carbon source but also is thought to function naturally as signalling molecule in vertebrates (141).

Of the gases that can be used by *C. autoethanogenum* CO is preferential to CO_2 and H_2 in terms of growth support and solvent production. CO as an electron donor is more energetically favourable then H_2 as electron donor but the organism inherently produces CO_2 on this carbon source (142). The produced CO_2 could be used as carbon source. This would need an alternative electron donor such as H_2. However, besides reports of co-consumption of H_2 and CO (60, 137, 140) there are reports that H_2 is not used if CO is present in significant proportions (142, 143). The reasons for this are, or thermodynamic in nature (143) or caused by the fact that CO inhibits the hydrogenases (142). Indeed, we found that CO at high partial pressures or flow rate can be detrimental to the cells, even to cells that are growing on CO (chapter 3).

Solubility of the gasses in water is an important parameter for the growth. While both CO and H_2 have poor solubility of about 1-2% w/v at biological relevant temperatures and pressures, CO_2 has a much higher solubility (144–146). However the solubility of CO_2 in water is a more complicated issue, as next to temperature and partial pressure, pH plays an important role. A small proportion of the CO_2 will react with water to form carbonic acid which will, depending on pH, dissociate to bicarbonate and carbonate. The reaction between CO_2 and carbonic acid (or bicarbonate) and vice versa will equilibrate spontaneously. However, the equilibration reaction is apparently too slow for life since most organisms harbour carbonic anhydrase enzymes to catalyse the interconversion (Chapter 3 & 4).

The hexose fructose and the pentose xylose both support growth of *C. autoethanogenum* very well. Growth on the methyl-pentose rhamnose has been reported by Arbrini *et al* (13) but they did not discover (or report) that *C. autoethanogenum* generates other products than acetate and ethanol during growth on this sugar; I identified that also 1,2-propanediol and propanol are also formed (Chapter 5 & 6).

In addition to these sugars, pyruvate was used to support growth as the carbon source that mimics gas growth since processes like gluconeogenis needs to be activated on both of these carbon source.

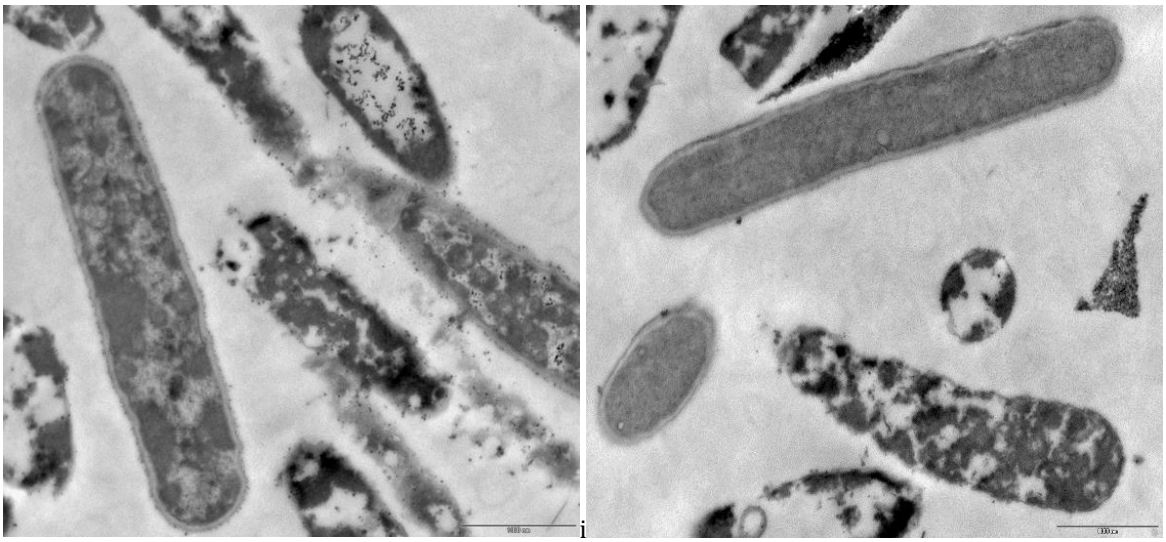

Figure 1-3 Transmission electron microscopy pictures of *C. autoethanogenum.*

The typical rod shape and fimicute type cell wall are visable as well as some variation in appearance. Sample preparation and microscopy by: by Florence J Annan, Ronja Breitkopf, Pawel Piatek, Bart Pander and Denise McLean

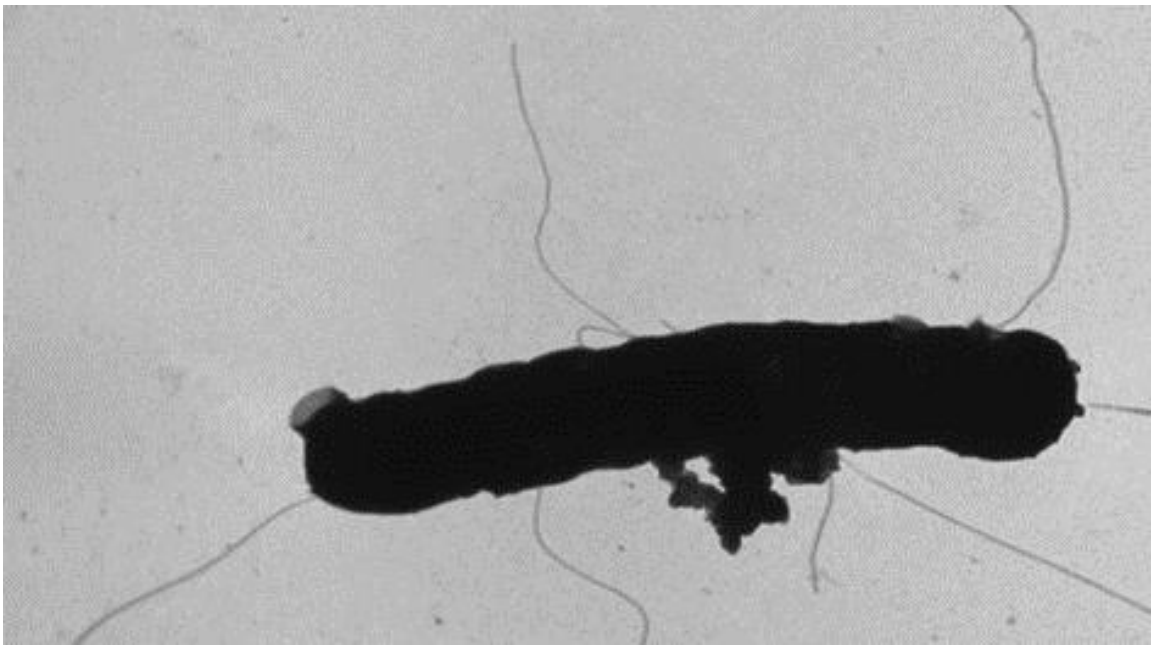

Figure 1-4 Electron microscopy pictures of *C. autoethanogenum.*

Multiple flagella are visable. The rough appearance and attachment was found more often in older cell cultures. Sample preparation and microscopy by: by Florence J Annan, Ronja Breitkopf, Pawel Piatek, Bart Pander and Denise McLean.

1.7.1.2 Nitrogen, phosphor and sulphur sources

Nitrogen is the fourth most common element in life as is obvious from the importance of proteins in almost any cellular function. *C. autoethanogenum* can utilise several nitrogen sources. Yeast extract or other amino acid sources such as tryptone, cas-amino acids are commonly added to semi defined and rich media. Growth of *C. autoethanogenum* is increased, more stable and predictable when these complex additives are part of the media but they muddle analysis and characterisation of subtle mutants is not always possible in rich media. It has been suggested recently that the amino acid arginine specifically enhances growth (147) thus addition of this amino acid might be a solution to the problem of unpredictable growth in fully defined medium.

Inorganic nitrogen sources are employed for fully defined autotrophic growth conditions. Several salts of ammonium are used as the primary nitrogen source for autotrophic conditions in most published methods and also in our lab. Dinitrogen (nitrogen gas) can be fixed (148, 149) by *C. autoethanogenum* and nitrate utilisation is expected to be possible (138) but pilot experiments by members of our lab did not yield significant growth (personal communication Pawel Piatek and Anne M. Henstra). N_2 utilisation is only preferential when other nitrogen sources are low, as N_2 fixation is energy intensive.

Phosphor atoms are present, in the form of phosphate, in all nucleotides, NADP, cofactors, phosphorylated proteins and metabolic intermediates. As such, phosphate plays an essential role in metabolism and intracellular signalling. Many aqueous ecosystems are under phosphate limitation, so when external phosphate is added to these ecosystems, problems of eutrophication arise (150). Indeed the growing phosphate demand, caused by the need to feed a growing world population, has caused some concern for a potential phosphate scarcity crisis (151, 152). Therefore from a sustainability perspective it is advantageous to limit phosphate use. Phosphate limitation is often employed in science and industry to limit growth and direct the metabolism to optimise product yields. In a similar fashion as ammonium limitation, phosphate limitation directs the metabolism to the more reduced, more valuable natural products of *C. autoethanogenum* (Chapter 5).

Sulphur atoms are found in a diverse range of essential molecules in the metabolism of life, and in anaerobes such as Clostridia specifically. Next to the amino acids cysteine and methionine, sulphur atoms are found metabolic intermediates such as the Co-enzyme A and in the iron-sulphur clusters that often function as electron transfer and electron carrying in redox reactions with ferredoxin as a prime example. The most commonly used sulphur sources in anaerobic microbiology are cysteine and sodium sulphide. Sulphate salts are part of many growth media but these are thought not to be utilised as source of sulphur atoms in *C. autoethanogenum* since the genome does not encode the required machinery (140).

1.7.1.3 Other mineral requirements

C. autoethanogenum requires a range of other elements for growth (Table 1-1). Amongst them are a range of metal ions usually required for all organisms. These ions act to maintain osmotic homeostasis and in as essential cofactors in enzymes and other proteins. A few classic examples of these are magnesium acting in all enzymes acting on nucleotides, and zinc in a diverse range of enzymes ranging from carbonic anhydrase to alcohol dehydrogenases (153, 154). Besides these elements *C. autoethanogenum* requires some specific elements. One example is tungsten that was first to be discovered to be biologically active in acetogens (155) and indeed *C. autoethanogenum* harbours tungsten containing enzymes in the form of aldehyde:ferredoxin oxidoreductases (AOR)(142) and formate dehydrogenase (FDH)(60). The later enzyme is one example where also the non-metal element selenium plays an important role since it incorporates selenocysteine residues.

1.7.1.4 Vitamin requirement

We generally add a rich mix of vitamins to the growth media although genome analysis reveals that *C. autoethanogenum* requires just three vitamins: pantothenate, biotin and thiamine. Pantothenate is a precursor of Coenzyme A (CoA) (156). Biotin is a cofactor in carboxylation and decarboxylation enzymes where it acts in transferring CO_2 or bicarbonate to or from the substrates (157). Thiamine is an essential cofactor in pyruvate ferredoxin oxidoreductase (PFOR) in *C. autoethanogenum* (158).

Two other substances in our vitamin mix (Chapter 2), cobalamin and folate, are important in the metabolism of acetogens. The cobalamin forms an important corrinoid cofactor in the WLP. Tetrahydrofolate are the cycling moieties in the methyl branch of the WLP on which a formyl group gets reduced stepwise to methyl.

Table 1-1 Overview of elements used by *C. autoethanogenum*

Element/nutrient	Sources	function
Carbon (C)	CO, CO_2, Pyruvate, Fructose, Xylose, Rhamnose, Arabinose, Glutamate, Fumarate	Backbone of all macro molecules, metabolic intermediates, products
Hydrogen (H)	H_2O, H_2, Carbohydrates (C-sources)	macro molecules, metabolic intermediates, products, proton motive force
Oxygen (O)	C-sources, H_2O	macro molecules, metabolic intermediates, products,
Nitrogen (N)	NH_4Cl, N_2, $NaNO_3$, amino acids	Amino acids, nucleotides
Phosphorus (P)	H_3PO_4, NaH_2PO_4, KH_2PO_4	All nucleotides, cofactors, metabolic intermediates, cell signalling
Sulphur (S)	Cysteine, Na_2S	Amino acids, CoA, FeS clusters
Iron (Fe)	$FeCl_2$, $Fe(SO_4)_2(NH_4)_2$	Several different cofactors, FeS, Fe^{2+}
Potassium (K)	KCl, KH_2PO_4	Osmotic homeostasis, transport
Magnesium (Mg)	$MgCl_2$	Cofactors in enzymes
Sodium (Na)	NaCl	Osmotic homeostasis
Calcium (Ca)	CaCl	Cofactors in enzymes
Chlorine (Cl	NaCl, KCl, CaCl, $MgCl_2$	Anion homeostasis
Selenium(Se)	Na_2SeO_3	Selenocystein
Zink (Zn)	$ZnCl_2$	Cofactors in enzymes
Nickel (Ni)	$NiCl_2$	Cofactors in enzymes
Cobalt (Co)	$CoCl_2$	Cofactors in enzymes
Molybdenum(Mo)	$NaMoO_4$	Cofactors in enzymes
Manganese (Mn)	$MnCl_2$	Cofactors in enzymes
Tungsten (W)	Na_2WO_4	Cofactors in enzymes

1.7.2 Products

The native products generated by *C. autoethanogenum* give us valuable information on how the cells are acting in the culture, through their identity, yield and ratio in which they are present. Products are formed for several reasons; energy conservation, redox and pH homeostasis or to get rid of toxic metabolites.

C. autoethanogenum, produces acetate/acetic acid, which acidifies the growth medium, which in turn leads to inhibition of growth. To counteract this acidification, we add considerable amounts of buffering agents to the medium for batch growth and control pH in bioreactors growth with bases such as sodium hydroxide or ammonium hydroxide. Also high concentrations of the product ethanol can inhibition growth.

The other two native aqueous products of *C. autethanogenum* are 2,3-butanediol and lactate, but under most conditions these are formed in relatively low amounts (0.1-10mM). These amounts are too low to inhibit growth, but also too low to be commercially interesting and therefore optimisation of the production of these is a goal of metabolic engineering. Measuring the concentration of these products gives us important information about the metabolic state of the cells. Both 2,3-butanediol and lactate are derived from pyruvate and it has been reported that increasing the CO_2 partial pressure will lead to increased production of pyruvate derived products (159).

1.7.3 Internal metabolism: inside the black box

In Figure 1-5 a summary of the current understanding on the metabolism of *C. autoethanogenum* is displayed. I distinguish four modules in this network that I will discuss in some detail: the WLP, sugar catabolism, end-product formation and energy conservation. These modules are obviously intertwined and interdependent in the metabolic network. This is illustrated by the fact the WLP is still active during growth on sugars, as was revealed by transcriptomics, modelling and metabolomics (136, 139). Certain parts of are necessary only under specific conditions. A mutant with part of the WLP disrupted is still able to grow on sugars (160) and sugar catabolism is mostly unnecessary for autotrophic growth.

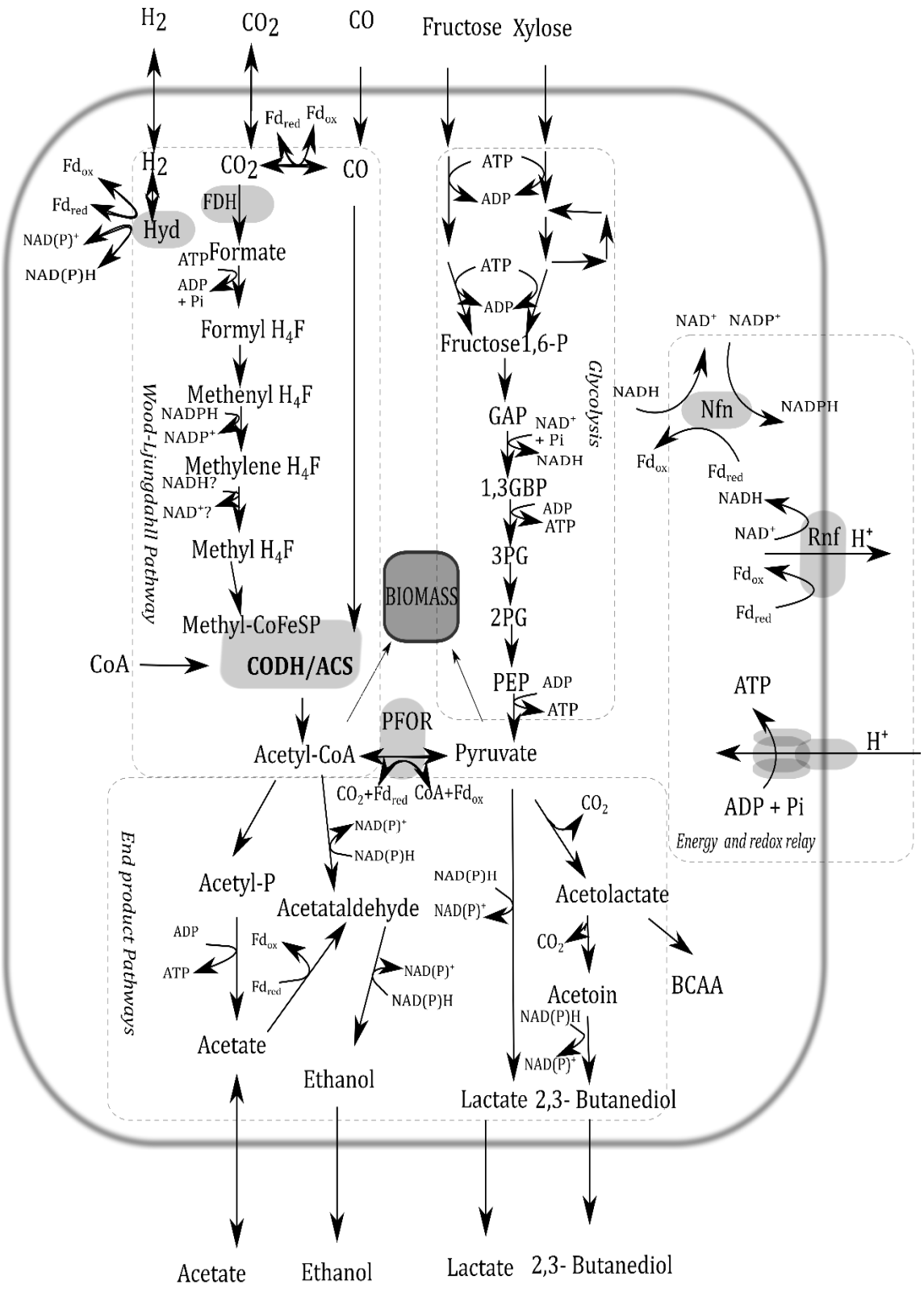

Figure 1-5 Overview of the metabolism of *Clostridium autoethanogenum.*

This overview illustrates several options of carbon and energy sources. A mixed use of carbon sources is possible where both organic substrates such as monosacherides and anorganic sources, CO, CO_2 of H_2 are consumed (mixotrophy). The boxed pathways can be considered modules that interact in redox balancing. Boxed pathways are discussed in detail in sections 1.8.5 (Wood-Ljungdahl Pathway), 1.8.6 (end product pathways), 1.8.7 (energy and redox relay) and 1.8.8 (glycolysis and sugar metabolism).

1.7.4 Wood-Ljungdahll pathway

The WLP of *C. autoethanogenum* can function both with CO and with CO_2 as the primary carbon source. As noted before, CO_2 as carbon source requires supply of an electron donor such as H_2 or carbohydrates such as fructose or xylose. In the following detailed description (Figure 1-6) I assume CO is the primary carbon source but shows the more generalised view. The WLP generates acetyl-CoA, by fusing CO with a methyl group and a CoA to acetyl-CoA

1.7.4.1 The hart of the WLP and the carbonyl branch

The WLP is traditionally said to consist of two branches, the methyl and the carbonyl branch. However if we consider this pathway with CO as the carbon source, this division might seem somewhat contrived as the carbonyl branch is seemingly just one step in this case. This step, the condensation of CoA, CO and a methyl group is the final step of the pathway.

This key reaction of the WLP is catalysed in the CO-methylating acetyl-CoA synthase (ACS), which is generally assumed to form a complex with a CO dehydrogenase (CODH) in acetogens like *C. autoethanogenum* (160). The crystal structure of ACS/CODH complex from *M. thermoacetica* was determined (161) In *M. thermoacetica*'s ACS/CODH it seems that the CO that reacts with the CoA and the methyl group is preferentially derived from CO_2 that was reduced in the enzyme and not CO from outside of the complex (162). The methyl group that enters the enzyme complex on a corrinoid-Fe-S protein is produced in the methyl branch. In this methyl branch, 6 electrons reduce CO_2 to a methyl group in a stepwise fashion.

1.7.4.2 Preparation stage: from CO to CO_2

When grown on pure CO, the CO_2 that will go into the methyl branch of the WLP pathway is formed by oxidation of CO on a CODH by reduction of ferredoxin. The CO/CO_2 reduction potential is approximately -530 mV which is more than the reduction potential of H_2 (H_2/H^+ E_0'= -414 mV) (142, 163). The reduced ferredoxin produced in this step provides, direct and indirect, almost all of the reduction power and energy for the rest of the metabolism. It is likely that this step is limited by the reoxidation of ferredoxin further on in the metabolism and the oxidation of CO can cause over reduction of the cell (60).

C. autoethanogenum contains 3 CODHs (CLAU_1578 (*acsA*), CLAU_2924 (*Coos1*), CLAU_2924 (*Coos2*)). The oxidation of CO to CO2 is thought happen on the CODH in the ACS/CODH complex (160). Only disruption of *acsA* gene abolished autotrophic growth. Like AcsA, CooS1 is highly expressed and gene disruption creates a clear effect, whereas disrupting Coos2 does not seem to have much effect nor does it show significant expression (160).

1.7.4.3 The first step of the methyl branch: CO_2 to Formate

In first reduction step of the methyl branch of the WLP, a formate dehydrogenase (FDH, CLAU_2712 - 2713) catalyses the conversion of CO_2 into formate. This FDH is complexed with a NADP specific electron bifurcating hydrogenase (HytABCD (CLAU_2718 - 2722)), which is an important reduction vent (60). Not surprising the genes coding for FDH/Hyt are amongst the highest expressed in *C. autoethanogenum* using the WLP. *C. autoethanogenum's* genome harbours five more hydrogenases (164) however except for CLAU 1534 – 1537 all other hydrogenases are expressed at low levels in all available datasets. and CLAU_0115 appears to be lacking amino acid residues for hydrogenase activity (136, 137, 165).

1.7.4.4 Step two: Formate to Formyltetrahydrofolate

Formyltetrahydrofolate synthase (CLAU_1576, FhsCO) catalyses the reaction between formate and tetrahydrofolate to form formyltetrahydrofolate. This reaction requires the hydrolysis of ATP to ADP and Pi. This ATP investment was one reason why acetogens where once thought to be energy starved since there was only one substrate level phosphorylation reaction known to recycle the ADP: the dephosphorylation of acetate phosphate to acetate. Since these two steps equal out there is not net ATP production and indeed as detailed below, ATP is produced using a proton motive force (PMF).

1.7.4.5 Formyltetrahydrofolate to methylenetetrahydrofolate

A methenyltetrahydrofolate cyclohydrolase (CLAU_1575, FchA) subsequently converts formyltetrahydrofolate to methenyltetrahydrofolate by a condensation reaction, and a NADPH specific methylene-THF dehydrogenase (CLAU_1574, FolD) reduces this further to methylenetetrahydrofolate.

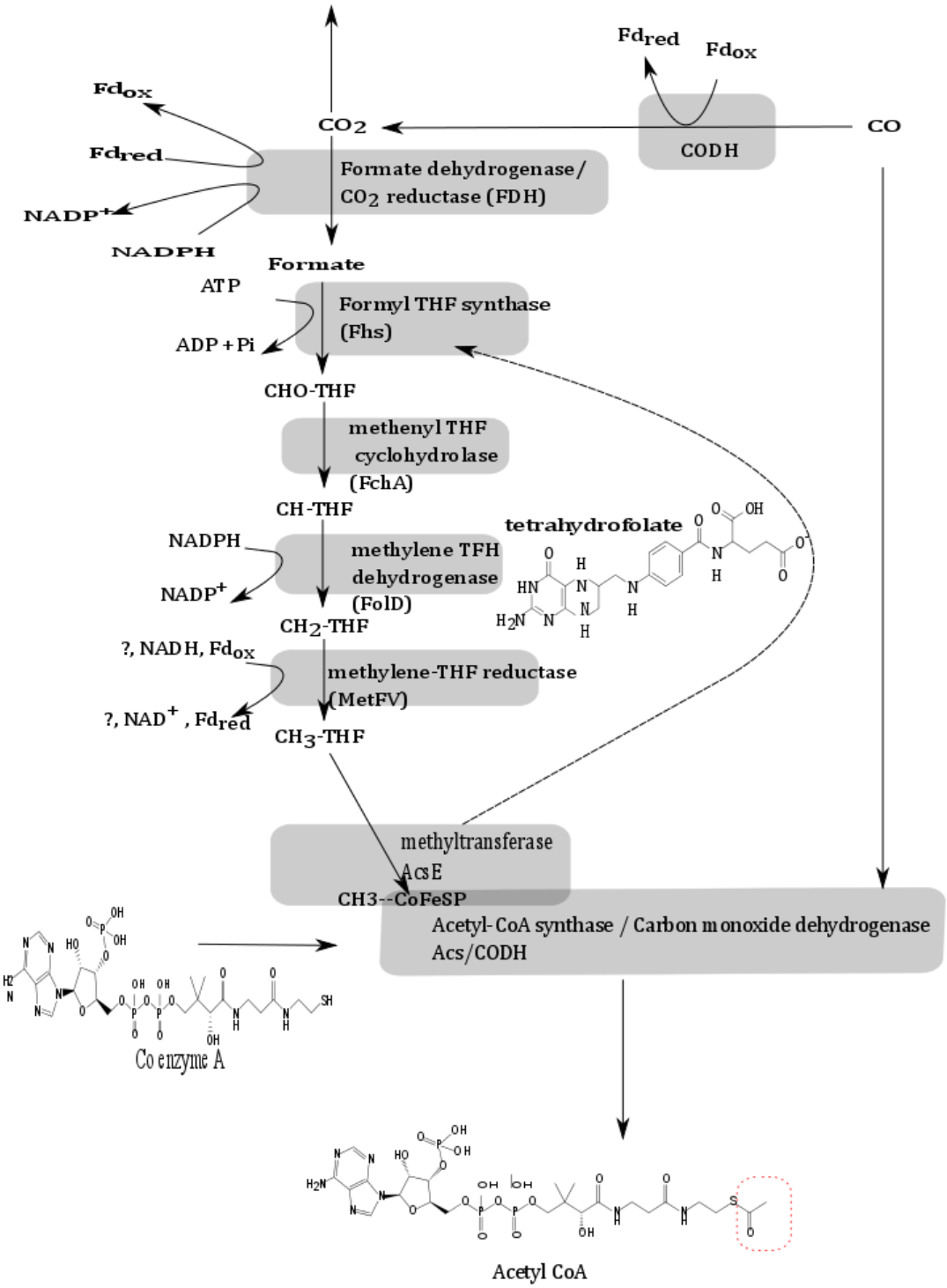

Figure 1-6 Wood- Ljungdahl or reducing acetylCoA pathway as it would flow when grown on CO.

CO enters the pathway either by being oxidised to CO_2 at a CODH while Fd_{ox} is reduced to Fd_{red} or by combining the CO with a methyl group and CoA in a Acs/CODH complex to create acetyl-CoA. The methyl group is formed, step wise, from CO_2, via formate, formyltetrahydrofolate, methenyltetrahydrofolate, methylenetetrahydrofolate, methyltetrahydrofolate and methyl-corrinoid-FeS-protein. Picture is based on information referenced in this chapter. The structure of some key intermetdiates (Co enzyme A, Tetrahydrofolate) are taken from Chemdraw (Perkin-Elmer). Acetyl group of acetyl-CoA is marked with a red box. The acetyl group forms the basis of all further carbon metabolism when CO (or CO_2) is the carbon source.

1.7.4.6 Methylenetetrahydrofolate to methyltetrahydrofolate.

Conversion of methylenetetrahydrofolate to methyltetrahydrofolate is catalysed by a methylentetetrahydrofolate reductase which is encoded by two genes (CLAU_1572-1573(MetFV)). It is still unknown what redox carriers facilitate this step (60, 165). However since it is often assumed that this step conserves energy (probably by reducing ferredoxin), experimental knowledge about this step is desired (89, 137, 165).

1.7.4.7 Methyltetrahydrofolate to methyl-corrinoid-FeS-protein

Subsequently the methyl group of methyltetrahydrofolate is transferred to the cobalt group of the corrinoid-FeS-protein by a methyltransferase. The methyl group is now available in the ACS/CODH for the final step of acetyl-CoA production.

1.7.4.8 Downstream of the WLP

The acetyl-CoA that is formed in the ACS/CODH complex from CoA, CO and the methyl group, forms the basis of all further metabolism in the case of autotrophic growth.

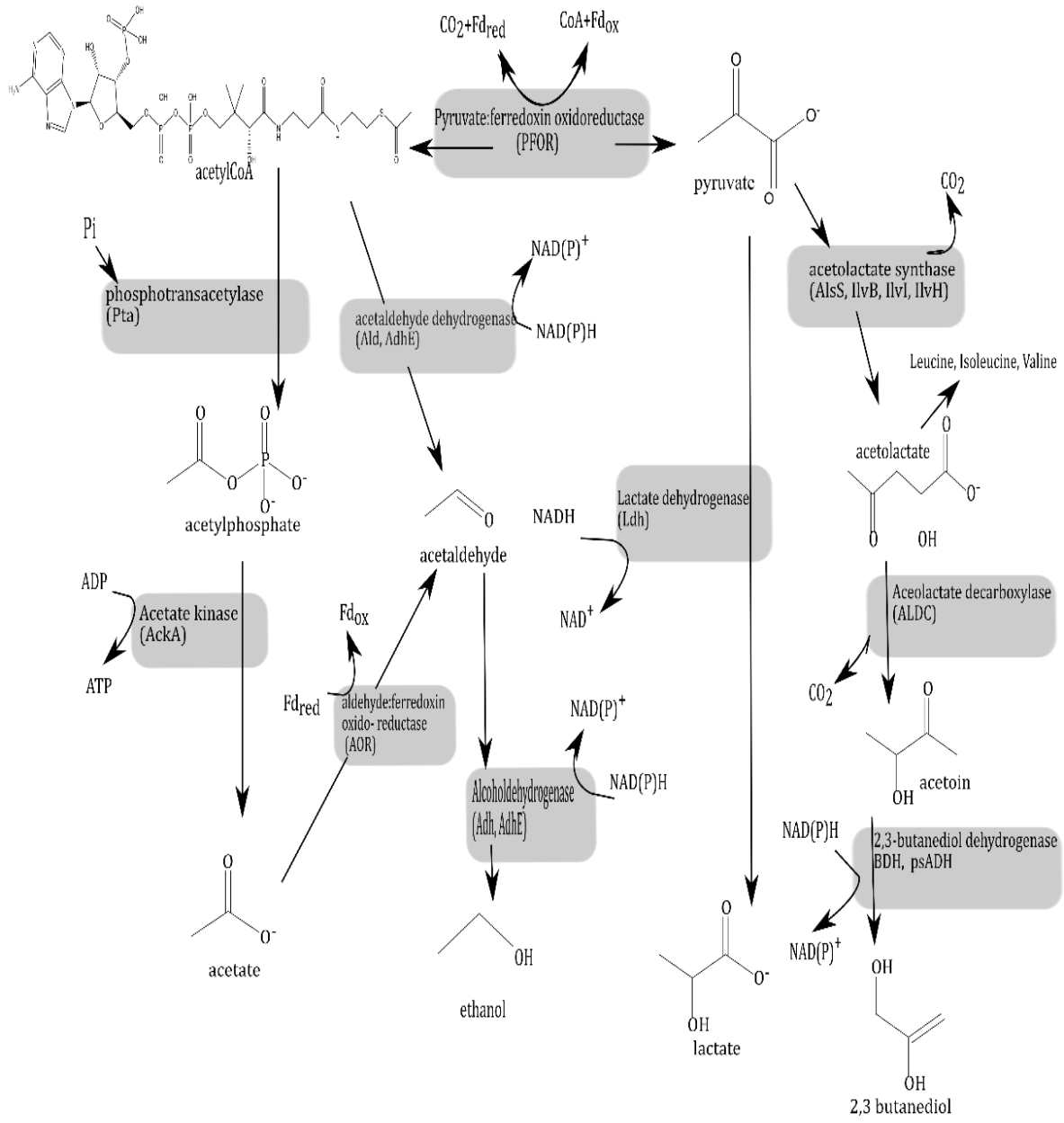

Figure 1-7 Pathway to liquid products from acetylCoA or pyruvate. The carboxylic acids are drawn in their deprotonated form which not necessarily reflects the most common state at the assumed pH of the cells. Acetate is formed to generate ATP. Since the WLP requires 1 ATP per produced AcetylCoA the acetate formation balances ATP so that no net ATP is formed this way. The other products, ethanol, lactate and 2,3 butanediol are formed at the expence of reducing electron cariers, Fd_{red}, NADH or NADPH and are expected to be formed at relatively higher levels under more reduced circumstances. Ethanol can be formed via two routes, from acetylCoA via an acetaldehyde dehydrogenase catalysed reaction to acetaldehyde or from acetate via an Aor catalysed reaction to acetaldehyde. The acetaldehyde is in both cases reduced to ethanol.

1.7.5 Pathways to biomass and products

The acetyl-CoA formed in the WLP feeds into approximately 20 reactions that can be grouped in the direct end product formation (catabolism) of acetate and ethanol, and the build-up of biomass (anabolism). The end products lactate and 2,3-butanediol branch of from pyruvate. About 80% of the acetyl-CoA will go to acetate and ethanol (Chapter 3).

1.7.5.1 Acetate

Acetate is formed from acetyl-CoA in the two-step process catalysed by phosphotransacetylase (Pta, CLAU_3274) and actate kinase (AckA, CLAU_3275), whereby ATP is formed by substrate level phosphorylation.

1.7.5.2 Ethanol

Although there is a possible route to ethanol formation from acetyl-CoA, via acetaldehyde, most the ethanol is formed from acetic acid via aldehyde ferredoxin oxidoreductase (Aor) that oxidises Fd_{red} (140, 166). Aor can only catalyse acetic acid and not deprotonated acetate (pKa 4.76) and this process is there for pH dependent (140).

The disruption or knocking out o genes involved in acetaldehyde formation result in somewhat surprising higher ethanol yields for aor2 (CLAU_0099), adhE1 (CLAU_3655) and adhE2 (CLAU_3656) when grown on CO. Only the disruption of aor1 (CLAU_0081) decreased the ethanol formation significantly while much more lactate was formed in this case (166). There exist three more genes that putatively encode for enzymes able to produce acetaldehyde (166). These three Ald genes (CLAU_1772, 1783, 3204) are part of two micro compartment gene clusters.

The acetaldehyde produced by any of the processes is then reduced by alcohol dehydrogenases (Adh). *C. autoethanogenum* genome contains at least 12 genes for Adhs but only some have been characterised. Interestingly when grown with CO as substrate, NADH and NADPH dependent Adh activity was detected while only NADH dependent activity was found with H_2 and CO_2 as carbon and energy source (165).

1.7.5.3 Pyruvate derived products

The remaining ~20% of the acetyl-CoA formed in the WLP will be transferred to other processes. This is mostly biomass formation but two other end products can be formed via pyruvate: lactate and 2,3-butanediol. Central enzyme in this step is pyruvate: ferredoxin oxidoreductase (PFOR1, CLAU_2947, PFOR2, CLAU_0896), which during heterotrophic growth produces acetyl-CoA while reducing ferredoxin and the reverse reaction happens during autotrophic growth. CLAU_2947 is much higher expressed than CLAU_0896 and is the primary PFOR (87). To produce pyruvate from acetyl-CoA, CO_2 is needed and it has been claimed that higher CO_2 partial pressures push the reaction towards more pyruvate production under certain circumstances (159).

1.7.5.4 Lactate

Lactate can be formed in one enzymatic step by lactate dehydrogenase (Ldh) for which one gene codes for a NADH dependent LDH (CLAU_1108) (167).

1.7.5.5 2,3-Butanediol

2,3-Butanediol production requires three enzymatic steps. This first step produces acetolactate from two pyruvate molecules. This step is catalysed by three different acetolactate synthases (ALS) for which 4 genes (AlsS (CLAU_1694), IlvIH (CLAU_0119-0120) and IlvB (CLAU_0388)) are present in *C. autoethanogenum*. This catalytic redundancy is required because the proteins have slightly different functions. AlsS is a catabolic ALS which is most important for product formation, while IlvIH and IlvB are anabolic ALS that provide the acetolactate for the production of the branch chained amino acids leucine, isoleucine & valine (87). The acetolactate destined towards 2,3-butanediol is first decarboxylated by acetolactate decarboxylase (Aldc/BudA CLAU_2851) to acetoin which finally is reduced to 2,3-butanediol by an NADH dependent butanediol dehydrogenase (Bdh, CLAU_0370) or an NADPH dependend primary-secondary alcohol dehydrogenase (CLAU_0532) (167).

1.7.6 Energy conservation

The ATP in the metabolism is produced by a substrate level phosphorylation (SLP) at AckA and by a proton motive force (PMF) driven ATP-synthase. It is unknown what amount of protons is needed to form one ATP out of ADP and Pi but can be assumed to be between 3 and 4 (137, 165). The PMF is generated by the Rnf complex that couples proton-translocation to ferredoxin:NAD+ oxidoreductase activity (*Rnf*$_{abcdefd}$, CLAU_3144-3149). When grown on CO most of the NADH needed in other parts of the cells metabolism is produced in this step. A *C. ljungdahlii* strain with a disrupted Rnf was unable to grow autotrophic and unable to grow without a fixed nitrogen source (148). Rnf and ATP-synthase are the drivers of the chemiosmotic based ATP synthesis and producer of the important electron carrier NADH.

When grown on CO the third electron carrier NADPH is formed on a flavin-based bifurcating enzyme, NADH-dependent ferredoxin-NADP+ oxidoreductase (Nfn). This enzymecomplex works as a redox relay station where the three most important redox carriers can be interconverted. The one high potential carrier, ferredoxin (-400-500mV) Fd_{red}, and one lower potential NADH (-320 mV) transfer their electrons to two molecules of the mid potential NADP+, forming two NADPH (-360 mV)(168).

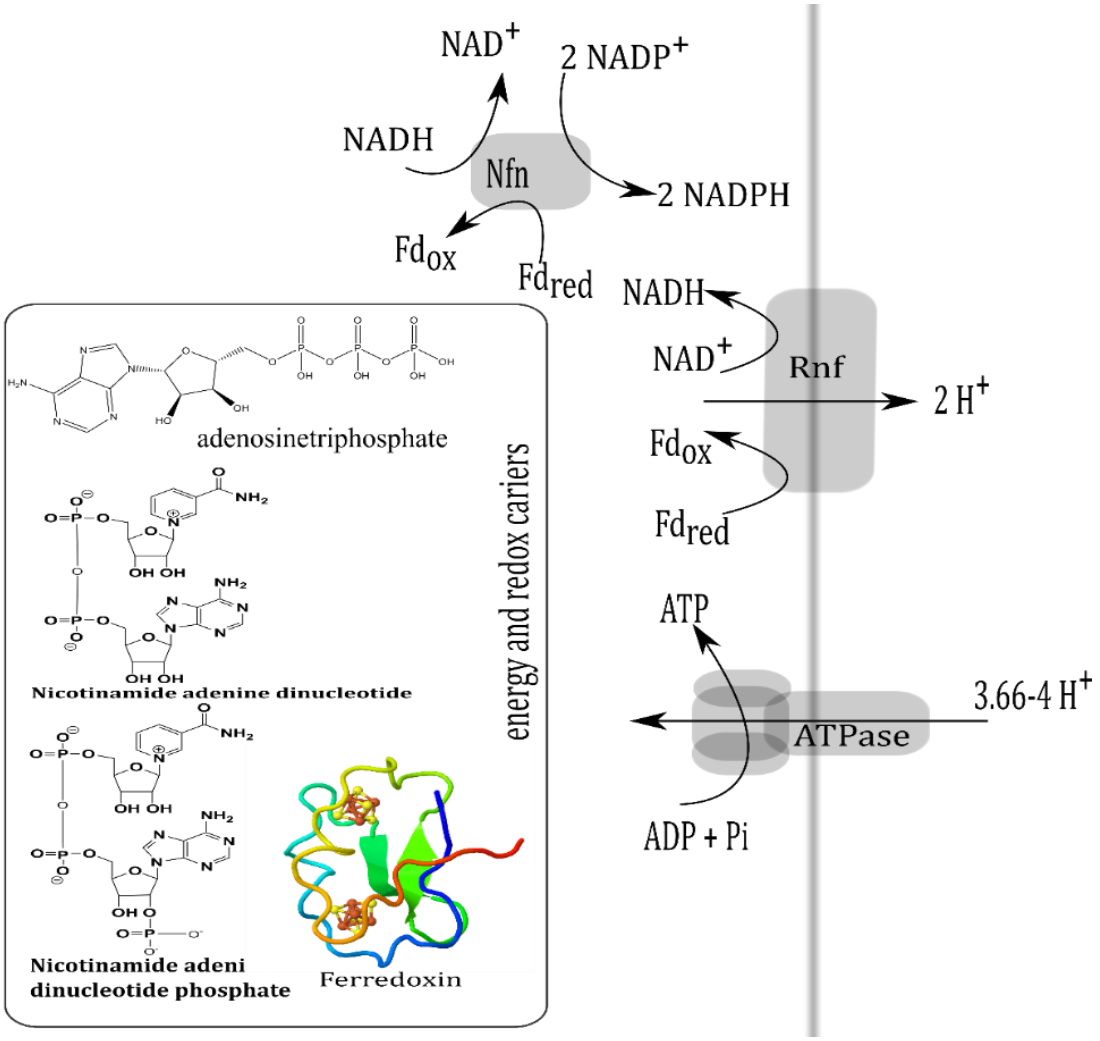

Figure 1-8 Overview of the energy conservation and redox relay system of *C. autoethanogenum*.

The structure of the energy and redox carriers is given in a separate box. At RnF a protons are transported creating a proton motive force (PMF). This PMF is then used at an ATP synthase to produce ATP. The energy for this comes from transferring electrons from Fd_{red} to NAD^+. The required Fd_{red} is produced at CODH and likely at MetFV, when the bacterium is grown on CO. Nfn functions in transferring electron from NADH and Fd_{red} to $NADP^+$ and vice versa.

1.7.7 Sugar metabolism

Fructose is used in the Embden-Meyerhof-Parnas (EMP) version of glycolysis, while xylose starts off in the penthose-phosphate pathway (PPP). These pathways generate pyruvate, CO_2, ATP and NAD(P)H. The pyruvate can be transformed at the PFOR generating Fd_{red}, acetyl-CoA and CO_2. The NAD(P)H, Fd_{red}, CO_2 and ATP can then be used in the WLP generating another acetyl-CoA molecule. The acetyl-CoA yields ATP via the substrate level phosphorylation with acetate as a product, as described before. This coupling of the EMP and the WLP gives the highest yield of ATP of any anaerobic sugar degradation (52).

Under autotrophic growth many of the metabolic intermediates of the glycolysis are still essential and these need to be formed by gluconeogenesis, in which pyruvate is transformed to phosphoenolpyruvate (PEP) and further towards fructose phosphate etc. Most PEP is probably not formed in a direct route but via oxaloacetate (137).

1.8 Genetics

This PhD was part of a larger project called the GASCHEM project. One goal of this project was to use genetic tools to optimise production of the native products of *C. autoethanogenum,* or to introduce pathways to new products. This is depended on the detailed knowledge on the genome and transcription on one hand, and the availability of tools for transformation on the other. At the start of the project both were not well developed, hampering our engineering attempts.

1.8.1 Whole genome analysis

The sequencing of the genome of *C. autoethanogenum* was complex because of the relatively low G+C content and the high amount of repeats (164). The first genome draft published in 2013, elucidated using 454 GS FLX Titanium and Ion Torrent PMG, was therefore submitted in 100 contigs (169). Besides that a fully closed genome of *C. ljungdahlii* (149)was available. In 2014, a Pac-Bio sequenced closed version of the *C. autoethanogenum* genome sequence came available(164). However the quality of the available genome sequences of *C. autoethanogenum* was lacking rigour since we found multiple unlikely inconsistencies such as frame shifts and premature stops in important genes in the available genome, when we compared to the *C. ljungdahlii* genome sequence. Therefore, we employed Illumina MiSeq to sequence a newly acquired stock of *C. autoethanogenum* from DSMZ, and produce a high quality genome sequence. About 10% discrepancies between our sequence and the other genomes were sequenced using Sanger sequencing, which in all cases agreed with our MiSeq data. Another issue with many bacterial genome sequences is the annotation of genes, which is almost universally fully automated, leads to propagation of mistakes in previously sequenced genomes. Since our project consist of a sizeable group of people, every member of the GASCHEM project manually curated 336 genes. This elevated the annotation of 482 genes from the 'hypothetical protein' status in the previous genome sequences to an assigned function, and in 131 instances the annotation of a gene product was made less specific or reduced to 'hypothetical protein'. Most human errors were corrected by a double check by another member of the team in case of significant differences with previous automated annotations. The effort resulted in a high quality genome sequence with good annotation (170). Shortly before the publication of our own genome sequence update, the groups that published the previous two genome sequences also published an update where they compared multiple next generation sequencing techniques: Roche 434, Illumina Truseq technology, Ion torrent, PacBio RS II, and Sanger sequencing (171). This means there are now multiple high quality genome sequences of *C. autoethanogenum* available in public data bases.

The genome of *C. autoethanogenum* is 4352627 bp of which 84.7 % is coding for its 4039 genes; it has a GC content of 31.09 %. This is somewhat smaller than the 4.6 Mbp *C. ljungdahlii* genome which contains 4198 predicted genes (149). Compared to *C. ljungdahlii*, the *C. autoethanogenum* genome has extra genes associated with functions in mannose metabolism and extra genes for aromatic compound degradation. In the central carbon and energy providing pathways of metabolism, *C. autoethanogenum* harbours an extra gene coding a Fe/Fe hydrogenase on an operon together with NuoF-like oxidoreductases. This operon is reported to be highly expressed under conditions of CO_2/H_2 grown condition and it is expected to be advantageous during growth on syngas (164).

The genomes provide a possible explanation for another noteworthy difference between *C. autoethanogenum and C. ljungdahlii.* Where *C. ljungdahlii* can be genetically transformed by electroporation or by conjugation (172), the only way we managed to transform *C. autoethanogenum* is conjugation. The presence of active methylation- restriction systems is an important reason for electro transformation failing in Clostridia (173). *C. autoethanogenum* contains at least 4 type IV restriction systems and a CRISPR system (clustered regularly interspaced short palindromic repeats) that are both lacking in *C. ljungdahlii.* A claim is made in a patent that electrotransformation of *C. autoethanogenum* is possible if type I methylated DNA is used (174). In line with the lower number of protective systems in *C. ljungdahlii,* it's genome harbours more prophage sequences (164, 175). This higher level of phage protection systems in *C. autoethanogenum* might yield advantages in industrial settings where phage attacks can be an issue (175, 176) however , it also makes gene editing much harder.

1.8.2 Transcriptomic studies

In recent years, the ease and decreasing price of RNA sequencing (RNAseq) has revolutionised the study transcriptomics. Many transcriptome datasets are now available of *C. autoethanogenum* comparing different growth conditions such as heterotrophy vs autotrophy (136) or different gas compositions (165), agitation rates (137), and pH and gas supply rate (unpublished data Henstra et al.).

1.8.3 Genetic modification tools

At the beginning of our project *C. autoethanogenum* was already shown to be genetically tractable. Both disruption of genes by intron insertion, allelic exchange and plasmid based expression was demonstrated (14, 166, 177, 178) however, compared to other Clostridia, the process is very much hit and miss, with more misses than hits. This low success rate of genetic engineering is probably caused by the previous mentioned phage defence systems such as CRISPR-CAS and the type IV restriction systems.

Even though genome editing is not straight forward, the possible gains are very significant and thus worth the pursuit. By deleting genes metabolic pathways get interrupted and energy and carbon flux can be steered. This can be done in more central metabolic routes, such as disrupting acetate or ethanol production. Optimisation can also be achieved by disrupting more peripheral pathways that are energy or carbon consuming but are unnecessary for growth such as flagella and exopolysaccharides. Deletion of genes can be used in a non-directed way, for example the random insertion of a mariner transposon can be used to produce and screen for useful functional mutations (179).

Not very long ago the amount genome editing that was possible in clostridia was fairly limited, however, in the last decade several tools have been established that enable engineering of clostridia.

1.8.4 Plasmid transfer

To transfer plasmids to *C. autoethanogenum* transformation by electroporation or heat shock and similar techniques is extremely inefficient and therefore cannot be employed effectively. Therefore conjugative *E.coli* strains are used for DNA transfer. An *E.coli* HBlOl with a R702 plasmid that harbours the conjugative machinery (180), the CA434 strain, is the most used strain for conjugation with Clostridia (160, 179, 181–184). However, this strain contains DNA cytosine methyltransferase (Dcm^+) which methylates the second cytosine of 5'-CCWGG sequences that can be attacked by the type IV restriction systems on *C. autoethanogenum*. Although CA434 has been used to transfer DNA to *C. autoethanogenum,* only a small set of plasmids could be used and with low frequencies. Therefore Craig Woods (PhD student in the our laboratory) transferred the R702 plasmid to a Dcm^- NEBexpress (BL21 derivative) strain. The resulting strain, colloquially named "Sexpress", was not only up to 750 times more efficient in transferring plasmids that were known to be transferable such as pMTL83151, but allowed plasmids with replicons that were previously impossible such as pMTL81151 to transfer. This opened up more complex gene editing of *C. autoethanogenum.*

1.8.5 The pMTL8000 plasmid series

The plasmids used in *C. autoethanogenum* are of the so called pMTL80000 series. This is a modular system allowing easy tailor-made plasmid construction that can be used in all genetically tractable clostridia and many other bacterial species (181). Special attention should be drawn to the several gram positive replicons that are available. For genome editing tools it is essential that the plasmid can be lost and thus replicons with fairly low segregationally stability such as pCD6 should be used, while for plasmid-based expression high stability supplied by replicon pBP1 is essential.

1.8.6 Clostron

The most successful technique to disrupt genes in *C. autoethanogenum* is group II introns based ClosTron technique which has been successfully employed in multiple studies (160, 166, 167). Using the *Lactoccus lactis* Ll.ltrB intron and the intron encoded protein LtrA, this system can be programmed to insert into a targeted region of the genome. Using a computer algorithm (185) and chemical synthesised DNA, ClosTron offers a way to disrupt genes (182, 186, 187). However since this is a technique using a mobile genetic element unspecific insertion is possible and southern blot or genome sequencing screening for double insertion and gene complementation are essential (173). Another issue with this technique is the possibility of polar effects. The target gene is disrupted by insertion of an intron which causes a frame shift, and also introduces an antibiotic resistance marker that is expressed. Both can cause effects on the genes surrounding the target genes.

1.8.7 Allele coupled exchange

Allele coupled exchange circumvents the problems associated with the ClosTron technique. It is based on double cross-over homologous recombination that can result in clean deletions of genes and clean insertions of genes. A positive/negative selection marker is the key to this system. The selection we deployed in *C. autoethanogenum* was based on the *pyrE* gene that encodes for an orotate phosphoribosyltransferase, an enzyme that is essential for uracil biosynthesis. The orotate phosphoribosyltransferase converts fluoroorotic acid (FOA) to 5-fluoro-uridine mono phosphate (FUMP), which leads to cell death. Deleting this gene thus results in a uracil auxotrophy and (FOA) resistance while the wild type or any strain carrying a *pyrE* is sensitive to FOA but a uracil prototroph. This Δ*pyrE* strain can then be used to delete other genes

after which the *pyrE* can be repaired by a repair plasmid, again using the positive/negative selection. Instead of just repairing the *pyrE* we can also insert genes at this locus. It was reported that 5-FOA is a mutagen (188) however we did not find evidence for this in *C. autoethanogenum (Chapter 7)*. This system was successfully employed in *C. autoethanogenum* and has been used to knock out one of the two *aor* genes (166), *alssS* (chapter 7), *ldh* (personal communication Chris Humphreys) and a the Agr quorum sensing system (personal communication Pawel Piatek). However this technique suffered from low success rates and is labour and time intensive.

1.8.8 CRISPR based editing

By the end of 2016, a superior gene editing technique became available for *C. autoethanogenum* (189, 190). This system is based on the use of the CRISPR-associated system, CRISPR-Cas, as a specific selection marker that can be targeted against any gene. CRISPR-Cas is a bacterial acquired immune system to combat phage infections which has revolutionised the gene editing in eukaryotes but now also prokaryotes. The system relies on a Crispr associated nuclease (Cas9) that is guided to its target by a 20-nucleotide guide RNA (sgRNA) it introduces a double-stranded break. By employing two homology arms that can recombine the flanking region of a target gene and a sgRNA that targets the gene, one creates a strong selection against cells containing the gene and thus selective advantage for the cells lacking the target genes. The introduction of this system has decreased the gene deletion cycle time from more than a month with ACE or ClosTron to about 10-15 days and makes gene introduction at any locus possible (personal communication Pete Rowe).

1.9 Classical microbiology and systems biology

Our insight into growth, metabolism and product formation by *C. autoethanogenum* have increased significantly in recent years. Many studies which contributed to this knowledge compared growth of a wild type under different conditions and measure growth by optical density and product formation by gas chromatography (GC) or high pressure liquid chromatography (HPLC). More recently, the previously discussed transcriptomics and not yet discussed metabolomics gave us a glimpse of the inner working of the cells, on a "systems" level, which in turn makes the building of properly curated computer models of the metabolic network possible.

1.9.1 Batch growth

The easiest method to grow *C. autoethanogenum* is in batch growth in tubes or bottles. Microbiologist are often focused on the exponential phase, but other phases should not be ignored, in *C. autoethanogenum* the pyruvate derived products are mostly formed during stationary phase or very late exponential phase (87). Batch growth can be done in a semi open tubes in an anaerobic cabinet where the head space is kept constant or in closed bottles or tubes. In the closed systems it is possible to create an elemental mass balance which is not possible for the open systems. In all cases of batch growth, all parameters affecting the bacteria are in constant flux, substrates are used up, cells and products are formed. Because of this it is hard to model the metabolism of cells in batch and thus to fully understand what is happening in the cells. Notwithstanding the drawbacks of batch growth, due to its simplicity it is most used method to study optimisation of product formation and to characterise growth, both of wild type and of mutant strains (13, 87, 160, 166, 191–193).

1.9.2 Growth in bioreactors

Bioreactor growth is more complex on a technical/material level, but has many advantages, most importantly that most growth parameters can be controlled and once the initial set up is accomplished it straightforward to get high quality samples. Since large bioreactors are used by industry, using bioreactors in the lab also yields information which is more transferable to the industrial process. Not surprisingly bioreactors were used in multiple recent studies (137, 140, 194)

Batch growth can also be established in bioreactors, but although better control of some parameters is possible, the constant flux of substrates and products as described above is still a drawback.

1.9.3 Fed-batch growth

Fed batch is growth in a bioreactor where most of the culture medium is not replaced but one or more substrates are added at a set rate. This mode of growth is stable and allows for very high cell densities to be established, and therefore, is a favourite growth mode in industry. It is also the growth mode employed to prepare the cultures for continuous growth.

1.9.4 Continuous growth in bioreactors at steady state (chemostat)

Continuous growth can be achieved in a bioreactor by adding new growth media at a set rate (D) and removing an equal volume of the growth media. The constant dilution of the growth media allows for constant growth at a constant rate (specific growth rate: μ) this means after a while, a steady state is established where all growth parameters are continuous at the same level. Operating under these conditions is known as chemostat culture. Since under these circumstances the dilution rate determines the growth rate, the growth rate of the population can be set at will. Obviously there is a maximum dilution rate and thus growth rate which is determined by the dilution rate at which more cells wash out than are being produced. The minimum dilution rate is less easy to define as no dilution would be essentially batch growth where a steady state is not possible but even a very slow dilution might lead to steady states.

All growth is restricted by limiting factors but only under chemostat conditions can these factors be precisely manipulated. Not surprisingly, much bioreactor work on other organisms have been under pre-defined limiting condition. This is in contrast to the bioreactor work on *C. autoethanogenum,* where the limiting conditions are often assumed but not known. This is in part caused by the fact that most bioreactor growth of *C. autoethanogenum* and its relatives is on gaseous substrates. In most chemostat studies with other organisms, all substrates (except oxygen) are added at a rate determined by the dilution rate. However in the case of gas fermentations the substrate and growth media are not added at the same rate. Generally these cultures are assumed to be carbon limited unless results yield reasons to believe otherwise (137, 140). Although the term carbon limited is used in literature, it is somewhat problematic. This is because a potential carbon source, CO_2, is produced and thus available one cannot really say the culture is carbon limited. A better term might be energy limitation.

In a true steady state it is assumed no changes in internal and external metabolite concentrations are occurring. This is only true on a population level, as individual cells still need to go through the cell cycle. By

adding phosphate to a phosphate limited culture with a frequency similar to the growth rate, one can cause cell cycle synchronicity, which can be useful to study the cell cycle of the bacteria but is something to avoid in most cases. Substrate addition should be as continuous as possible to avoid periodic effects.

1.9.5 Computer Modelling of the metabolism

An important spin-off of genome sequencing is the possibility to build a genome scale metabolic model. Metabolic modelling can provide a deeper understanding of the organism behaviour. There are multiple ways to model organisms; a rough distinction can be made between smaller kinetic models vs larger genome scale models (GSM). Kinetic models which incorporate detailed knowledge such as enzyme kinetics can at this time only be built of small subsets of the metabolic network. Genome scale modelling incorporate many more reactions, but since kinetic parameters are missing, flux balance analysis is possible only under the steady state assumption. Both types of modelling are slowly becoming intertwined. Using these different kinds of modelling can give the levels of insight needed to truly engineer an organism (195–198). Genome scale models are available for both *C. ljungdahlii* (138) and *C. autoethanogenum* (136, 137)

In the GASCHEM project Rupert Norman built a genome scale model of *C. autoethanogenum* using ScrumPy (199). This model revealed, amongst other findings, that ethanol production is strongly affected by nutrient limitations other than carbon limitation as is confirmed by the work presented in chapter 5.

There is another published GSM of *C. autoethanogenum* (136). This model combined with a poly-omics study suggested that pyruvate carboxykinase is the rate-limiting step of gluconeogenesis, predicted a novel glyceraldehyde-3-phosphate dehydrogenase that lowers the ATP consumption of the gluconeogenesis (136) and that the addition of arginine strongly boosts growth on the gaseous substrates (147).

1.9.6 Metabolomics

Under the steady state assumption of flux balance analysis, not only remain levels of external metabolites, substrates and products constant over time, the internal metabolite concentration remains constant too. This means that determining the concentrations of the internal metabolites is a good way to validate the metabolic models. Determining internal metabolites can also be rewarding in more explorative approaches to gain understanding of the phenotype of a mutant (chapter 4) or the metabolism of a novel substrate (chapter 6).

Two of the most commonly used methods to determine the internal metabolites are nuclear magnetic resonance (NMR) or a combination of chromatography and mass spectrometry (GC-MS or LC-MS). NMR allows living sample analysis and can detect many smaller molecules simultaneously. Modern MS techniques are more sensitive, and more quantitative than NMR but require more laborious sample preparation

In chapter 4 and chapter 5 LC-MS is used to determine the internal metabolites in both targeted and untargeted approaches. The difference between targeted and untargeted is in that a targeted approach uses a standard of the metabolites of interest so these metabolites can be quantified while untargeted uses the full output of all that is detected. This untargeted approach can be used to detect unexpected differences between growth conditions or mutant strains and to test if these differences are reproducible.

1.10 Research objectives

The overall aim of the research presented in this thesis is to explore the physiology of *C. autoethanogenum* during gas fermentations with CO and CO_2 as carbon sources, specifically in relation to nutrient limitation. Chapter 5 describes the effects of phosphate limitation on the product formation while chapter 6 explores the effect of carbon source availability

Availability of CO_2 and bicarbonate is an important parameter for the growth. Chapter 3 describes the discovery and characterisation of the carbonic anhydrase enzymes of *C. autoethanogenum*. Chapter 4 describes their physiological function.

I added two chapters that record more preliminary work, as record for other researchers on this topic. Chapter 7 describes the start of an exploration of the pathway for 2,3-butanediol through a mutant of alsS. Chapter 8 describes the analysis of a promoter library, results of which may be used a synthetic biology approach to engineer the *C. autoethanogenum* metabolism towards desired products.

Chapter 2:

Methods

“It's still magic even if you know how it's done.”

— Terry Pratchett, A Hat Full of Sky

2 Methods

This chapter describes the methods used in Chapters 3-6.

2.1 Software

2.1.1 Bioinformatics

2.1.1.1 Primer design and in silico cloning

For primer design, *in silico* cloning and analysing sanger sequencing results, Ugene (200) and Benchling (https://benchling.com/) were used combined with Microsoft Notepad for storing and editing Fasta files.

2.1.1.2 Phylogenetic and alignment tools

Sequences were aligned using MUSCLE (201)combined with manual editing, unless specified otherwise. Alignments were visualised using Ugene (200), Mega7.0 (202) or Jalview (203). Phylogenetic analysis was performed using Mega7.0 (202) for maximum likelihood(ML), neighbour joining (NJ) tree construction and mrBayes (204) for Bayesian trees. Optimal evolutionary model selection was performed using Mega7.0 (202) or Prottest (205). Phylogenetic trees were visualised using Figtree (206)or Mega7.0 (202).

2.1.1.3 Protein parameter prediction software

Structural protein modelling was done by Phyre2 (207, 208) and models were visualised and graphicaly edited using DeepView/Swiss-PdbViewer (209). Protparam of the ExPASy server (210) was used to calculate parameters of proteins.

2.1.1.4 DNA and Protein database searches

The protein basic local alignment search tool (BLASTP) from National Center for Biotechnology Information (NCBI) was used homologous protein sequences and nucleotide basic local alignment search tool (BLASTn) for to identify homologous DNA sequences (211–214). Standard settings were used unless otherwise stated.

2.1.2 Graphical and analytical software

2.1.2.1 Metabolomics analysis

Dionex HPLC and Trace 1310 GC data were acquired, analysed and transformed to SI units using Chromeleon software. An agilent 490 micro-GC was used to measure the inflow gasses and headspace of the bioreactors; this GC data were acquired and analysis using OpenLab EZchrom (Agilent). The transformation of peak areas to SI units was done using Microsoft Excel (Microsoft Office 2013) or Matlab (MATLAB R2016a, The MathWorks Inc., Natick, MA, 2000)

LC-MS metabolite data were analysed using Xcalibur (Thermo Fisher Scientific, Hemel Hempstead, UK). Identifications were carried out using accurate mass to 5 decimal places (error<5ppm) and confirmed further using retention time. Calibration curves were further analysed using Graphpad PRISM 7.0. Untargeted data were analysed using SimcaP multivariate analysis software using standard settings where applicable. Principal component analysis (PCA) was always performed first to determine unsupervised discrimination was possible if this was shown to be the case further analysis such as partial least squares discriminant analysis (PLS-DA) and orthogonal projections to latent structures discriminant analysis (OPLS-DA) were performed.

Targeted data analysis was further analysed MetaboAnalyst (215). As before: only if unsupervised method such as PCA showed discrimination in expected groups further analysis was performed.

2.1.3 Other software use

General data processing was performed using Excel. Graphs other than for metabolomics were produced using MS-Excel and Graphpad Prism. Statistics was performed using Graphpad Prism. Graphical editing and drawing of schemes was performed using Inktscape, Chemdraw, MS-powerpoint or MS-Word. Mendeley was used as reference manager and for generating a bibliography for this thesis.

2.2 Materials

Enzymes used for cloning and PCR were purchased from New England Biolabs (NEB, MA, USA). Chemicals were purchased from Sigma Aldrich and Fisher Scientific unless specified otherwise. Yeast extract and tryptone was acquired from Oxoid. Kits for the extraction and purification of nucleic acids were acquired from Zymo Research, Sigma Aldrich or New England Biolabs. Glasgerätebau Oschs Gmbh or Duran provided glassware and accessories for storage of media, buffers and chemicals as well for aerobic and anaerobic culturing in closed and open containers. Both a MG1000 Mark II anaerobic work station (Don Whitley Scientific Ltd) and an anaerobic chamber (Coy Laboratory Products) were used for semi open cultivation and other work requiring an anaerobic atmosphere. The atmosphere in the MG1000 was kept close to 80 % N_2, 10 % CO_2 and 10 % H_2 at 37 °C while the gas composition and temperature in the Coy anaerobic chamber was undefined but close to 85-95 % N_2, 5-10 % CO_2 and 2-4 % H_2 and 20 °C. BOC provided the gases and gas mixtures (Argon, Helium, Carbon monoxide, Carbon dioxide, Nitrogen, Hydrogen anaerobic gas mixture and calibration mixture).

2.3 Strains and growth conditions

Incubations of *C. autoethanogenum* and *E. coli* were carried out at 37 °C unless otherwise stated. Static incubations were performed in a static incubator or the anaerobic workstation. Serum bottle cultures or Erlenmeyer conical flasks agitated incubations were carried out inside New Brunswick Innova 44 shakers (Eppendorf) with agitation at 225 rpm.

2.3.1 C. autoethanogenum

C. autoethanogenum strain JA1-1 (DSM10061) was obtained from the German culture collection DSMZ. The strain was grown in liquid Yeast, Trypton, Fructose (YTF) media (Table 2-1) in the anaerobic workstation until late exponential growth phase, after which -80 °C stock were prepared by adding DMSO to a final concentration of 10%, in 2 mL polypropylene screw-cap micro-tubes (Sarstedt). Five types of media for growth of *C. autoethanogenum* were used in this study (Table 2-1). A rich YTF medium was employed for reviving -80 °C stocks and during creation of mutant strains. A MES buffered mineral medium with vitamins (PETC-MES) was used for batch growth experiments. For rich medium PETC-MES was complemented with 1% w/v yeast extract, and for semi-defined medium with 0.1% casamino acids. A mineral reactor medium with vitamins (MRMV) was used for all bioreactor experiments. Growth media were sterilised by autoclave at 121°C for 15 minutes, or by filter sterilisation using 0.2µm filters PES syringe filters (Minisart, Sartorius-Stedim) for small batch or Sartobran 300, Sartorius-Stedim for 20 l batches. After autoclaving, antibiotic, inducers, reducing agents or carbon sources were added as appropriate (Table 2-1, Table 2-3).

YTF was prepared in ambient air and incubated in anaerobic workstation for a minimum of 4 hours for agar plates or 8 h for liquid cultures, reducing agents were added prior to use. PETC-MES used in the anaerobic workstation was treated similar as YTF, PETC-MES used in closed bottle or tubes was prepared in ambient air, then brought to boil in a microwave oven and cooled on ice while sparged with N_2 gas. The medium was transferred to the Coy anaerobic chamber and then 50 mL for 200 ml serum flasks or 5 ml for Hungate tubes, was dispensed. Glassware had been incubated in the anaerobic chamber for a minimum of 10 h prior to use. Alternatively bottles and tubes were filled while being sparged with N_2 and cooled. Glassware was sealed with a butyl rubber septum (Rubber B.V., Netherlands) and Supelco 20 mm aluminium crimp cap (Sigma-Aldrich), and subsequently sterilised by autoclave. Carbon sources and reducing agents were added after autoclaving from appropriate stock solutions. Gases were added to head space through 0.2 µm sterile filters to 100-200 kPa gauge pressure using a GW6400 gas exchange (GR intruments, the Netherlands).

MRMV(216) medium was prepared using the ingredients as in Table 2-1. For filling up bioreactors, phosphoric acid (0.38mL 85% H3PO4 per L medium) was added as source of phosphorous instead of NaH_2PO_4 to prevent precipitation of minerals. Vitamins that were added after autoclaving. For media used to feed bioreactor during continuous growth, pH of the final medium was titrated to 3.6 with 3 M NaOH before filter sterilisation into autoclaved 20 L glass bottles. The media was sparged with N_2 at least 2 days prior to starting of media addition and sparging continued to maintain anaerobic condition.

2.3.2 Strains of E.coli

E. coli strains were available in the culture collection on our research group or were acquired from Novagen, NEB, or the Coli Genetic Stock Center (CGSC) of Yale University. All *E. coli* were grown on LB (Table 2-1) medium with appropriate antibiotic or inducers (Table 2-3). *E. coli* -80 °C stocks were prepared in 2 ml Microbank™ vials with beads.

Table 2-1 Ingredients of growth media.

Ingredients	YTF(170)		PETC-MES(87)		MRMV(216)		LB(217)	
Undefined nutrients	g l^{-1}	Mol l^{-1}	g l^{-1}	Mol l^{-1}	g l^{-1}	Mol l^{-1}	g l^{-1}	Mol l^{-1}
Yeast extract (YE)	10	NC	(10)[a]	NC	(1)[g]		5	NC
Tryptone	16	NC					10	NC
Casamino acids			(1)[a]	NC				
Macronutrients								
NH_4Cl			1	$1.87*10^{-2}$	1	$1.87*10^{-2}$		
NaCl	$2.00*10^{-1}$	$3.42*10^{-3}$	$8.00*10^{-1}$	$1.37*10^{-2}$			10	$1.71*10^{-1}$
KCl			$1.00*10^{-1}$	$1.34*10^{-3}$	$1.50*10^{-1}$	$2.01*10^{-3}$		
$MgCl_2.6H_2O$					$5.00*10^{-1}$	$2.46*10^{-3}$		
$MgSO_4.7H_2O$			$2.00*10^{-1}$	$8.11*10^{-4}$				
$CaCl_2$			$2.00*10^{-2}$	$1.80*10^{-4}$	$3.70*10^{-1}$	$3.33*10^{-3}$		
KH_2PO_4			$2.00*10^{-1}$(b)	$1.47*10^{-3}$				
$NaH_2PO_4.2H_2O$					$8.66*10^{-1}$(b)	$5.55*10^{-3}$		
Micronutrients								
$Fe(SO_4)_2(NH_4)_2.6H_2O$			$5.80*10^{-2}$	$1.48*10^{-4}$				
$FeCl_2.4H_2O$	$7.80*10^{-4}$	$3.92*10^{-6}$			$1.94*10^{-2}$	$9.73*10^{-5}$		
$MnCl_2.4H_2O$	$2.30*10^{-4}$	$1.16*10^{-6}$			$3.96*10^{-4}$	$2.00*10^{-6}$		
$MnSO_4.H_2O$			$1.00*10^{-3}$	$5.92*10^{-6}$				
H_3BO_3	$1.00*10^{-4}$	$1.62*10^{-6}$			$1.24*10^{-4}$	$2.01*10^{-6}$		
$CoCl_2.6H2O$	$1.03*10^{-4}$	$4.33*10^{-7}$	$2.00*10^{-4}$	$8.41*10^{-7}$	$4.76*10^{-4}$	$2.00*10^{-6}$		
$NiCl_2.6H_2O$	$6.02*10^{-4}$	$2.53*10^{-6}$	$2.00*10^{-5}$	$8.41*10^{-8}$	$1.19*10^{-3}$	$5.01*10^{-6}$		
$ZnCl_2$	$7.80*10^{-5}$	$5.72*10^{-7}$			$6.90*10^{-4}$	$5.06*10^{-6}$		
$ZnSO_4.7H_2O$			$2.00*10^{-4}$	$6.96*10^{-7}$				
$CuSO_4.5H_2O$	$5.00*10^{-5}$	$2.00*10^{-7}$						
$CuCl_2.2H_2O$			$2.00*10^{-5}$	$1.17*10^{-7}$				
$AlK(SO_4)_2.12H_2O$	$5.00*10^{-5}$	$1.05*10^{-7}$						
Na_2SeO_3	$5.80*10^{-5}$	$3.35*10^{-7}$	$2.00*10^{-5}$	$1.16*10^{-7}$	$3.46*10^{-4}$	$2.00*10^{-6}$		
Na_2WO_4	$5.30*10^{-5}$	$1.80*10^{-7}$	$2.00*10^{-5}$	$6.81*10^{-8}$	$4.78*10^{-4}$	$1.63*10^{-6}$		
$Na_2MoO_4.2H_2O$	$5.20*10^{-5}$	$2.15*10^{-7}$	$2.00*10^{-5}$	$8.27*10^{-8}$	$4.84*10^{-4}$	$2.00*10^{-6}$		
Vitamins								
p-Aminobenzoate	$5.70*10^{-5}$	$4.16*10^{-7}$	$5.00*10^{-5}$	$3.65*10^{-7}$	$5.00*10^{-4}$	$3.65*10^{-6}$		
riboflavin	$5.20*10^{-5}$	$1.38*10^{-7}$	$5.00*10^{-5}$	$1.33*10^{-7}$	$5.00*10^{-4}$	$1.33*10^{-6}$		
Thiamine	$1.00*10^{-5}$	$3.77*10^{-8}$	$5.00*10^{-5}$	$1.88*10^{-7}$	$5.00*10^{-4}$	$1.88*10^{-6}$		
Nicotinic acid	$1.03*10^{-5}$	$8.37*10^{-8}$	$5.00*10^{-5}$	$4.06*10^{-7}$	$5.00*10^{-4}$	$4.06*10^{-6}$		
Pyridoxine	$2.55*10^{-5}$	$1.51*10^{-7}$	$1.00*10^{-4}$	$5.91*10^{-7}$	$1.00*10^{-4}$	$5.91*10^{-7}$		
Ca-pantothenate	$5.20*10^{-5}$	$1.09*10^{-7}$	$5.00*10^{-5}$	$1.05*10^{-7}$	$5.00*10^{-5}$	$1.05*10^{-6}$		
Cyanocobalamin	$3.90*10^{-5}$	$2.88*10^{-8}$	$1.00*10^{-6}$	$7.38*10^{-10}$	$1.00*10^{-6}$	$3.69*10^{-7}$		
Biotin	$1.10*10^{-5}$	$4.50*10^{-8}$	$2.00*10^{-5}$	$8.19*10^{-8}$	$2.00*10^{-5}$	$8.19*10^{-7}$		
Folate	$2.40*10^{-5}$	$5.44*10^{-8}$	$2.00*10^{-5}$	$4.53*10^{-8}$	$2.00*10^{-5}$	$4.53*10^{-7}$		
Thioctic acid	$2.50*10^{-5}$	$1.21*10^{-7}$	$5.00*10^{-5}$	$2.42*10^{-7}$	$5.00*10^{-5}$	$2.42*10^{-6}$		
Carbon sources								
Sodium pyruvate			(7.21)[c]	$6.55*10^{-2}$	(5)[g]	$4.5*10^{-2}$		
Xylose			(7.21)[c]	$4.80*10^{-2}$				
Fructose	10	$5.55*10^{-2}$	(7.21)[c]	$4.00*10^{-2}$				
Rhamnose			(7.21)[c]	$4.39*10^{-2}$				
Acetate			(8.2)[c]	$1*10^{-1}$	(8.2)[g]	$1*10^{-1}$		
Sodium formate					(5)[g]	$7.3*10^{-2}$		
Carbon monoxide			(6.9)[c]	$4.48*10^{-1}$	[d]			
Carbon dioxide			(1.44)[c]	$3.28*10^{-2}$	[d]			
Buffers and chelators								
Nitrilotriacetic acid (NTA)			$5.80*10^{-2}$	$3.03*10^{-4}$				
2-(N-morpholino)-ethanesulfonic acid (MES)			20	$1.02*10^{-1}$				
Reducing / Sulphur sources [e]								
Cystein.HCl	$4.00*10^{-2}$	$2.54*10^{-4}$	($4.00*10^{-2}$)	$2.54*10^{-4}$	($4.00*10^{-2}$)[g]	$2.54*10^{-4}$		
Na2S·9H2O			($1.20*10^{-2}$)	$5.00*10^{-5}$	$5*10^{-1}$(f)	$2.08*10^{-4}$		
Ti-NTA reducing agent	(10 ml l^{-1})		(10 ml l^{-1})					
Hydrogen (headspace)			($6*10^{-1}$)	$6*10^{-1}$				
Redox indicator								
Resazurin	$5.00*10^{-4}$	$2.18*10^{-6}$	$5.00*10^{-4}$	$2.18*10^{-6}$	$5.00*10^{-4}$	$2.18*10^{-6}$		
Solidifying agent								
Agar	15		15				15	

Footnote Table 2-1 tableAll ingredients are given in g l^{-1} & Mol l^{-1} for ease of comparison. Micronutrients and Vitamins were added from 100x or 500x concentrated stocks except for Fe(SO4)2(NH4)2.6H2O in PETC-MES of which 5.0 *10-2 was added as macro nutrient and 0.80*10-2 as micronutrient. Ingredients between brackets were optional. [a]=YE only added for rich and Casamino acids only to semi defined PETC-MES . [b]= Phosphate source concentration of standard medium. For phosphate limitation studies concentrations are as discussed in chapter 3. The MRMV for the bioreactor prior to autoclaving contains phosphoric acid (0.38 mL 85% H_3PO_4 (L medium)$^{-1}$) to avert precipitation of phosphates. [c] = A carbon source must be selected. Most used concentration is given. Carbon monoxide, carbon dioxide & hydrogen were added in headspace. [d]= gasses supplied to bioreactors at flow rates standard at 15 ml min^{-1} but varied as described in chapter 3. [e]= At least one sulphur source (cystein or sodium sulphide) was added and optional extra reducing agents was

added if necessary, hydrogen only added to this level for growth with carbon dioxide. [f] = Sodium sulphide concentration is estimation based on dilution rate and consumption in bioreactors. [g]= only added during start up phase or crash recovery

Table 2-2 Ti-NTA reducing agent composition. Produced with anaerobic distilled water.

Ti-NTA reducing agent	Concentration ($g\ l^{-1}$)
NTA (Nitrilotriacetic acid)	76.4
Na_2CO_3	53.3
$TiCl_3$	62.7 mM

Table 2-3. Selective and inductive supplements

Supplement / antibiotic	Stock		Solvent	Concentration for *E. coli*		Concentration for *C. autoethanognum*	
	$g\ l^{-1}$	$Mol\ l^{-1}$	$Mol\ l^{-1}$	$\mu g\ mL^{-1}$	mM	$\mu g\ mL^{-1}$	mM
Ampicillin(Amp)	50	$1.4*10^{-1}$	Water	100	$2.8*10^{-1}$		
Chloramphenicol (Cm)	25	$7.7*10^{-2}$	Ethanol	25	$7.7*10^{-2}$		
Erythromycin (Em)	50	$6.8*10^{-1}$	Ethanol	500	$6.8*10^{-1}$		
Trimethoprim(Tmp)	10	$3.4*10^{-2}$	DMSO	10	$3.4*10^{-2}$		
Spectinomycin (Spt)	10	$3.0*10^{-1}$	Water	250	$7.5*10^{-1}$		
Kanamycin (Kan)	50	$1.0*10^{-1}$	Water	50	$1.0*10^{-1}$		
Thiamphenicol (Tm)	15	$4.2*10^{-2}$	DMSO			15	$4.2*10^{-2}$
Clarithromycin (Cla)	6	$8.0*10^{-3}$	DMSO			6	$8.0*10^{-3}$
D-cycloserine(Dcs)	50	$4.9*10^{-1}$	Water	250		4	$4.9*10^{-1}$
Tetracycline(Tet)	5	$1.1*10^{-2}$	0.7 Ethanol	10	$2.2*10^{-2}$	10	$2.2*10^{-2}$
5-Fluoroorotic acid (FOA)	15	$8.6*10^{-2}$	DMSO			1500	$8.6*10^{-1}$
Uracil	1	$8.9*10^{-3}$	Water			20	$8.9*10^{-3}$
Sodium azide (NaN_3)	6.5	$1*10^{-1}$	Water	6.5	$1*10^{-4}$		
IPTG	238	1	Water	238	1		

Table 2-4 Strains used in this study.

Strain name *Clostridium* strains	Description	Created by / obtained from
C. autoethanogenum JAl-1 DSM 10061	Wild type	Abrini *et al.*(13) / DSMZ
C. ljungdahlii DSM 13528	Wild type	Tanner *et al.*(218)/DSMZ
C. autoethanogenum ΔPyrE	*ΔPyrE strain*	This thesis/ Ronja Breitkopf / SBRC
C. autoethanogenum bCA::CT	bCA::CT strain	This thesis
C. autoethanogenum gCA::CT	gCA::CT strain	This thesis
C. autoethanogenum ΔAlss	ΔAlsS	This thesis
C. autoethanogenum pMTL82252-bCA	bCA overexpression	This thesis
C. autoethanogenum promoter library strains 12x	12 different strains, each containing plasmids with a promoter driving a *catP* gene.	This thesis
C. ljungdahlii DSM 13528 promoter library strains 12x	12 different strains, each containing plasmids with a promoter driving a *catP* gene.	This thesis
Escherichia coli strains		
E. coli DH5α	Cloning strain. *fhuA2Δ(argF-lacZ)U169 phoA glnV44 Φ80Δ (lacZ)M15 gyrA96 recA1 relA1 endA1 thi-1 hsdR17*	D. Hanahan *et al.* (219) / NEB (Ipswich, MA, USA)
E. coli TOP10	Cloning strain. F- mcrA Δ(mrr-hsdRMS-mcrBC) φ80lacZΔM15 ΔlacX74 deoR recA1 araD139 Δ(ara-leu)7697 galU galK rpsL(StrR) endA1 nupG	Invitrogen Ltd
E. coli XL1-Blue MRF` Kan	Cloning strain. Δ(mcrA)183 Δ(mcrCB-hsdSMR-mrr)173 endA1 supE44 thi-1 recA1 gyrA96 relA1 lac [F'proAB lacIqZΔM15 Tn10 (TetR)]	Stratagene
E. coli CA434 (HB101 + plasmid R702)	Conjugation strain. thi-I hsdS20 (rБ, mБ) supE44 recAB ara-14 leuB5proA2 lacYl galKI rpsL20 (StrR) xyl-5 mt1-1	M. Young, UCW, Aberystwyth, UK/ CRG Culture collection (180)
E. coli BL21(DE3) pLysS	Expression strain. F- ompT hsdSB (rB-mB-) gal dcm (DE3) pLysS (CamR)	Novagen (Madison, WI, USA)
NEB express	Expression strain. fhuA2 [lon] ompT gal sulA11 R(mcr-73::miniTn10--TetS)2 [dcm] R(zgb-210::Tn10--TetS) endA1 Δ(mcrC-mrr)114::IS10	NEB
NEBexpress R702 (sexpress)	Conjugation strain, as *NEB express* plus plasmid R702	Craig Woods
E. coli BL21(DE3) pLysS-pET16b-bCA	Caut-bCA expression strain	This thesis
E. coli BL21(DE3) pLysS-pET16b-gCA	Caut-gCA expression strain	This thesis
E. coli EDCM636	*ΔcanA1::FLK2(lacZ,kan)*, *λ⁻*, *Δfnr-267*, *rph-1. R*equires high CO_2 or sodium azide addition for growth	Merlin et al.(220)/ CGSC (New Haven, CT, USA)
E. coli EDCM636-pMTL82252-bCA	CAN<FLK> mutant complemented with *pMTL82252-bCA not need* sodium azide	This thesis
E. coli EDCM636 pMTL82252-bCAStrepC	CAN<FLK> mutant complemented with *pMTL82252-bCAStrepC not need* sodium azide	This thesis
E. coli EDCM636 pMTL82252-gCA	CAN<FLK> mutant with *pMTL82252-gCA* needs high CO2 or sodium azide addition for growth	This thesis
E. coli EDCM636 pMTL82252-gCAstrepC	CAN<FLK> mutant with *pMTL82252-gCAStrepC* needs high CO2 or sodium azide addition	This thesis

Footnote Table 2-4 this list only contains strains that are characterised or used as a tool. Intermediate strains such as all the conjugative donor strains with transferable plasmids or cloning strains containing plasmids are not listed.

2.3.3 Growth conditions

2.3.3.1 Bioreactor setup

The bioreactor culture volume was 1.5L culture in a 3 L total volume jacketed continuously stirred tank reactor. The reactor was fitted with Bioflo115 baffles, Rushton impellers at a setting adapted from (221), and an open-pipe sparger made by removing the head from a standard BioFlo115 micro-sparger. Gas flow was controlled using Smartrak thermal mass flow controllers (SmartTrak C100, Sierra Instruments) except for the pilot phosphate limitation when El-Flow thermal mass flow controlers were used (Bronkhorst Ruurlo, The Netherlands). Bioreactor cultures were controlled using a New Brunswick Scientific BioFlo 115 bioreactor system (Eppendorf) and BioCommand Batch Control software (Eppendorf). A BioFlo115 headplate with 13 ports fitted with harvest tube, non-standard low dead-volume sample port, sample port, thermowell, non-standard septum (Z164437, Sigma) fitted to a 12mm compression port, tri-port, plugged, level tube, exhaust condenser, sparger, ORP probe (Pt4805-DPAS, Mettler Toledo), pH probe (405-DPAS, Mettler Toledo), and growth medium addition tube. A peristaltic pump (Masterflex L/S precision, Cole-Parmer) fitted with two pump-heads and Marprene pump tubing (Watson-Marlow) was used to add growth medium to the culture at a constant rate and remove excess liquid (waste) from the culture using a larger bore tubing. The pilot phosphate limitation reactor used additional Waston Marlow pumps for pH control (controlled using an analogue input/output module (Eppendorf) with the BioCommand software to control pH), media supply at a constant rate, and excess culture removal pump set to a volumetric rate at least two times the media supply rate. Sodium hydroxide, sodium sulphide and antifoam were added to the medium through the tri-port with system pumps. Sodium hydroxide was added as pH control while sodium sulphide and antifoam were added at constant rate. If acidic control was needed (during unstable growth situations), acetic acid or hydrochloric acid was added using a hypodermic needle through the septum using the peristaltic pump on the controler. The signal from the ORP probe was recorded through a separate analytical transmitter (M300, Mettler-Toledo) that was connected through an analogue input/output module (Eppendorf) with the BioCommand software. Exhaust gas was cooled through a 10 °C condenser bubbled through a 70 - 80 cm water column to generate backpressure which facilitated exhaust gases to a gas chromatograph.

Figure 2-1.Set up of pilot phosphate limitation bioreactor.
From left to right: waste receptacle, pumps, in front of the pump the NaOH bottle, bioreactor, BioFlo contoler. Close up on the right shows pump set up.

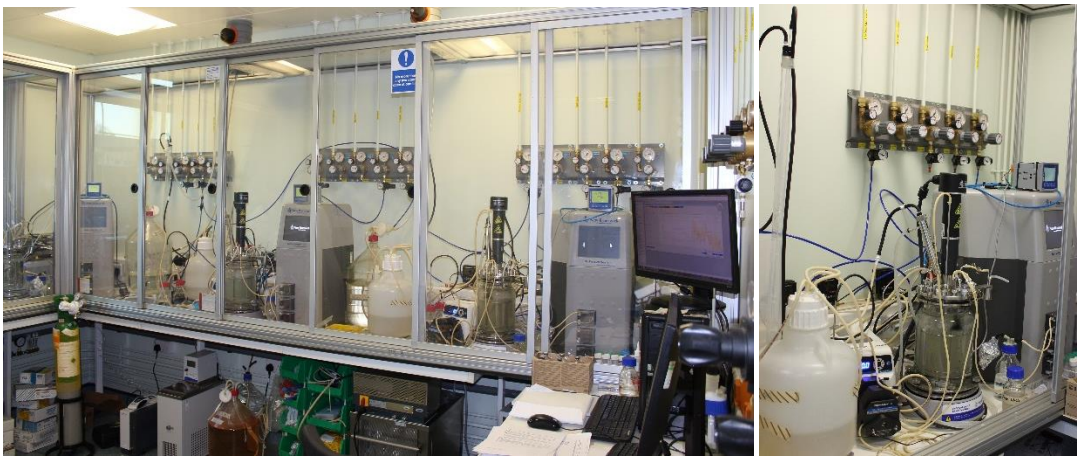

Figure 2-2. Picture of the Bioreactor room.
Room where the experimental reactors were run on left picture, right reactor set up detail. Picture by Anne M. Henstra.

2.3.3.2 Bioreactor growth

Prior to inoculation of the bioreactors the media in the sterile bioreactor was made fully anaerobic trough continuous sparging with N_2. The pH was set to 5. To ease the start-up of the culture, sodium acetate, cysteine and yeast extract were added from stock solutions. Growth was started off with 20 ml min^{-1} carbon monoxide flow but with low agitation rates (200 RPM). When significant growth and rise in pH was detected agitation was slowly raised in a step wise fashion to the normal running agitation of 600 RPM. The carbon monoxide flow rate was then lowered to 15 ml min^{-1} unless otherwise specified in chapters 3 and 5.

2.3.3.3 Bioreactor sampling

5-15 ml samples were taken at least once a day during periods of interest. Before samples were taken, a volume of 3-5 ml culture was wasted to flush the dead space in the tubing. 1 ml of sample was dispensed in 1.5 ml Eppendorf tubes in triplicate. The tubes were centrifuged at maximum *g* at 4°C in a small benchtop centrifuge for 5 minutes and supernatant and cell pellet were separated and stored at -20°C. For LC-MS analysis, samples of 1.5 ml volume were treated in the same way except cell pellets and supernatant were flash frozen in liquid nitrogen.

Optical densities of samples were measured using a Jenway 7300 Spectrophotometer (Bibby Scientific Ltd). For samples above OD_{600} value of 0.8, samples were diluted 10-fold. Biomass was calculated by conversion factor of 0.34 $g_{(cell\ dry\ weight)}\ l^{-1}\ OD_{600}^{-1}$. This conversion factor was calculated by Thomas Millat from measurements performed by Anne M. Henstra and is comparable to published conversion factors of *C. autoethanogenum* and *C. ljungdahlii* (70, 137, 222). The approximation of the elemental composition of biomass (dry weight) of *C. autoethanogenum* generally used for elemental balancing in our project is $C_4H_8O_2N$ which is similar to approximations published for other organisms (223–225). Samples were regularly evaluated via microscopy to assess contamination and cell health.

2.3.3.4 Batch growth and sampling

Unless otherwise stated, *C. autoethanogenum* wild-type (WT) and mutant strains were cultivated in triplicates on minimal PETC-MES. Pre-cultures were grown inside anaerobic workstation and active growing culture was washed with PETC-MES without carbon sources and bottles were inoculated to a start OD_{600} of 0.05. When grown on carbon monoxide, initial incubation was static and only when growth was clearly observed the bottles were transferred to shaking incubator. 1-2 mL of liquid samples were harvested at several time points by hypodermic needle and syringe, samples were treated similar as bioreactor samples above except that pH was regularly measured in supernatants previous to -20°C storage. Headspace pressure was measured using a Digital Pressure Gauge DPG120 (Omega Engineering, Inc.). To confirm absence of contaminations, regular microscopy and PCR with strain specific primers was performed at end points.

2.4 Genomic tools

To analyse and produce genetically modified clostridium strains, molecular genetic tools such as polymerase chain reaction, DNA purification, restriction digest, ligations, were used as detailed below.

2.4.1 PCR

Polymerase chain reaction (PCR) (226, 227) was used to specifically amplify and modify DNA. For reactions that required high fidelity, the Q5-polymerase master mix (NEB) was used which contained standard buffer and nucleotides, while for reactions that required lower fidelity OneTaq quick load standard buffer mix (NEB) was used. PCR reactions were performed in T3000 Thermocycler (Biometra) or SensoQuest Gradient Labcycler (Geneflow Ltd) according to the manufacturors instructions. All oligonucleotides primers were obtained from Sigma-Aldrich.

To join the homology arms of in-frame deletion vectors (Splicing by) Overlap Extension (SOE) PCR was performed (228, 229) or NEB HiFi assembly was used.

Table 2-5 Primers used in this study

Primer name	Sequence (5'-3')	Use / template	Design
EBSuniversal	CGAAATTAGAAACTTGCGTTCAGTAAAC	Clostron screening	(182)
FPCA1	GTTGTCCATATGATAAGAAAATTTGAACAACATTACATACCAG	Caut-γCA gene	This study
RPCA1	GTTGTTGGATCCCTAATATTCACTATAATTTTTAGCCC	Caut-γCA gene	This study
BCAECPF	GTTGTCCATATGTTGAACAGTGATTTTGCTGTATTG	Caut-βCA gene	This study
BCAECPR	GTTGTTGGATCCCTAAAGTTTTTCCACTTCG	Caut-βCA gene	This study
alsS F1	ATATATCCGCGGGATAATATACTAAAAAAAACTGC	alsS flanking region	This study
alsS R1	TTTACATATTATTCATAATTTTAATTAAATAATTTCAG	alsS flanking region	This study
alsS F2	AATTATGAATAATATGTAAAGTGGAGGAATAAAATG	alsS flanking region	This study
alsS R2	ATATATGGCGCGCCGCAAGTAAAAATTTATCAACAAGG	alsS flanking region	This study
Bart_PPfwd	GAGCTGGTGAAGTACATCACC	pMTL8xx5x module	This study
Bart_PPrev	CTGCGTGATGAACTTGAATTGC	pMTL8x1xx module	This study
JWC_pET16b_F	GATCCCGCGAAATTAATACGA	pET16b MCS flanking	Jon Baker
JWC_pET16b_R	GCTTATCATCGATAAGCTTT	pET16b MCS flanking	Jon Baker
M13F	TGTAAAACGACGGCCAGT	M13 sites in plasmids	unknown
M13R	AGCGGATAACAATTTCACACAGGA	M13 sites in plasmids	unknown
ACE pyrE FSP	GAGCTTATGCAATTCAAGTAGGTACTGCAAAC	pyrE flanking region	C.M. Humphreys
ACE pyrE RSP	CATCAAAGCTATACTATTTTCCGTATTTACATTTGGG	pyrE flanking region	C.M. Humphreys
F1gCAifd	tataccgcggGTA ATT TCC CTG TTT AGC ACC AC	Caut-γCA flanking	This study
R1gCAifd	TCTAATATTCTATCATATAATTTACTCTCCTTAAGAATTTA	Caut-γCA flanking	This study
F2gCAifd	TTATATGATAGAATATTAGAAAACAATACATTAATCACAT	Caut-γCA flanking	This study
R2gCAifd	tataggcgcgccCCATCTGGATTTACCATTGGAAC	Caut-γCA flanking	This study
bCAF1	tataccgcggCTT GAA TAG CCT TAG TAT ACT TAT AAG	Caut-βCA flanking	This study
bCAR1	CCTAAAGTTTGTTCAAAGCAATCCACCCCTTA	Caut-βCA flanking	This study
bCAF2	TGCTTTGAACAAACTTTAGGTATTTATCATTTACATTTAAG	Caut-βCA flanking	This study
bCAR2	tataggcgcgccCAGTTTTACTTGCAAAATCTCTGC	Caut-βCA flanking	This study
FgCALHA	GCA AGC AGA AGC CTG AGT C	Caut-γCA flanking	This study
RgCARHA	CCA CCT TAT AAG TTC ATT ATA AAA CG	Caut-γCA flanking	This study
FbCALHA	GGA GAA ATA TAA GCA AGG TAT AGG	Caut-βCA flanking	This study
RgCARHA	CAA TTT ACT TCC ATA ATT ACT CCA G	Caut-βCA flanking	This study
FpMTL8xx5x	GAA GTA CAT CAC CGA CGA GC	pMTL8xx5x module	This study
RpMTL84xxx	CTT TTT GAC TTT AAG CCT ACG AAT AC	pMTL84xxx module	This study
Fpet16Hisinsertc	TAATAAGAGCTCACCATGGGCCATC	pET16b MCS+his flank	This study
Rpet16Hisinsert	CTTTGTTAGCAGCCGGATCCTC	pET16b MCS+his flank	This study
Fpet16his2	TATAGAGCTCCCATGGGCCATCATCATC	pET16b MCS+his flank	This study
Rpet16his2	GCTTTGTTAGCAGCCGGATC	pET16b MCS+his flank	This study
Univ-0027-F	GCGAGAGTTTGATCCTGGCTCAG	16s rRNA coding gene	Universal
Univ- 1492 -R	CGCGGTTACCTTGTTACGACTT	16s rRNA coding gene	Universal

2.4.2 DNA isolation

DNA isolations, both genomic and plasmid DNA, were performed with previously described kits according to supplied instructions from overnight *E. coli* or 2-5 day old *C. autoethanogenum* culture. For the latter samples, 20 mg mL^{-1} of chicken lysozyme pre-treatment was employed with incubation at 37°C for 30 min followed by the lysis and purification steps.

For high DNA yields phenol-chloroform extractions were used. Here 1-2 ml culture was harvested using centrifugation at max speed on a bench top centrifuge. Resulting cell pellet was resuspended in 180 µl phosphate buffered saline solution(PBS) with 20 mg ml^{-1} of chicken lysozyme and 4µl RNase and incubated at 37°C for 30 min. 25 µl proteinase K solution, 85 µl ddH_2O and 110 µl 10% w/v SDS was added and incubated at 65°C for 30 min with gentle agitation. 400 µl phenol/chloroform/Isoamyl Alcohol (pH 8) was added, mixed, transferred to tubes containing Phase Lock Gel™ (Quantabio) and centrifuged for 3 minutes at max speed. This phenol/chlorophorm/isoamyl alcohol step was repeated two times after which DNA in aqueous phase was precipitated by ethanol precipitation and resulting DNA was washed twice using 70% ethanol.

2.4.3 Restriction Digests

Restriction digests for diagnostic or cloning purposes were performed according to NEB supplied instructions although incubation times were frequently up to twice longer than prescribed.

2.4.4 Electrophoresis and quantification of DNA

DNA electrophoresis was performed on 0.8 – 1% w/v agarose in TAE buffer (40 mM Tris, 1mM EDTA, 0.1% Glacial acetic acid). To visualise DNA SYBR Safe (Life Technologies) was added to the liquid agarose. If small size bands were poorly visible post staining with SYBR safe in TAE was performed for 2 h. NEB loading buffers (6X concentration) were used for all DNA sample except for the PCRs performed with OneTaq quick load. Electrophoresis was performed 80 – 120 V for 30-90 min in TAE buffer. DNA was subsequently visualized in Odyssey Fc Imager (LI-COR, Inc.). Further DNA quantification was performed using Nanodrop ND1000 (Thermo Scientific).

2.4.5 Dephosphorylation and Ligation of DNA Fragments

If self-ligation problems of restriction digested vectors were likely (compatible sticky ends), Antarctic Phosphatise (NEB) treatment was performed. T4 DNA ligase (NEB) was used to ligate purified and linearised DNA fragments. Ligation reactions were incubated on melting ice overnight.

Table 2-6 Plasmids used in this study

Plasmid name	Features of interest	Use/description	Marker	Carriers	Made by
pMTL-AMH101	*pMTL84151 + C. Acetobutylicum* PyrE gene / *C.autoethanogenum* homology arms of pyrE flanking region	Deleting *pyrE*	Cm/Tm	Top10, CA434, *C. autoethanogenum*	A. M. Henstra
pMTL-CH20	*pMTL84151 + pyrE repair homology*	Repairing *pyrE*	Cm/Tm	Top10, Sexpress, *C. autoethanogenum ΔpyrE*	C. M. Humphreys
pMTL-BPdelbCA	*pMTL84151 + C. Acetobutylicum* PyrE gene / *C.autoethanogenum* βCA flanking homology arms.	Deleting bCA	Cm/Tm	Top10, CA434, Sexpress, *C. autoethanogenum ΔpyrE*	This thesis
pMTL-BPdelgCA	*pMTL84151 + C. Acetobutylicum* PyrE gene / *C.autoethanogenum* γCA flanking homology arms	Deleting gCA	Cm/Tm	Top10, CA434, Sexpress, *C. autoethanogenum ΔpyrE*	This thesis
pET16b	P*lac1,* 10xHis tag	IPTG induced expression, His tagged	Amp	Top10	Novagen
pET16b-CAETHG_2776	N-terminal HIS-tag sequence to inserted gene	Overexpression *gCA* CAETHG_2776 in *E.coli*	Amp	Xl1-Blue, Bl21(DE3)pLysS	This thesis
pET16b-CAETHG_3103	N-terminal HIS-tag sequence to inserted gene	Overexpression of *bCA* CAETHG_3103 in *E.coli*	Amp	DH5α, Bl21(DE3)pLysS, NEBexpress	This thesis
pET16b-CpfrbetaCA	N-terminal HIS-tag sequence to inserted gene	Overexpression of the synthetic CpfrbetaCA in *E.coli*	Amp	Top10 Bl21(DE3)pLysS,	This thesis
pET16b-mtcamh	N-terminal HIS-tag sequence to inserted gene	Overexpression of the synthetic mtcamH in E.coli	Amp	Top10, Bl21(DE3)pLysS,	This thesis
pMTL007C-E2-CTgCA79s	ClosTron	Disrupt CAETHG_2776 at 79 bp after start codon	Cm/Tm	Top10, CA434, *C. autoethanogenum*	This thesis
pMTL007C-E2-CTgCA331s	ClosTron	Disrupt CAETHG_2776 at 331 bp after start codon	Cm/Tm	Top10, CA434, Sexpress, C. autoethanogenum	This thesis
pMTL007C-E2-CTbCA30s	ClosTron	Disrupt CAETHG_3103 at 30 bp after start codon	Cm/Tm	Top10, CA434, Sexpress, C. autoethanogenum	This thesis
pMTL84422	Pthl+MCS	To produce pMTL82252	Tet	Top10	(181)
pMTL82251	pBP1, ErmB, ColE1+TraJ	To produce pMTL82252/ negative control	Em/Cla	Top10	(181)
pMTL82252	pBP1, ErmB, ColE1+TraJ, Pthl+MCS	Overexpression in Clostridia and *E.coli*	Em/Cla	DH5α, *EDCM636, C. autoethanogenum*	This thesis
pMTL82252-bCA	Caut- bCA	Overexpression of the Caut-bCA in *E. coli* and Clostridia	Em/Cla	DH5α , *EDCM636, C. autoethanogenum*	This thesis

pMTL82252-bCAstrepC	Caut- bCAstrepC	Overexpression of the Caut-bCA-Streptag C-terminal in *E. coli* and Clostridia	Em/Cla	DH5α , *EDCM636,*	This thesis
pMTL82252-bCAStrepN	Caut- bCAStrepN	Overexpression of the Caut-bCA-Streptag N-terminal in *E. coli* and Clostridia	Em/Cla	DH5α , *EDCM636*	This thesis
pMTL82252-bCAHisC	Caut- bCAHisC	Overexpression of the Caut-bCA-His tag C-terminal in *E. coli* and Clostridia	Em/Cla	DH5α , *EDCM636*	This thesis
pMTL82252-gCA	Caut- gCA	Overexpression of the Caut-gCA in *E. coli* and Clostridia	Em/Cla	DH5α , *EDCM636*	This thesis
pMTL82252-*gCAstrepC*	Caut- *gCAstrepC*	Overexpression of the Caut-gCA-Strep tag C-terminal in *E. coli* and Clostridia	Em/Cla	DH5α , *EDCM636*	This thesis
pMTL82252-gCAStrepN	Caut- gCAStrepN	Overexpression of the Caut-bCA-Streptag N-terminal in *E. coli* and Clostridia	Em/Cla	DH5α , *EDCM636*	This thesis
pMTL82252-gCAHisC	Caut- gCAHisC	Overexpression of the Caut-bCA-His tag C-terminal in *E. coli* and Clostridia	Em/Cla	DH5α , *EDCM636*	This thesis
pMTL82251_Csp_fdx-catP	PCsp_fdx-catP	Test ferredoxin promoter from C. sporogenes/ biological positive control	Em/Cla	CA434, *C. ljungdahlii, C. autoethanogenum*	Kovács, Wilson, Mansfield
pMTL82251-Cac_thl-catP	PCac_thl-catP	Test thiolase promoter from C.acetobutylicum / biological positive control	Em/Cla	CA434, *C. ljungdahlii, C. autoethanogenum*	Kovács, Wilson, Mansfield
pMTL82254_catP	Promoterless catP	Biological negative control in the promoter study.	Em/Cla	CA434, *C. ljungdahlii, C. autoethanogenum*	(181)
pMTL8225x_TT_Cbe_fdx_CAChlRBS_catP	PCbe_fdx-catP	Test ferredoxin promoter from Clostridium beijerinckii	Em/Cla	CA434, *C. ljungdahlii, C. autoethanogenum*	Kovács, Wilson, Mansfield
pMTL8225x_TT_Cte_fdx_CAChlRBS_catP	P Cte_fdx-catP	Test ferredoxin promoter from *Clostridium thermocellum*	Em/Cla	CA434, *C. ljungdahlii, C. autoethanogenum*	Kovács, Wilson, Mansfield
pMTL8225x_TT_Sac_fdx_CAChlRBS_catP	PSac_fdx-catP	Test ferredoxin promoter *Clostridium thermocellum*	Em/Cla	CA434, *C. ljungdahlii, C. autoethanogenum*	Kovács, Wilson, Mansfield
pMTL8225x_TT_Clk_fdx_CAChlRBS_catP	PClk_fdx-catP	Test ferredoxin promoter from *Clostridium kluyveri*	Em/Cla	CA434, *C. ljungdahlii, C. autoethanogenum*	Kovács, Wilson, Mansfield

pMTL8225x_TT_Cpf_fdx_CAChlRBS_catP	PCpf_fdx-catP	Test ferredoxin promoter from Clostridium perfringens	Em/Cla	CA434, *C. ljungdahlii, C. autoethanogenum*	Kovács, Wilson, Mansfield
pMTL8225x_TT_Cbe_thl_CAChlRBS_catP	PCbe_thl-catP	Test thiolase promoter from C. beijerinckii	Em/Cla	CA434, *C. ljungdahlii, C. autoethanogenum*	Kovács, Wilson, Mansfield
pMTL8225x_TT_Cpf_thl_CAChlRBS_catP	PCpf_thl-catP	Test thiolase promoter from *C. perfringens*	Em/Cla	CA434, *C. ljungdahlii, C. autoethanogenum*	Kovács, Wilson, Mansfield
pMTL8225x_TT_Ccv_thl_CAChlRBS_catP	PCcv_thl-catP	Test thiolase promoter from *Clostridium cellulovorans*	Em/Cla	CA434, *C. ljungdahlii, C. autoethanogenum*	Kovács, Wilson, Mansfield
pMTL8225x_TT_Cby_thl_CAChlRBS_catP	PCby_thl-catP	Test thiolase promoter from *Clostridium butyricum*	Em/Cla	CA434, *C. ljungdahlii, C. autoethanogenum*	Kovács, Wilson, Mansfield

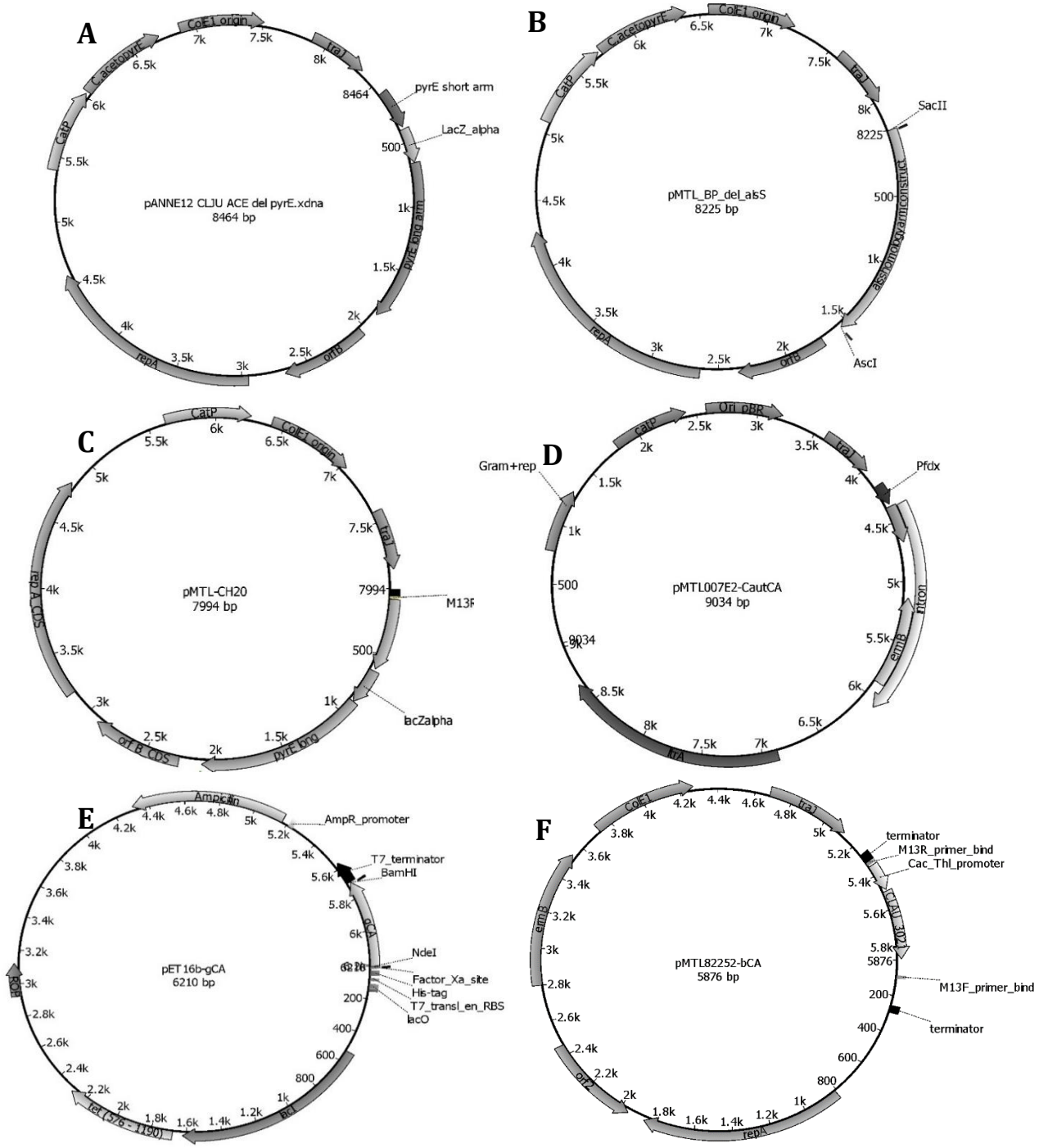

Figure 2-3. Plasmid maps. Representative examples of all plasmids used in this study.

Panel A (top left) depicts the pMTL-AMH101 (pANNE CLJU delPyrE is an alternative name) used for creating a pyrE knock out. Panel B (top right) depicts pMTL-BP-delAlsS which was used to create inframe deletions. Panel C (middle left) shows pMTL-CH20 used to repare the pyrE locus. Panel D (middle right) shows pMTL007E2-CautCA used to make ClosTron disruptional mutants. Panel E shows pET16b-gCA that represents all pET16b-based protein expression plasmids used. Panel F depicts pMTL82252-bCA a representative of pMTL expression plasmids.

2.4.6 Competent cell production and transformations of *E.coli*

Chemically competent cells were produced by inoculation of 100 mL LB medium in Erlenmeyer conical flask 500 µl overnight grown culture. The 100 ml culture was grown with agitation until an OD_{600} of 0.3 - 0.5, then chilled on ice for 10 min. Cells were harvested by centrifugation at 2700 x g at 4 °C for 10 min and resulting cell pellet was resuspended in 20 mL ice-cold calcium chloride buffer (100 mM $CaCl_2$, 10% v/v glycerol) and chilled on ice for 15 min. The cells were washed by centrifugation and resuspension once more before incubated at 4 °C for 1 hour after which 100 µL aliquots of were stored in -80 °C freezer. To transform *E. coli* DH5α, *E. coli* Top 10, *E. coli* Xl1-Blue, *E. coli* NEB express, *E. coli* Sexpress, and *E. coli* BL21(DE3)pLysS, plasmid DNA (1-10 µl) was mixed with 50 – 100 µl competent cells and incubation on ice for 30 min, followed with a 45 s heat shock at 42 °C. The cells were quickly cooled on ice and recuperated in 1 ml SOC medium at 37 °C for one hour. A selective step on liquid or solid LB medium with selective antibiotics ensured selection of cells harbouring the target plasmid.

The production of electro-competent *E. coli* CA434 cells was performed in similar fashion as chemical competent cells described above except instead of calcium chloride buffer, ddH_2O was used for washes, 10% glycerol was used for final resuspension incubation prior to aliquoting was skipped. *E. coli* CA434 cells were transformed using electroporation. 1- 5 µl plasmid DNA and 50 µl electro-competent cells were mixed and incubated on ice for one min after which an electric pulse was provided with a Gene Pulser (25 µF capacitor, 200 Ohm). 1 ml of SOC medium was added, cells recuperated for 1h at 37 °C after which they were transferred to selective media with appropriate antibiotics.

2.4.7 DNA transfer via conjugation

Conjugation with CA434 strains or Sexpress as donor strains was the standard method to transform *C. ljungdahlii* and *C.autoethanogenum.* The donor harbouring the plasmids were grown for 10-16 h in LB containing antibiotics. 1.5 mL of conjugative donor was spun down for 2 min at 4000 rpm and washed once with 500 µL Phosphate Buffered Saline (PBS). The cell pellet was moved to the anaerobic cabinet and resuspended with 200 µL of a 3 day old *Clostridium* culture. This conjugation mixture was spotted on YTF agar plates without antibiotics and incubated over-night inside the anaerobic cabinet. The spotted conjugation mixture was then transferred to YTF agar with 10 µg ml^{-1} trimethoprim and the appropriate antibiotic for plasmid selection.

2.4.8 Sanger Sequencing

Sanger sequencing (230) was performed by Source bioscience (Nottingham, UK) or by Eurofins (Ebersberg, Germany)

2.4.9 Next generation sequencing

Genome sequencing was performed by DeepSeq (University of Nottingham) or by MicrobesNG (University of Birmingham) using Illumina HiSeq or MiSeq.

2.5 Protein methods

2.5.1 Cell lysis

Cells for protein purification or enzyme activity were lysed using sonication with a Bioruptor® (Diagenode) or QS1 probe sonicator (Nanolabs, MA, USA), or by using BugBuster® Plus Lysonase™. Protein purifications were performed anaerobic if oxygen tolerance of target proteins was unknown. Fisher protease inhibitor cocktail VII was added if deemed necessary.

2.5.2 PAGE, Western Blotting and protein concentration determination

All samples were analysed on 4-12% NuPAGE™ Novex™ 4-12% Bis-Tris Protein Gels (ThermoFishcher, Waltham, MA USA) for purity and yield (231). His-tagged samples were western blotted at least once using Novex™ system and protocol. Samples were prepared by diluting to normalise if needed and by using NuPAGE LDS Sample Buffer (4X) and denaturation at 98 °C for 5-10 minutes. NEB Colour protein ladder was used as a molecular weight reference. Protein concentration was further measured using a Nanodrop photospectrometer (Thermoscientific, Wilmington, DE, USA) or using the Bradford assay (232) with bovine serum albumin as a standard.

2.6 Analytics

2.6.1 Gas Chromatography

Headspace of the bioreactors were analysed every 30 minutes using a micro-GC (model 490, Agilent) fitted with 10m 5A molsieve (M5A) and 10m poraplot Q (PPQ) columns with backflush thermal conductivity detectors (TCD). The injector and M5A channel column were heated to 100 °C and the PPQ channel to 80°C. The column pressures were 200 kPa and 150 kPa, respectively. Argon was used as carrier gas/mobile phase. A 16 port dead-end sampling valve (VICI) allowed automated serial sampling of multiple gas streams.

For head space of bottles and tubes a Thermo Scientific Trace 1310 with a Restek ShincarbonST column was used. Injector was at 100 °C while the column was programed to start at 40 °C for 3 minutes, followed by a temperature ramping of 7 minutes to 230 °C and a hold for 2 minutes. Helium was used as carrier gas and a TCD to detect gasses.

Calibration standards for the gases were a certified gas mixture of 97% N_2, 1% CO, 1% CO_2 & 1% H_2, and mixtures prepared from pure gases at 10%, 30%, 50% and 100% were used.

2.6.2 High pressure liquid chromatography

HPLC was employed to analyse, acetate, ethanol, lactate, 2,3-butanediol, MES, sugars, phosphate, pyruvate, 1,2-propandiol and propanol in the supernatants of cultures. For this a Thermo Scientific dionex Ultimate 3000, with RI and DAD detectors and Rezex ROA organic acid H+ column at 35 °C (Phenomenex) was used. 0.01 mM H_2SO_4 at was used as mobile phase at 0.5 mL/min. Standards were prepared with acetate, ethanol at 400 mM stock concentration, lactate, formate, 2,3-butanediol, 1,2 propanediol, propanol pyruvate and sugars at 100mM stock concentration and sodium phosphate concentration at 10mM. This stock was serial diluted in 9 steps of 0.5x each.

2.6.3 Liquid Chromotography-Mass Spectrometry

The LC-MS method was developed by Laudina Safo, Sarah Schatschschneider and Salah Abdelrazigh and carried out side by side with Laudina Safo. The method uses an internal standard of ^{13}C labeled *Clostridium pasteurianum* cell lysate created by Laudina. A calibration standard of all 133 target metabolites in 50 % v/v methanol: water to a final concentration of 1 mM was produced by Laudina. We prepared a serial dilution ranging from 0.5 µM to 200 µM. 40 µL of the ^{13}C labelled *C. pasteurianum* was added to 40 µL of each calibration standard mixture with each of the dilution series. *C. autoethanogenum* cell pellet samples were mixed with internal standard and extracted by a validated freeze thaw, methanol and chloroform method (PhD-thesis Laudina Safo, UoN). Both samples and calibration standards were thoroughly mixed and kept at 4 °C in the autosampler prior to LC-MS analysis. An injection of 10 µL was used for analysis. This analysis was performed on a Dionex LC system with a ZIC-pHILIC 150 mm × 4.6 mm, 5 µm particle size column (Merck Sequant, Roxley Green Business Park, Watford, UK) followed by Hybrid Quadrupole Orbitrap mass spectrometer (Q-Exactive, Thermo Fisher Scientific, Hemel Hempstead, UK). A 8 min linear gradient starting at 80% acetonitrile/ 20% 20 mM ammonium carbonate pH 9.1 ending at 5% acetonitrile/95% 20 mM ammonium carbonate followed by a, 2 min from reverse gradient back to 80% acetonitrile and 5 min re-equilibration at 80% The flow maintained between 300 and 400 µl min^{-1} and column temperature at 45 °C.

Heated electrospray ionisation (HESI-II) probe was used for MS. Polarity-switching mode of ionisation and the parameters for the MS were optimised using settings of (233, 234). Resolution was set at 140000, automatic gain control was 1 × 106, m/z ranging from 70 - 1400, sweep gas 1, auxiliary gas 20, sheath gas 40, capillary temperature 250 °C and probe temperature 275 °C. Source voltage +4 kV, tube voltage +70 kV, capillary voltage +50 V and skimmer voltage +20 V was used for positive mode ionisation while negative mode ionisation was performed at source voltage of -3.5 kV, tube voltage -70 V, capillary voltage -50 V and skimmer voltage -20 V. Both polarities were calibrated using at least 5 mass ranges before analysis.

Chapter 3:

The identification and characterisation the carbonic anhydrases of *Clostridium autoethanogenum*

"Bart, do you know if there are any carbonic anhydrases in C. autoethanogenum?" **Thomas Millat, December 2013**

3 The identification and characterisation the carbonic anhydrases in *Clostridium autoethanogenum*

3.1 Introduction

Many reactions in microbial metabolism exist where either CO_2 or bicarbonate (HCO_3^-) are substrates or products (235). A chemical equilibrium between CO_2 and HCO_3^- establishes readily in aqueous solution (eq 1) however this reaction appears to be too slow for many organisms. It is for instance proposed that without a mechanism for the rapid interconversion of carbon dioxide and bicarbonate, the necessary turnover rates of common carboxylation reactions that consume HCO_3^- would not be feasible in *Escherichia coli* (220). This interconversion of CO_2 and HCO_3^- is catalysed by carbonic anhydrases (CA), enzymes which are found in all branches of the tree of life. To optimise product formation and carbon fixation, knowledge about CA activity can be important (236, 237). It was unknown if *C. autoethanogenum* harboured CAs, a knowledge gap that is addressed in this chapter.

Carbonic anhydrases (CAs, EC 4.2.1.1) are metalloenzymes that catalyse the reversible conversion of carbon dioxide and water to bicarbonate and protons (eq 1) and are essential for most organisms.

$H_2O + CO_2 \leftrightarrow HCO_3^- + H^+$ (eq 1)

There are 3 major classes of carbonic anhydrases: α-CA, β-CA, and γ-CA. In addition, δ-CA, ζ-CA and η-CA classes were proposed for non-canonical CA enzymes present in diatoms and *Plasmodium sp*. (238). An initially identified ε-CA class of carboxydosome specific CAs was reclassified as a sub group of β-CA after it was recognised that these enzymes were structurally similar, despite little sequence similarity (239). This specific subclass will be referred to as the E-clade β-CA in the remainder of this thesis.

All known CAs function with a Zn^{2+} metal ion cofactor in their active site. In γ-CAs of anaerobic microorganisms, Fe^{2+} or Co^{2+} can functionally replace Zn^{2+}, while the ζ-class CA is also functional with Cd^{2+} (154, 240). The metal ions are coordinated in the active-site by three histidines (For α-, γ-, δ- and η-class CA), or one histidine and two cysteines (for β- and ζ-class CA); these amino acids are arranged in a distinct motif for each CA class(241–244). The diverse class of β-CAs are divided in 5 clades, A-D(235) plus the E-clade (this thesis), with all members possessing the common metal coordinating active-site motif CxDxR-G-HxxC. The α-CAs are active in monomeric state while the β-CAs forms dimers that in turn can stack into tetramers or octamers. The γ-CAs finally form homotrimeric structures (241, 244, 245).

Most bacteria can grow under low carbon dioxide partial pressures but for this a CA gene seems to be essential. Species that need high carbon dioxide partial pressures (capnophiles) often have no detectable CA activity and some have lost CA genes(246, 247). In the capnophile *Campylobacter jejuni* a CA was found only active at high pH, but not active under normal physiological pH (248). ΔCA mutants often can only grow under high carbon dioxide partial pressures (220, 249, 250) making them functional capnophiles. In *E. coli* a specific CA, CynT, is part of a cyanate metabolism operon that is tightly controlled and induced by cyanide or azide (251). When the constitutively expressed CA gene (*Can*) of *E. coli* is disrupted, the mutant strain (*E. coli* EDCM636) is unable to grow under atmospheric carbon dioxide pressure. Addition of azide leads to expression of *CynT* and restores normal growth (220). This strain is useful for complementation studies to test for CA activity of products from putative CA genes.

Previously a diverse set of acetogens that were screened for CA activity showed a range of CA activities (252). One model acetogen, *Acetobacterium woodii* had high CA activity but the other model acetogen *Moorella thermoacetica* showed little to no activity. No close relatives of *C. autoethanogenum* were included in this screening.

Here I identify two putative CA genes in the genome of *C. autoethanogenum.* Only one gene, with β-class CA active site motif, could complement CA function the *E. coli* EDCM636 Δ-Can mutant strain. Further characterisation of the purified enzyme revealed this protein is a dimer. With a new high-throughput activity assay, CA activity was confirmed and found to be comparable to that of other CA enzymes. Further phylogenetic characterisation places this CA gene in a new clade of the β-CAs harbouring CAs with the shortest primary structure known.

3.2 Methods

To study the capability of two putative CA encoding genes bioinformatic analysis was followed by expression of the *C. autoethanogenum* genes in *E. coli* strains and protein purification. Purified enzymes were characterised using a colorimetric assay employing pH indicators to monitor the reaction was adapted to be used in a 96 wells plate reader with automated injection.

3.2.1 Production of protein expression strains

To make plasmids for heterologous overexpression of carbonic anhydrase genes, fragments were amplified with polymerase chain reaction (PCR) using genomic DNA of *C. autoethanogenum* as template and cloned them in several plasmids. The genomic DNA was isolated using the Genelute (Sigma) genomic DNA isolation kit. PCR was performed with primers (Table 2-5) FbCA and RbCA for an untagged version Caut-bCA, and primers FbCA and RbCAstrep for a C-terminal strep-taged version of the same gene. The primers FgCA and RgCA were used for Caut-gCA, and FgCA, RgCAStrep for a C-terminal strep-tagged version of the gCA gene. These PCR fragments were cloned in to pMTL82252 using NdeI and EcoRI and T4-ligase. To produce His-taged versions of Caut-bCA and Caut-gCA we performed PCR with primers BCAECPF and BCAECPR, or FPCA1 and RPCA1 respectively. The resulting fragments were cloned in to a pET16b (Novagen) plasmid using NdeI and BamHI and T4-ligase. *E.coli* DH5α chemically competent cells were transformed with these plasmids. Plasmids were isolated Sanger sequenced using the FpMTL8xx5x primer for the pMTL82252 plasmids and the pET16b_F primer for the pET16b plasmids.

E.coli BL21(DE3) pLysS and NEBexpress were transformed with pET16b-bCA and pET16b-gCA.

E.coli EDCM636 were transformed with pMTL82252-bCA, pMTL82252-bCAstrepC, pMTL82252-bCAStrepN, pMTL82252-bCAHisC, pMTL82252-gCA, pMTL82252-gCAstrepC, pMTL82252-gCAStrepN and pMTL82252-gCAHisC. The cells were plated on LB agar with erythromycin and on plates of LB-agar, erythromycin and sodium azide. A selection of the resulting colonies were streaked on LB with several selective conditions to study the ability of the Caut-bCA and Caut-gCA genes to complement the ΔCA mutation of E.coli EDCM636s.

3.2.2 Protein production and purification

To produce and purify the His-tagged putative CA enzymes from the *E. coli* BL21(DE3) cells, 5 ml LB was inoculated from a -80 °C stock and grown overnight at 225 rpm, 37°C. This O/N culture was used to inoculate 5x 100 ml LB in 500 ml Erlenmeyer flasks to a start OD600 of approximately 0.05 and incubated in a shaking incubator 225 rpm at 37 °C. At OD600 0.3-0.7 cells were induced with IPTG (Isopropyl β-D-1-thiogalactopyranol) a 0.5 mM final concentration and incubated at 30 °C for 3-5 h. Cells were harvested by centrifugation and cells were lysed with a QS1 probesonicator (Nanolabs, MA, USA) or with BugBuster® Plus Lysonase™. An additional centrifuge step was used to create cell free extract. We purified the protein using a 5-mL HisTrap® HP collumns (GE Healthcare Life Sciences, Buckinghamshire, UK) and 300 mM imidazole for elution buffer. For the production of the STREP-tagged enzyme 300 ml of overnight (LB, shaking, 37 °C) E.coli EDCM636 pMTL82252-bCAstrepC or EDCM636 pMTL82252-gCAstrepC were harvested by centrifugation and lysed using BugBuster® Plus Lysonase™ complemented with Avidin at one small crystal per 30 ml. The Caut-bCA protein was purified using streptavidin sepharose using 100 mM Tris pH 8 with 150 mM NaCl as wash buffer. For elution 0.5 mg ml^{-1} desthiobiotin was added to the wash buffer.

3.2.3 Carbonic Anhydrase assay

Carbonic anhydrase activity was determined using a Tecan m1000Pro (Männedorf, Switzerland) plate reader with auto injector. The assay is based on previously published methods (253–256)and provides an alternative to stop-flow devices that allows for reasonable accurate high-throughput measurements. We have validated the assay using bovine CA and *C. jejuni* β-CA CanB (248), kindly supplied by D.J. Kelly of the University of Sheffield. The assay buffer was 50mM HEPES, 50mM NaSO4, 50 mM MgSO4, 0.004 % (w/v) phenol red at several pH values. The substrate for the hydration reaction was carbon dioxide saturated water, produced by bubbling carbon dioxide through demineralised water at 20 °C for 30 minutes. This should result in 34 mM CO_2 (146) for lower concentrations the saturated water was diluted with demineralised water that had N_2 bubbled trough for 30 minutes. The substrate of the dehydration reaction was $KHCO_3$ at 100 mM. For the hydration reaction 120 µl of assay buffer was mixed with 10 µl enzyme sample or 10 µl sample buffer in a 96 well plate. After measuring the baseline for 4 s 120 µl of substrate was injected. For the dehydration reaction 140 µl and 10 µl enzyme sample or 10 µl sample buffer was used, after 4 s baseline measurement 50 µl substrate was added. Change of absorption was measures at 557 nm for 40 s at a temporal resolution of 200 ms. The average change in absorption s^{-1} of the first ten readings was taken as the initial speed of the reaction. The Km and Vmax were calculated using the Michaelis-Menten (257)curve fitting tool of GraphPad Prism 7.00.

3.2.4 Structural protein characterisation

Structural protein characterisation was performed externaly. Analytical ultracentrifuge was performed by Gemma Harrison. X-ray chrystallography was performed by Stephen Carr and Megan Cox. All structural characterisation is organised by David Scott.

3.3 Results

3.3.1 Gene identification

To establish if *C. autoethanogenum* harbours CA genes in its genome, 41 CA protein sequences of the α-, β-, γ-, & δ-CA classes of organisms from all domains of life were collected. Consensus sequences of the α-, β-, γ-CA classes were constructed using MUSCLE alignment in UGENE. Both the raw sequences and the consensus sequences were used to search the genome of *C. autoethanogenum* using BLAST algorithms.

3.3.2 Putative γ-CA encoding gene identification

One gene coding for a putative γ-CA (*Caut-gCA,* locus tag CLAU_2699) was identified with PSI-BLAST at E-value of 3e-50 and 54% identity to the γ-CA consensus sequence. This gene coding for a putative Caut-gCA is annotated as a transferase hexapeptide repeat containing protein. Three important metal binding histidine residues are conserved, but it lacks glutamic acid and asparagine residues that were found to be important in the canonical γ-CA (Cam) from *Methanosarcina thermophile* (241).

3.3.3 Putative β-CA encoding gene identification

A gene coding for a putative Caut-bCA (locus tag CLAU_3021), was found by using the β-CA consensus sequence in a PSI-BLAST E-value of 80. Despite the low similarity to other β-CAs this gene coded for a protein, that contained the motifs, CxDxR and HxxC, that are known to be important for the activity of β-CAs (235, 258).

3.3.4 Transcription

In recently published RNA seq data *Caut-bCA* is consistently expressed at a higher level than *Caut-gCA* (148.177 FPKM vs 71.7564 FPKM) (136), our own unpublished transcriptomics and proteomics support this (unpublished data, A.M. Henstra *et al, UoN*).

3.3.5 Genome region

The surrounding genetic regions (figure 3-1) of the identified genes do not provide much information that indicate a specific function. *Caut-gCA* has one neighbouring gene downstream in that codes for a peptidase M14 carboxypeptidase A, which has no obvious link to CAs except that both are Zn-metalloenzymes. *Caut-bCA* is part of a gene cluster (CLAU_3019-CLAU_3023) of 5 genes with similar expression pattern (unpublished data, A.M. Henstra *et al, UoN*). This gene cluster has features that suggest a phage origin, such as a *yopX* gene and a single stranded DNA binding protein encoding gene. The first gene downstream of *Caut-bCA* is a Deoxyuridine 5'-triphosphate nucleotidohydrolase which could indicate a function in pyrimidine metabolism where HCO_3^- is an important factor but this is not consistent with the rest of this cluster.

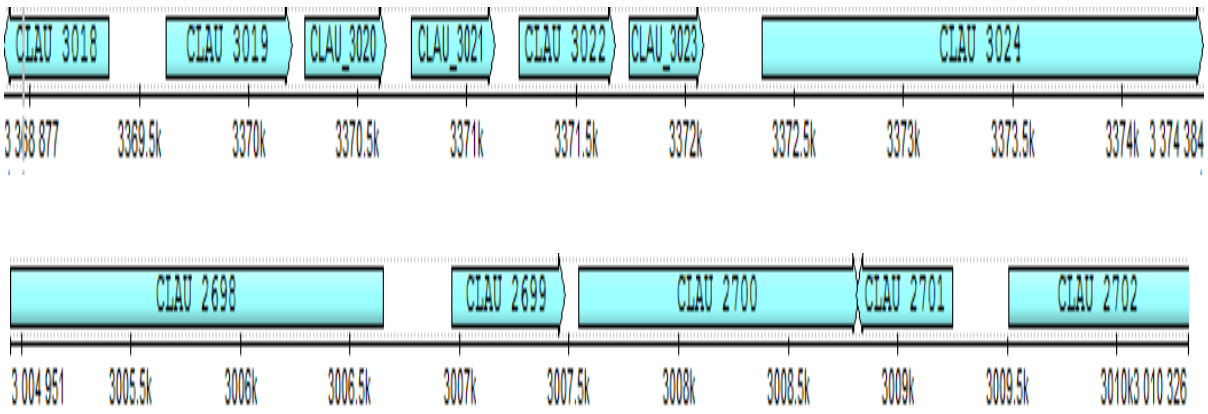

Figure 3-1 *C.autoethanogenum* genome regions containing the (putative) CA encoding genes.

Top figure shows the region containing the βCA gene (CLAU_3021) flanked by a YopX (CLAU_3120) and deoxyuridine 5'-triphosphate nucleotidohydrolase (CLAU_3021). The lower figure shows the genome region containing the γCA (CLAU_2699) which is upstream of a M14 peptidase gene (CLAU_2700). Neither regions give a clear indication of the function of the putative CA encoding genes.

3.3.6 Protein prediction

Protparam (210) analysis showed the 124 amino acid residues of Caut-bCA to form a stable protein with a molecular weight of 14.2 kDa and pI 5.3. The 168 amino acid residues of Caut-gCA are expected to form an unstable protein with a mass 18.3 kDa and pI 6.4. Phyre2 (207) structural modelling shows Caut-bCA coding for a small but not untypical β-CA protein with an accessible active site and Caut-gCA for a typical γ-CA (Figure 3-2).

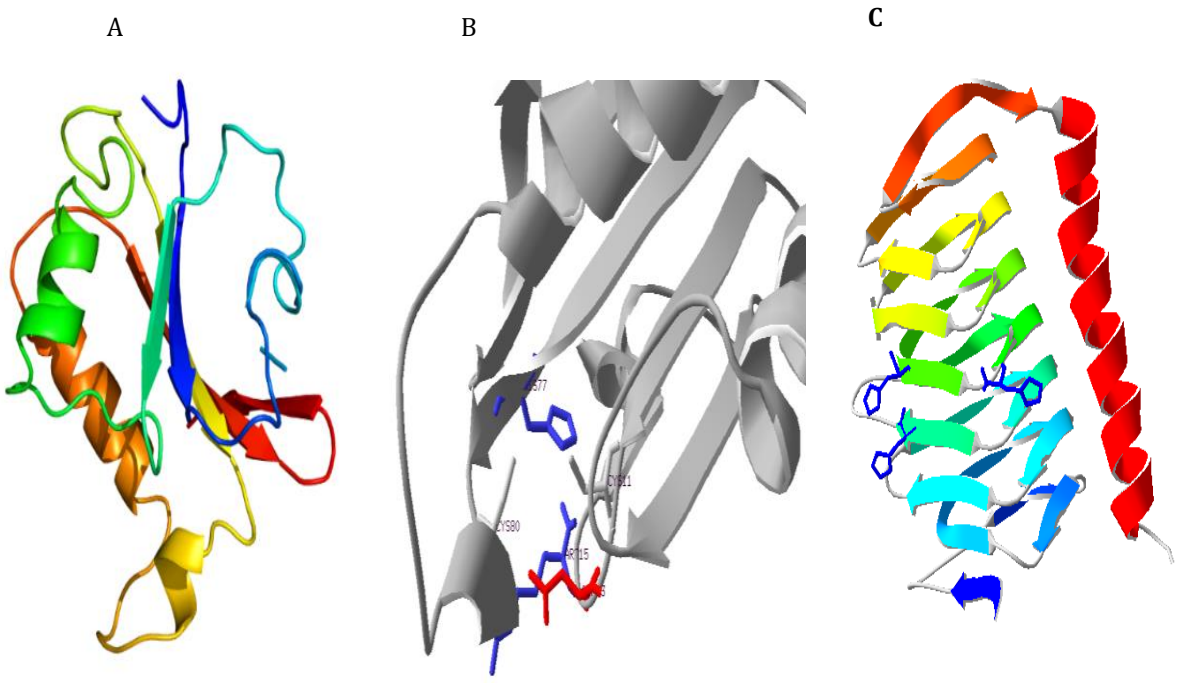

Figure 3-2 Protein structure models of the CA of *C. autoethanogenum*, calculated using Phyre2.

Picture A (left) shows the Caut-bCA monomer, picture B (middle) is a detailed view of active site with most conserved residues C11, D13, R15 and H77 & C80. The two cysteine and histidine residues are thought to bind a zink ion. Picture C (right) shows the Phyre2 model of Caut-gCA with the three conserved histidine side chains. Other γ-CAs are known to form trimers where a zink ion is bound to the two histidines of one monomer and another from another monomer.

3.3.7 Phylogeny and protein sequence alignments

Both protein sequences of Caut-bCA and Caut-gCA were aligned to sequences of other proteins from the respective class. Caut-gCA seems to be a typical member of the γ-CA family based both on sequence alignment comparison (figure 3-5) and phylogenetic analysis. Like some other members of this family (241, 248, 259, 260), it did not show CA activity and therefore no extensive further sequence and phylogenetic analysis was performed on this protein.

The low identity of the putative Caut-bCA with known β-CAs and the fact it was shown to possess CA activity (section 3.3.8) warranted further phylogenetic analysis. Using NCBI blastp with Caut-bCA as query sequence, I identified multiple hypothetical genes in both bacteria and archaea that encode putative β-CAs that have a distinct, shorter, sequence from previously described β-CAs. It was striking that these specific Caut-β-CA-like CAs sequences were relatively often found in the deposited genomes of uncultivable bacteria and archaea or recent isolates of candidate species. I did not include any of these in further analysis, which was limited to CAs from cultivable species.

3.3.7.1 Alignment analysis of the β-CAs

An alignment of 63 β-CA (Figure 3-3) protein sequences support a grouping of the β-CA family in 6 separate groups, the classic A-D clades, the E-clade and a clade of Caut-β-CA-like CA that was designated as the F-clade. An alignment of 160 β-CA protein sequences (appendix Figure 11-1) is summarised as consensus logos for all 6 identified sub-clades (figure 3-4). Only two motifs are fully conserved in all selected β-CAs, CxDxR and HxxC interspaced by 48-77 amino acids. These are the well-known metal binding Histidine and Cysteine residues and the Aspartic acid and Arginine that complete the active site (244). Additional motifs exist; A-, B-, C-clades all have a QxP 6 amino acids N-terminal of the CxDxR motif while D- and E-clades lack this motif; it is noteworthy that most of the novel F clade have a QxP motif on the C-terminal side of the CxDxR motif. The A,B and C clade further have conserved G[D,E]xFxxR motif between the CxDxR and HxxC motifs. In the E-clade only the GxxF is conserved. In the D-clade G[D,E] is conserved. The distance between CxDxR and HxxC are larger than average in the E-clade with approximately 75 aa, and to a lesser extent in the F-clade with average distance of 64 aa, where A-, B-, C- and D- clade have an average distance of 55 aa.

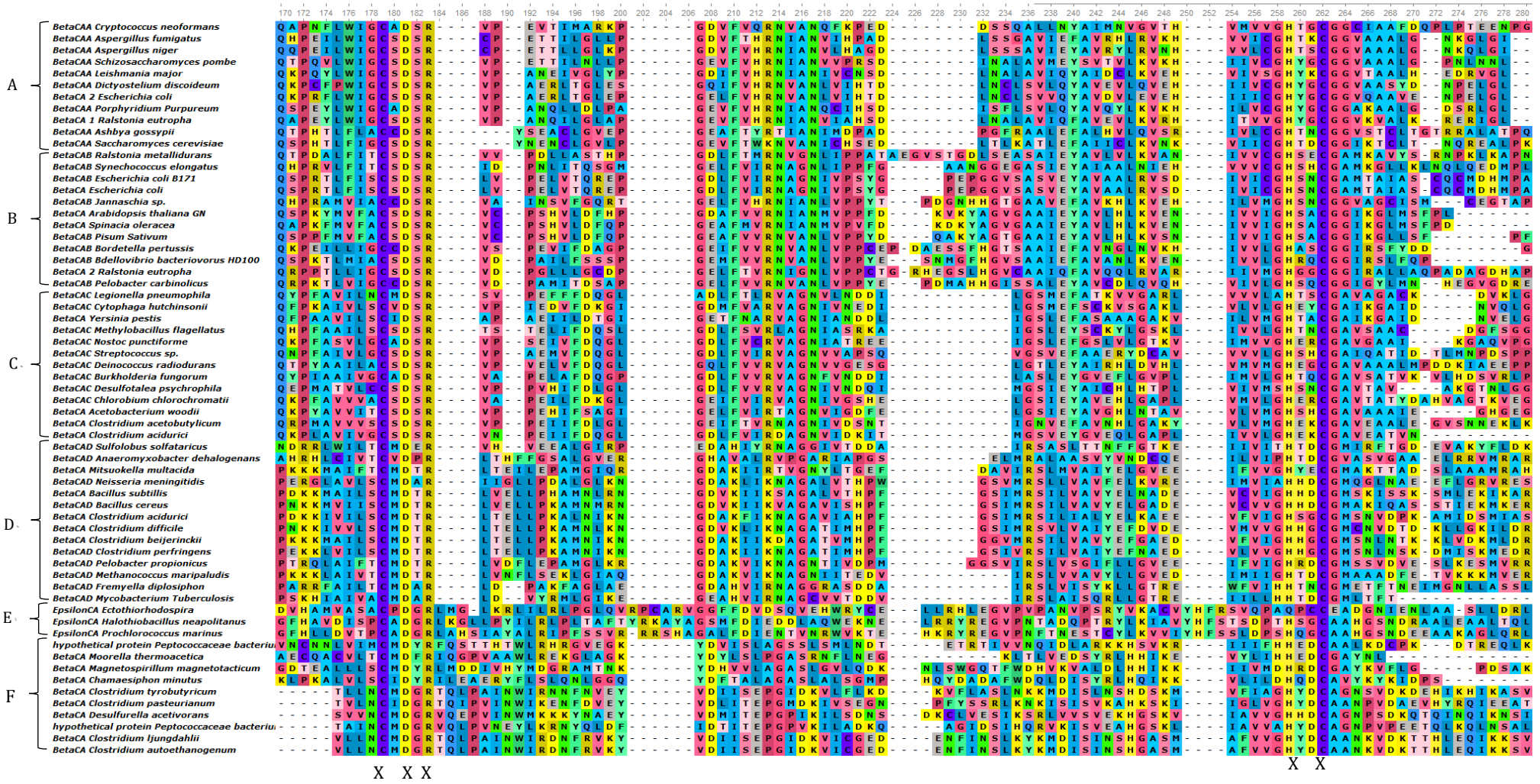

Figure 3-3 Active cleft region of an alignment of 63 βCAs.

The X below the alignment indicate most conserved amino acid residues. The cysteine of the 100% conserved CxDxR motif is thought to form a metal ion binding site together with the histidine and cysteine residues in the HxxC motif. To the left the names of the subclades are given. Although the F-clade βCAs are smaller in total length, the distance between the metal binding residues appears to be somewhat expanded in the primary structure. The level of conservation between and within groups are given

Figure **3-4**.

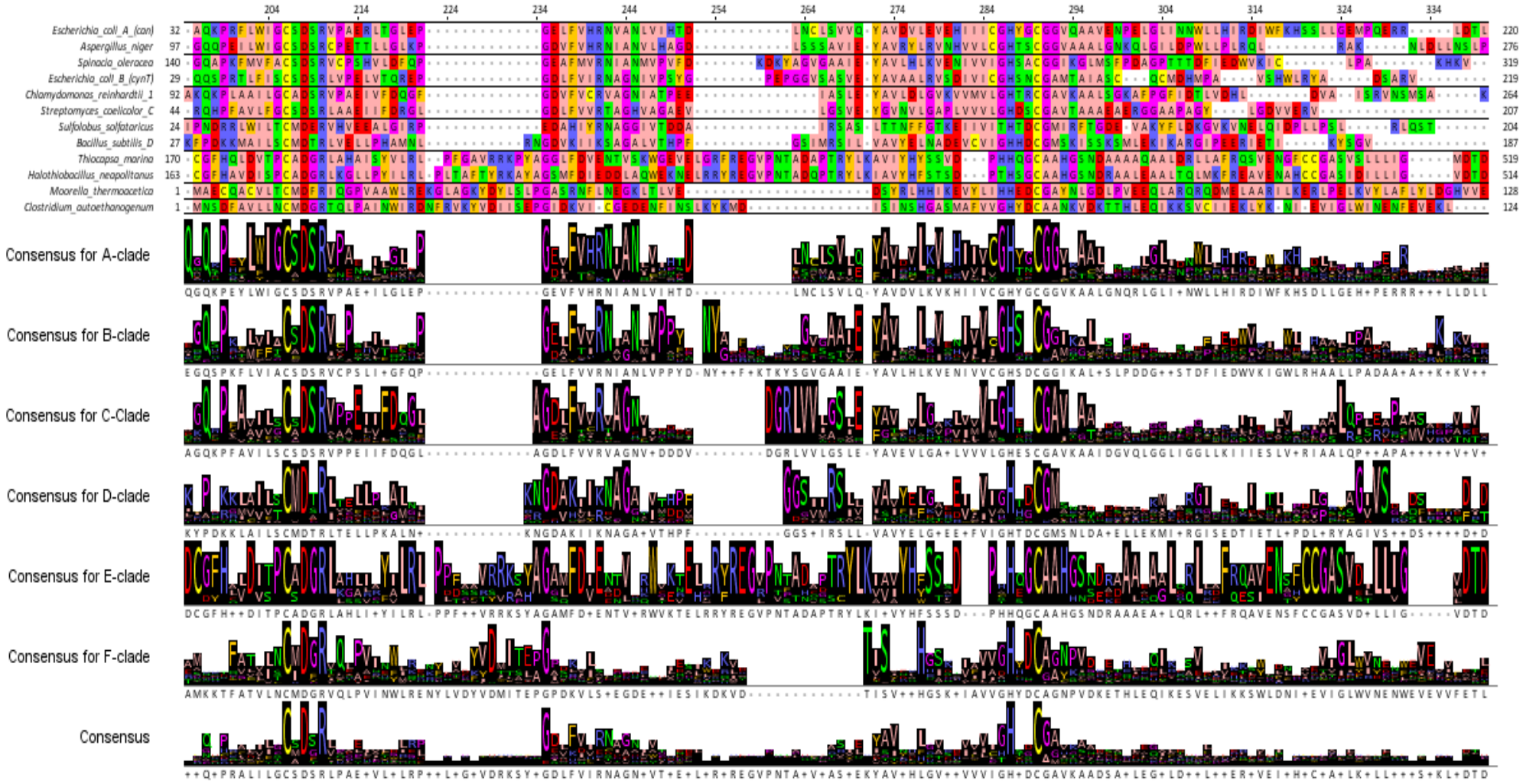

Figure 3-4 abstract of a 160 sequence alignment (appendix 10.1).

Here two examples of each clade are shown. The full sequence Caut-bCA is depicted, other sequences shown have parts of both ends removed. The numbers on right are preceding amount of residues numbers on left are total length of sequence. This illustrates the compact nature of the F-clade CAs. Below the alignments, the consensus logos of all 160 sequences (bottom) and of each clade consensus is depicted (alphabetic order top to bottom).

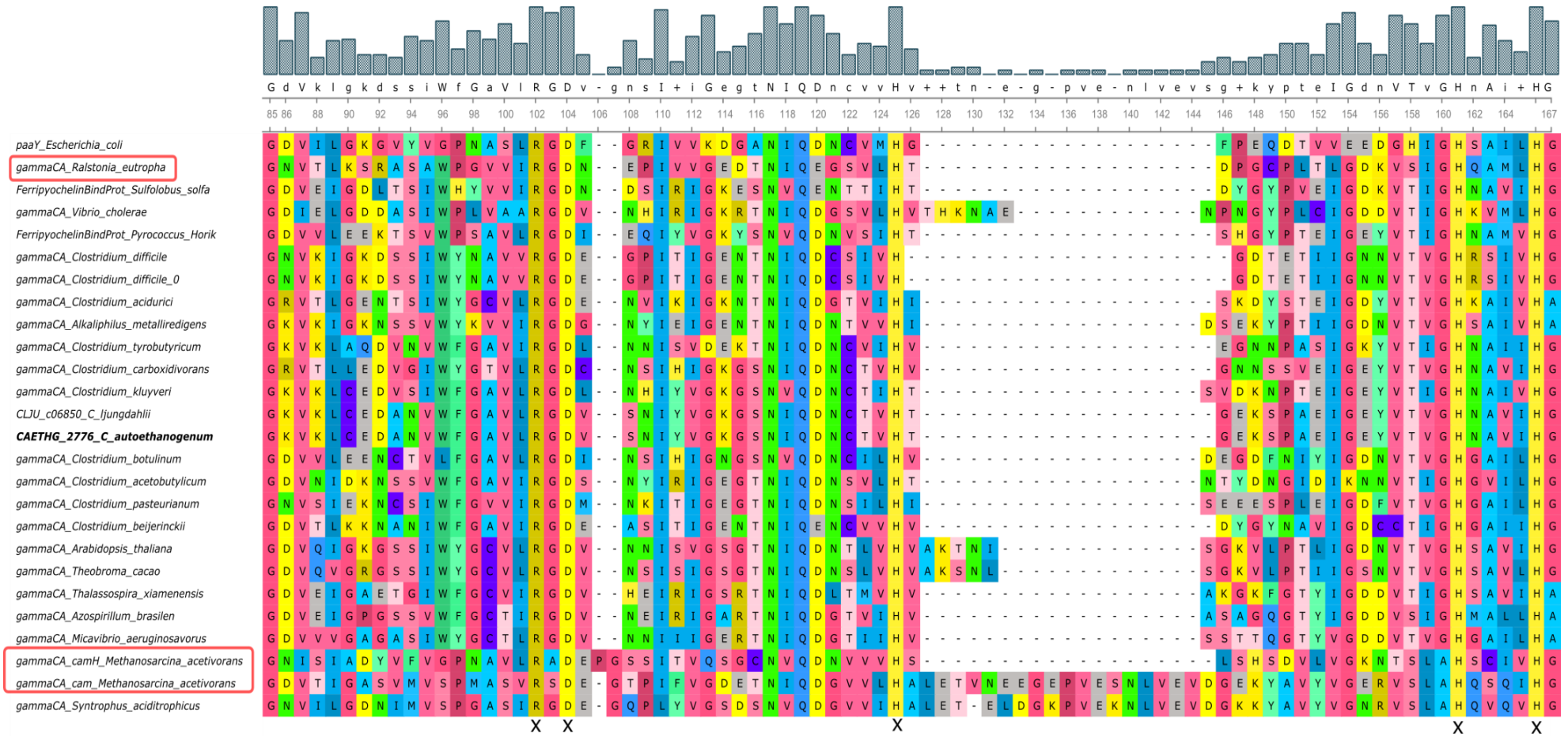

Figure 3-5 Alignment of selected γCAs.

The γCAs labels with a red box have confirmed CA activity. The predicted active residues are marked with an X. Residues 125 (Histidine), 161 (Histidine) & 166 (Histidine) are the metal ion binding residues. Residues 102 (Arginine) & 104 (Aspartic acid) are probably important for proton transfer in the reaction. Interestingly the Ferripyochelin binding proteins and paaY proteins included here are conserved on these positions

3.3.7.2 Phylogeny

Extensive phylogenetic analysis gave insight to how the Caut-β-CA-like CAs relate to the other β-CAs. Figure 3-6 depicts a Bayesian phylogenetic tree made with 60 β-CA sequences that presents the overall topology of identified clades, consistent with that found with other methods such as maximum likelihood and larger sets of β-CA sequences (appendix Figure 11-2, Figure 11-3, Figure 11-4). The analysis included sequences of the majority of previous described β-CAs as well as β-CAs from the major taxonomic groups of life. The Caut-bCA-like proteins formed a distinct clade (Clade F) of not previously studied β-CAs.

The grouping in 6 major clades within the β-CA family were replicated in the fast majority phylogeny analyses. However full consensus between the separate analyses cannot be found on how these group relate. The A & B clade group closely together in all analyses but the relationships that are found between the other clades differ somewhat in different analyses.

The divergent nature of the E clade makes exact placement in relation to other groups problematic. Other divergent sequences that are somewhat hard to place are those of some Archaea such as *Haloferax volcanii* that are likely divergent C-clade β-CAs and the insect β-CAs that are likely very divergent B-clade β-CAs. The newly proposed F-clade β-CAs are calculated to be closest related to E-clade, D-clade or C-clade in several analyses. If one ignores the E-clade the majority of the high quality calculations position the F-clade group closest to the D-clade. In the majority of the analyses with the E-clade, the F-clade forms a branch in between E- and D-clade (Figure 3-6).

Both phylogenetic and alignment analysis shows that the F-clade can further be divided in two sub-clades, one defined by the putative β-CA of *M. thermoacetica* (Mtherm-bCA-like) and the other by Caut-bCA. F-clade CAs have mostly shorter sequences than the previously described CAs of the other clades. The Mtherm-bCA-like sub-clade harbours 6 proteins of considerable length (172-183 aa). The Caut-bCA-like sub-clade consists of relatively shorter CAs with a length of between 124 and 142 residues. *M. thermoacetica* showed little CA activity in previous studies (252) and therefore some caution is in place to assume functionality on the Mtherm-bCA-like proteins without further study. The similarity of some of the Caut-bCA-like F-clade CAs to Caut-bCA implies these are likely active CAs. It is interesting to note that many of the species in which I found F-clade β-CAs are (chemolitho)autotrophic, anaerobes or have other uncommon types of metabolism which, partly, might explain the richness of this class in the genomes of recent isolates and uncultivable organisms.

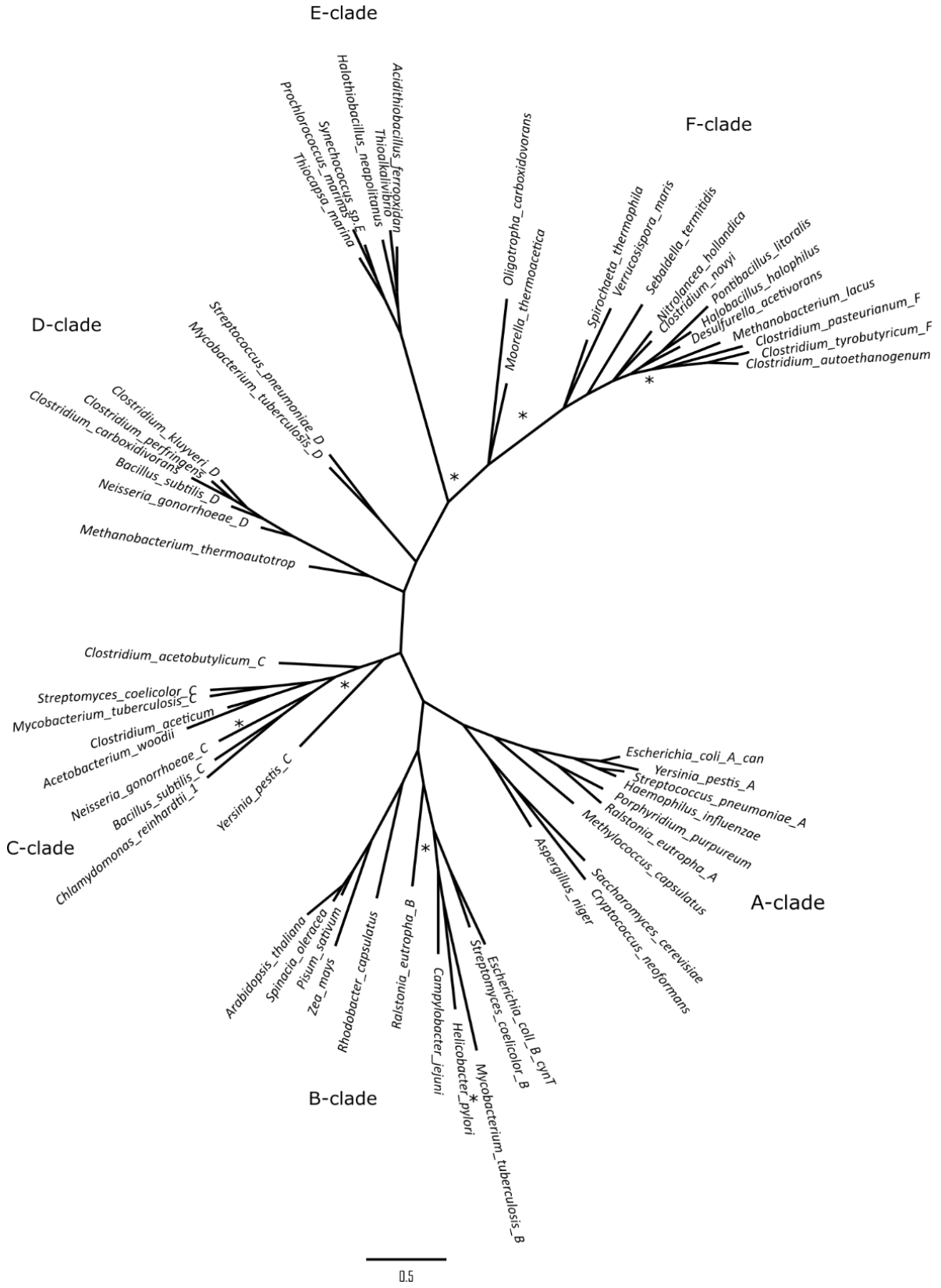

Figure 3-6 The phylogeny of β-CAs was reconstructed using MrBayes.
All Posterior probabilities are above 0.85 except for branches labelled with * which have a probability between 0.55 and 0.7. A similar topology was obtained with more extended sets of sequences, both with Maximum Likelihood method and Bayesian analysis (see appendix figures 10.2-10.5). The tree is edited for clarity using Figtree and Inktscape. The Caut-bCA-like proteins formed a distinct clade (Clade F) of not previously studied β-CAs. The A-D clades group in a similar fashion a previously described (235).The precice pacement of the E-clade within the β-CAs is complex and has, to my knowledge, not been reported previously.

3.3.8 Enzyme characterisation

3.3.8.1 Development of CA high-throughput activity assay method.

To establish whether the putative CA genes of *C. autoethanogenum* encode for active CA enzymes, a high-throughput activity assay in 96-well format was developed based on published methods (253, 254). To my knowledge this is the first description of performing CA-assays in 96-well format. This method allows fast measurements of many replicates reactions under a wide range of reaction conditions.

The details of the high-throughput method are described in the methods section. The performance of the assay was assessed with bovine α-CA at a range of dilutions which gave a nonlinear dose effect response within the range of 0.003 – 3 μg ml^{-1} of enzyme (figure 3-7). It was further validated by measuring the Km of bovine α-CA and the pH specific activity of the *C. jejuni* β-CA CanB (248). The method replicated the pH profile of *C. jejuni* CanB typical of type II β-CAs and the Km was determined as 4.7 ± 2 mM (data not shown). Al-Haideri et al found 34 ± 10 mM but at a temperature (4 °C) not replicable in the used Tecan m100Pro. The Km of bovine CA was determined as 17 ± 4 mM while published values vary between 12 mM and 1.1 mM (261, 262). These values are within an order of magnitude difference which validate the method for further use. This assay was applied in further characterisation of the putative CAs of *C. autoethanogenum*.

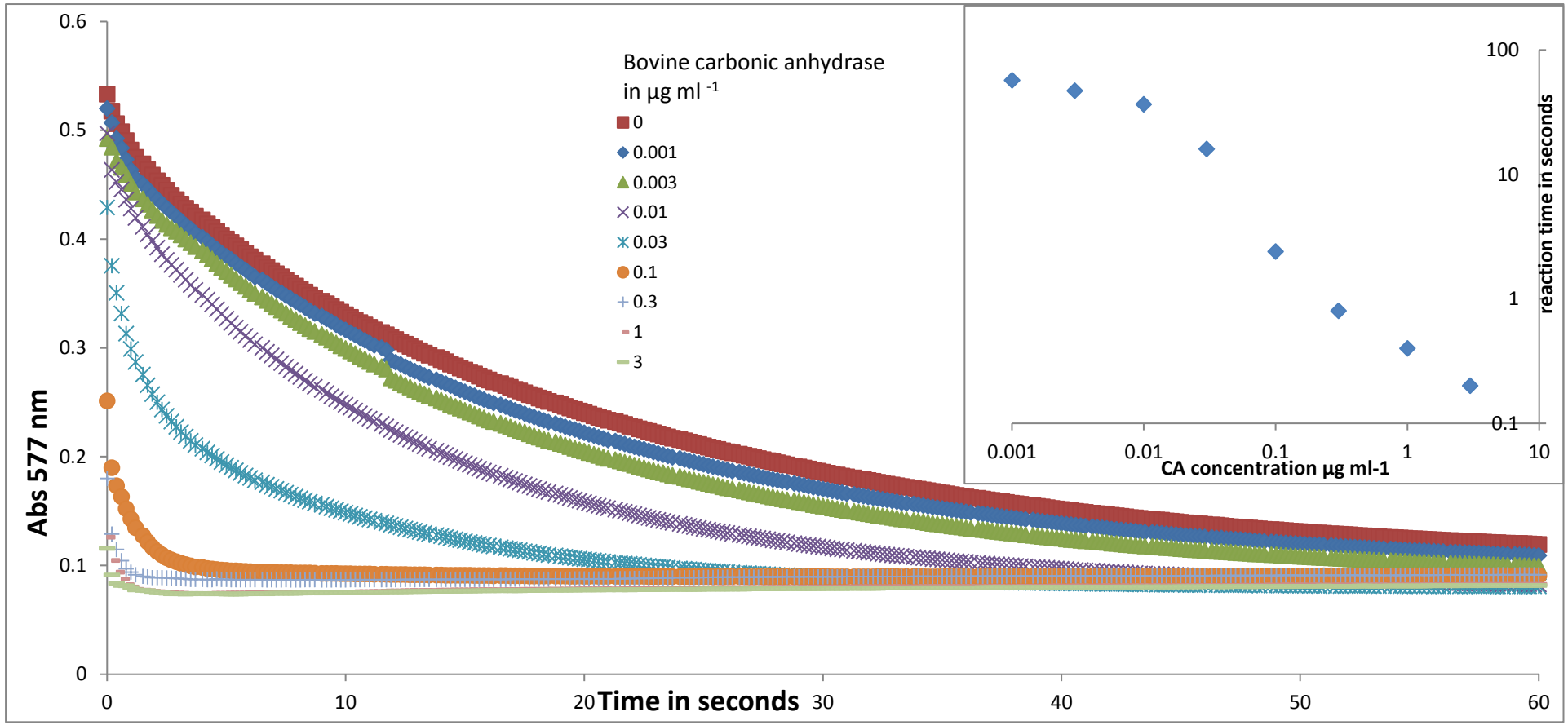

Figure 3-7 Validation of the CA-Asay performed in 96-wells plate reader with automated injection.

These graphs shows the effect of addition of different concentrations of Bovine Carbonic Anhydrase to assay the buffer when carbon dioxide saturated water is used as a substrate. The diagram in the lower left half shows averaged reaction curves of the 4 technical replicates from which reaction times can be calculated. The graph inserted the upper right corner shows a double logarithmic plot with reaction times plotted against the bovine CA concentration. This gives a clear dose-effect curve which validates the assay.

3.3.8.2 Protein purification

To determine the activity of the CAs of *C. autoethanogenum* the enzymes were produced, purified and assayed for activity. Purification of the Caut-bCA and Caut-gCA with a N-terminal His-tag(263) on a pET16b plasmid expressed in BL21(DE3) pLysS cells did not reliably yield active enzymes, although yield and purity were within acceptable range (Appendix Figure 11-6, Figure 11-7). In the case of Caut-bCA I suspect the bulky metal binding 10xHis residue close to the active site interferes with activity. A C-terminal STREPII-tagged (264) Caut-bCA protein, expressed from pMTL82252 in the *E.coli* EDCM636 strain, gave reliable activity and the purified protein produced with this system was used to characterise the enzyme. Since *E.coli* EDCM636 does not grow without the Caut-bCA complementation, Caut-bCA must be produced as an active enzyme which might improve reproducibility of this system.

No active Caut-gCA was acquired with any of the tested systems. Initially all growth and enzyme purification steps were performed anaerobically in a Coy anaerobic chamber. Only after it was discovered that the Caut-bCA was stable and active in air, aerobic purifications were employed.

3.3.8.3 Oligomeric state

Analytical ultracentrifugation on the purified protein indicates a dimeric oligomeric state (figure 3-8) which is consistent with previously reported β-CAs (Table 3-1). In contrast, preliminary X-ray crystallography results showed the basic building block of the crystal being a cube of sufficient dimensions to contain four copies of Caut-bCA. In this light it is interesting to note that some β-CAs have a pH dependent oligomeric state (265). The measured molecular weight of the dimer is close to some of the monomers of β-CAs of other species, illustrating the compact nature of Caut- β-CA.

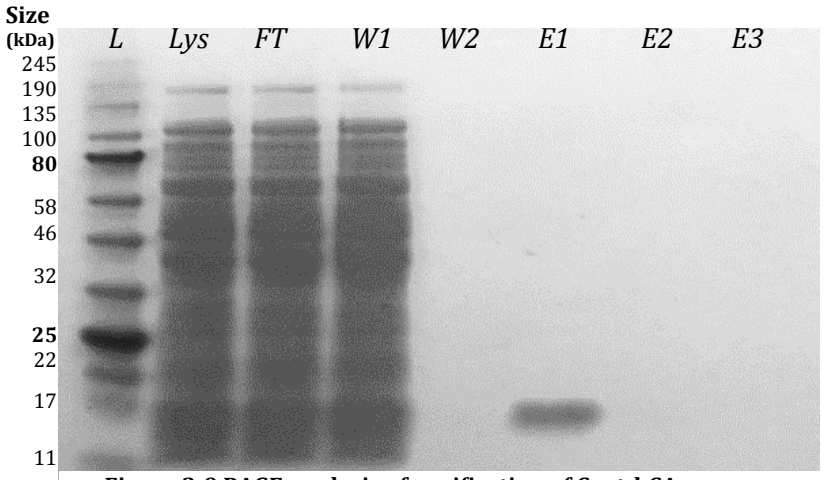

Figure 3-9 PAGE-analysis of purification of Caut-bCA.
NuPAGE™ Novex™ 4-12% Bis-Tris Protein Gel analysis showing StrepTag purified Caut- bCA in lane E1 with no noticeable second band in lane E1. Expected and observed size of StrepII-Caut-bCA protein is ~15.5 kDa. Lane legend: L=protein colour ladder, Lys=lysate, FT=column flow through, W1=initial wash, W2=final wash, E1-E3=Eluted fractions.

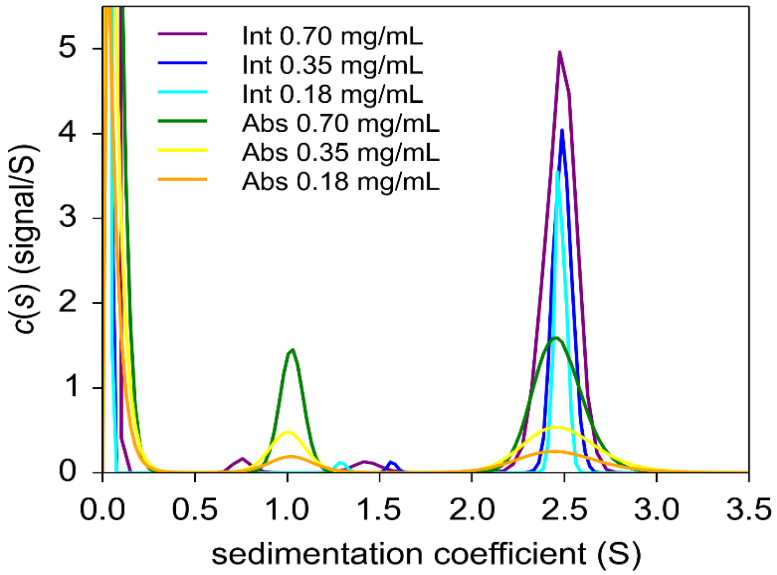

Figure 3-8 Analytical ultracentrifuge c(s) distributions for Caut-bCA.
This data suggests that Caut-bCA has a molecular weight of approximately 30 kDa (monomer 15.5 kDa) which would indicate a dimer as oligomeric state. Int - Interference data, Abs - Absorbance data. The sharp peak at ~0.1S is buffer salts.) This figure and the work it represents was performed by Gemma Harris at the Diamond light source.

3.3.8.4 Enzyme activity

The developed CA assay method was used to measure the kinetic parameters of the hydration reaction of the enzyme (figure 3-10) . The measured kinetic parameters are similar to other reported β-CAs (Table 3-1). The Km of 6.8 mM is intermediate compared to other prokaryotic CAs, slightly higher than that for the β-CAs of *Clostridium perfringens* and *Methanothermobacter thermautotrophicus* but lower than those of *Salmonella enterica* or *Helicobacter pylori.* The particularly low Km of the *C. perfringens* CA is interpreted as an indication for a function in retaining intracellular levels for anaplerotic CO_2 fixation reactions (249). I measured the dehydration reaction in the same fashion but I lack comparative parameters from many other β-CAs. The Caut-bCA protein retained activity at least 2 weeks in -20 °C. Incubation of the purified enzyme at 95 °C for 10 minutes caused total loss of activity (appendix Figure 11-8).

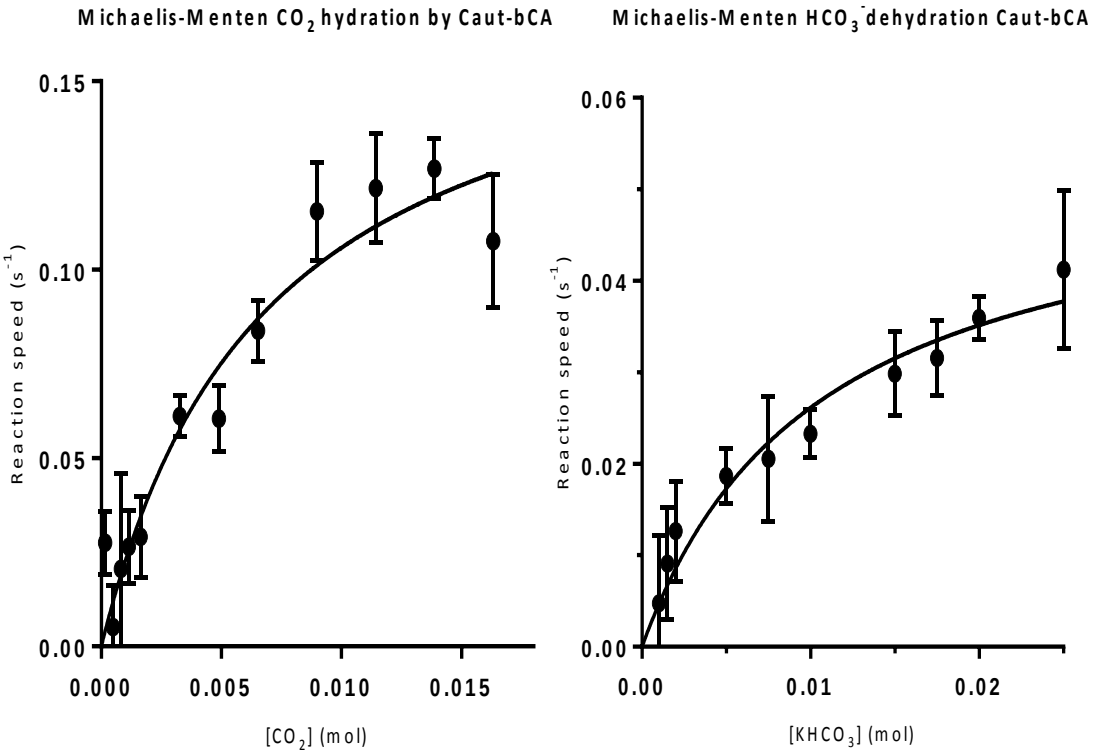

Figure 3-10 The reaction rates of CO_2 hydration (left) and $KHCO_3$ dehydration (right) are shown.

The values are the difference between the uncatalysed and catalysed rates measured by absorption at 557 nm. The enzyme was assayed in a buffer of 50 mM HEPES, 50 mM $MgSO_4$, 50 mm Na_2SO_4, 0.004 % (w/v) phenol red pH 8.3 with CO_2 as a substrate, and pH 6 for $KHCO_3$ substrate at 20 °C. The data points represent the mean and SD where N≥4. The curve is the fit to the Michaelis-Menten equation from which Km and Vmax were determined. The kinetic parameters derived from these measurments and those of other CAs can be found in in table3.1for comparison.

Table 3-1 A comparison of some parameters of previous described beta carbonic anhydrases with that of Caut-bCA.

Species	Monomer size (kDa)	Oligomeric state	Clade	Hydration		Dehydration		Ref.
				Kcat (s^{-1})	Kcat/Km ($s^{-1}M^{-1}$)	Kcat (s^{-1})	Kcat/Km ($s^{-1}M^{-1}$)	
Clostridium autoethanogenum	14.2	Dimer	F	2.1×10^5	3.1×10^7	6.3×10^4	6.0×10^6	This study
Pisum sativum	24.2	Octamer	B	4×10^5	1.8×10^7	NA	NA	(266, 267)
Cryptococcus neoformans	26	Dimer	A	3.9×10^5	4.3×10^7	NA	NA	(268)
Drosophila melanogaster	30.0	Dimer	B	9.5×10^5	1.1×10^8	NA	NA	(269)
Clostridium perfringens	21.3	Tetramer	D	1.5×10^4	4.8×10^6	NA	NA	(249)
Methanobacterium thermautotrophicus	18.9	Tetramer	D	1.7×10^4	5.9×10^6	NA	NA	(270)
Halothiobacillus neapolitanus	57.3	Dimer	E	8.9×10^5	2.8×10^7	4.6×10^4	4.9×10^6	(239, 271)
Salmonella enterica (stCAI)	24.8	NA	A	7.9×10^5	8.3×10^7	NA	NA	(272)
Salmonella enterica (stCAII)	26.6	NA	C	8.9×10^5	5.2×10^7	NA	NA	(272)

3.3.9 Complementation of E.coli Can<FLK2> mutant.

The *Can* disruption mutant of *E.coli* EDCM636 (220), which lacks a constitutively expressed CA and is unable to grow under atmospheric carbon dioxide pressure, can be complemented by Caut-bCA but not by Caut-γ-CA. Figure 3-11 shows LB-agar plates with *E.coli* DH5α (as a WT control), EDCM636, EDCM636 pMTL82252-bCA and EDCM636 pMTL82252-gCA strains; only the pMTL82252-bCA strain can grow with erythromycin and without azide. I found some indication that *E.coli* EDCM636 cells can spontaneously mutate at a very low rate (mutation rate not precisely determined) regaining the ability to grow without azide (as WT), possibly through loss of the FLK2 transposon that was used to disrupt the *Can* gene or by a mutation of the regulator of *CynT*. Therefore, I repeated this experiment three times with fresh batches of competent cells that did not contain WT phenotypes with the same result. *E.coli* EDCM636 cells containing a pMTL82252-bCAstrepC or pMTL82252-bCA could both grow without the addition of azide, indicating that the C-terminal strep-tag has no important influence on the CA activity. This further supports both the CA status of Caut-bCA and that Caut-gCA is not a functional CA.

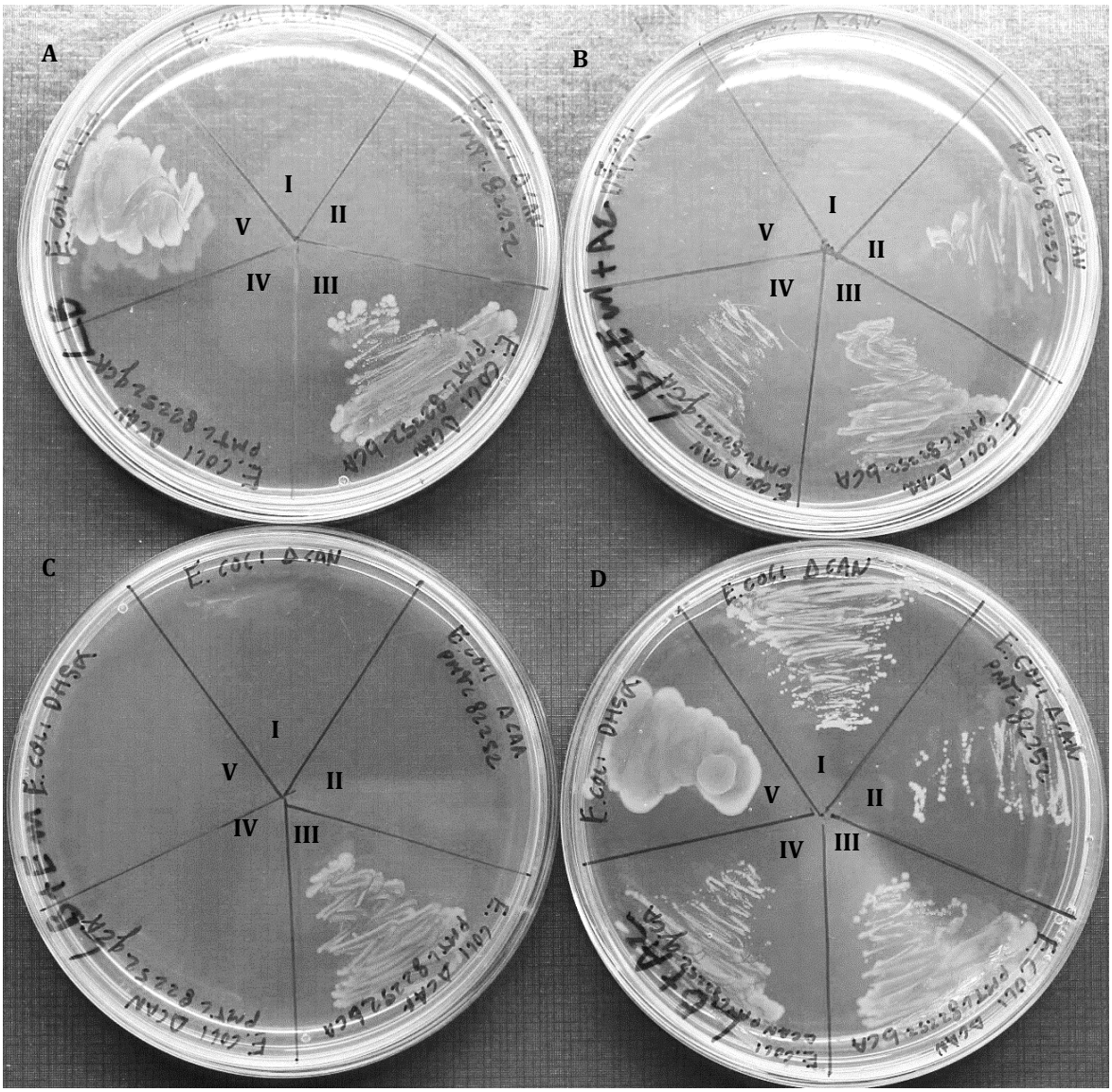

Figure 3-11 LB agare plates showing complementation of a ΔCan E.coli strain by Caut-bCA.

Starting at top moving clockwise the strains on each plate are (I) EDCM636 (ΔCan), (II) EDCM636 (ΔCan)-pMTL82252, (III) EDCM636 (ΔCan)-pMTL82252-bCA, (IV) EDCM636 (ΔCan)-pMTL82252-gCA, (V) DH5α. Plate A (top left) is LB, plate B (top right) is LB+ erythromycin + azide, plate C (bottom left) is LB + erythromycin, plate D (bottom right) is LB + azide. EDCM636 (ΔCan) is sensitive to erythromycin and can not grow without activation of the CynT gene by azide addition. The pMTL82252 plasmids contain an ermB antibiotic resistance marker gene. Only pMTL82252-bCA containing EDCM636 (ΔCan) cells can grow on media with erythromycin without azide showing the ability of Caut-bCA to complement the ΔCan mutation of the EDCM636 strain. The pMTL82252 and pMTL82252-gCA plasmidsdo not give this same ability to EDCM636 (ΔCan) cells. This is further evidence that Caut-bCA is active as a CA while Caut-gCA is not under any tested circumstance.

3.4 Discussion

The β-CA of *C. autoethanogenum* represents a new F-clade of β-CAs, which are the most compact β-CAs known to date. Although previously a *Rhodospirilum rubrum* CA was purified with a similar size (28kDa) at oligomeric state (dimer) no matching gene or protein sequence was identified. Later analysis of this species β-CA showed larger sizes of β-CA monomers (273, 274). Caut-bCA's sequence is quite distinct from other β-CAs but I did find similar kinetic parameters as other β-CAs. Closely related organisms but metabolically distinct species such as *C. kluyverii* and *C. autoethanogenum* harbour β-CAs of different sub-classes. This indicates a physiological or ecological reason for organisms to have evolved specific sub-clades. What this specific role of the separate sub-classes is, requires further research. CAs are inhibited by a range of substances and conditions including acetate and pH. They might shed a light on the importance of the differences between the 6 different subclasses described in this article.

I could not characterise Caut-gCA since I found no activity of purified protein. Whether this is because Caut-gCA does not possess CA activity or my methodology was unsuitable for this protein could not be determined. However, a lack of activity is reported for multiple γCAs in literature (241, 248, 259, 260). Caut-gCA was predicted by Protparam to be unstable. Some γCAs with Fe^{2+} as cofactor require strict anaerobic conditions (275). All growth and purifications were performed under strict anaerobic conditions but the assay that followed immediately after purification was performed under aerobic conditions which may have resulted in rapid loss of activity.

The studied *C. autoethanogenum* CAs sequence is identical in *C. ljungdahlii* and very similar in *Clostridium ragsdalei*, *Clostridium coskatii*. The industrial importance of these very similar strains (86) makes them prime target for metabolic engineering in which recent advances were made (14, 166) and make them likely the basis for future strains. Since optimisation of carbon fixation into useful substances is the prime goal, the research on CAs presented here might prove valuable, especially when engineering bicarbonate dependent carboxylation reactions (236). A recent example of heterologous expression of a pathway allowing for 3-hydroxypropionate (3HP) in *Pyrococcus furiosus* (which lacks native CAs) benefited from co-expressing CA genes improving production 3-fold (237). Since the kinetic parameters of Caut-bCA are similar to other bacterial CAs one can imagine Caut-bCA being used in a similar fashion. Since Caut-bCA is smaller than most other βCAs the metabolic strain of the protein production would be lower at comparative expression levels which might be advantageous. The CA activity shown in this chapter indicates that similar coexpression of CA in metabolic engineering *C. autoethanogenum* is unnescesary unless expression of the gene is not sufficient in the specific context.

This chapter provided evidence for the activity of one CA of *C. autoethanogenum*. The following chapter will discuss research that was performed to understand the function of this CA in the cells of C*. autoethanogenum*.

Chapter 4:

The physiological function of carbonic anhydrase studied by characterisation of a *Caut-bCA::CT* strain of *Clostridium autoethanogenum*

"There are times in life when people must know when not to let go. Balloons are designed to teach small children this." **Terry Pratchett**

4 The physiological function of carbonic anhydrase studied by characterisation of a Caut-bCA::CT strain of *Clostridium autoethanogenum*

4.1 Introduction

The previous chapter discussed the evidence that *C. autoethanogenum* has at least one active carbonic anhydrase encoding gene, Caut-bCA, that is expressed at intermediate level. The aim of this chapter is to present the research undertaken towards understanding the function of the Caut-bCA in the cells by characterisation a ClosTron disruption strain of Caut-bCA.

Considering the ubiquity of CAs in life, including microbial life, it might be found to be somewhat surprising that the precise function of carbonic anhydrases in microbes is not always clear. In many cases, we have little more than hypotheses about their function.

This in contrast to other groups of life where the function is not only known but the function was understood before the enzyme was discovered. The existence of carbonic anhydrases in animals was hypothesised before they were discovered because of the realisation that rapid gas exchange and pH-homeostasis would be too slow without some kind of catalyst (276, 277). Human CAs are still actively researched since CAs are common drug targets (278). In plants and algae CAs have well understood functions in carbon dioxide diffusion facilitation and carbon concentration mechanisms (279, 280). CAs in prokaryotes are proposed to be involved in a range of functions: carbon concentration (252, 281), carbon dioxide transport (253), facilitation of carbon dioxide or bicarbonate consuming or producing reactions (220, 235, 282), pH homeostasis (283), and acetate transport facilitation (252).

It has long been known that both high and extremely low CO_2 partial pressures are detrimental to growth in many bacterial species (284–287). The CA lacking capnophiles already mentioned in the introduction of the previous chapter need relatively high levels of CO_2 to support growth but even the growth of non-capnophilic organisms such as *E. coli* is severely hampered if CO_2 is removed from the supplied air (284, 287). This is because multiple steps in the central metabolism are carboxylation reactions and therefor require CO_2 or HCO_3^-. Without a mechanism for the rapid interconversion of these inorganic carbon species, the necessary turnover rates of common carboxylation reactions that consume HCO_3^- would not be feasible in *Escherichia coli* (220)

In autotrophicly growing *C. autoethanogenum* the bulk of the carbon fixation happens in the WLP and somewhat less in the PFOR reaction. However, there are 64 reactions in the metabolic network where carbon dioxide is involved of those about 21 produce carbon dioxide, 40 that might work in both directions and 3 that are thought only to be in the direction of carboxylation. In addition to these CO_2 carboxylation and decarboxylation reactions nine HCO_3^- dependent carboxylation reactions are thought to be important in the metabolism of *C. autoethanogenum* (Table 4-1), from genome scale model by R. Norman, UoN, unpublished).

With decreasing pH the available HCO_3^- decreases greatly since most of it gets protonated to carbonic acid (H_2CO_3). Especially within lower range of the growth supporting pH range (4.5 – 5.5) of *C. autoethanogenum* HCO_3^- availability can vary widely because of this. When little CO_2 is produced (at low cell densities) and very little is supplied, the bicarbonate depending carboxylation reactions might be limited by substrate availability. The rapid interconversion of carbon dioxide to bicarbonate provided by carbonic anhydrases might be essential in those cases.

In this chapter the creation and characterisation of the insertional disruption (ClosTron) mutants Caut-bCA::CT and Caut-gCA::CT mutant is discussed. The most common phenotype of a bacterial CA mutant is an inability to grow at low CO_2 partial pressures. These conditions were tested in initial pilot growth experiments for both mutants seemed to a lack a clear phenotype. Once CA activity for Caut-bCA protein was confirmed, efforts to find a phenotype for the Caut-bCA::CT strain were increased. Therefore the results presented here focus on the Caut-bCA::CT. The first indication of a possible phenotype was an indication of metabolic changes measured with LC-MS. Further investigation revealed that growth of the Caut-bCA::CT strain is affected at low pH combined with very low CO_2 partial pressures.

Table 4-1 A selection of carboxylating and decarboxylating reactions in the metabolism of *C. autoethanogenum.*

Carbon dioxide reactions (selection)
1 CARBON-DIOXIDE + 2 ATP + 1 AMMONIUM -> 1 CARBAMOYL-P + 1 Pi + 2 ADP
1 UREA + 1 CARBON-DIOXIDE + 1 ATP -> 1 Pi + 1 ADP + 1 urea-1-carboxylate
1 CARBON-MONOXIDE + 1 Fd_{ox} <> 1 CARBON-DIOXIDE + 1 Fd_{red}
1 PYRUVATE + 1 GAP <> 1 DEOXYXYLULOSE-5P + 1 CARBON-DIOXIDE
1 OROTIDINE-5-PHOSPHATE <> 1 UMP + 1 CARBON-DIOXIDE
1 L-ASPARTATE -> 1 L-ALPHA-ALANINE + 1 CARBON-DIOXIDE
1 CO-A + 1 PYRUVATE + Fd_{ox} <> 1 CARBON-DIOXIDE + 1 ACETYL-COA + 2 FD_{red}
1 GLUTACONYL-COA <> 1 CROTONYL-COA + 1 CARBON-DIOXIDE
2 PYRUVATE <> 1 CARBON-DIOXIDE + 1 2-ACETO-LACTATE
1 2-ACETO-LACTATE <> (R)-acetoin + 1 CARBON-DIOXIDE
1 OXALO-SUCCINATE -> 1 2-KETOGLUTARATE + 1 CARBON-DIOXIDE
2 FORMATE + 1 NADP + 1 Fd_{ox} <- 1 NADPH + 2 CARBON-DIOXIDE + 1 Fd_{red}
1 OXALYL-COA <> 1 CARBON-DIOXIDE + 1 FORMYL-COA
1 2-OXOBUTANOATE + 1 PYRUVATE <> 1 2-ACETO-2-HYDROXY-BUTYRATE + 1 CARBON-DIOXIDE
1 2-KETO-ISOVALERATE <> isobutanal + 1 CARBON-DIOXIDE
1 CARBON-DIOXIDE + 2 ATP + 1 AMMONIUM -> 1 CARBAMOYL-P + 1 Pi + 2 ADP
1 UREA + 1 CARBON-DIOXIDE + 1 ATP -> 1 Pi + 1 ADP + 1 urea-1-carboxylate
1 MAL + 1 NAD -> 1 NADH + 1 PYRUVATE + 1 CARBON-DIOXIDE
1 2-OXOBUTANOATE + 1 PYRUVATE <> 1 2-ACETO-2-HYDROXY-BUTYRATE + 1 CARBON-DIOXIDE
1 OXALACETIC_ACID + 1 ATP <> 1 PHOSPHOENOLPYRUVATE + 1 CARBON-DIOXIDE + 1 ADP
1 CO-A + 1 2-KETO-ISOVALERATE + 1 NAD <> 1 ISOBUTYRYL-COA + 1 NADH + 1 CARBON-DIOXIDE
Bicarbonate reactions (all)
1 PHOSPHO-ENOL-PYRUVATE + 1 HCO_3 → 1 Pi + 1 OXALACETIC_ACID
1 GLN + 2 ATP + 1 HCO_3 → 1 CARBAMOYL-P + 1 Pi + 1 GLT + 2 ADP
1 ACETYL-COA + 1 ATP + 1 HCO_3 -> 1 MALONYL-COA + 1 Pi + 1 ADP
2 ATP + L-glutamine + 1 HCO_3 + H2O → L-glutamate + carbamoyl-phosphate + 2 ADP + Pi + 2 H+
1 CO-A + 1 NAD + 1 CH3-MALONATE-S-ALD → 1 PROPIONYL-COA + 1 NADH + 1 HCO_3
1 5-PHOSPHORIBOSYL-5-AMINOIMIDAZOLE + 1 HCO_3 + 1 ATP→1 Pi + 1 N5-carboxyaminoimidazole ribonucleotide+ 1 ADP
1 BCCP-dimers + 1 HCO_3 + 1 ATP → 1 Pi + 1 Carboxybiotin-BCCP + 1 ADP
1 THR + 1 ATP + 1 HCO_3 → 1 PPI + 1 L-threonylcarbamoyladenylate
1 PYRUVATE + 1 HCO_3 + 1 ATP -> 1 Pi + 1 OXALACETIC_ACID + 1 ADP

4.2 Methods

To gain some insight in the function of CAs ClosTron mutants were created as discussed in detail below. Several growth conditions were tested with the mutant strains and WT strains. Growth on CO, with and without CO_2 was tested in batch and in continuous culture while growth on other carbon sources (CO_2 + H_2, fructose & pyruvate) only tested in batch. Product formation was measured using GC and HPLC. Internal metabolite concentration using LC-MS.

4.2.1 Mutant construction

To disrupt the β-CA and γ-CA genes Clostrons were designed using the automated design system on the web site (http://www.clostron.com/clostron1.php) and DNA was synthesised by DNA2.0 (186, 187). For the β-CA one clostron was designed to insert at position of bp 30 (bCA30s::CT) and for γ-CA two different Clostron fragments were designed, one to insert at position of bp 79 of CAETHG_2776 (gCA79s::CT) and one to insert at bp 331of CAETHG_2776 (gCA331s::CT). The Clostron fragment containing pMTL007C-E2-CT plasmids were supplied in lyophilised format and ready cloned in *E. coli* DH10 cells by DNA2.0. The plasmid with the γ-CA clostrons were transferred to *E. coli* CA434 and the β-CA clostrons in Sexpress. The donors were used in a conjugational mating with WT *C.autoethanogenum* as described above. First selection on thiamphenicol YTFagar selected for acquisition of the pMTL007C-E2-CT. Colonies then restreaked at least 3 times om YTF agar with clarithromycin and plates containing thiamphenicol (streaked from clarithromycin plates 2^{th} -4^{th} iteration). 8 colonies that did grow on clarithromycin but not thiamphenicol plates were selected as they should be gCA::CT and bCA::CT strains. The resulting strains were grown up in 15 ml liquid YTF. At OD_{600} of approximately 1.0, 0.9 ml was used to make -80 °C stock, 14 ml was harvested, the cells centrifuged and washed once with PBS. Phenol-chlorophorm-isoamylalchohol extraction of genomic DNA was then performed on the cell pellets. The purity and concentration of the DNA was checked on the Nanodrop and by gel electrophoresis. A PCR was performed using the primer combination FPCA1 - EBSuniversal and FPCA1- RPCA1 for the Caut-gCA or FbCALHA-RgCARHA for the Caut-bCA. 10 µl of the PCR product was checked with gel electrophoresis, on 40µl of the PCR products with the right fragment a PCR clean-up was performed using a PCR-clean-up kit. Cleaned up DNA fragments were then send off for Sanger sequencing.

An effort was carried out to produce both bCA and gCA in frame deletions. These were carried out in similar fashion as described above except F1gCAifd, R1gCAifd, F2gCAifd, R2gCAifd, bCAF1, bCAR1, bCAF2, bCAR2 were used to produce the plasmids *pMTL-BPpdelbCA, pMTL-BPdelgCA.* Both *E. coli* CA434 and *E. coli* Sexpress were used as conjugative donors and primers FgCALHA, RgCARHA or FbCALHA, RgCARHA were used to screen for single cross and double crossover events.

4.3 Results

Three independent gCA (**Figure 4-1** A) and four independent bCA (**Figure 4-1** B) mutants were obtained. PCR and Sanger sequencing confirmed correct insertion of the ClosTrons in the genes. The properties of the resulting strains were explored by several growt experiments.

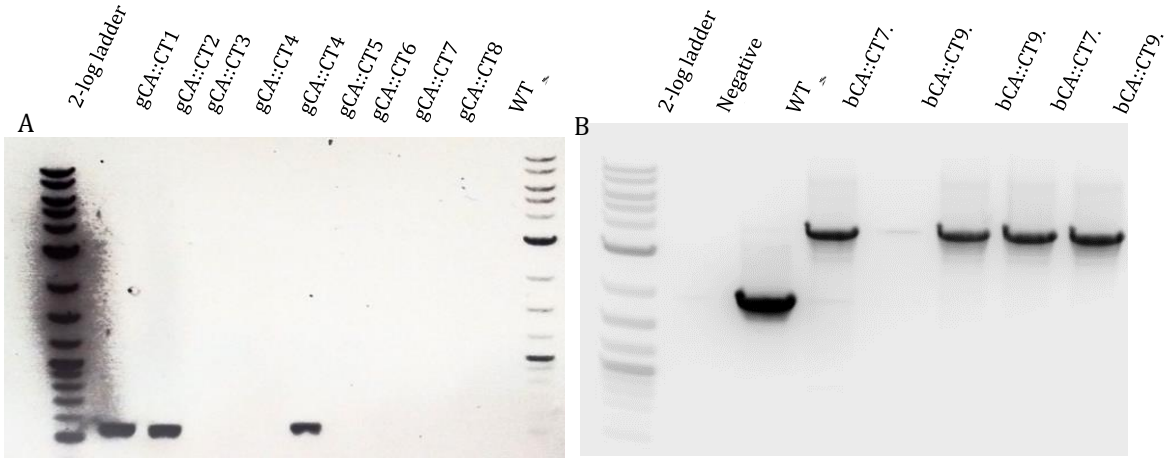

Figure 4-1 PCR screening of Caut-gCA (picture A) & Caut-bCA (picture B) ClosTron mutants.

Performed using the primer combination FPCA1 – EBSuniversal for the Caut-gCA with expected fragment size: 578 bp (gel picture A) or FbCALHA-RgCARHA for the Caut-bCA with expected fragments: 1.9 kb for WT, 3.3 kb for ClosTron insertions (gel picture B). 2-log lader band size top to bottom 10 kb, 8 kb, 6 kb, 5 kb, 4 kb, 3 kb, 2 kb, 1.5 kb, 1.2 kb, 1.0 kb, 0.9 kb, 0.8 kb, 0.7 kb, 0.6 kb, 0.5 kb, 0.4 kb, 0.3 kb, 0.2 kb, 0.1 kb.

4.3.1 Batch culture

4.3.1.1 Comparison of bCA::CT vs WT growth on PETC-MES and CO

The bCA::CT mutant and WT strains preculture was grown up in PETC-MES with fructose which contained clarithromycin in the case of bCA::CT strains. This pre-culture was used to inoculate PETC-MES (with 10 g l^{-1} MES instead of 20 g l^{-1}) in anaerobic serum flasks. These bottles were prepared in the Coy-anaerobic chamber after which the head space was replaced with N_2 via 6 cycles of vacuum and filling and then autoclaved. After cooling, sodium sulphide was added. The medium in the bottles was inoculated to initial OD_{600} ~0.1 and head space was changed for 200 kPa gauge pressure with CO. Bottles were incubated static at 37 °C until first the signs of growth appeared in most bottles when bottles were put in a shaking incubator. When pressure had dropped to ~100 kPa gauge pressure in at least one bottle all bottles were topped up with CO to 200 kPa gauge pressure.

Samples for, OD, pH, LC-MS and HPLC were taken. Headspace pressure was measured at every sample point and its composition was analysed using GC twice, at ~70h and at ~254 h.

Results of this experiment show somewhat slower growth, faster drop in pH, somewhat lower ethanol/acetate ratios and lower 2,3-butanediol level in the bCA::CT strain vs WT however the variation between cultures was high so this is not significant (Figure 4-2). At ~70 h bottles of both strains contained approximately ~24 kPa (8%) CO_2 and had consumed ~30 kPa CO (10%). At ~254 h the WT had 80 kPa CO left while bCA::CT had ~69 kPa CO left while both had ~120 kPa CO_2 in the headspace.

Untargeted LC-MS was performed by Laudina Safo. Although the growth as measured according the parameters mentioned above was varied and no clear phenotype was found, a principal component analysis (PCA) showed separation between WT and bCA::CT. Therefore partial least squares discrimination analysis (PLS-DA) could be performed and discriminated strongly between the two strains. PLS-DA discrimination on its own should not be used as evidence for a phenotypical difference between the strains since PLS-DA is known for strongly overfitting data. However the loading table of PLS-DA of metabolomics can be used to identify compounds that might discriminate between strains. An attempt to identify the top 20 metabolites of the loading table of PLS-DA showed that most compounds could not be identified with certainty (appendix figure 10.1) however the metabolite that was found highest differentiating for the mutant was likely ketoisovaleric acid or a related compound. This likely difference between the WT and the mutant inspired further experiments.

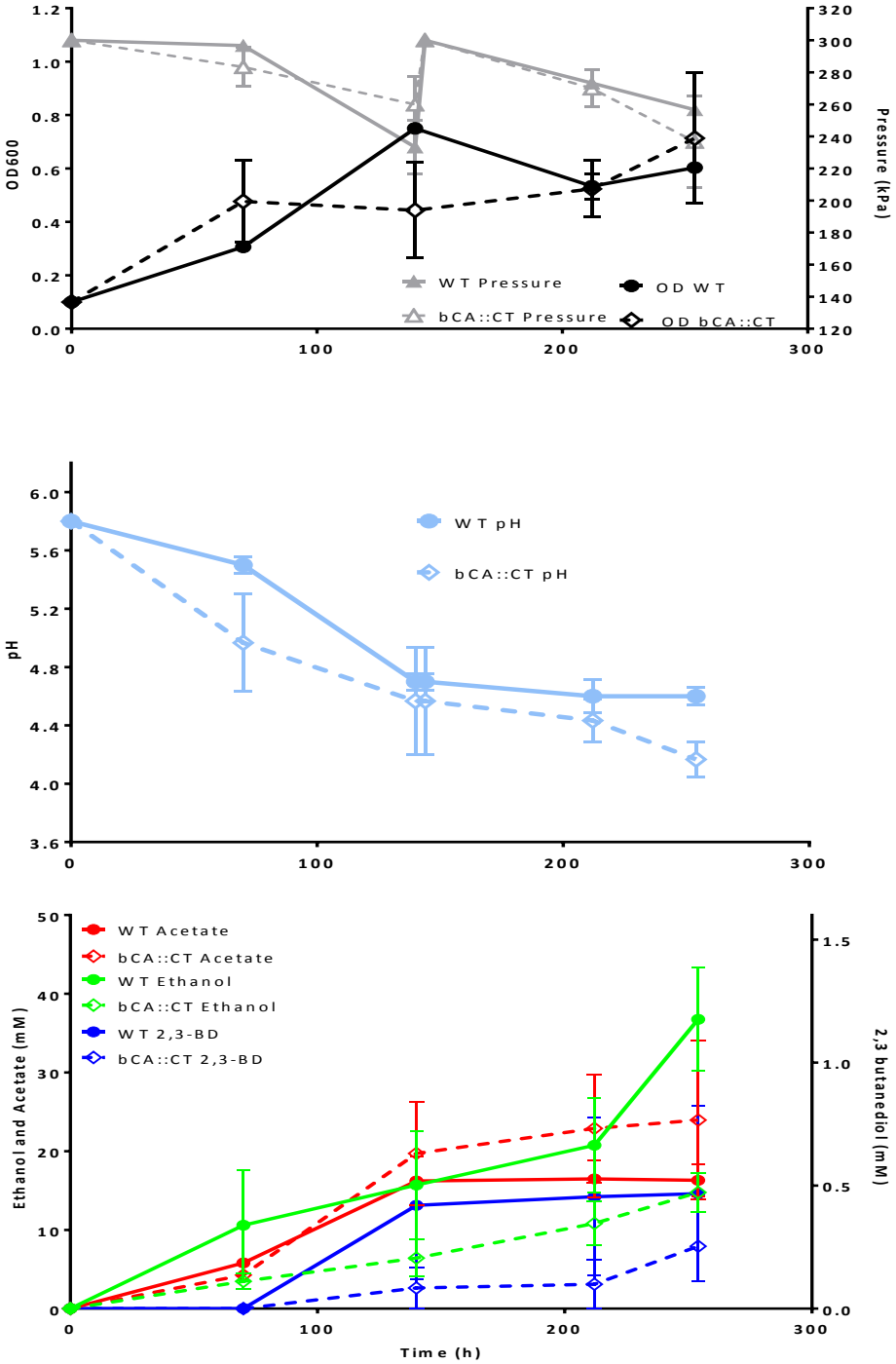

Figure 4-2 Growth of the bCA::CT compared to WT.

The graphs depict the measured parameters of the growth experiment. Top graph shows headspace pressure and optical density, middle graph shows the pH, bottom graphs show the product concentrations. At 144 h CO was added to the headspace to all bottles so all bottles had 300 kPa in headspace. Results show slightly slower growth, faster drop in pH, somewhat lower ethanol/acetate ratios and lower 2,3-butanediol level in the bCA::CT strain vs WT however the variation between cultures was high and result not significant.

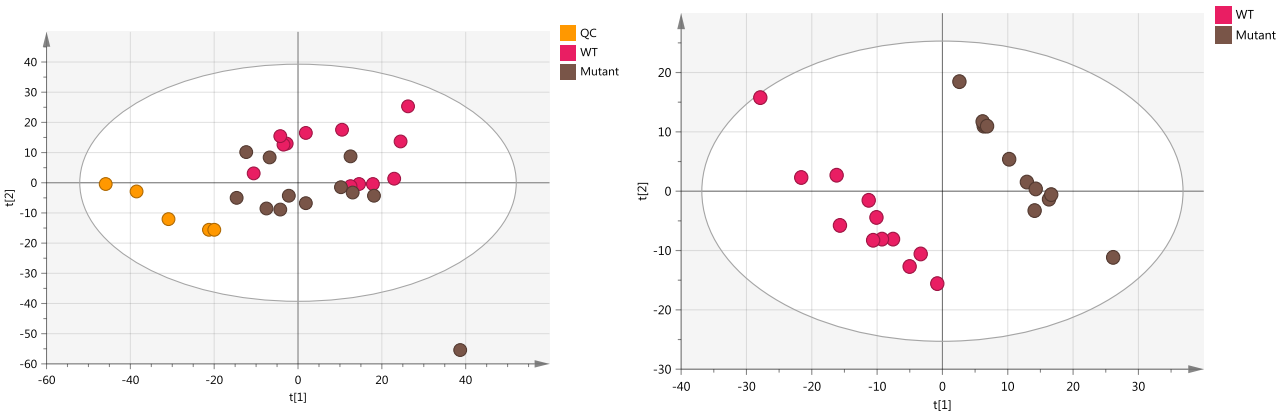

Figure 4-3 Multivariate analysis of WT and bCA::CT strains untargeted metabolomics.

PCA score plot on the left and PLS-DA on the right. Analysis performed and figures produced by Laudina Safo. The QC plotted in the PCA should be found in the centre between the WT and mutant howver since QC, WT and bCA::CT mutant groups are somewhat separated a PLS-DA was performed.

4.3.1.2 Effect of CO_2 on bCA::CT and WT growth with PETC-MES and CO

Since the LC-MS results of the previous described experiment indicated some difference in metabolism between the strains a follow up experiment was performed under slightly different conditions. Differences with above described experiment were the use of standard PETC-MES, lower initial ODs, and inclusion of, low CO_2 (none added, similar as previous experiment) and high (~50 kPa) CO_2 concentration in head space. LC-MS was performed targeted and untargeted allowing for quantified metabolite concentrations. Initial total pressure in the headspace was 250 kPa (150 kPa gauge). Head space was 'topped up' twice, once at 230 h and once at 390 h both with pure CO to 200 kPa gauge pressure.

Results of all growth parameters except for internal metabolites are summarised in

Figure 4-4. It appears that WT initially grew faster than the bCA::CT strain, specifically in the high CO_2 atmosphere. Again no indication of the expected phenotype was found as both strains grew in low CO_2 partial pressures. Otherwise no significant differences were found in this experiment.

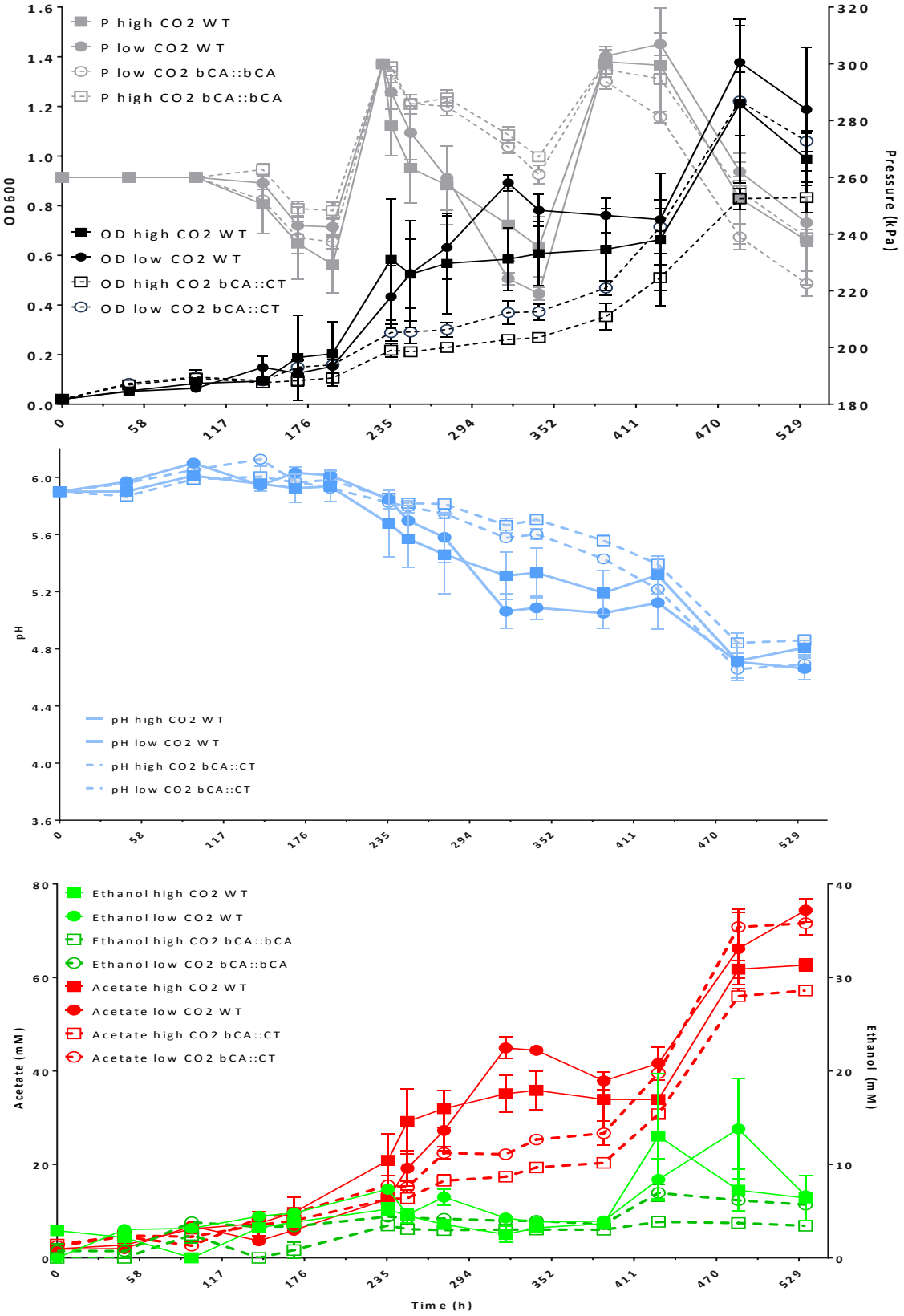

Figure 4-4 Growth of WT and Caut-bCA::CT strains on CO in low and high CO2 gas phases.

Overview of second growth experiment. In the top graph the optical density and headspace pressure are plotted, middle graph depicts the pH and the product concentrations are plotted in the bottom graph. At 230 h and at 390 h CO was added to a total pressure of 300 kPa. The Caut-bCA::CT strains initialy reach lower optical densities however at the end of this experiment these differences had disappeared.

Untargeted LC-MS performed (in collaboration with Laudina Safo) on the samples show discrimination between both strains and conditions as shown by PCA and OPLS-DA plots (Figure 4-5). The targeted analysis could quantify 68 compounds. These were further analysed using metaboanalyst. As with the untargeted analysis discrimination in WT vs bCA::CT mutant was possible with PCA alone, however only principal component 1 (PC1) discriminates between these groups while other PCs do not discriminate much for the strain differences. A PLS-DA discriminates only slightly better. Both PC1 and PC2 add to the discrimination between the strains in the case of the PLS-DA.

The loading plot of this PLS-DA and the clustered Heatmap analysis of the top 14 metabolites show that the mutant metabolome is enriched with 2-keto-isovalerate, hydroxyisocaproic acid and 3-phosphoglycerate. Wildtype compared to bCA::CT strain is enriched in glyoxylic acid, oxalic acid, mesaconic acid and citraconic acid amongst others.

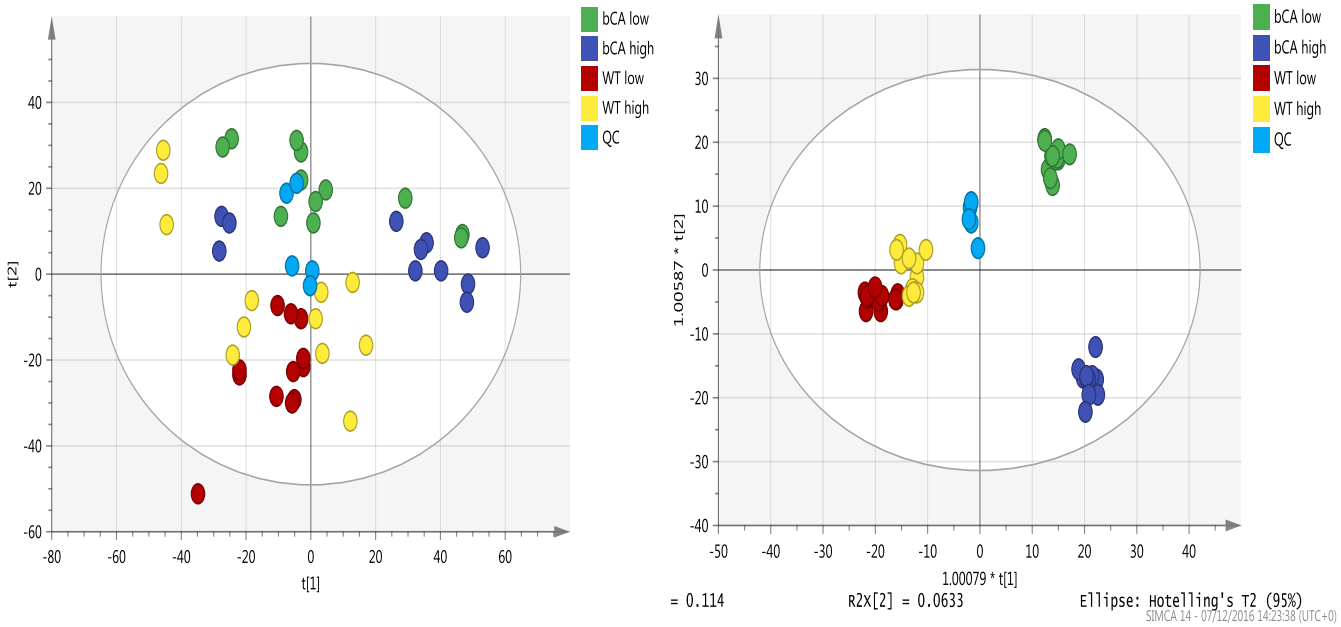

Figure 4-5 Untargeted metabolomics results multivariate analysis of WT and bCA::CT strains.

PCA analysis (left plot) and OPLS-DA (right plot) show discrimination between the four tested conditions. As a quality control (QC) an even mixture of all samples is included which should show up in the centre of the plots. The QC was found in the centre of the plots and in both analyses the strains sample groups cluster closer together than the initial CO_2 condition samples.

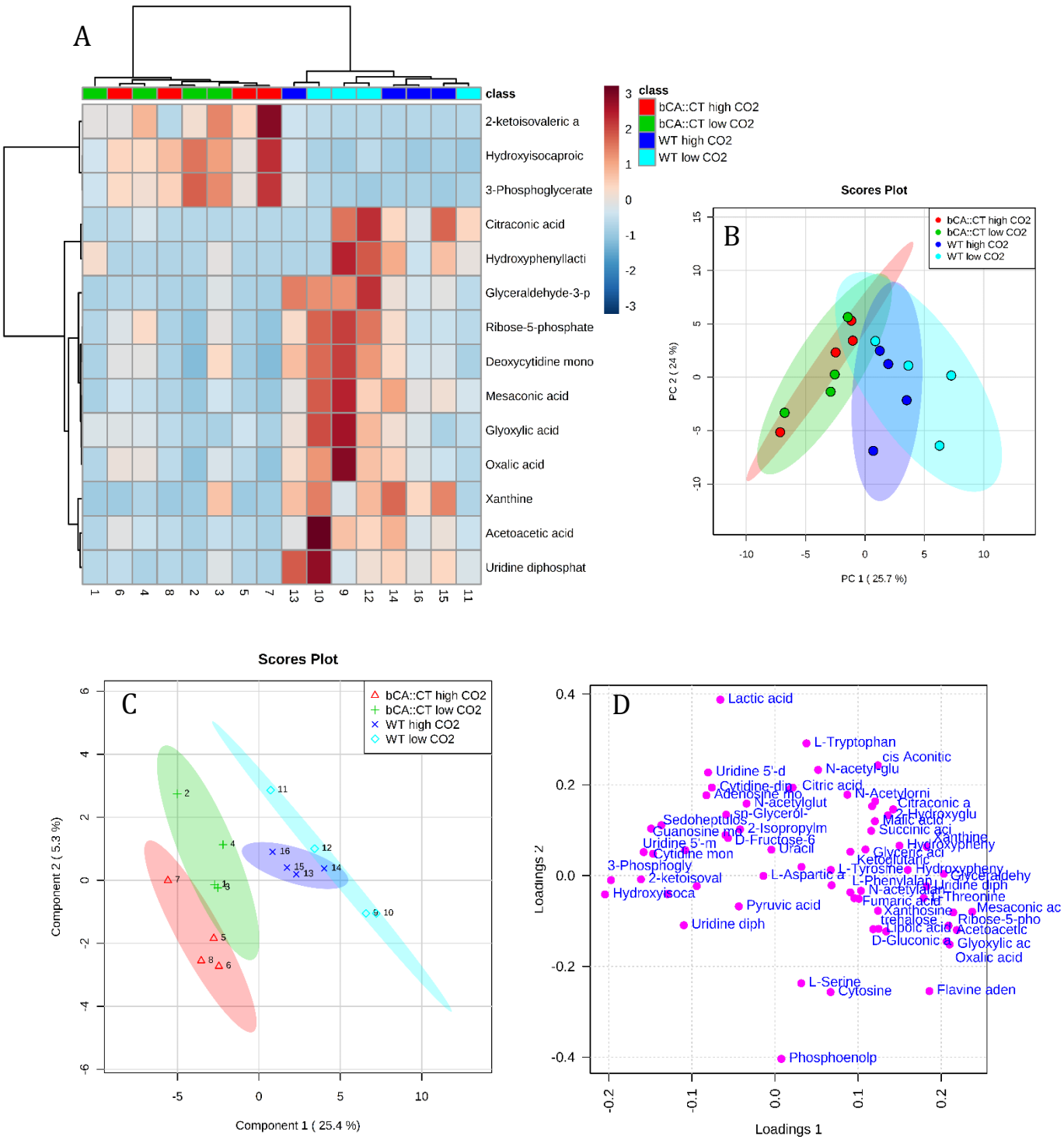

Figure 4-6 Multivariate analysis of metabolomics of WT vs mutant growth on CO with low and high CO_2.

Panel A (top left) is a clustered heatmap of the top 14 most differentiating metabolites, **panel B** (top right) is PCA score plot, **panel C** (bottom left) is PLS-DA score plot, **panel D** (bottom right) is the loading plot of the PLS-DA analysis. The mutant metabolome is enriched with 2-keto-isovalerate, hydroxyisocaproic acid and 3-phosphoglycerate. Wildtype compared enriched in glyoxylic acid, oxalic acid, mesaconic acid and citraconic acid amongst others.

4.3.1.3 Growth on Carbon dioxide and Hydrogen

In a serum bottle based growth experiment on carbon dioxide as carbon source and hydrogen as energy source. The headspace consisted of 100 kPa N_2, 150 kPa H_2 and 30 kPa CO_2. After no further increase of optical density nor significant further decrease of headspace pressure was observed for three days the headspace was topped up to 180 kPa with H_2. End point measurement of product formation show not significant (p value=0.3) 8 x lower ethanol concentrations in the mutants.

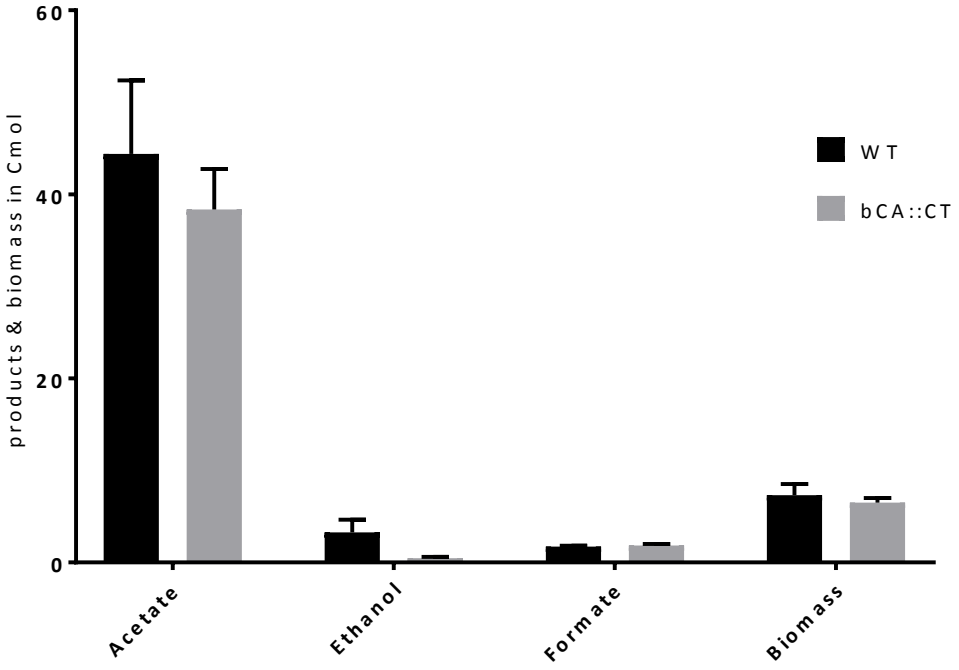

Figure 4-7 End point values of WT and bCA mutant strain comparison grown on CO_2 and H_2.

Acetate, ethanol and biomass are lower at endpoint and formate slightly higher however none of these differences were significant.

4.3.1.4 Effect of initial pH on growth of WT vs bCA::CT with pyruvate and fructose

To study the potential effect of pH on HCO_3^- availability on the growth of the bCA::CT and WT strains these grown at several different pH very low CO_2. For this experiment media was prepared without exposure to the high CO_2 anaerobic chambers atmosphere. The carbon and energy sources used were pyruvate and fructose for these experiments.

Growth was tested at pH 3.5, 4.5, 5.0, 6, 7 and 8. As expected no growth was observed in at pH 3.5 , 7 and 8. Growth for WT was limited at pH 4.5 while the mutant showed no growth at that same pH at all. At pH 5.0 one out of three tubes inoculated with the mutant did not show signs of growth but the other two grew to similar end OD as WT although with prolonged lag phase. At pH 6 one tube out of three inoculated with WT did not show signs of growth while the other two tubes grew as normal (Figure 4-8). An interesting side observation is that more ethanol was formed at pH 4.5 vs higher pH.

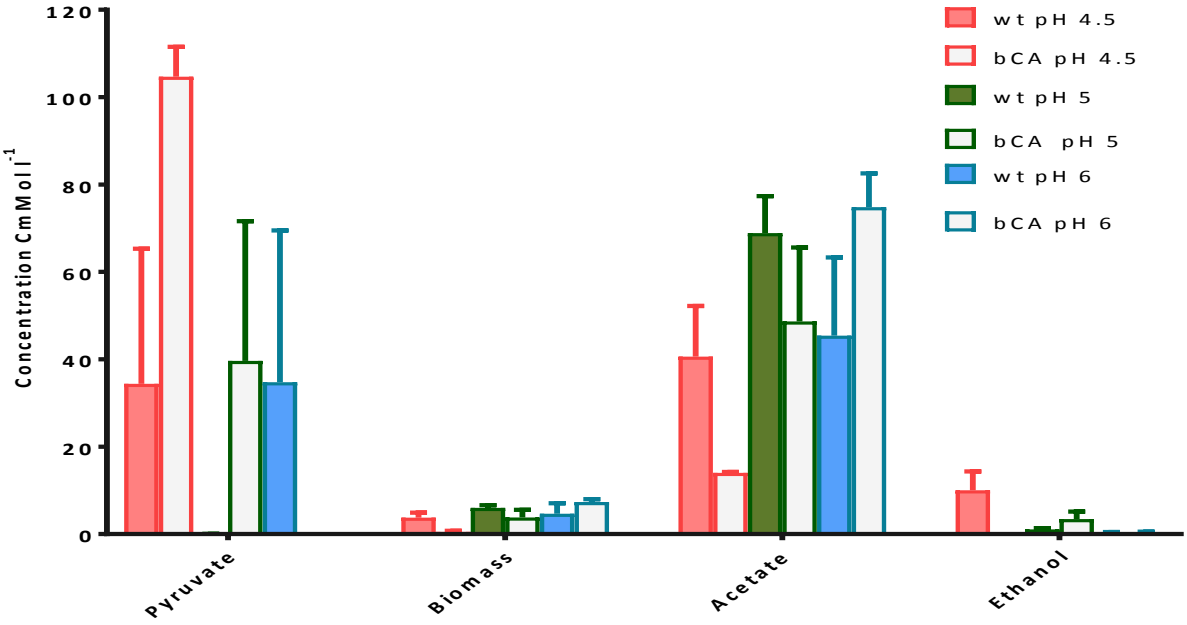

Figure 4-8 The end point parameters of WT and bCA::CT mutant strains at 3 different pH.
The cultures with an initial pH 4.5 only showed growth for WT while the bCA:CT mutant no visisble biomass accumulated.

Using fructose as carbon source at initial pH 4.5, pH 5.0 and pH 5.5 gave similar but more consistent results. At pH 4.5 no growth was observed with fructose for any bottle (N=3) inoculated with the mutant strain and WT growth was severely hampered. At pH 5 no growth was notable for mutant strains while WT reached a close to normal end OD while both strains behaved as wild type at pH 5.5 (Figure 4-9).

pH 5.5		pH 5.0		pH 4.5	
WT	bCA::CT	WT	bCA::CT	WT	bCA::CT

OD_{600}	1.7	1.8	1.3	0.07	0.08	0.06

Figure 4-9 A photograph of fructose grown cultures at initial of pH 5.5, pH 5.0 and pH 4.5.

Below the bottles is the average OD_{600} of three replicates. At lower initial pH the growth of the bCA::CT mutant is hampered compared to WT. This difference is most clear at the initial pH of 5.0 where WT reaches an OD_{600} of 1.3 while none of the mutant strains showed significant growth. A side observation visable on this picture is the colour of the culture. The cultures are more amber/yellow coloured at pH 5.5 while the WT cultures at pH 5 were lighter in colour. This is in line with other observations where cultures of *C. autoethanogenum* that are growing closer to optimal conditions are more amber/yellow while cultures under conditions that are expected to be more stressful are more pale in colour.

4.3.1.5 The effect of CO_2 and pH on growth of bCA::CT in continuous culture

Growth of the *C. autoethanogenum* bCA::CT mutant was studied in continuous culture. We used standard reactor medium and CO as carbon and energy source. Bioreactors were inoculated with 150 ml active growing culture (OD_{600} 0.6-0.9) in PETC-MES with sodium sulphide as sulphur source and carbon monoxide as carbon source. CO_2 addition to the gas feed was essential to start up cultures of the mutants successful which is not necessary for WT. Two attempts of starting up a bioreactor with this strain failed and only when we started to add CO_2 to the gas feed growth was observed. This CO_2 addition could be stopped at higher biomass concentrations when CO_2 production resulted in higher partial pressures. It is likely that CO_2 partial pressure (without CO_2 addition) at low cell densities was lower than in our bottle experiments since the medium is continuous stripped of dissolved gases by the sparging of the N_2 and CO gas mixture.

A switch from pH 5 to pH 4.5 was attempted in decreasing steps of 0.1 pH per day without addition of CO_2 in gas feed. At pH 4.7 the culture became unstable and a crash could not be avoided. After recovery another decrease the pH to 4.6 was attempted with CO_2 added to the gas flow which did not result in a crash however we did not test if this pH could be hold prolonged periods.

Addition of CO_2 to the gas flow resulted in lower ethanol/acetate molar ratio. If this is specific for this mutant or if this is also true for WT is unknown since no experiment with CO_2 addition on WT was performed.

A comparison of all LC-MS data from all bioreactors in this thesis distinguishes the different conditions. The PCs beyond PC3 still explain variation and PC5 together PC1 distinguish best between the mutant and WT strains. The loading plot of a PLS-DA plot and heat map show again the differentiating feature of 2-ketoisovaleric acid although this was only clear for two of the sampled periods.

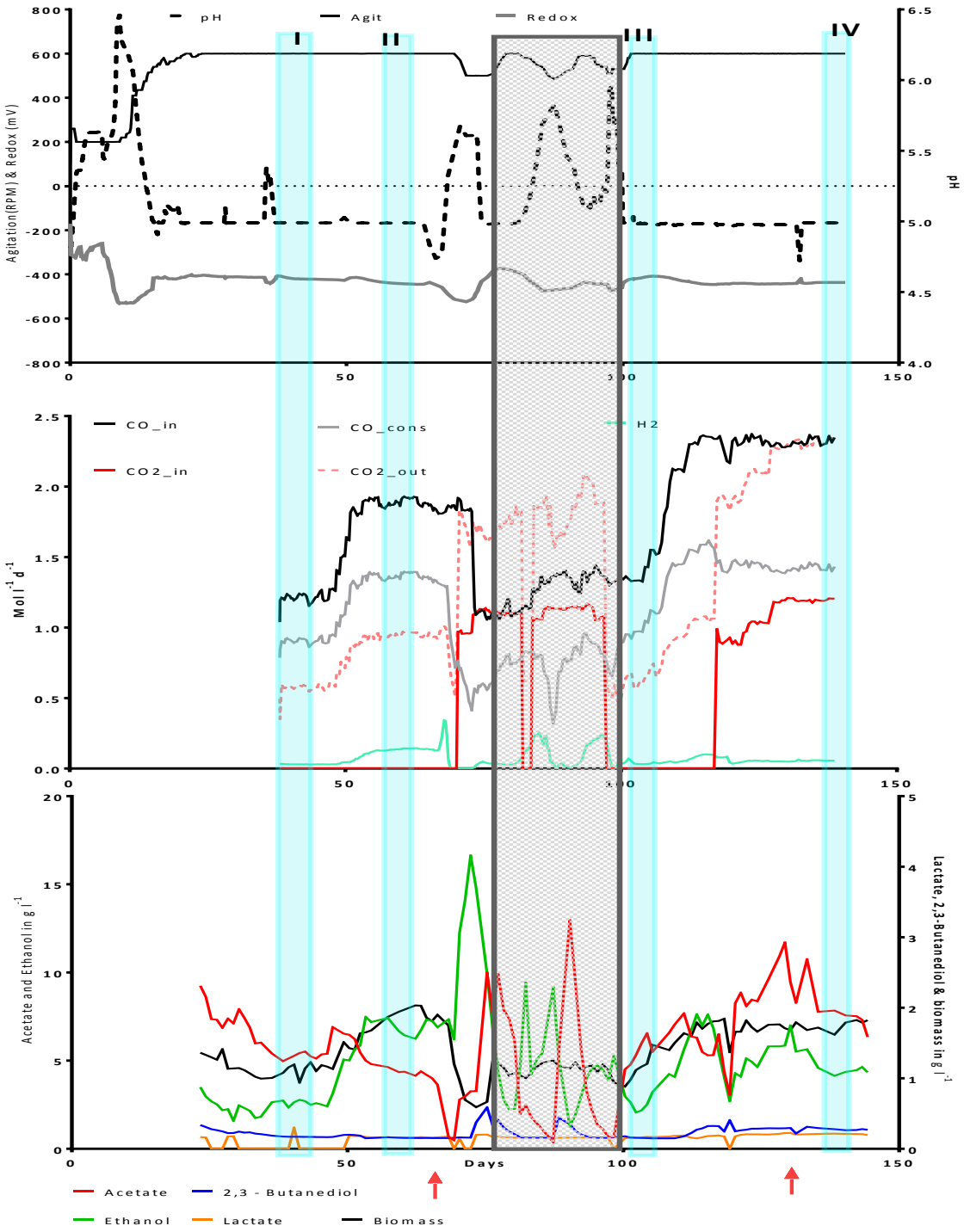

Figure 4-10 Overview of the variables of the reactor run with bCA::CT.

For a while this reactor was suffering from a faulty vitamin stock solution used to make the media (see chapter 5) this period is marked by the grey box. Blue boxes indicate metabolomics sample periods. Red arrows indicate pH decrease caused by stopping pH control by NaOH addition. A pH lower than 4.7 without CO_2 adittion was not sustainable as the bioreactor culture crashed. With pH addition this same pH was apparently more stable. These experiments ware not repeated but are in line with out findings in batch. CO_2 addition was beneficial at the low biomass levels during the initial culture start up but could be omitted when the culture produced significant CO_2

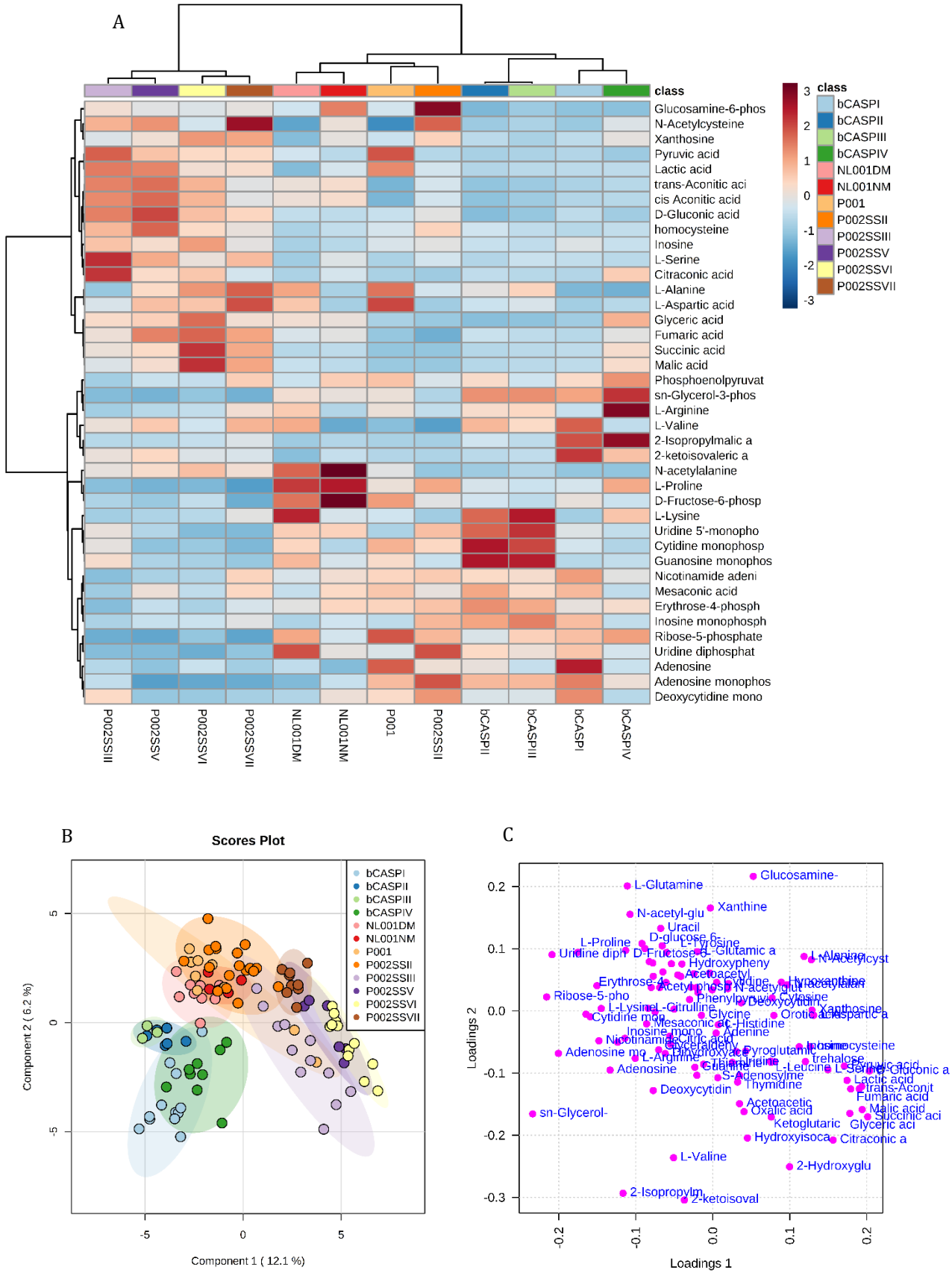

Figure 4-11 Multivariate analysis of metabolomics of bCA::CT strain bioreactor and WT bioreactor runs.

Panel A (top figure) is a clustered heatmap analysis with top 40 most discriminating metabolits as determined by PLS. Panel **B** (bottom left) is the scores plot of PLS-DA and **panel** C (bottom right) the loading plot of same PLS-DA**.** snGlycerol 3-phosphate, 2-isopropylmalate and 2-ketoisovalerate are the metabolite contributing strongest to the discrimination of bCA::CT and WT

4.4 Discussion

Initial experiments of growth of the *Caut-bCA::CT* on CO without CO_2 addition did not yield the phenotype expected of a CA mutant i.e. no growth at low CO_2 partial pressures. This can have multiple possible causes: insufficient CO_2 removal, closed bottles causing a CO_2 rise due to non-growth associated metabolism, carbon source depended effects, pH dependent effects. All of these likely have played a role in not identifying the phenotype.

Although the initial growth experiments did not show the typical growth phenotype of a CA mutant, the metabolomics results of those experiments pointed toward some effects of CA disruption. The mutation showed higher levels of intracellular 2-ketoisovaleric acid and to a lesser degree to other leucine precursors in most of the LC-MS data. 2-keto-isovalerate is a precursor of hydroxycaproic acid and can be decarboxylated to isobutanal or isobutyrylCoA, reactions that might suffer from high CO_2 concentration and thus might benefit from CA activity. This might also explain the somewhat surprising fact that the mutant was reaching somewhat lower end ODs at in the higher CO_2 conditions in the batch growth experiment. It is unclear why specifically this metabolite is so differentiating and why other decarboxylation reaction do not suffer equally from the mutation. Another finding was that glyoxylate and aconitate were more abundant in the WT. These metabolites are part of, or related to the glyoxylate cycle/citric acid cycle which is thought to benefit from presence of CA activity because the so called anapleurotic reactions that produce oxalacetic acid are bicarbonate consuming.

Our bioreactor run culture did not start initial growth without CO_2 in the gas flow. This CO_2 addition could be stopped at higher biomass concentrations when CO_2 production resulted in higher partial pressures. WT does not require CO_2 for start-up phase. It is likely that CO_2 partial pressure (without CO_2 addition) at low cell densities was lower in our bioreactor set-up than in our bottle experiments since the medium is continuous stripped of dissolved gases by the sparging of the N_2 and CO gas mixture.

The mutant bioreactor culture was instable below pH 4.8 without CO_2 addition. Previous experiments performed in our lab showed that bioreactor culture of WT *C. autoethanogenum* under similar conditions can be stable at pH 4.5 (personal communication A. M. Henstra). The combination of these observations of a need for CO_2 addition at low cell densities and instability at lower pH implied that the classical phenotype could be found by removing CO_2 more thoroughly and / or by lowering pH to lower equilibrium HCO_3^- concentration.

Indeed, at least on pyruvate and fructose, a pH depended phenotype was found when we thoroughly removed CO_2. This pH dependency is likely caused by the fact that at lower pH less HCO_3^- is dissolved.

Why was it so hard to find a phenotype for *Caut-bCA::CT* strains if the phenotype for the *E. coli* Can::FLK2 is so clear? Next to all the reasons already mentioned for initially not finding a phenotype one can speculate that it is an effect of growth rate and metabolic rate. Little is known about minimal growth rates of specific organisms (in contrast to maximum growth rates) however it is easy to imagine that an organism that has about ten times higher maximum growth (*E.coli* μ_{max}=~2 h^{-1} vs *C. autoethanogenum* μ_{max}=~0.15 h^{-1} (288, 289) also has a higher minimum growth since the system is optimised for faster growth. If this is true this might mean that lower metabolic rates are viable in *C. autoethanogenum.* This in turn might mean that lower levels of CO_2 can provide HCO_3^- at a rate that is proficient to keep *C. autoethanogenum*'s metabolism working, while that of *e.coli* would not be able to cope with this.

It that cannot be fully discarded that *C. autoethanogenum* has two carbonic anhydrases. No activity was found for the putative γ-CA nor did pilot growth screening of a Caut-gCA mutant show a phenotype however it is possible that this is a functional CA under certain physiological conditions. Attempts to make a double knock out with our allelic exchange in-frame deletion system failed. This cannot be seem as evidence for the essentiality of the genes since most attempts to create mutants with the system in this organism failed. The very recent development of our CRISPR-CAS based system would likely allow for a double knock-out to be produced.

Together with the findings presented in chapter 3, this chapter provides evidence for a functional CA in *C. autoethanogenum*.

Chapter 5:

The effects of nutrient limitation on the metabolism of *Clostridium autoethanogenum* studied in batch and continuous stir tank reactors

"Theoretically I am supposed to divide my time between finding what life is and trying to preserve it by saving the world, at present the world seems to be beyond saving, and that leaves me more time free for biology." **Leo Szilard, Inventor of the Atomic chain reaction and of the Chemostat.**(290)

5 The effects of nutrient limitation on the metabolism of Clostridium autoethanogenum studied in batch and continuous stir tank reactors

5.1 Introduction

This chapter discusses the effects of phosphate limitation on the metabolism and product profile of *C. autoethanogenum.* Nutrient limitation induced shift in product formation is a well-known phenomenon of which just a few examples follow. Non-carbon limitation is a common way to induce Polyhydroxybutyrate (PHB) production in bacteria such as *Cupriavidus necator* (*Ralstonia eutropha*) and *Rhodobacter sphaeroides* (291–293). Phosphate limitation was successfully employed to optimise butanol, acetone and ethanol production by *Clostridium acetobutylicum* (294). In *Clostridium sphenoides* phosphate limitation can induce the methylglyoxal pathway and production of 1,2- propanediol and lactate (295).

As mentioned before(Chapter 1), the first ethanol production by an acetogen was discovered under phosphate-limiting conditions (80). It is no surprise then that nutrient limitations (Ammonium, phosphate, trace elements, vitamins) investigated in several successful attempts to increase ethanol production in the Clostridial acetogens of industrial importance (193, 296–299).

The two most recent publications that study *C. autoethanogenum* or *C. ljungdahlii* in continuous stir tank reactors (CSTR) at steady state did not have predefined non-carbon limitation. However nutrient limitation played a role in these studies. Richter *et al.* used a two stage continuous fermentation approach with *C. ljungdahlii*, with first a 1-L reactor stage operated at acidogenic condition, followed by a 4-L reactor with a cell recycler operated at solventogenic conditons. The transcriptomic analysis revealed a severe sulphur limitation in the second stage which they concluded causes the change in metabolism, from mostly acetate formation in the first reactor stage to a metabolic state that produced mostly ethanol in the second (140).

Valgepea *et al*. employed a single stage CSTR approach where gas transfer to cells was regulated by agitation (137). At higher agitation rates higher gas-liquid mass transfer rates cause higher cell densities which they claim cause a shift in molar ethanol/acetate ratio from 0.16 to 1. Their reactors did not seem to be able to have better ratios then 1 at steady states. Based on transcriptomics data they assume their cultures to be in carbon limitation at all stages.

It is generally assumed that nutrient limitation is binary/discrete, in the sense that only one nutrient is limiting in one situation. This binary model has the advantage that it is simple and makes sense when one nutrient is predominantly limiting. However, this model does not properly describe a transition from one type of nutrient limitation to another. In this model the transition would be sudden from one state where one of the nutrients is limiting to the other state where the other is limiting. However, if the cell metabolism is adapting to the change from one type of nutrient limitation to another then dual nutrient limitation is possible (300).

To investigate the effects of nutrient limitation on product formation in *C. autoethanogenum*, I started with small scale batch pilot experiments with 4 different organic carbon sources with distinct properties at a series of phosphate levels. Next to the common carbon sources pyruvate, fructose and xylose, the interesting methyl-pentose rhamnose was included. Rhamnose is one of the few biologically active L-enantiomer sugars and its degradative pathway is quite dissimilar to that of other sugars in most bacteria. It is remotely related to the previously mentioned methylglyoxal pathway. In *E.coli* lactate is the main product of rhamnose degradation when grown aerobically, while under anaerobic conditions 1,2 propanediol is the main product (301). In the Clostridiales *Acetonema longnum* and *Clostridium phytophermentans,* rhamnose strongly induces microcompartments and products not produced under other conditions such as 1,2-propanediol and 1-propanol (302, 303). This chapter and chapter 6 will provide evidence that *C. autoethanogenum* also produces these two products when grown on rhamnose.

From these pilot batch experiments we learned that phosphate limitation affects product formation and had an indication what level of phosphate would be growth limiting. To follow this up I started the first bioreactor experiment (PL001) which was used to establish the phosphate concentration that causes a shift in the product formation and to establish the minimum of phosphate required at steady state. When these parameters obtained we started a second bioreactor. In this reactor several phosphate limited and carbon limited steady states were established and it was used to investigate the effect of increased CO gas flow under phosphate limited conditions.

5.2 Batch growth studies on phosphate limitation

5.2.1 Methods

A batch growth experiment to find the phosphate limitation threshold with several carbon sources was performed as pilot experiment for the bioreactor studies. Inoculum was grown in minimal PETC-MES with Fructose. The inoculum was washed with PETC-MES without carbon source and phosphate. PETC-MES media was adapted so that a series of phosphate concentrations (0 – 4.4 mM) was produced by adding appropriate amounts of potassium phosphate. Standard PETC-MES contains 1.47 mM phosphate. Each carbon source, pyruvate, xylose, fructose and rhamnose, was added at a concentration of 40 mM. Optical density, substrate consumption and product formation were measured.

5.2.2 Results

The results shown in Figure 5-1 and discussed below are end-point results taken at least 5 days after maximal OD had been reached in all cultures of the carbon source. In the case of the fructose and xylose cultures with 0.15 mM phosphate and higher the carbon source was still present indicating that something else than carbon source availability was limiting (Figure 5-1 C & D). Higher ethanol / acetate ratios were found associated with higher phosphate ratios (Figure 5-2 A). At phosphate concentrations <0.15 mM less biomass was formed and accordingly carbon source was consumed less in a dose response fashion indicating that phosphate was likely limiting at that threshold. Growth limitation does not limit non-growth associated metabolism as at lower phosphate levels the mass ratio of product / biomass rises sharply for fructose and xylose (Figure 5-2 C).

Rhamnose was consumed fully in all cases above the phosphate limitation threshold except for the highest phosphate concentration in which lag phase was more prolonged and maximum optical density lower and some precipitate had formed after inoculation (confirmed by microscope that this was not biological growth). Biomass was lower at phosphate concentrations <0.15 mM and decreased in line with the phosphate decrease. To my knowledge, this pilot experiment was the first time products of *C. autoethanogenum* grown on rhamnose were analysed and the first time 1,2-propandiol as a native product was noticed. At higher phosphate concentrations (>0.15 mM) 1,2-propanediol molar ratios were approximately 0.6 while for lower phosphate concentrations those ratios dropped below range from 0.18 to 0.1 (Figure 5-2 B). The products / biomass mass ratio did not rise as sharply at lower phosphate concentration as those of fructose and xylose (Figure 5-2 B).

Lactate is a product of rhamnose degradation in aerobic grown *E.coli*. In our experiments, lactate was found in two rhamnose grown cultures. A small, initially unidentified, peak was observed in the HPLC data of the rhamnose grown cultures. It was suspected to be 1-propanol and indeed in subsequent growth experiments on rhamnose this product could be identified and quantified as will be discussed in the next chapter.

2,3-Butanediol was only above detection limit in the pyruvate grown phosphate limitation experiments. The high detection limit is caused by the fact that the 2,3-butanediol peak falls within the shoulder of the MES peak in our HPLC data which makes detection and quantification challenging. It is likely that the some 2,3-butanediol was also formed in the other cultures.

Pyruvate was consumed fully in all tubes containing more than 0.015 mM phosphate indicating that for most of the dilution range carbon was not added in excess. In the pyruvate cultures the growth appears to be limited by phosphate concentration below 4.5 mM unlike what was found in any other condition, including the bioreactor studies described below. However in the cultures with 0.15mM and below a shift in product formation was noted with lower levels phosphate relate to higher ethanol levels (Figure 5-2 a). In the case of the three previously sugars the products / biomass mass ratio did not change much above 0.15 mM phosphate but a strong rise in this ratio was noted at lower phosphate concentrations. In contrast, the pyruvate cultures showed a higher ratio with each decrease in phosphate concentration except at 0.0 mM phosphate (Figure 5-2 C).

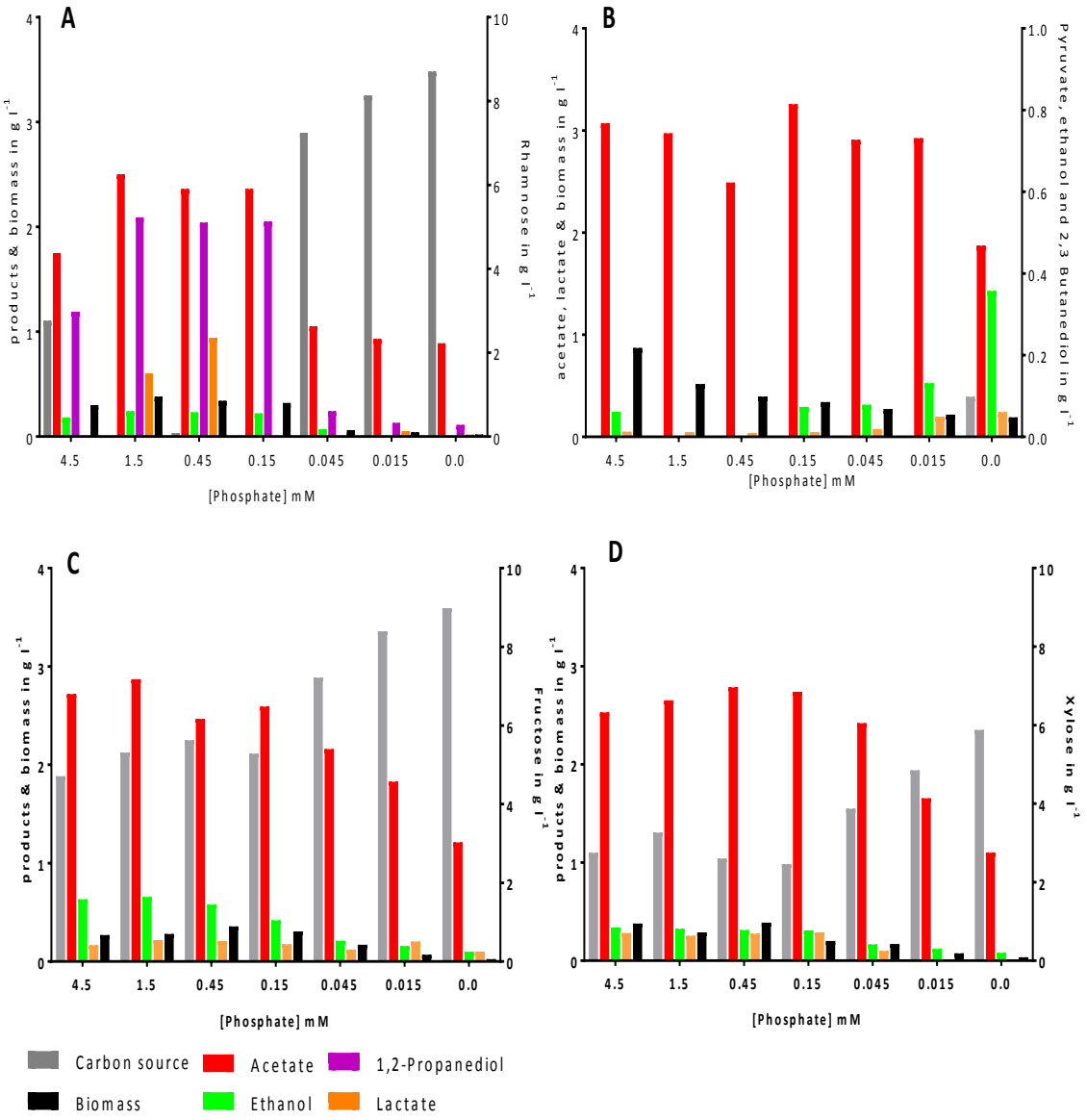

Figure 5-1 Effect of phosphate limitation on product formation and growth in *C. autoethanogenum* with four different carbon sources in open tubes in an anaerobic workstation. Results shown are end point results taken at least 5 days after maximum OD had been reached in all tubes of the carbon source. Panel A shows the results of rhamnose panel B those of pyruvate, C of fructose and D the results with xylose as carbon source. All graphs have the same axes scaling except the right axes of the pyruvate graph. Phosphate became growth limiting below 0.15 mM in the case of rhamnose, xylose & fructose. In the case of fructose and xylose something else than carbon source availability was limiting since carbon source was still present at end point at >0.15mM. Pyruvate was consumed fully in all tubes above 0.015 mM phosphate. In the pyruvate cultures the growth appears to be limited by phosphate concentration below 4.5 mM. However in the cultures with 0.15mM and below the expected shift in product formation was noted with lower levels phosphate relate to higher ethanol levels.

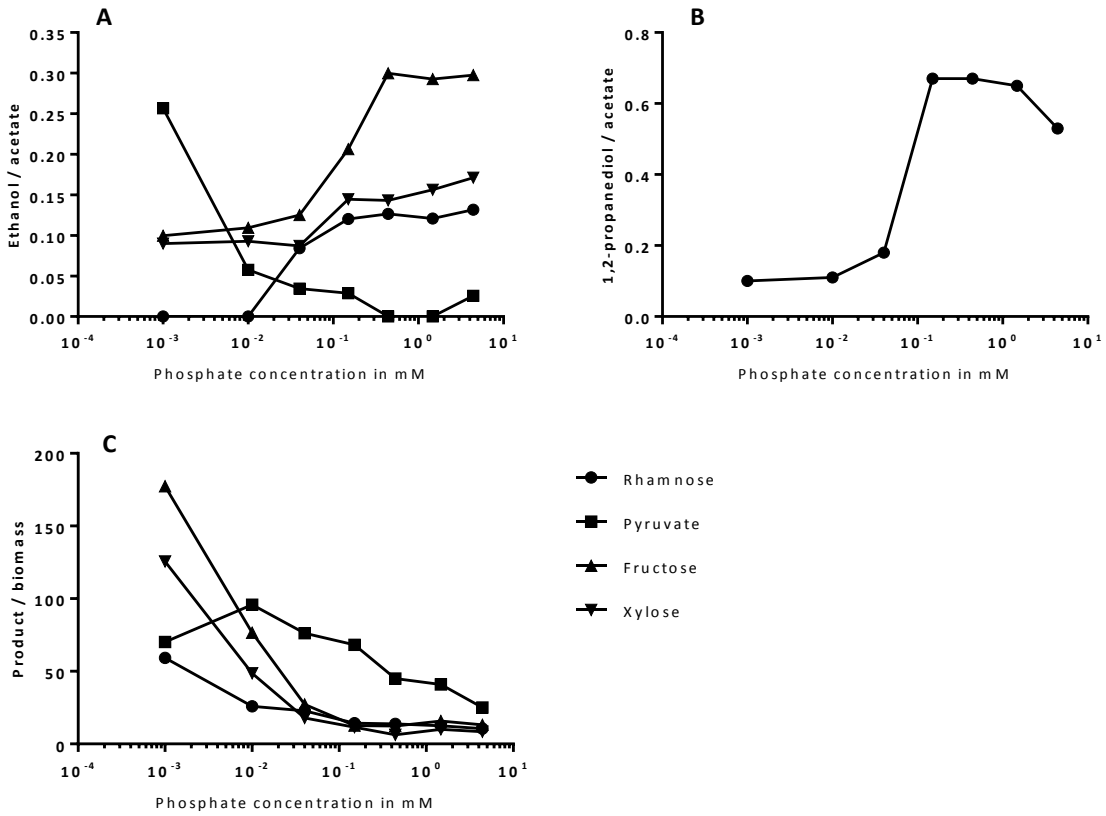

Figure 5-2 The effect of phosphate limitation on product ratios.

Panel A shows the ethanol / acetate molar ratio, panel B shows the 1,2-propanediol/acetate ratio and panel C the total product mass / biomass ratio. The ratios are plotted against the phosphate concentration at logarithmic scale. Ethanol /acetate ratios are higher with more phosphate for fructose, xylose and rhamnose while the situation is opposite for pyruvate where lower phosphate concentrations lead to higher ratios. In the rhamnose culture the 1,2-propanediol/acetate ratio follows a similar course as the ethanol/acetate ratios. The bottom shows there is only limited effect on the total product/biomass ratio for pyruvate grown culture. In the case of fructose, xylose and rhamnose ratios are close to 10 at and above 0.15 mM phosphate and the ratios go much higher below that threshold.

5.2.2.1 Discussion of batch growth experiments

The expectation was that reducing the phosphate levels would lead to a shift toward more ethanol and less acetate. This was not observed for the three sugars, fructose, xylose and rhamnose however it was observed for pyruvate. The pyruvate experiment is in that sense more like the carbon monoxide grown phosphate limited steady state cultures discussed further on in this chapter since phosphate limitation leads to more ethanol and lactate production. Another expectation was that at phosphate limitation conditions the ratio of product / biomass would be higher. The reasoning here is that less biomass per available energy and carbon source can be formed and thus more of the substrate is available for the product formation. This was observed for the three sugars and less strong for the pyruvate grown cultures.

In the case of the fructose and xylose tubes with 0.15 mM phosphate and higher the carbon source was still present indicating that something else than carbon source availability was limiting. Acidification (pH) was not measured in this experiment but based on the fact that a substance with a high pKa (the sugar) is consumed and one with a low pKa (acetate) produced and the experience with other cultures (Chapter 4) it is likely that pH decreases. This would explain why ethanol/ acetate ratios are higher at higher phosphate concentration for these sugars since at lower pH acetate is more protonated and ethanol production via Aor becomes more favourable (140).

In the case of rhamnose something similar was observed. At higher phosphate levels with relatively high levels of acetate high levels of 1,2-propanediol were formed while at lower phosphate concentration with lower levels acetate only little of the neutral product 1,2-propandiol was formed and acetate was the predominant product.

What can explain the difference between the results of the three sugar grown cultures and the pyruvate culture? One fact that might explain the difference is the different nature of the carbon sources. The sugars are more energy dense than pyruvate. Fructose is for instance more energy dense (915.38 kJ mol^{-1}) than pyruvate (474.63 kJ mol^{-1}) and in especially in anaerobes more energy can be released from fructose then from pyruvate (163). Another explanation is that the acidic nature of pyruvate/pyruvic acid. Where pyruvate's pKa is 2.5, that of acetate is pKa 4.5 which might mean that the pH in pyruvate cultures is not decreasing by the formation of acetate in contrast to the sugar grown cultures. This in turn does not increase ethanol production at the higher phosphate levels as seen in the sugars. At the lower phosphate concentration the reducing potential that is would be used for biomass production can go to more reduced products. One final important difference is that the concentration of the carbon sources was set at 40 mM and since the molecular weight of pyruvate is roughly half that of the sugars, not only less energy but also less carbon was available for biomass production which might influence the ratios further. In the next chapter the effect of initial carbon source concentration is discussed.

The aim of this pilot study was to establish at which phosphate concentration we might expect growth limiting effects. Based on the samples of the three sugar carbon sources this level was close to 0.15 mM phosphate. With this knowledge we started continuous bioreactor cultures of WT *C. autoethanogenum*

5.3 Bioreactor studies

5.3.1 Method

To study the effect of phosphate limitation on the product spectrum two CSTR studies were performed on *C. autoethanogenum* with carbon monoxide as carbon and energy source.

The first phosphate limitation bioreactor (PL001) was inoculated with 150 ml from active growing culture (OD_{600} 0.6-0.9) in PETC-MES with sodium sulphide as sulphur source and carbon monoxide as carbon source. The second phosphate limitation reactor medium (PL002) was inoculated with 100 ml from the PL001 reactor. During the culture start-up phase acetate was added to the medium and carbon monoxide sparged trough, mixed by low agitation rates (200 RPM) at first. This low agitation caused low gas-liquid mass transfer which is needed since carbon monoxide is inhibits growth severely at high concentrations. At the start pH was set close to 5. Sodium sulphide is added to the medium which leads to increased pH since there is only a base (sodium hydroxide) for pH control under normal circumstances. The cells of the inoculum start to consume acetate and carbon monoxide and produce hydrogen this combination leads to further pH increase until the pH rise slows and peaks somewhere between pH 5.75 and 7 after which the pH starts to decrease caused by net acetic acid production. At this point it was assumed that the cells consume mostly carbon monoxide and are likely in a carbon limiting circumstance. Increasing the agitation then leads to higher CO supply to the cells which causes increased biomass and a further decrease of the pH. When OD_{600} ~3 was reached continuous culture was started by medium addition.

The definition of steady state used is a period of more than two reactor volume turn-overs with 10 % or less change in biomass, acetate and ethanol levels. With a dilution rate (D) of 0.6 reactor volumes per day this means that about four days of less than 10% change in those parameters is a steady state. Obviously longer periods are preferred as they indicate higher levels of stability.

The two bioreactor runs yielded a total of 13 steady states of which 6 were under phosphate limited growth conditions.

5.3.2 Results run description

5.3.2.1 Phosphate limitation reactor run 1 (pilot, PL001)

To establish the phosphate concentration at which growth is limited in CSTR, a bioreactor (PL001) was set up as described previously (chapter 2). The headspace GC data was not analysed due to technical issues with one of the columns. Metabolomics samples were taken from three separate steady states. An overview of the PL001 reactor run can be found in in Figure 5-3.

After the start up at standard phosphate concentration medium, continuous addition with a medium containing 1 mM phosphate was started. This 1 mM was estimated, based on the batch experiments, not to be a limiting concentration for the ~1.2 g l^{-1} d^{-1} biomass that establishes at the 15 ml min^{-1} carbon monoxide flow rate in our bioreactor set-up.

Indeed after ten days a steady state (PL001 I) established which behaved similar as previous carbon limited reactors under the same settings (personal communication A.M. Henstra). Phosphate concentration of the feed medium was then lowered to 0.5 mM. At day 44 another steady state that lasted for 5 days established (PL001 II). There was no indication that phosphate was limiting growth at this level so the concentration was decreased to to 0.25 mM. This concentration was clearly growth limiting since the optical density of the culture dropped from ~3.5 to ~2 (biomass ~1.1 g l^{-1} d^{-1} & ~0.6 g l^{-1} d^{-1} respectively) the ethanol/acetate ratio changed in a similar fashion. On the days 67, 68, 69 & 70 a steady state (PL001 III) was established.

This steady state was interrupted by maintenance work with a temporary gas shut down which caused a crash in the culture. By addition of yeast extract, increasing the phosphate concentration and lowering the agitation I revived the culture. After another steady state had established with 1mM phosphate medium under carbon limiting conditions I lowered the phosphate concentration of the feed media to 0.125 mM. After ten days on this feed regimen the culture crashed. Prior to the full crash we seen significant less NaOH use and an increase of pH at a later stage. Based on the hypothesis that this was caused by to high carbon monoxide partial pressures per cell I tried to control conditions by lowering agitation however culture collapse was not prevented.

By increasing the phosphate concentration, lowering agitation and adding yeast extract the culture was revived and after a few days at 1mM phosphate level feed media I switched back to 0.25 mM phosphate medium. This resulted the same drop in biomass yield as observed before but not the same strong shift in product spectrum. I therefore lowered the phosphate concentration to 0.2 mM which resulted in slightly lower biomass yields and the same shift in product spectrum as before.

It resulted in a steady state of six days where the ethanol/acetate molar ratio was about ~1.3 followed by two intermediate days and a steady state of ratios of five days with ratios of ~1.9 after which we had an emergency gas shut of that lasted for 2 days after which we did not attempt to revive this culture.

The primary goal of this reactor was to find the phosphate concentration at which we found the expected shift in product spectrum towards more reduced liquid products. It was found that a phosphate concentration of about 0.2-0.25 mM phosphate gives this result. The lowest level at which non-limitation effects were noticed was 0.5 mM phosphate while 0.125 mM did not yield stable reactor cultures.

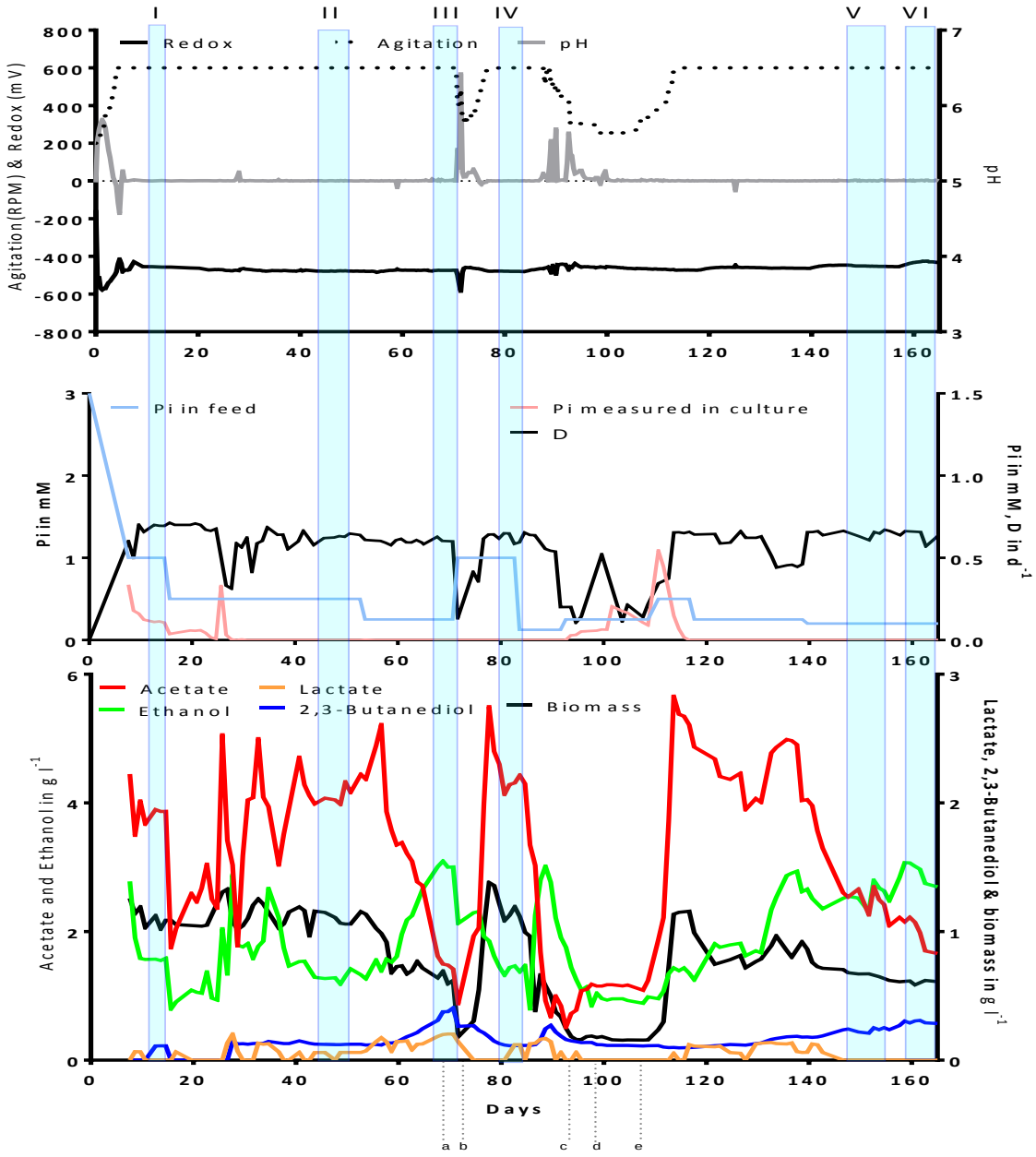

Figure 5-3 overview of the PL001 bioreactor run.

Top diagram shows parameters and settings measured by bio command software (agitation, redox potential & pH), middle diagram the dilution rate (D) and phosphate concentrations as set in feed media and measured in culture media with HPLC. Bottom diagram shows the products and biomass as measured by HPLC (products) and photo spectrometer (biomass calculated from optical density). Blue boxes with roman numerals mark steady states. Events marked are: a= temporary gas supply shut off because of maintenance, b= Added 2 ml glacial acetic acid, 0.1 g KH_2PO_4 10 ml 10% YE, c= added 0.08 g KH_2PO_4, d= Added 0.2 g, NaH_2PO_4, 0.1ml acetic acid, 10ml YE, e= added 4 ml YE and 0.5g NaH_2PO_4

5.3.2.2 *Phosphate limitation reactor run* 2 (PL002)

To investigate the effects of phosphate limitation in an independent bioreactor run I started the second bioreactor (PL002, Figure 5-4). This reactor was inoculated from PL001. At day 35 continuous mode was stated with standard reactor medium containing 5.5 mM phosphate running at steady state for two periods (PL002 I & II) and changed to 0.2mM phosphate medium at day 48. The exponential decay from 5.5 mM phosphate to ~0.2 mM phosphate took approximately 9 days. While phosphate was approaching limiting conditions product spectrum shifted to higher ethaol / actetate molar ratios, and biomass and hydrogen production decreased. Since both strong decrease and increase of hydrogen production were associated with pre-crash situations and experience showed fast changes can cause instabilities. To prevent a crash phosphate was added to the bioreactor which turned product spectrum back to that indicative of carbon limitation.

At day 64 a 20 litre bottle of 0.2 mM Phosphate medium was attached which contained a medium that had too little pantothenate (1/10 of normal concentration). Since initially it was thought the instabilities that followed were caused by phosphate limitation it took until day 105 to understand what must have gone wrong. Interestingly during this unstable period we did not detect the much lower biomass production associated with the phosphate limiting conditions. Limitation of pantothenate was stable since we reached a steady state (PL002) but eventually this medium led to a culture collapse/crash. After recovery from this crash and having determined the cause of the instability, the bioreactor culture was run under the intended phosphate limitation experimental conditions. As before, the biomass production was lower under the phosphate limiting conditions compared to the carbon limiting conditions. Three more steady states (V, VI and VII) were run at true phosphate limitation. V and VII were under lower carbon monoxide flow rates (17 and 15 ml min^{-1} respectively) while VI was under higher carbon monoxide flow rates(27 ml / min^{-1}) creating a gas induced shift under limitation controlled conditions. The 7 days steady state VII was the longest steady state we established under phosphate limiting conditions and it was as stable as carbon limited steady states.

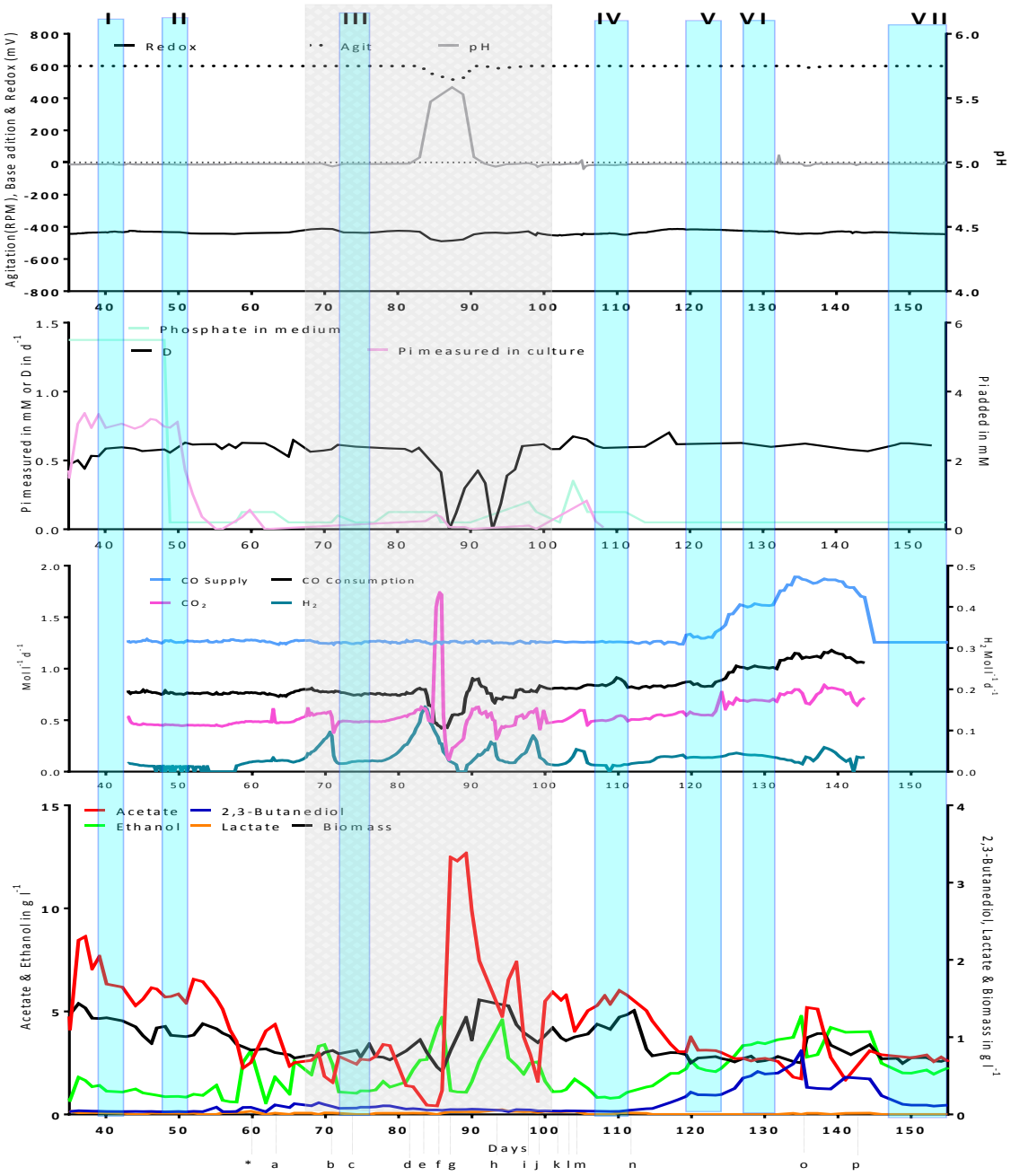

Figure 5-4 The overview of the PL002 bioreactor run.

Top graph gives reactor parameters. Second from the top the dilution rate (D) and the phosphate concentrations as added and as measured in culture. Third from the top indicates the gasses produced and consumed as measured by the GC, after day 143 CO supply was determined from mass flow controller setting. Bottom graph shows the production in the liquid phase. Steady states are indicated by light blue boxes and labelled on top with roman numerals. Grey box is period where pantothenate was at low concentration. Some significant events are labelled * & a-p below. *=Phosphate injection, a=start 0.2 mM Pi medium with faulty vitamin batch, b=0.04 g KH2PO4 added, c=changed 0.2 mM Pi medium to ~0.4 mM, d=set up NaH2PO4 injection as an acid control for 2 days, i=added 0.05 g NaH2PO4, e=CO_2 in gas mix 20 ml/m 2 days, f=Set up 25% acetic acid pH at set point 5.7, g=added 2g YE 2g pyruvate 0.5 g formate, h=added 0.5 g YE 0.05 NaFormate, i=added 0.05 g NaH2PO4, j= changed medium to 0.5 mM Pi medium, k=changed back to 0.2 mM medium, l=added 0.2g NaH2PO4, m=changed medium to 0.5 mM Pi medium, n=changed to new 0.2 mM Pi medium, o=added 0.05 g NaH2PO4, p=GC broke

5.3.3 Results

5.3.3.1 Correlation analysis of full runs

Analysis of all data of each bioreactors shows a clear relation between phosphate concentration and the all products except lactate. Correlation was calculated from the values of each day for all variable using both Pearson and Spearman correlation methods. These gave similar values for most variables where phosphate variable showed most difference. Results of the Spearman correlation method are depicted in Table 5-1 for the values of PL001 and Table 5-2 for PL002. Spearman was chosen over Pearson since it was unknown if the linear assumption of the Pearson method can be met, specifically for the phosphate concentration. Linear regression results supporting the use of Spearman over Pearson can be found in Appendix figure 1 for biomass, phosphate and CO supply.

The correlation analysis (Table 5-1 & Table 5-2) shows significant positive correlation between phosphate concentration and biomass, acetate while a significant negative correlation exists between phosphate and production of ethanol, 2,3-butanediol, CO_2, H_2 and CO consumption. The strongest positive correlations are between the productions of ethanol, 2,3-butanediol, CO_2, H_2 and CO consumption, and the biomass and acetate production. The strongest negative correlations are between acetate, and ethanol and 2,3-butanediol.

Table 5-1 Spearman correlation coefficients matrix of PL001. *=P<0.05 **= P<0.005

PL001	Acetate	Ethanol	Lactate	2,3-Butanediol	Pi in feed
Biomass	0.789**	-0.128	0.064	-0.434**	0.753**
Acetate		-0.017	0.196*	-0.315**	0.525**
Ethanol			0.304*	0.759**	-0.430**
Lactate				0.191*	-0.114
2,3-Butanediol					-0.606**

Table 5-2 Spearman correlation coefficients matrix of PL002. P*=P<0.05 **= P<0.005

PL002	2,3-Butanediol	Acetate	Ethanol	Lactate	CO Sup	CO_2	H_2	CO Cons.	Pi	D
Biomass	-0.722**	0.818**	-0.674**	0.340**	-0.577**	-0.660**	-0.729**	-0.448**	0.498**	-0.148
2,3-		-0.751**	0.909**	-0.387**	0.673**	0.887**	0.760**	0.801**	-0.517**	0.094
Acetate			-0.729**	0.246	-0.653**	-0.717**	-0.688**	-0.551**	0.399**	-0.241
Ethanol				-0.369*	0.689**	0.805**	0.732**	0.709**	-0.405**	0.143
Lactate					-0.100	-0.394*	-0.525**	-0.392*	0.300*	-0.115
CO Sup.						0.672**	0.505**	0.678**	-0.415**	0.054
CO_2							0.844**	0.913**	-0.415**	-0.025
H_2								0.667**	-0.365**	0.014
CO Cons.									-0.342**	-0.035
Pi										-0.083

5.3.3.2 Steady state data analysis

An overview of the product spectra of the liquid phase during the steady states is given in Figure 5-5A. As before the phosphate limitation leads to more ethanol and 2,3- butanediol and less acetate and biomass production. It is interesting to note that the effect of phosphate limitation was stronger in PL001. Prior to the second culture crash in PL001 significant levels of lactate were formed during steady states which was not found during any stable period after that.

Figure 5-5B gives the mean of biomass and product yields of all carbon limiting steady states and of all phosphate limitation steady states of which data was collected at low CO flow rates. It was found that the differences in product spectrum are significant for biomass, acetate, ethanol and 2,3-butanediol and not for lactate.

In PL002 the headspace was analysed from day 43 until day 143. For this period a full carbon balance can be made. The carbon balance was within 10% for most days except for the days of culture crash and steady state III. Figure 5-6 gives the carbon balance of the five steady states of which PL002 III is the only steady state where carbon balance was approximately 12% off which was more than twice the percentage for the other steady states.

Figure 5-7 gives an insightful representation of what happens during a phosphate limitation induced product spectrum shift. In this example, the shift started at day 56 of the PL001 bioreactor run. At carbon limited conditions there are more oxygen atoms and less hydrogen and carbon atoms in the dissolved products in the liquid phase, relatively to the phosphate limited condition.

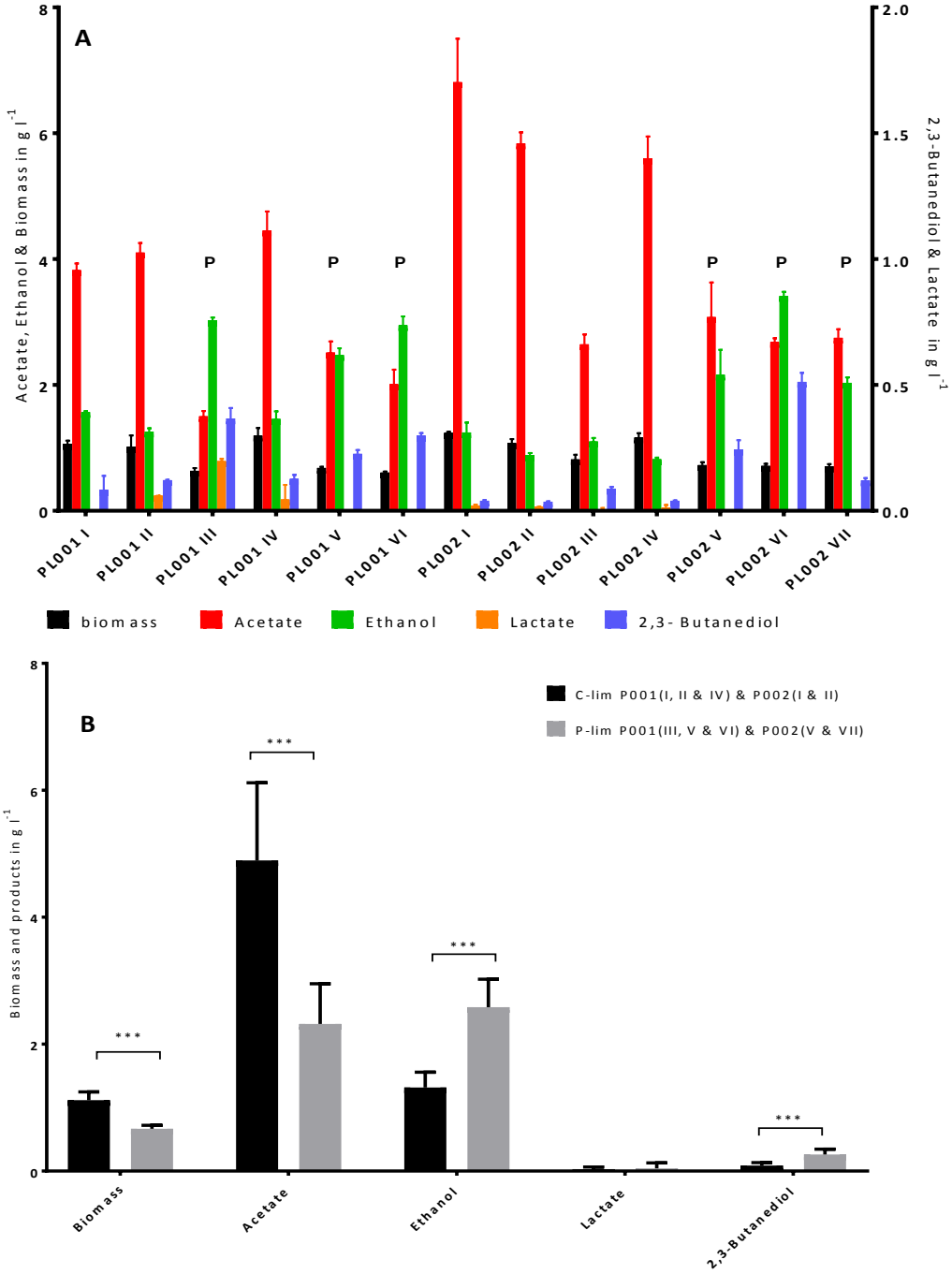

Figure 5-5 A comparison of the steady states.

Panel A (top) depicts the products in the liquid phase in each steady state. The P indicates the steady states that under phosphate limited growth conditions with 0.25 mM phosphate in PL001III and 0.2 mM phosphate for the other 5 steady states. **Panel B** (bottom) compares the two conditions, carbon limited steady states (C-lim) and phosphate limited steady states (P-lim) at low CO flow rate (PL002 VI excluded). Multiple T-tests comparison show the results for biomass, Acetate, Ethanol and 2,3-Butanol to be highly significant. ***= P<0.0005. Combined these two graphs show clearly that under phosphate limitation the production of ethanol and 2,3-butanol is higher while that of acetate and biomass is lower.

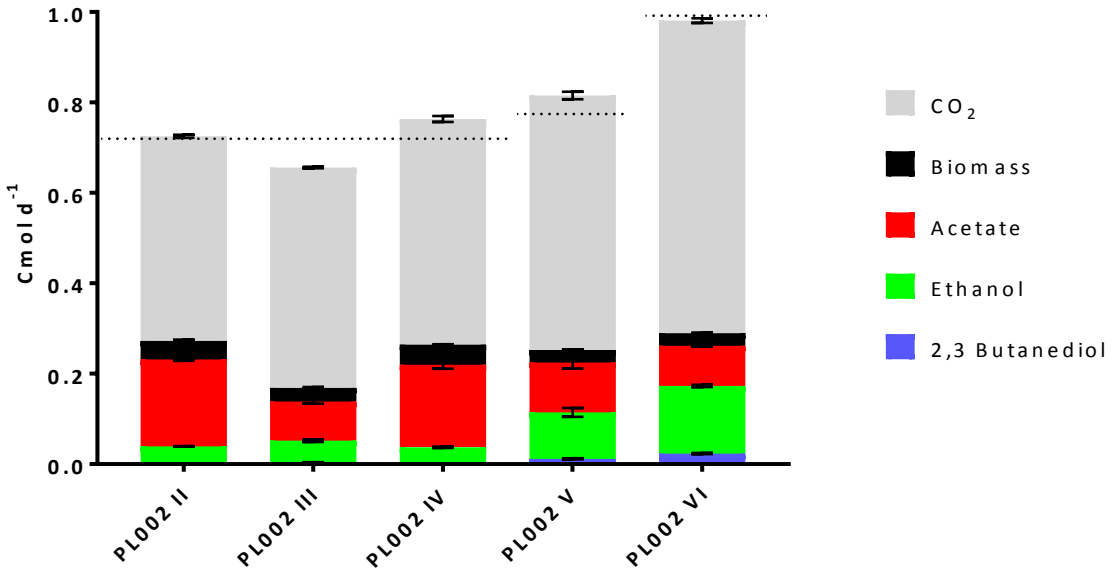

Figure 5-6 A bar diagram depicting the carbon balance of the steady states in the PL002 run.
Dotted line indicates average carbon consumption as calculated by the carbon monoxide levels going in the reactor minus the carbon monoxide in the headspace. Steady states PL002 II & PL002 IV were carbon limited, PL002 III was likely pantothenate limited while PL002 002 V and PL002 VI were under phosphate limitation. Error bars represent standard deviation.

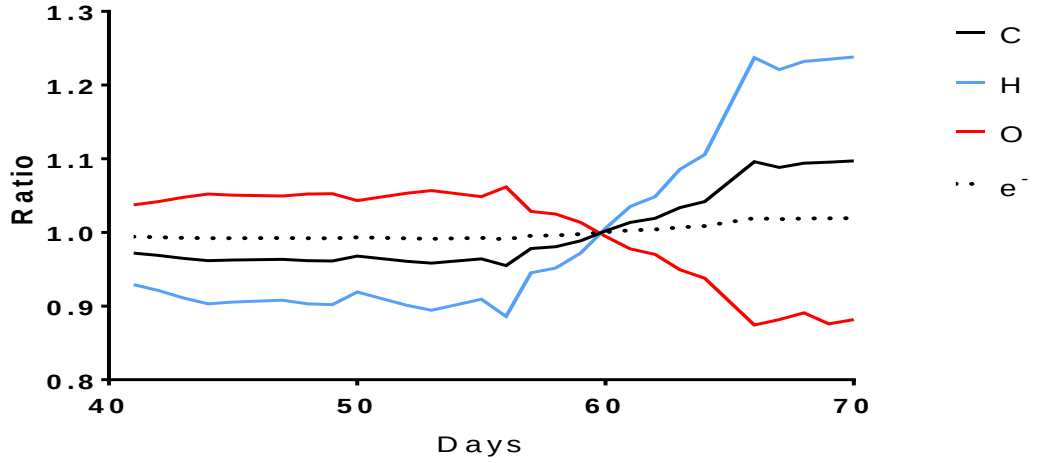

Figure 5-7 Elemental composition of the liquid products during phosphate limitation induced shift in PL001.
The ratio is the elemental concentration normalised on the daily total amount of atoms and the mean over the time period of the element.

5.3.4 Metabolomics

5.3.4.1 PL002

The analysis of the internal metabolites for PL002 steady state II- VII were performed in a targeted and untargeted approach. PCA and PLS-DA analyses of the untargeted data shows steady state III, V, VI & VII clustering together and II as an outlier group. The untargeted approach can be powerful to find unexpected patterns and unexpected differentiating metabolites. The results discussed in this chapter are results of the targeted approach which uses quantified LC-MS results for the 94 metabolites that could be quantified at reasonable levels of certainty. These targeted results give similar results in principal component analysis (PCA) clustering as the untargeted results.

During phosphate limitation malate, succinate, fumarate and branched chain amino acids have a higher relative abundance while during the carbon limited steady state (Pl002 II / SSII) some nucleotides and nucleotide precursors together with amino acids such as proline and tryptophan had a higher relative abundance.

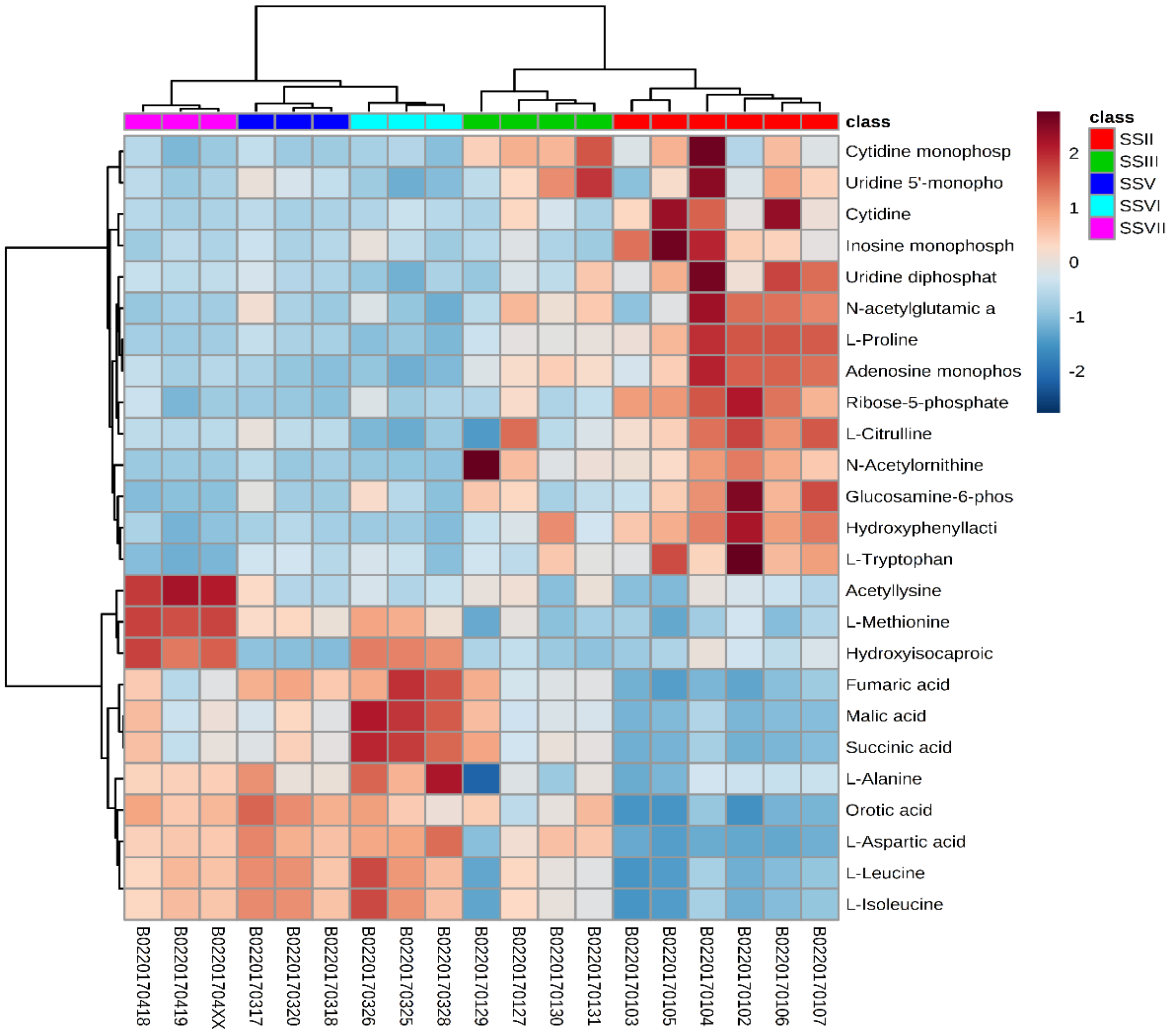

Figure 5-8 Clustered heat map of the metabolomics data from steady states II, III, V, VI & VII of PL002.

Since the analysis software only allows groups of a minimal 3 replicates an average of the two samples of SSVII was added. The samples taken under phosphate limitation were found to have relatively higher levels of fumarate, malate, succinate, orotate, leucine, isoleucine and aspartic acid.

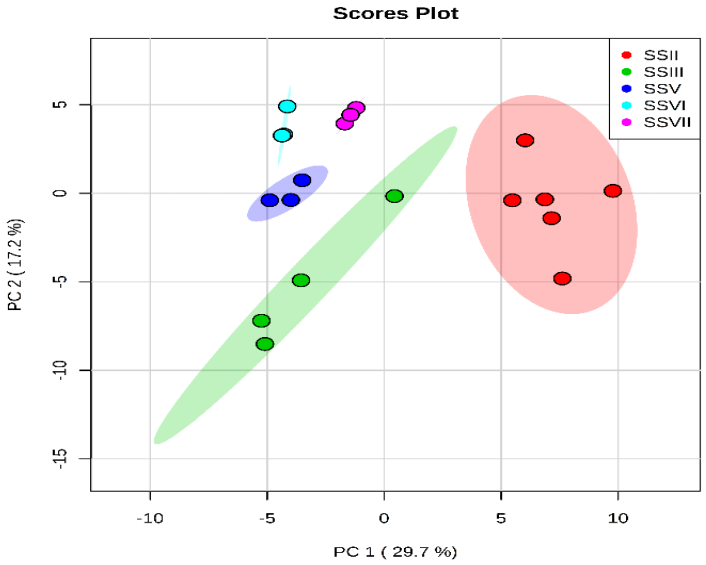

Figure 5-9 PCA of the five steady states of which LC-MS samples were taken.

This PCA shows a clustering of the samples of the separate steady states. The phosphate limited cultures cluster more to the top left quadrant.

5.3.4.2 Results of PL001 combined with PL002

To test if we can cluster the PL001 samples in phosphate limited and carbon limited samples based on the metabolomics, we analysed the samples of PL001 together with PL002. Only three steady states were sampled of PL001, day per steady state (each in technical triplicate). Two at high phosphate concentrations (07-07-2016/Day18/SSI, 09-12-2016/Day 80/ SSIV) and one day at phosphate limiting condition (08-30-2016 / day 68/ SSIII). If there is any significant reproducible effect of phosphate limitation, clustered correlation analysis and PCA, should group the phosphate limiting conditions together in one group and the carbon limiting conditions together in another. Indeed, this is what we find. The PCA analysis shows that the first principal component (PCA1) is heavily determined by batch effects. However PCA 2 explains 15.8 % of the variation and clearly distinguishes the effects of limitation (Figure 5-10 B, C & D). Clustered correlation analysis gives the same overall results (Figure 5-10 A).

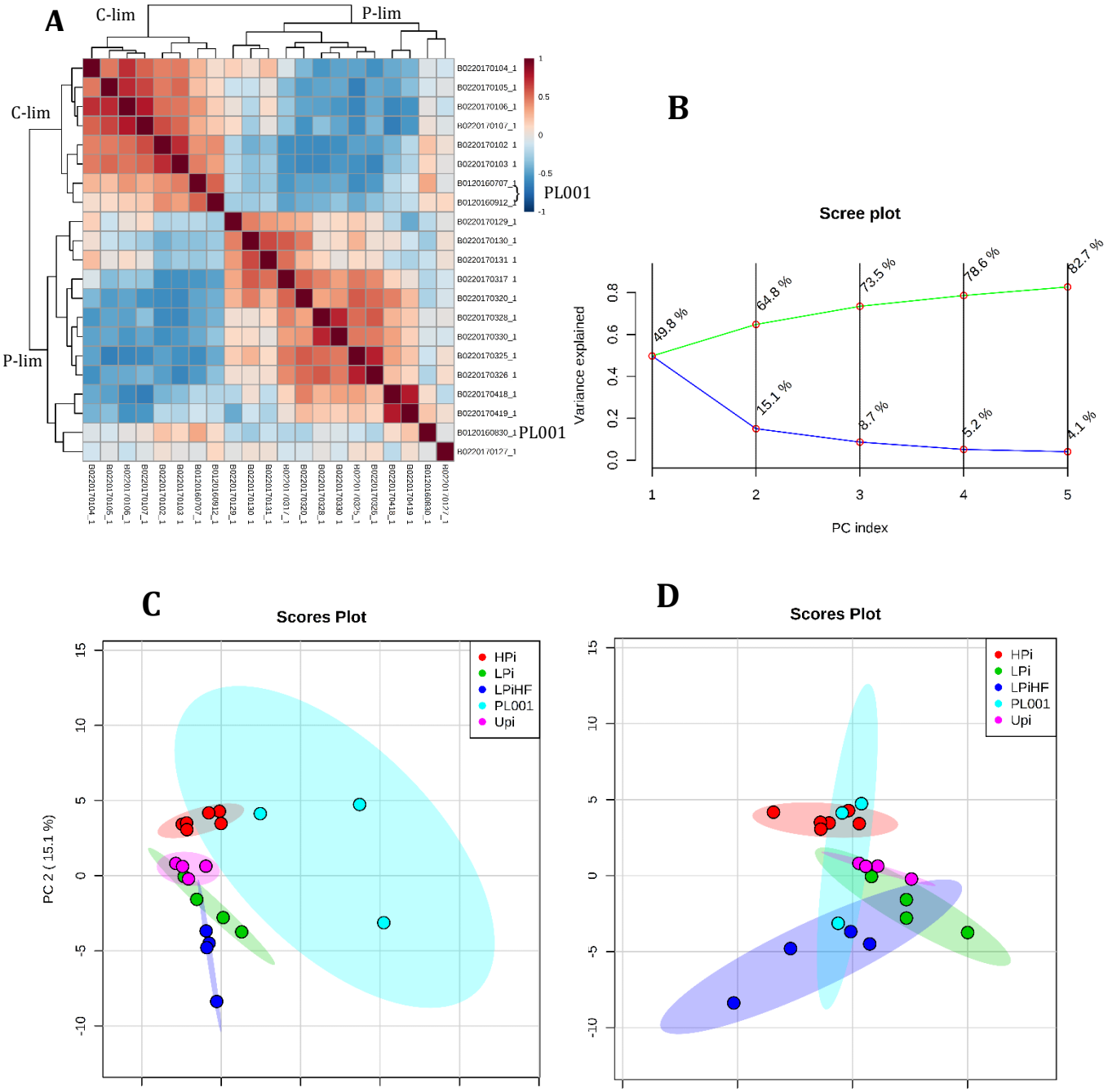

Figure 5-10 Multivarate analysis of PL001 & PL002

Panel A (top left) depicts the clustered correlation analysis in a heatmap with clustering tree diagram**. Panel B** (top right) is the Scree plot that shows the contribution of the five principal components that were calculated by Metaboanlyst. The green line shows the accumulated variance explained, the blue line depicts the variance explained by individual PC. **Panel C** shows the scores plots of the PCA PC1 vs PC2 and **Panel D** shows the scores plot of PCA with PC4 and PC2. HPi=High phosphate (PL002 SSII), LPi= Low phosphate (PL002 SSV & SSVII), LPiHF=Low Pi, high CO flow rate (SSVI) , Upi= Unknown limited (SSIII). The left bottom graph shows that the batch effects are strongly represented in PC1 while PC2 strongly distinguished limitation. The PL001 sample that cluster together with both LPi groups is the phosphate limiting PL001 SSIII while the PL001 samples that cluster with the high phosphate samples of PL002 indeed are the high phosphate samples of PL001

Since grouping into a phosphate limited and carbon limited groups is validated, we can see which metabolites are most affected by these specific conditions with relatively high certainty. By applying a fold change cut-off of 2-fold and a significance cut-off P value of 0.05 we find 24 out of the 94 metabolites that are significantly different between the two types of limitations (Figure 5-11). Using these parameters only four metabolites are found at significantly higher levels during high phosphate levels (Acetyl phosphate, Erythrose-4-phosphate, Inosine monophosphate (IMP), and hydroxyphenyllactic acid. Amongst the twenty metabolites with significantly higher levels during phosphate limitation are the branched chain amino acids, phosphorylated nucleosides and citric acid cycle intermediates such as malate and fumarate (Figure 5-12).

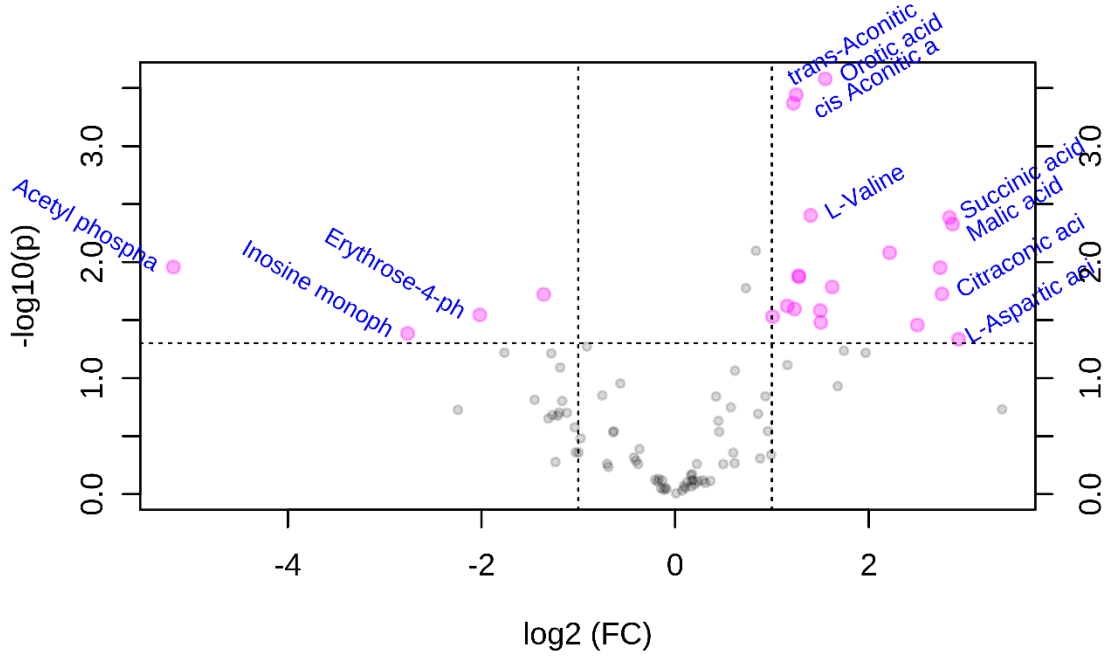

Figure 5-11 Vulcano plot of the compbined metabolomics data of PL001 and PL002.
The effect is plotted on the x-axes and statistical significance on the y-axes. The metabolites in the top left section have both higher abundance at high significance under carbon limited culture conditions while top right sections are considered significant and high abundant under phosphate limited conditions. . In phosphate limited cells relatively higher levels of fumarate, malate, succinate, orotate, leucine, isoleucine, valine are found amongst 19 other compounds. In the cells fed high phosphate medium inosine monophosphate, hydroxyphenyllactic acid, erythrose-4-phosphate and acetyl phosphate are found at a relatively higher level. Figure 5-12 gives a heatmap representatation of the same data.

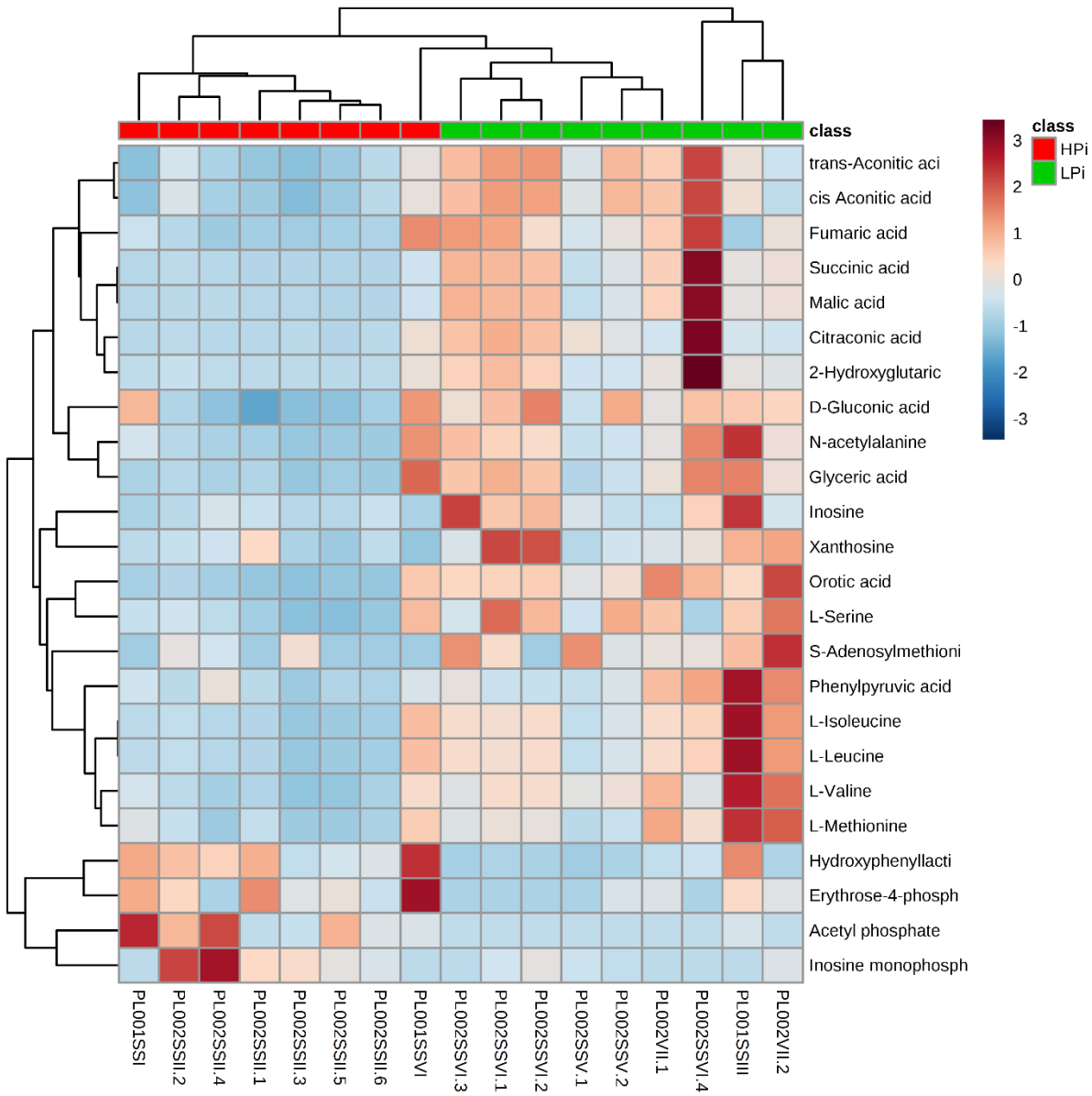

Figure 5-12 Heat map analysis of pooled samples of PL001 & Pl002.

The 24 most significant metabolites are shown. Colour code depicts mean-centred divided by standard deviation of the metabolite concentration. In phosphate limited cells relatively higher levels of fumarate, malate, succinate, orotate, leucine, isoleucine, valine are found amongst 19 other compounds. In the cells fed high phosphate medium inosine monophosphate, hydroxyphenyllactic acid, erythrose-4-phosphate and acetyl phosphate are found at a relatively higher level.

5.4 Discussion

Nutrient limitation affects product formation significantly. We expected that phosphate limitation would shift the product profile to more reduced dissolved products. Indeed this was found in our bioreactor studies and pyruvate batch studies. However the phosphate dilution series of fructose and xylose did not follow our prediction. This is likely explained by product limitation or change in pH having a stronger effect in than the effect of lower phosphate concentrations. Another reason might be that the effect of phosphate limitation on the metabolism with fructose and xylose was not as strong since some of the biomass can be created from intermediates from glycolysis and pentose phosphate while on pyruvate and CO these intermediates need to be produced by gluconeogenesis.

The bioreactor results very clearly show the ability of phosphate limitation to induce a shift towards higher ethanol yield while lowering acetate production. The effects are similar to those found by Richter *et al*. who likely were running their reactor at sulphur limitation(140) and to unpublished results in our group that were likely running reactors at nitrogen limitation (personal communication A.M. Henstra, UoN).

Valgepea *et al*. (137) explain their results in of higher levels of ethanol production at higher agitation rates from the fact that this leads to higher biomass and to higher acetate concentration. The higher acetate diffusion would partly uncouple PMF and thus ATP production. To solve this ethanol is formed from acetate via the Aor route which requires relatively higher levels of CO oxidation for ferredoxin reduction. This model explains their observations. However, to explain the higher ethanol production this model requires higher biomass while the data presented in this chapter shows a strong negative correlation between biomass with ethanol, since phosphate limitation decreases biomass production but increases ethanol production.

A likely explanation for the effect of non-carbon limitation, such as the phosphate studied here, is that it results in lower anabolic metabolism while other metabolic processes continue. Since anabolism requires both ATP and reducing equivalents it functions as a sink for both. When growth is limited due to phosphate limitation this sink can take up less reducing equivalents. The redox state needs to be balanced in a different way. This can be done via multiple routes. Acetate can be reduced to ethanol via the Aor route which oxidises one NAD(P)H and one Fd_{red}. Ethanol can be further be produced from acetyl-CoA via the ALDH route that consumes two NAD(P)H. Acetyl-CoA can be reduced to pyruvate by oxidising Fd_{red}. This pyruvate in turn can be further reduced to malate via oxaloacetate, or to lactate. Two pyruvate molecules can fuse and decarboxylate to acetolactate which in turn is the start of pathways that acts as electron sink both towards 2,3-butanediol and towards the branch chain amino acids. The production of hydrogen finally is another electron sink. This means phosphate limitation should lead to more ethanol, 2,3-butanediol, lactate and hydrogen production. Extracellular lactate production was not significantly affected by phosphate limitation although internal lactate concentrations were found higher in the phosphate limited cultures. However higher levels of the products ethanol, 2,3-butanediol, lactate and hydrogen were detected together with higher intracellular concentrations of malate and branched chain amino acids. Similar to these findings, Richter *et al*.(140) found higher levels of citrate, alanine, aspartic acid and succinate during solventogenesis (sulphur limited). In contrast acetyl-phosphate was found at higher levels during solventogenis in their data while, in the data presented in this chapter, this metabolite has a higher relative abundance during the carbon limited conditions (140). This is likely a reflection of the different limitation condition between their and this study.

The stability of the steady state is an issue that needs to be addressed. Prolonged culturing under phosphate limitations was not attempted as our goal was cycling through multiple steady state conditions. The seven days steady state of PL002 VII was the longest steady state we established under phosphate limiting conditions and during that time it was as stable as carbon limited steady states. This shows that a prolonged steady state under phosphate limitation is possible, however during this steady state the ethanol/acetate molar ratio was only slightly above 1 (~1.03). Valgepea *et al.* claim that this ratio is the highest possible ratio for true steady states as found in their experiments (137). In this experiment, the highest ethanol/acetate ratio at steady state is ~1.7 which was at high carbon monoxide flow (27 m/min) rates but this state just lasted 4 days. Future work should therefore include prolonged (>10 days) running of phosphate limiting steady state at higher CO flow rates.

One issue with long bioreactor runs is strain evolution. The probability of strain evolution is enlarged by the crash and recovery bottlenecks we employed. From the perspective of studying a WT strain this is obviously not ideal. However the trade-off is creating evolved reactor strains which are sought after in industry (304). Since the culture preparation, bioreactor start up and growth is rather slow and the lack of available bioreactors it was decided to be more effective to repeat experimental conditions in the same bioreactor culture then to run less experiments in many independent replicates.

The standard concentration of 5.5 mM phosphate in our bioreactor medium is about ten times higher than 0.5 mM phosphate, the lowest level we did not find clear growth limiting effects. This means phosphate is added in excess and it is likely possible to reduce the concentration without negative effects. In an industrial setting the lowering of phosphate levels can improve environmental impact even when the reactors are chosen to be run at a different type of nutrient limitation. Phosphate limitation might lead to lower relative levels of nucleotides in the biomass which would increase the suitability of the spend cells to be used as animal feed (305, 306). It seems advisable to run ethanol production bioreactors at a non-carbon nutrient limitation due to the more reduced and thus more valuable product spectrum. The choice of which nutrient to limit requires an economic analysis that is outside the scope of this thesis. However both the environmental and the animal feed argument argue for phosphate limitation as a good type of nutrient limitation for product optimisation.

One surprising finding of the heterotrophic batch growth experiments was the discovery of 1,2-propanediol as a native product during growth on rhamnose. These batch experiments further prompted the question on how initial carbon source concentrations influence product formation. Both issues will be further explored in the next chapter.

Chapter 6:

The effect of initial substrate concentration on product formation during heterotrophic growth

"The most exciting phrase to hear in science, the one that heralds new discoveries, is not "Eureka!" but "That's funny."" **Isaac Asimov**

6 The effect of initial carbon source concentration on product formation.

The batch growth experiments to determine the effect of phosphate concentration on growth instigated questions about the effect of the initial carbon source concentration on growth and carbon source. It is known that the partial pressure of CO in the head space has a strong effect on the product spectrum (307). However not much is known about the effect of the initial concentration of carbon sources used for heterotrophy in the clostridial acetogens. Heterotrophy in acetogens has recently received an excellent review. This concludes that the combination of the WLP, electron bifurcating enzymes and Rnf based PMF allows for flexible redox balancing which allows for a very diverse set of carbon sources to be used in anoxic environments (52).

The batch growth experiment to determine the effect of phosphate limitation described in chapter 3 showed fairly similar behaviour for the hexose fructose and the pentose xylose while the behaviour was very dissimilar for the methylpenthose rhamnose and the ketoacid pyruvate. The use of rhamnose as carbon source leads to the production of 1,2-propanediol and 1-propanol next to the standard products such as acetate and ethanol. Pyruvate grown cultures reacted very different to phosphate limitation compared to the cultures that were supplied with one of the three sugars. Pyruvate behaved more like the gas grown cultures.

In the CO grown cultures the supply rate or the headspace pressure influences the product spectrum (307–309). Analogous to this it can be hypothesised that the concentration of the dissolved organic carbon sources influences the product spectrum. It was expected that at low carbon source concentrations (severely carbon limited growth) *C. autoethanogenum* would produce mostly acetate and very little by-products. Increasing carbon source concentrations should then yield increasing by-products such as ethanol, lactate and 1,2-propandiol.

To test this hypothesis a growth experiment was performed in similar fashion as the phosphate limitation series form in chapter 5. In this case the phosphate was added at the standard concentration for PETC-MES and the carbon source was the added at different concentrations. Since this experiment was performed after the identification of the 1-propanol peak in our HPLC results an effort was made to quantify this novel native metabolite as well.

C. autoethanogenum can use substrates mixotrophicaly where both CO and an organic carbon source are co-consumed. To test if the CO and rhamnose can be co-consumed, a pilot culture was grown with rhamnose in PETC-MES and CO in the headspace. Although both carbon sources were used, the CO did not increase the yield of 1, 2-propanediol. However there seemed to be a slightly higher 1-propanol/1, 2-propanediol ratio (data not shown). This pilot spurred some further investigation of the influence of the head space composition on the 1-propanol/1, 2-propanediol ratio which did show a reducing headspace to indeed lead to higher 1-propanol yield.

6.1 Results

6.1.1 The effect of initial carbon source concentration on the product spectrum

To test the effect of initial carbon source concentration 15 ml falcon tubes were filled with standard PETC-MES. The four carbon sources tested were added at 20 g l^{-1}, 15 g l^{-1}, 10 g l^{-1}, 5 g l^{-1}, 3 g l^{-1}, 1 g l^{-1}, 0.5 g l^{-1}, 0.3 g l^{-1}, 0.1 g l^{-1} and 0.03 g l^{-1}. In comparison to the phosphate limitation experiment where all carbon sources were added at 40 mM this translates to 4.4 g l^{-1} sodium pyruvate, 7.2 g l^{-1} fructose, 6.6 g l^{-1} rhamnose and 6 g l^{-1} xylose. Inoculum was grown in PETC-MES with fructose and washed in PETC-MES without carbon source. Media was inoculated to start OD_{600} of approximately 0.05.

End point samples were taken at least 5 days after no further OD increase was seen in all tubes. Product formation and substrate uptake were analysed using HPLC (Figure 6-1). This revealed that ≤ 5 g l^{-1} fructose not all fructose was consumed and from 10 g l^{-1} and above no further increase in biomass was measured (Figure 6-1 C). This indicates another growth limitation which seems to be substrate inhibition. Low levels of ethanol and lactate were only detected at the higher fructose starting concentrations <1 g l^{-1}.

Xylose is fully consumed in all cultures with starting concentrations of 5 g l^{-1} and below (Figure 6-1 D). In this case the residual carbon source is not as clearly caused by substrate limitation as it was in the case of the fructose grown culture. The biomass concentrations did not vary much between the cultures of 5 g l^{-1} and above. Low levels of ethanol and lactate were only detected at the higher xylose starting concentrations of 1 g l^{-1} and higher. One surprising finding is that on this carbon source trace amounts of 1,2-propanediol were detected at the xylose starting concentrations of 3 g l^{-1} and above.

The 1,2-propanediol production was expected for rhamnose. Some cultures using rhamnose as carbon source had not reached their end point since rhamnose was fully consumed in the 5 g l^{-1} starting concentration but not in 0.3, 1 and 3 g l^{-1} rhamnose starting concentration. Growth on rhamnose inoculated from fructose pre-culture, as in this experiment, has a lag-phase of over 6-8 days compared to 1-4 days for the other tested carbon sources. The 0.5 g l^{-1}, 5 g l^{-1}, 15 g l^{-1} and 20 g l^{-1} tubes were inoculated from a different pre-culture tube and started growing after 8 days while the other rhamnose tubes showed somewhat longer delays. The cultures were harvested assuming growth had ceased 5 days before but the results reveals this might not have been the case.

Notwithstanding this issues, the rhamnose experiment shows that at higher starting concentration similar mass concentrations were reached for actetate and 1,2-propanediol while at lower concentrations acetate is the predominant product (Figure 6-2). The phosphate limitation experiment showed that 1,2-propanediol/ acetate ratios were highest when phosphate was least limiting and thus when most of the sugar was consumed. Biomass increased with all increasing starting concentrations of rhamnose. 1-Propanol was only found in from 5 g l^{-1} and higher starting rhamnose concentrations. Lactate was only found above 0.5 g l^{-1} rhamnose concentrations. Ethanol was formed in the cultures containing 5 g l^{-1} and higher and increased with rhamnose availability.

Pyruvate was consumed at end-point in all but the highest starting concentration tube and biomass increased with every increase of pyruvate concentration (Figure 6-1 B). Ethanol /acetate ratios were higher at higher pyruvate concentrations. Formate is a common side product of acetogens but in the case of *C. autoethanogenum* it rarely reaches levels above the detection limit unless cultures are grown on carbon dioxide and hydrogen. Here with growth on pyruvate low levels of formate were detected.

A comparison of the ethanol / acetate molar ratios is shown in Figure 6-2 A. The most striking finding in this was the difference between the results of pyruvate and the sugars. Cultures with all carbon sources at ≤ 1 g l^{-1} have ethanol / actetate ratios < 0.1. These ratios rise to ~0.2 for xylose and fructose while those fed with pyruvate reach 0.5. The 1,2-propanediol molar ratio increases to 0.9 for rhamnose while those for xylose stay well below 0.05 (Figure 6-2 B). The product mass / biomass ratio (Figure 6-2 C) is about ~12 for all carbon sources at 20 g l^{-1} . This ratio is similar for the sugars between 0.5-20 g l^{-1} initial carbon source concentrations while it rises for the pyruvate at these concentrations. At ≤ 0.3 g l^{-1} the rhamnose and xylose cultures the ratio increased sharply.

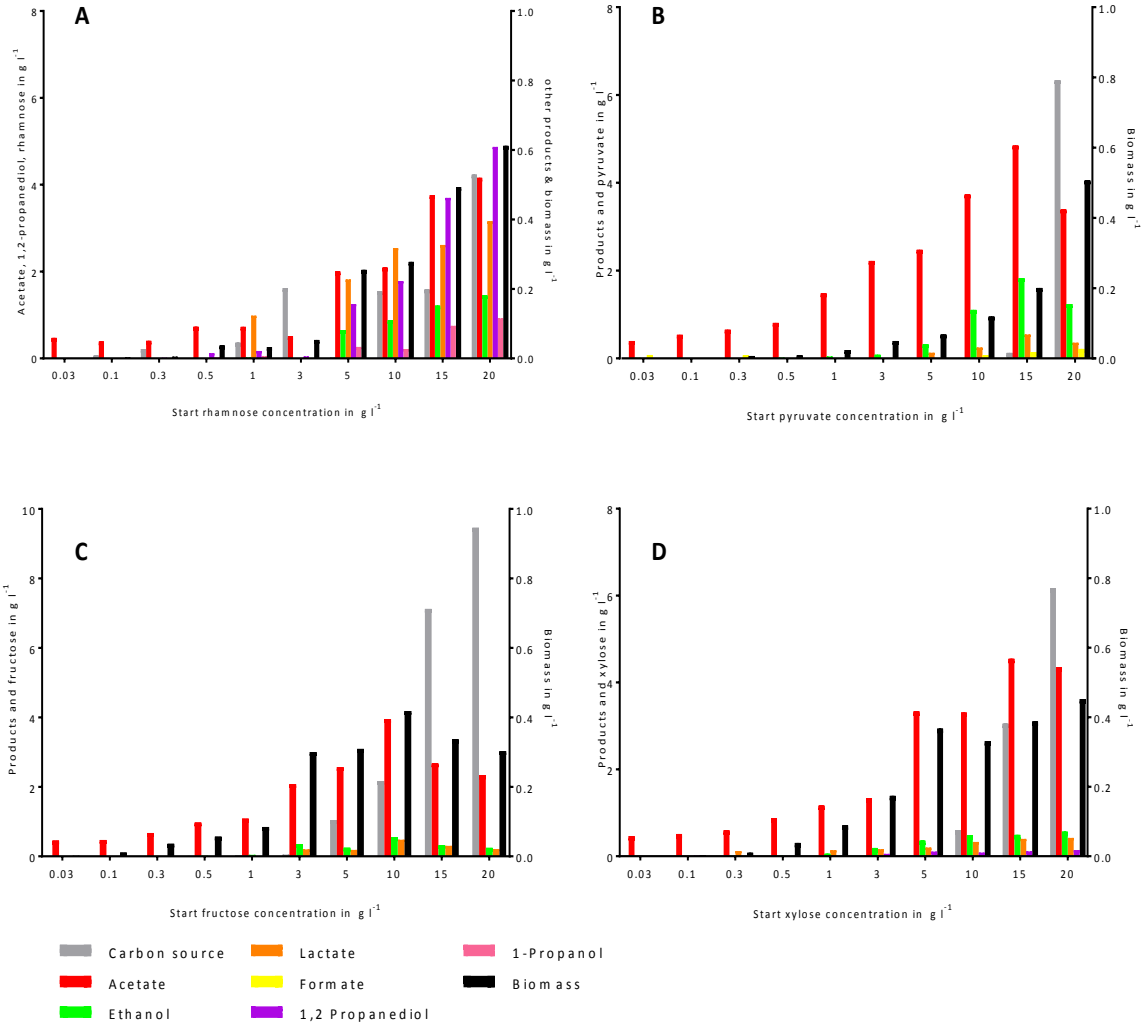

Figure 6-1 the results of the carbon limitation batch growth experiments.

Panel A (top left) depict the results of rhamnose, B (top right) those of pyruvate, C (bottom left) fructose and finally panel D (bottom right) xylose. Rhamnose cultures show an increase of 1,2 propanediol and 1-propanol with increasing rhamnose levels until at the highest level of rhamnose equal amounts of 1,2 propanediol and acetate are found. 1-propanol was only found at above 3 g l^{-1} rhamnose. Rhamnose was not fully consumed in the 0.1 g l^{-1}, 0.3 g l^{-1}, 1 g l^{-1}, 3 g l^{-1}, 10 g l^{-1}, 15 g l^{-1} & 20 g l^{-1} while it was in the in 0.03 g l^{-1} & 0.5 g l^{-1} rhamnose cultures. For the lower concentrations this is likely caused by premature end-point. Pyruvate is fully consumed in all cultures with ≤ 10 g l^{-1} pyruvate. At the higher pyruvate concentrations ethanol and lactate is formed. In the fructose based cultures of 10 g l^{-1} and above no further increase in biomass was measured. Low levels of ethanol and lactate were only detected at the higher fructose starting concentrations <1 g l^{-1}. Xylose is fully consumed in cultures with starting concentrations of 5 g l^{-1} and below. The biomass concentrations did not vary much between the cultures of 5 g l^{-1} and above. Low levels of ethanol and lactate were only detected at the higher xylose starting concentrations Trace amounts of 1,2-propanediol were detected at the xylose starting concentrations of 3 g l-1 and above.

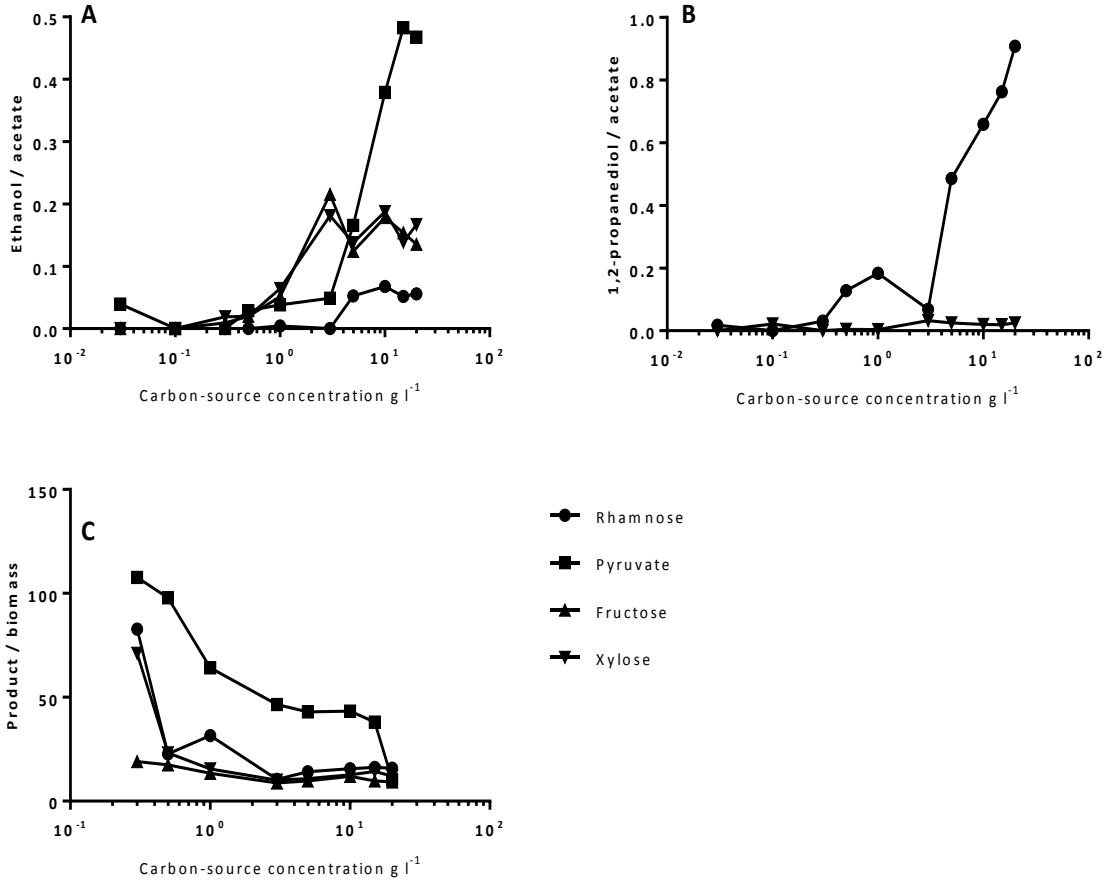

Figure 6-2 The product ratios at different carbon source conditions.

Panel A shows the ethanol/acetate molar ratios. This show the strongest shift for pyruvate grown cultures. **Panel B** gives the 1,2- Propane diol/acetate ratios also that also shifted considerably with increased rhamnose concentration but not xylose. At higher starting concentration similar mass concentrations were reached for acetate and 1,2-propanediol**. Panel C** gives the product/biomass ratios that are is highest for pyruvate except at the highest concentration of pyruvate tested where the it is about 12 similar to the other carbon sources.

6.1.2 Effect of headspace composition on 1, 2-propanediol and 1-propanol formation

In one pilot bottle growth experiment higher 1-propanol levels were produced if CO was present in the headspace (data not shown). To investigate this further WT *C. autoethanogenum* was grown at three different rhamnose concentrations (10 g l^{-1} , 1 g l^{-1} and 0.1 g l^{-1}) with three different headspace compositions (100 kPa Nitrogen + 50 kPa carbon monoxide, 100 kPa nitrogen + 50 kPa carbon dioxide and 100 kPa nitrogen + 50 kPa hydrogen) in Hungate tubes. After 8 days some carbon monoxide was consumed and all tubes were topped up to total gauge pressure of 150 kPa with CO, CO_2 or H_2, respectively. The formation of 1-propanol and 1,2-propanediol and other products was measured with HPLC.

Compared to the headspace containing carbon dioxide 30x more 1-propanol was produced with carbon monoxide (Figure 6-3 C&F) and 15x more with hydrogen in the head space (Figure 6-3 E&F). It seems that initially 1,2-propanediol is formed which is subsequently transformed into 1-propanol. This can be inferred from the observation that in the CO and H_2 headspace cultures 1,2-propanol levels at 169h were higher at 500h while the values were inversed for 1-propanol. In the case of lowest rhamnose concentrations with CO headspace no 1,2-propanediol was detected but 1-propanol was.

Since carbon monoxide was the only headspace that can support growth on its own growth on lower rhamnose concentration show a combined profile of rhamnose and CO use, whereas the cultures with CO_2 and H_2 seem to use rhamnose as primary carbon and energy source (Figure 6-3). The tubes with carbon monoxide reached higher optical densities faster and had already consumed nearly all rhamnose after 168 hours while CO_2 and H_2 headspace both had somewhat longer lag phases and less rhamnose consumed after 168 hours.

The headspace pressure decreased over time in all tubes (Figure 6-3 B). Except in the case for the CO headspace cultures this decrease is likely caused by escaping gas. Indeed butyl rubber is much more permeable for CO_2 than for H_2 (310). Furthermore the H_2 and CO_2 cultures with lowest rhamnose starting condition had the strongest decrease and the cells consuming rhamnose likely produce CO_2 and H_2. Therefore, if no gas had escaped pressure would have increased in these tubes.

Other noteworthy observations include the higher ethanol concentrations in the reducing atmospheres (CO & H_2), most lactate is formed under a carbon dioxide atmosphere and the finding of formate in both CO_2 and H_2 containing tubes.

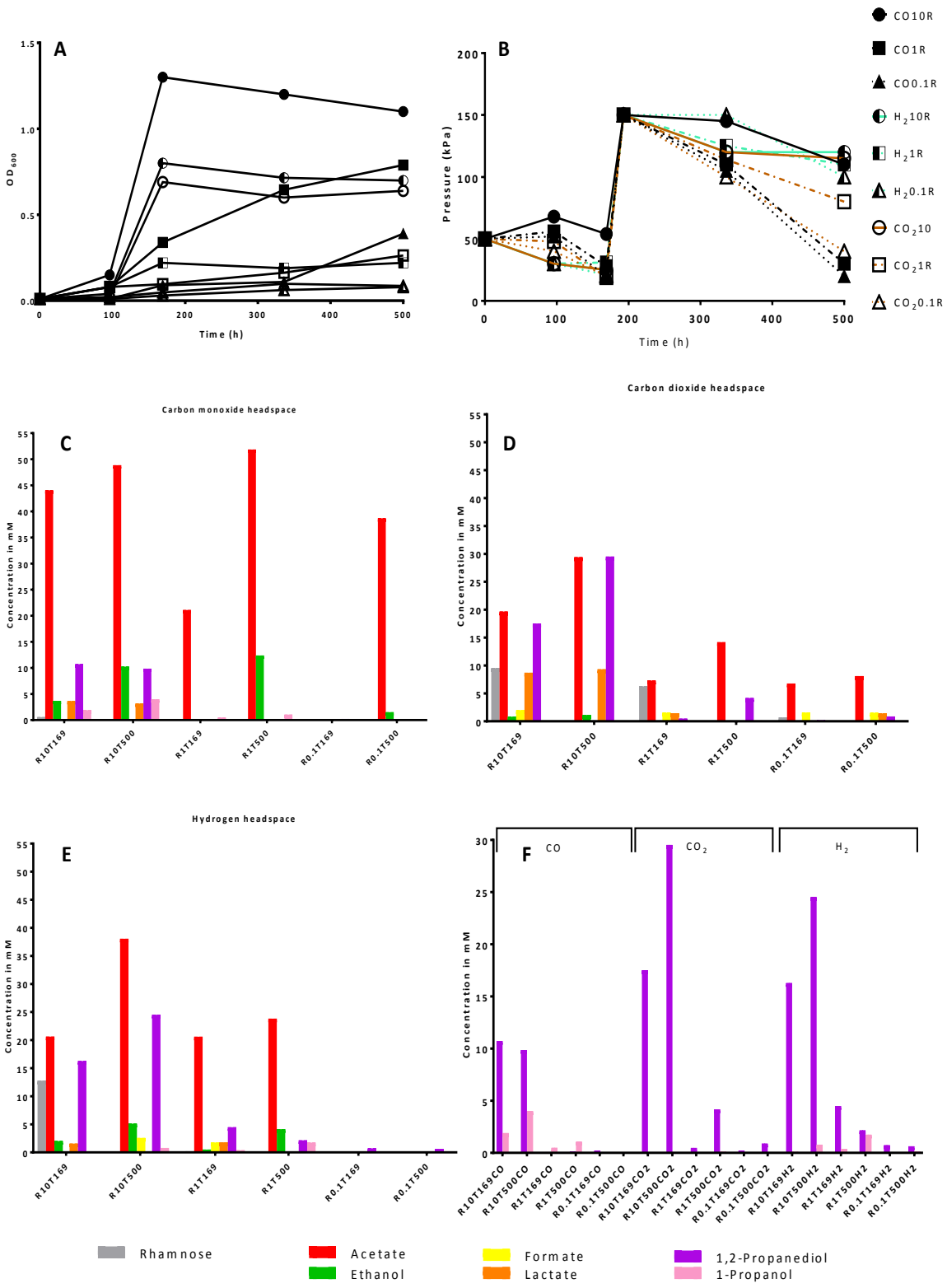

Figure 6-3 The results of the rhamnose growth experiment with different headspace compositions.

Panel A depicts the optical density of the tube culture plotted against time. **Panel B** depicts the headspace pressure, **C** depicts the product formation of the rhamnose grown cultures with CO in the head space, **D** shows the cultures containing CO_2 in the headspace, **E** shows the results for the H_2 headspace tubes. In all three of the product spectrum (C, D &E) from left to right: 10 g l^{-1} rhamnose tube at 169 h (R10R169), 10 g l^{-1} rhamnose at 500 h (R10T500), 1 g l^{-1} rhamnose tube at 169 h (R1T169), 1 g l^{-1} rhamnose at 500 h (R1T500), 0.1 g l^{-1} rhamnose tube at 169 h (R0.1T169), 01 g l^{-1} rhamnose at 500 h (R0.1T500). **Panel F** finally focuses only on 1,2-propanediol and 1-propanol concentration of these same time point comparing all three types of head space in one graph. This graph shows the effect of head space composition: where the carbon monoxide and the hydrogen containing tubes show 1-propanol, the carbon dioxide cultures do not show this substance.

6.2 Discussion

The starting concentrations of the carbon source influences the product spectrum. More reduced products such as ethanol and 1,2-propanediol are formed at higher carbon source levels. I expected that at very low carbon concentrations *C. autoethanogenum* would act somewhat as a homoacetogen i.e. that acetate is its sole product. Indeed, this is more or less what we found. At ≤0.1 g l^{-1} carbon source, only amounts close to detection limit or no product besides acetate were found. Although the trend in all carbon sources was found to shift to relatively more acetate at lower starting concentrations it is not absolutely certain acetate is the sole product at the lowest carbon source. Since all products are at lower concentration at lower initial carbon source concentration it cannot be fully ruled out that the finding is partly an artefact of the metabolite levels getting close to detection limit of our HPLC. However the observed trend is not an artefact of this since the higher values were in the range of our calibration series.

The ratio between product mass and biomass was the opposite of what was expected. It was expected that at higher substrate levels something else than the carbon source would be growth limiting which in turn would mean that more total product per biomass might be formed. What we did observe however was that at lower substrate levels relatively more product was formed per biomass. This is somewhat puzzling. It might be an artefact from the optical density measurements used that are increasingly imprecise at low levels of growth. A biological explanation could be that the thermodynamics at very low product concentration are more favourable for product formation.

This chapter gives the first quantification of native 1-propanol and 1,2-propanediol production by *C.autoethanogenum*. Although these compounds are produced from the rather costly rhamnose, it shows unequivocally that the organism has the necessary pathways to produce these substances. In our genome annotation of *C.autoethanogenum* genes coding for enzymes that catalyse the rhamnose degradation steps to dihydroxyacetone phosphate (feeds into glycolysis), and (S)-lactaldehyde were annotated: L-rhamnose mutarotase (CLAU_2032), L-rhamnose isomerase (CLAU_2035), Rhamnulokinase (CLAU_2036), and Rhamnulose-1-phosphate aldolase (CLAU_2034). (S)-lactaldehyde can subsequently be reduced to 1,2 propanediol by a lactaldehyde reductase. For this enzyme no gene has been annotated however multiple candidates (alcohol dehydrogenases) can be found of which CLAU_1460 is the most likely candidate since it this has the highest identity with the lactaldehyde reductase from *C. carboxidivorans* and is annotated in other related (*C. ljungdahlii*) species as a 1,3-propanediol dehydrogenase. This same gene might also code for the enzyme responsible for the further reduction from propanal to 1-propanol however another candidate gene (CLAU_3196) coding is also likely responsible for this step. No gene was identified that could encode an enzyme catalysing the dehydration reaction from 1,2-propanediol to propanal. At the moment I can only hypothesise on what the exact pathway is that is used but an elucidation of that pathway might lead us a way to use those native pathways to produce these products from carbon monoxide.

In *Clostridium phytofermentans* propionate (next to 1-propanol) has previously been shown to be a product with growth on fucose and rhamnose(302). This product was not observed in the experiments described in this chapter, however we did not specifically look for this compound either. Propanol was found because there was a previously unidentified peak in our HPLC spectra. There were no obvious further unidentified peaks in our HPLC spectra. However we did not ad a standard for this product so it might be that our method is relatively insensitive for proprionate. The cultures grown on rhamnose did not have noticeable odour of propionate. Since headspace composition was not monitored for this experiment it is not possible to make a full carbon balance it is therefore possible that a small amount proprionate is produced next to 1,2-propanediol and 1-propanol.

There are trace amounts of 1,2-propanediol formed on xylose. Why this is the case is not fully clear. Xylose is degraded via the pentose phosphate pathway which is also used in the opposite direction to produce many important metabolites such as ribose-5-phosphate. The pentose phosphate pathway produces glyceraldehyde 3-phosphate (GAP) and fructose 6-phosphate which both are intermediates of the glycolysis. In the glycolysis fructose 6-phosphate is further phosphorylated to fructose 1,6 phosphate and split in dihydroxyacetone phosphate (DHAP) and GAP. DHAP and GAP interconversion is catalysed by triose phosphate isomerase. If for any reason GAP is not metabolised fast enough this might lead to GAP and DHAP build-up. If the DHAP reaches high levels, the methylglyoxal pathway is activated forming 1,2-propanol as end product (311). It is unclear why this pathway seems to be specifically active on xylose and not on fructose for which much of the other behaviour is similar.

Chapter 7:
In frame deletion of the
alsS gene.

7 In frame deletion of the alsS gene

7.1 Introduction

To increase or understanding of the central metabolism of *C. autoethanogenum* a collaborative effort of our lab was made to knock out all pathways that that are implicated in converting either Acetyl-CoA or Pyruvate towards the products, Acetate, Ethanol, Lactate and 2,3-butanediol. The genes to knock out were divided between all six PhD students and two post-docs. The intention was to use in-frame deletion to first produce a *ΔpyrE* which then would be used to make further deletion strain of the specific genes after which the pyre locus would be repaired. A secondary reason to work in parallel and close collaboration was to investigate the mutation build up during the strain production with the allelic exchange method. Especially the use of FOA was thought to be a likely mutagenic factor (188).

Acetolactate synthase (ALS) catalyses the conversion of pyruvate to acetolactate (eq 2), which is an essential step in the production of the branched-chain amino acids (valine, leucine & isoleucine) and thus is ubiquitous in nature.

$$2\ \text{pyruvate} \xrightarrow{\text{ALS}} \text{acetolactate} + CO_2 \quad \text{(eq 2)}$$

Acetolactate is also a precursor for 2,3 butanediol production in *C. autoethanogenum* and a gene encoding ALS, *alsS (*CLAU_1694), has been cloned and the catalytic properties of ALS confirmed by Köpke *et al*(167). The gene *alsS encodes* for a catabolic acetolactate synthase. Next to this gene the genome contains 3 more genes encoding anabolic acetolactate synthases; *ilvB, ilvI, ilvH* (CLAU_0388, &CLAU_0119-0120).

Here I will report on some of my effort to make an in-frame deletion of *alsS.* The in-frame deletion of the a*lsS* gene was produced using the allelic exchange method in the Δ*pyrE* strain background. The deletion was the first successful gene deletion in in this background strain and thus was an important prove of concept. Preliminary strain characterisation showed that growth on minimal medium was similar as wild type but medium containing 5 g l^{-1} cas amino acids improved growth in WT while it this was less the case for the Δ*alsS* mutant.

7.2 Methods

To construct the inframe deletion of the *alsS* gene, first a Δ*pyrE* strain was created. This strains allows for positive/negative selection using uracil and FOA as selective agents. This strain was used to produce a Δ*pyrE* Δ*alsS C. autoethanogenum* which was then used to produce a Δ*alsS C. autoethanogenum* strain. This strain was then grown on CO in rich, semi-defined and minimal media for strain characterisation.

7.2.1.1 ΔpyrE strain construction

The Δ*pyrE* strain was constructed by conjugating a CA434-pMTL-AMH101 with a wild type *C.autoethanogenum* and selected on YTF plates with trimethoprim and thiamphenicol. Of these 35 colonies where selected and plated on YTF plates containing 1mg/ml 5-FOA. The colonies that appeared were restreaked on PETC-MES with YE and PETC-MES without YE but with CAA to further select for uracil auxotrophs. The auxotrophs where once more restreaked on YTF (with uracil) and PETC-MES lacking uracil after which 8 colonies were selected to grown up in liquid YTF. These liquid cultures were used to make -80 ^{o}C stocks and to isolate genomic DNA . The genomic DNA was used as a template for a PCR with to amplify the *pyrE* region and the resulting PCR fragment was send for sequencing with the fsppyre primer. Genomic DNA was isolated and fully sequenced by DeepSeq and Δ*pyrE* with least polymorphisms were used for further work.

7.2.1.2 ΔalsS construction

The AlsS deletion plasmid was constructed with the pMTL-AMH101 plasmid as backbone from which the *pyrE* homology arms where cut out by restriction using SacII and AscI, followed by antarctic phosphatase treatment and separation of the fragments by gel electrophoresis on 1% agarose and plasmid DNA from gel. The *alsS* flanking homology arms insert was constructed using primer pair alsS F1, alsS R1 for left homology arm and primer pair alsS F2, alsS R2 for right homology arm using genomic *C.autoethanogenum* DNA as template. Both fragments were purified using a Sigma PCR-clean up kit and used as template for SOE-PCR with primer pair alsS F1, alsS R2. The resulting fragment was restricted with SacII and AscI and ligated to the plasmid backbone. The resulting plasmid was used to transform Top 10 cells followed by growth on LB agar + chloramphenicol. Result was screened by colony PA colony PCR with primer pair alsS F1, alsS R2. The correct plasmids were isolated and sequenced. This plasmid was then transferred to *E. coli* CA434 which were then used to transfer plasmids to Δ*pyrE C. autoethanogenum*. The colonies that appeared on selective YTF+ Tmp + TP plates were restreaked after which single colonies were screened for single crossover events using alsSflankF Bart_PPrev or alsSflankR Bart_PPfwd primer pairs. Positive colonies were streaked on YTF+FOA+Uracil plates. Colonies that appeared on these plates were replica plated on YTF, semidefined PETC-MES plates with and without uracil to test for uracil auxotrophy. The auxothophic colonies were restreaked to YTF and screened for inframe deletion using alsSflankF alsSflankR as primer pair and Sanger sequencing. In de confirmed Δ*pyrE* Δ*alsS* strains plasmid pMTL-CH20 was used to repare the Δ*pyrE* back to its WT. For this the pMTLCH20 in an *E. coli* Sexpress strain was used to conjugate with the Δ*pyrE* Δ*alsS C. autoethanogenum* strains. Succesfull conjugant colonies were transferred to semidefined media without uracil. The DNA of the resulting colonies was screened with PCR for Δ*alsS* deletion and *pyre* repair with primer pairs alsSflankF + alsSflankR and ACE pyrE FSP + ACE pyrE RSP.

7.3 Results

7.3.1 ΔpyrE strain construction

The *ΔpyrE* strain was constructed by conjugating a CA434-pMTL-AMH101 with a wild type *C.autoethanogenum* following the procedure described above. The genomic DNA of the resulting uracil auxotrophs was isolated. The genomic DNA was used as a template for a PCR with ACE pyrE FSP, ACE pyrE RSP to amplify the *pyrE* region and the resulting PCR fragment was send for sanger sequencing with the fsppyre primer. Genomic DNA was also send of to be Illumina sequenced. Both methods of sequencing confirmed the construction of a clean *ΔpyrE* strain. Since this part of work was done in parallel by six people a comparison between produced strains could give insight to how mutagenic the strain construction process with a FOA step was. Table 7-1 gives an overview of the results of the genome sequencing. Every researcher had multiple strains created and chose one to send for genome sequencing. One (Sam) sent a strain that underwent the full procedure but reverted to WT in the final step. It is clear that the procedure yields some mutations however much less than we feared based on previous experience in other species of Clostridia (personal communication Christopher Humphreys). The strain created by Ronja had least mutations and went on to be the standard background strain.

Table 7-1 genome sequencing results

Bart	*ΔpyrE* 3 SNV, 1 deletion (1 nt), 1 insertion (1 nt)
Chris	*ΔpyrE* 1 insertion (15 nt)
Pawel	*ΔpyrE* 2 SNV, 1 deletion (1 nt)
Pete	*ΔpyrE* 1 SNV, 1 insertion (15 nt)
Ronja	*ΔpyrE* 1 SNV
Sam	WT, 3 SNV, 1 Insertion (1 nt)

7.3.2 ΔalsS construction

The *alsS* deletion plasmid was constructed with the pMTL-AMH101 plasmid as backbone with the *alsS* flanking homology arms inserted. The plasmids were used to create the *ΔalsS* in the *ΔpyrE* background strain. Strains were checked with PCR (Figure 7-1) and Sanger sequencing. The pMTL-CH20 plasmid was used to correct the *pyrE* locus restoring uracil prototrophy (Figure 7-2) and creating a *ΔalsS* as a final product. The a*lsS* deletion was confirmed by PCR and Sanger sequencing.

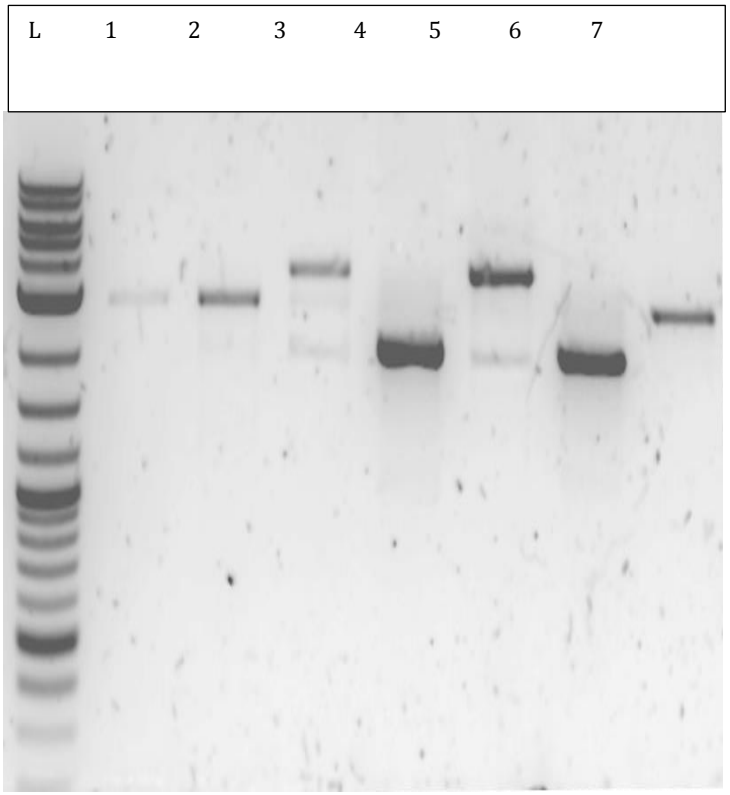

Figure 7-1 Electrophoresis of PCR for *alsS* deletion screening

Primer pair alsSflankF, alsSflankR. L=Log2 ladder, 1-7 are PCR products of produced strain. Strains 3 and 5 are wild type with small proportion of *ΔalsS,* strains 4 and 6 are *ΔalsS* strains. While 1,2 & 7 gave unclear sequencing results which were not further analysed. Expected fragment size WT is 3.8 kb while *ΔalsS* strains should yield 2 kb. 2-log lader band size top to bottom 10 kb, 8 kb, 6 kb, 5 kb, 4 kb, 3 kb, 2 kb, 1.5 kb, 1.2 kb, 1.0 kb, 0.9 kb, 0.8 kb, 0.7 kb, 0.6 kb, 0.5 kb, 0.4 kb, 0.3 kb, 0.2 kb, 0.1 kb.

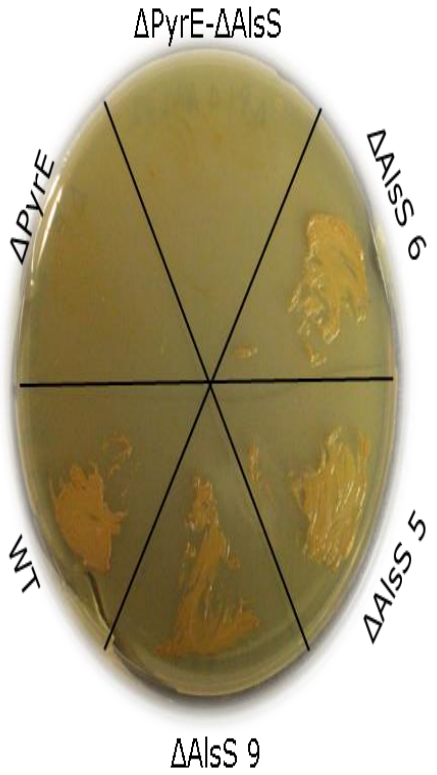

Figure 7-2 PETC-MES agar plate

without uracil showing restoration of uracil prototrophy in the *ΔalsS* strains. No growth was observed in either *ΔalsS and ΔpyrE ΔalsS* as expected from uracil auxotrophs

7.3.3 Preliminary strain characterisation

The strain was characterised in a preliminary growth experiment. In this growth experiment WT and *ΔalsS* strains were grown on CO and PETC-MES without Cas amino acid (CAA) (minimal medium), 0.5 g l^{-1} CAA (low AA medium) and 5 g l^{-1} CAA (rich medium) .The data (Figure 7-3) shows differences when Cas amino acid (CAA) were present in the media. While the WT displayed increased growth when CAA were added the *ΔalsS* did not benefit in the same way. Although some initial benefit of CAA addition to growth was apparent, the mutant strain did not reach the same final OD. Figure 7-3 further more shows no significant difference was noticeable on minimal medium between the strains. The low level CAA addition had a similar effect but less pronounced (appendix figure Figure 11-11). The product formation showed some differences between the strains. WT produced higher levels of acetate when amino acids are present while this was not significant for the mutant.

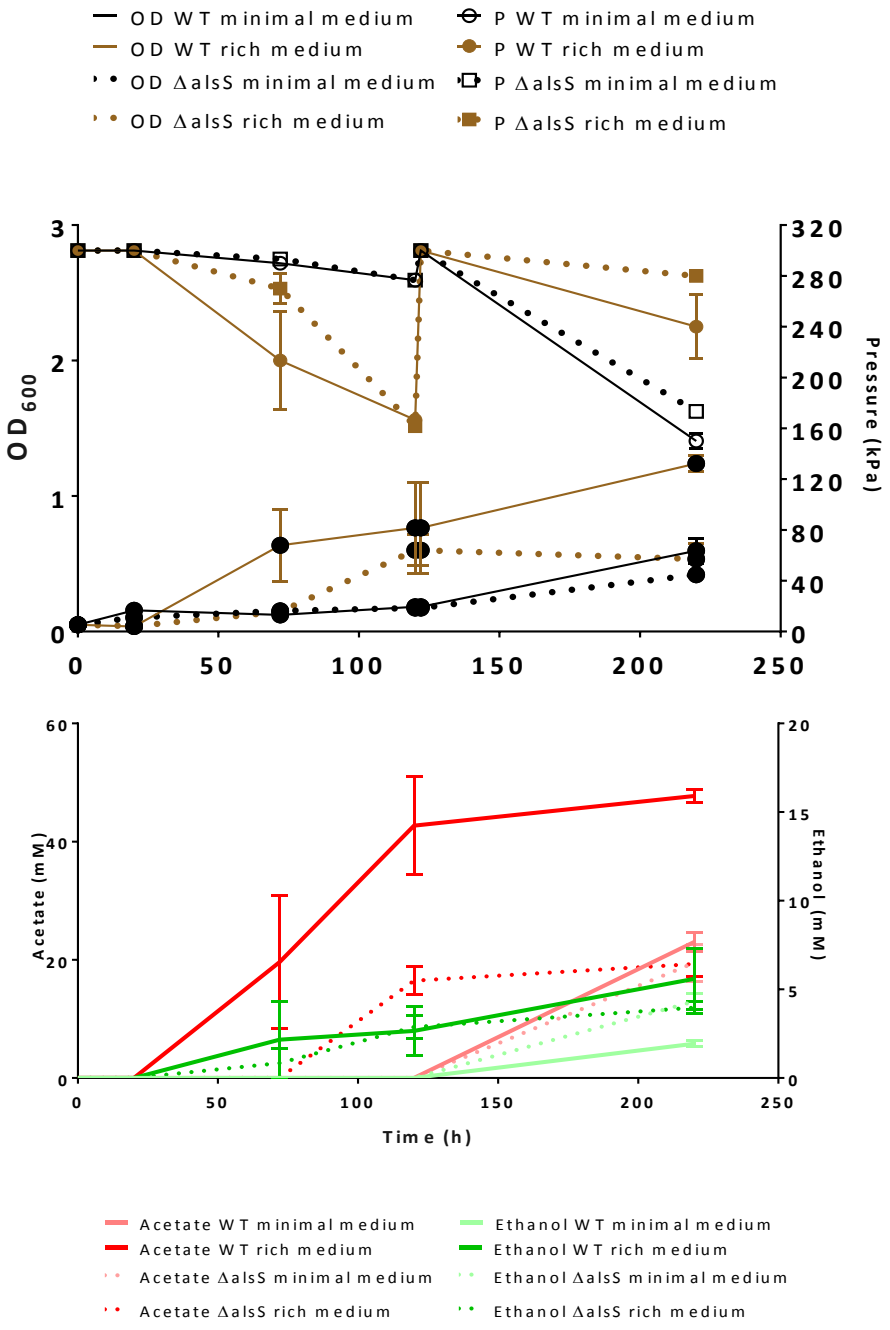

Figure 7-3 Overview of growth of the WT and *ΔalsS*.

Top graph shows the headspace pressure and optical density of the cultures. Bottom graph shows the product formation. The *ΔalsS* behaves similart to WT when grown on minimal medium. WT benefits more from addition of cas amino acids compared to *ΔalsS*.

7.4 Discussion

The *ΔalsS* strain was the first mutant created using the allelic exchange based in-frame deletion/ACE system in *C. autoethanogenum* in this background strain. Somewhat previous to this creation our lab member Fung Min Liew created an in frame deletion of *aor2* in a different *ΔpyrE* background strain (166). Together these two strains were a good prove of concept of the allelic exchange method to create in-frame deletions. Others moved on and created three more knock out mutants (personal communication Pawel Piatek and Christopher Humphreys). However many, if not most, other attempts to create knock-out mutants using this method failed. Partly because of the troubles creating these mutants, partly because other lines of research were more fruitful, this line of research was abandoned and no proper characterisation of the *ΔalsS* strain was performed.

If CAA are present there appears to be some difference in growth between WT and *ΔalsS.* This can be explained by the fact that the anabolic acetolactate synthases (ilvB, IlvI & ilvH) are often inhibited by the branch chain amino acids (312) while it is likely that the catabolic AlsS is induced by acetate as is the case in *B. subtilis* (313). In minimal medium the amino acid pools are likely relatively low. However in medium with high amino acid concentratio the internal pools might be higher which in turn inhibit the anabolic acetolactate synthases. In WT the catabolic acetolactate synthase (alssS) can still catalyse the reaction however in the ΔalsS mutant this is not possible (figure 7-4). One can speculate that this in turn leads to build up of pyruvate which both acidifies the cell and makes the PFOR reaction less thermodynamically favourable which might cause lower ferredoxin recycling. It follows that the redundant nature of the ALS enzymes is of important in environments that are rich in branch chained acids and acetate.

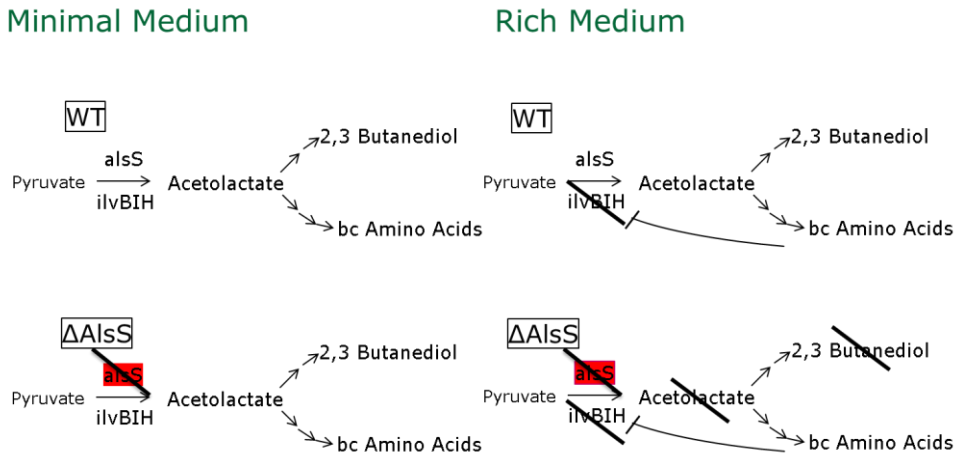

Figure 7-4 model to explain the difference in behaviour between WT and *ΔalsS* strains .
In minimal medium pyruvate can be transformed into 2,3-butandiol, and branched chained amino acids in both strains. In rich medium (with branched chain amino acids) the mutant strain cannot remove excess pyruvate to the same amount as WT.

Chapter 8:

Determining the promotor strength of eleven heterologous thiolase and ferredoxin promotors in *C. ljungdahlii* and *C. autoethanogenum*

8 Determining the promotor strength of eleven heterologous thiolase and ferredoxin promotors in *C. ljungdahlii* and *C. autoethanogenum*

8.1 Introduction

Gene expression, either from a plasmid or from the genome, requires a promotor region and a ribosomal binding site (RBS) upstream of the gene. For this the standard pMTL8000 plasmids offer a choice of two different promoters and RBS upstream of a multiple cloning site (181). These promoters and RBS are derived from constitutively and highly expressed genes; the thiolase gene (*thl*) from *Clostridium acetobutylicum* ATCC 824 (314) and the ferredoxin gene (*fdx*) from *Clostridium sporogenes* NCIMB 10696(315).

Other Clostridia species harbour variations of these promoters which may vary in strength. For engineering purposes it is useful to have a larger set of promotors to choose from. A library of 11 different P_{fdx} and P_{thl} promoters combined with a RBS of the *thl* gene of *C. acetobutylicum* cloned upstream of a *catP* reporter gene in pMTL8225x plasmids. The *catP* gene encodes a chloramphenicol acetyltransferase, the activity of which can be measured colorimetric. Using this colorimetric assay, the 11 constructs have been used to determine their promoter strength in *C. acetobutylicum* and in *C. sporogenes (*B.Wilson, R. Mansfield, K. Kovács & Dr A. Kubiak). Here I will report the introduction and expression of these 11 constructs in *C. ljungdahlii* and *C. autoethanogenum* and compare the strengths of the different promoters in these organisms.

This data of this promotor library screening has proved useful in subsequent work by Pete Rowe and Florence J. Annan. Pete Rowe continued with producing and testing an RBS library.

8.2 Method

8.2.1 Promoter library strain production, growth and lysis of cells

Dr Katalin Kovács kindly provided 12 *E.coli* CA434 strains containing the constructs with the different promoters to test. These strains were used as donor strains in conjugation to both WT *C. ljungdahlii* and *WT C.autoethanogenum.* From the selective plates 3 colonies of each strain were selected. These strains were grown up in YTF from a start OD_{600} of 0.05. After OD_{600} of approximately 1 was reached 20 OD equivalents of cells were pelleted and resuspended in 10mM Tris + 2% protease inhibitor cocktail VII to a total of 2 ml. 200 µl of the cell suspension was lysed by sonication. Plasmids were isolated and used as a template for a PCR with Bart_PPfwd, Bart_PPrev primer pair. The PCR products were sequenced with the M13R as sequencing primer.

8.2.2 Chloramphenicol acetyl esterase (CatP) assay

Chloramphenicol acetyltransferase (catP) activity of the crude lysates of promoter test strains was measured by a catP assay performed in triplicate using a Tecan M1000Pro plate reader. Of each crude lysate 5 µl was pipetted in a well of a 96-wells transparent plate. To start the assay reaction 195 µl of the catP assay mixture (27 ml 100mM Tris buffer pH 7.8, 1 ml 5,5'-Dithio-bis(2-Nitrobenzoic Acid) (DNTB) 1.0 mg/ml solution, 1ml of Acetyl CoA 4.68 mg/ml solution and 0.5 ml chloramphenicol 3mg/ml solution) was injected in the well. Immediately the absorbance at 413 nm was measured for 90 seconds. The measurements were recorded in a Microsoft Excel spreadsheet. This data was used to determine the maximum speed of the reaction as a measure for the amount of catP in the cell lysates. As an alternative measurement catP production was also assessed by a cell growth antibiotic halo assay. Small rounds (d = 5 mm) of filter paper were soaked in 15mg/ml thiamphenicol solution and placed in the centre of a YTF plate on which 100 µl of liquid culture of the promoter test strains was spread evenly. The size of the produced halo was used as a measure of catP activity.

8.2.3 CatP reporter assays

Chloramphenicol acetyltransferase (catP) activity of the crude lysates of the promoter test strains was measured by a catP assay performed in triplicate using a Tecan M1000Pro plate reader. The units of enzyme per OD_{600} equivalent were used as a measure of the transcription driving strength of the promoters. The strain NoP-CatP strain had no promoter upstream of the *catP* gene and was used as a biological negative control. A water sample was used as a non-biological negative control to all data.

Table 8-1 List of the promotors used with the species of origin.

Promoter tag	Origin
Ferredoxin promoters	
Csp_fdx	*Clostridium sporogenes*
Cbe_fdx	*Clostridium beijerinckii*
Sac_fdx	*Clostridium saccharoperbutylacetonicum*
Cpf_fdx	*Clostridium perfringens*
Cte_fdx	*Clostridium tetani*
Clk_fdx	*Clostridium kluyveri*
Thiolase promoters	
Cac_thl	*Clostridium acetobutylicum*
Cbe_thl	*Clostridium beijerinckii*
Ccv_thl	*Clostridium cellulovorans*
Clk_thl	*Clostridium kluyveri*
Cby_thl	*Clostridium butyricum*
Cpf_thl	*Clostridium perfringens*

8.3 Results

The promotor strength of the 11 different *fdx* and *thl* promoters was tested in *C. ljungdahlii* and *C. autoethanogenum* using the CatP reporter assay. The results (Figure 8-1) show that six promotors are fairly strong: the pMTL8000 standard *Csp_fdx* & *Cac_thl* promoters, and further, *Cpf_fdx* , *Cpf_thl* are all of similar strength in both species while *Cby_thl* and *Cte_fdx* are somewhat less strong(0.4-0.8x of *Cac_thl*) while *Sac_fdx* was relatively weak (0.05-0.2x *Cac_thl*).

The promotors *Clk_fdx* and *Ccv_thl* showed great variation between the replicates and between the host species. Sequencing of the plasmids of these replicates revealed mutations in the relevant section, mainly caused by *E.coli* insertion elements. In the Cbe_thl CatP plasmids of all replicates of *C. ljungdahlii* and *C. autoethanogenum* contained insertion elements.

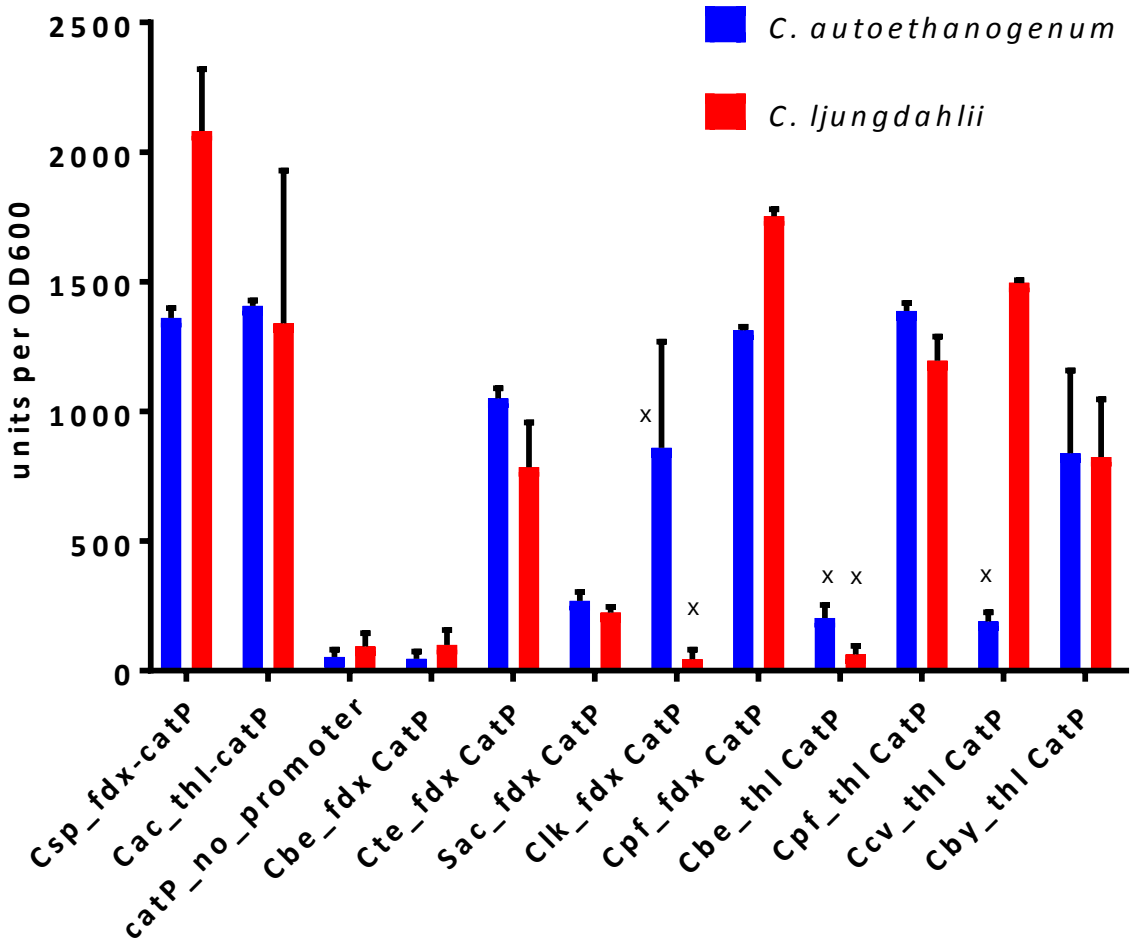

Figure 8-1 The units of CatP activity per OD equivalent of promoter-catP constructs of *C.ljungdahlii* and *C.autoethanogenum*.

For every construct there are three replicates per species. Error bars represent standard error of the mean. *Csp_fdx* & *Cac_thl*, *Cpf_fdx* and *Cpf_thl* apparently are of equal high strength, *Cby_thl* and *Cte_fdx* are somewhat weaker. The weakest promoter with significant results for both species was P*fdx* of *C. saccharoperbutylacetonicum*. The x indicates that sequencing revealed mutations in essential parts of the plasmid, mostly caused by insertion elements.

The results of the promoter strength test results of four species, *C. sporogenes, C. acetobutylicum*, *C. autoethanogenum* and *C. ljungdahlii* were compared with the promoter strengths normalised to *Cac_thl-catP* for each species (Figure 2). The constructs with Cte_fdx-CatP, Sac_fdx-CatP and *Cpf_fdx CatP* have all higher relative expression levels in *C. autoethanogenum* and *C. ljungdahlii* than in *C. acetobutylicum* and *C.sporogenes*.

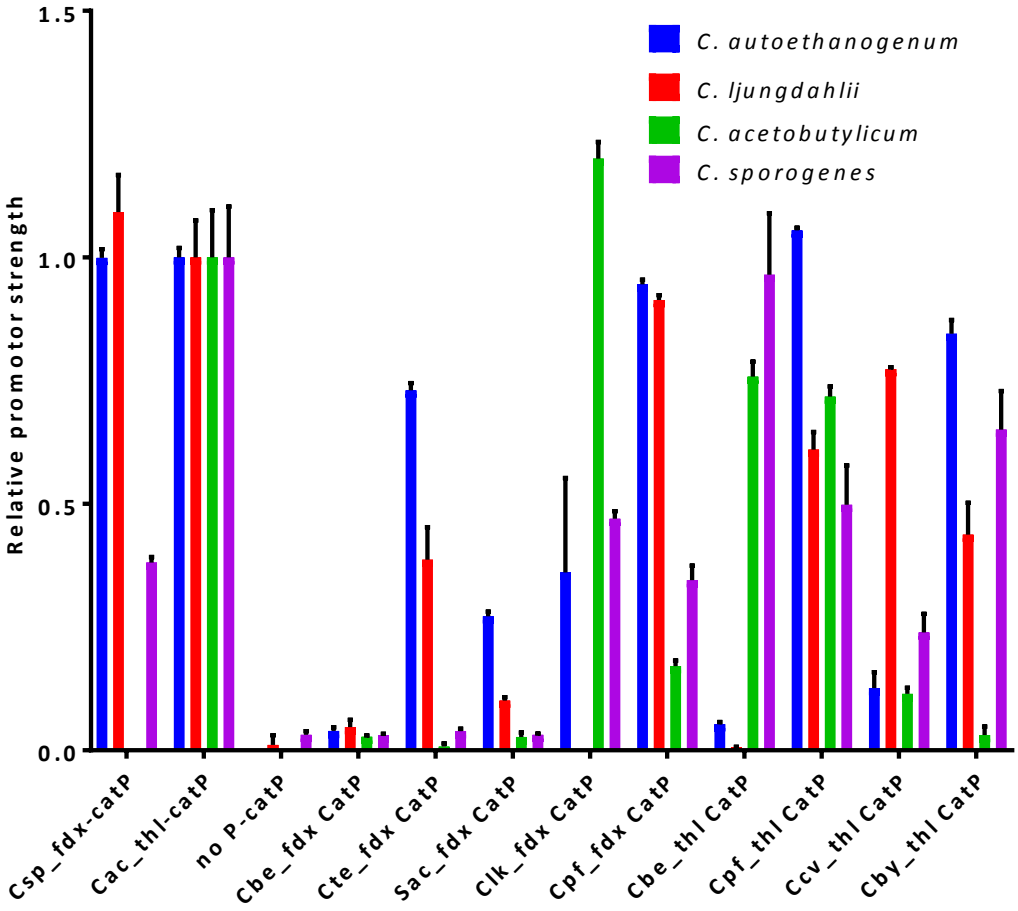

Figure 8-2 the relative promoter strengths of Clostridial promoters in four different Clostridial species.
Because of slight methodological differences comparison can only be relative and the values of the test strains of one species were normalised by the values of *Cac_thl-catP* of the same species. Error bars represent the standard error of the mean. Data of *C. acetobutylicum* by B.Wilson, R. Mansfield, K. Kovács and data of *C. sporogenes* by Dr A. Kubiak.

Promoter strength was also assessed by a cell growth antibiotic halo assay. Small rounds (d = 5 mm) of filter paper were soaked in 15mg ml^{-1} thiampenicol solution and placed in the centre of a YTF plate on which 100 µl of liquid culture of the promoter test strains was spread evenly. The size of the produced halo was used as a measure of catP activity. The results of the antibiotic resistance halo assay are shown in Figure 8-3. The construct with a catP gene without promoter shows no sign of growth on the YTF agar plates with chloramphenicol in the centre. The constructs with very low promoter activity (such as Cbe-fdx-catP) show approximately 1 cm halo while the all the stronger promoters show no sign of halo. In the catP assay Cbe-fdx-catP barely showed any significant activity while this halo assay shows clearly shows some effect of this promoter.

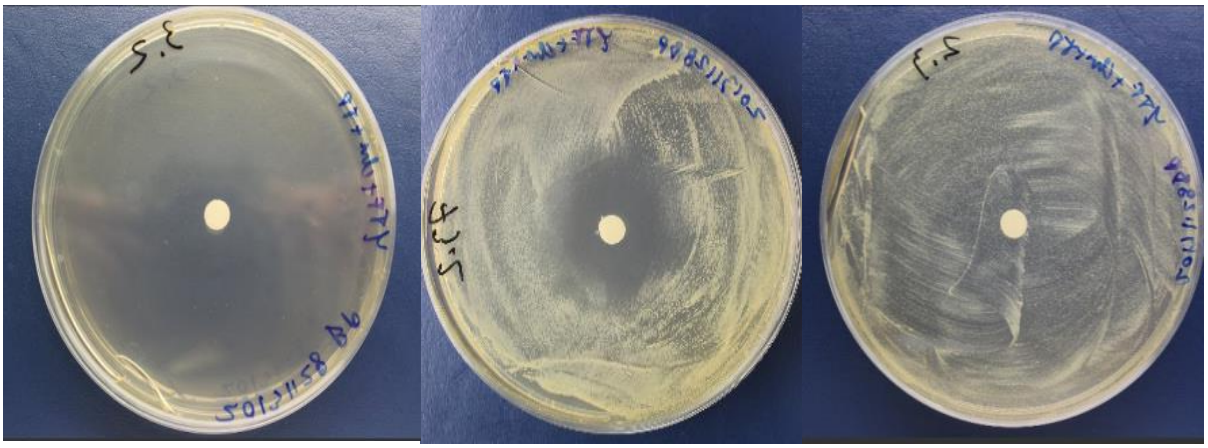

Figure 8-3 Thiamphenicol resistance halo assay.
From left to right on these plates: *C.ljungdahlii*_pMTL82254 (no promoter-catP), *C.ljungdahlii*_pMTL8225x_ Cbe_fdx CatP and *C.ljungdahlii*_pMTL8225x_Cac_thl-catP.

8.4 Discussion

The testing of the promoter library in *C. autoethanogenum* and *C. ljungdahlii* confirmed the finding that the promoters P_{thl} and P_{fdx} of different species have different expression driving strengths in different species. It showed that standard P_{thl} and P_{fdx} of the pMTL80000 plasmids are strong promoters in *C. autoethanogenum* and *C. ljungdahlii*. Furthermore *Cpf_fdx*, *Cpf_thl* promoters were shown to be suitable for high level expression, *Cby_thl* and *Cte_fdx* for only slightly lower levels and *Sac_fdx* for significant lower levels of expression.

C. autoethanogenum and *C. ljungdahlii* are closely related which is reflected in the fact that the average patterns of expression of the constructs are similar. The biggest difference between *C. autoethanogenum* and *C. ljungdahlii* not explained by mutations are in the Cte_fdx-CatP constructs.

Because five strains showed mutations in the constructs the results of these should not be used as indication of the promoter strength. The mutations in the constructs could be caused by the very high levels of CatP in the cells (both *E.coli* CA 434 and the *Clostridia*) providing selective pressure for mutants with lower amounts of CatP activity. This could mean that the Cbe-thl and Clk promoters are is in fact strong promoters. To reduce likelihood of mutations of the construct adding some thiamphenicol to the medium could help by applying some selective pressure for active catP. As most mutations were caused by insertion elements of *E.coli*, the use of a strain without these types of elements would reduce most of these problems (316).

The activity of the constructs Cbe_fdx_CatP appear to be close to the average activity of the biological negative controls but promoter strength was also tested by antibiotic resistance halo assay (Figure 8-3) and the halos for Cbe_fdx_CatP were smaller than those for NoP-CatP. This indicates that the colorimetric catP assay as applied here is not sensitive for lower levels of CatP even though these amounts are enough to cause antibiotic resistance.

Since the goal of establishing the ability of these promoters to work in *C. autoethanogenum* and *C. ljungdahlii* and preferably to find some variation in promoter strength was reached no further optimisation was performed. Combined with the RBS library produced by Pete Rowe (appendix 10.12) this promotor library allows future researchers to control gene expression at a desired level in these Clostridial acetogens.

Conclusion

"*Thus, from the war of nature, from famine and death, the most exalted object of which we are capable of conceiving, namely, the production of the higher animals, directly follows. There is grandeur in this view of life, with its several powers, having been originally breathed into a few forms or into one; and that, whilst this planet has gone cycling on according to the fixed law of gravity, from so simple a beginning endless forms most beautiful and most wonderful have been, and are being, evolved.*"

From: On the Origin of Species by Means of Natural Selection, or the Preservation of Favoured Races in the Struggle for Life. Charles Darwin (317)

9 Conclusion

In a sustainable economy, waste must be used as a resource. Municipal waste and biological waste are carbon rich substances that can be converted to synthesis gas (syngas) by pyrolysis. Industrial processes, such as steel production, release syngas as off gas (14, 112, 318) Syngas has been successfully employed as a substrate for production of a range of organic compounds ever since Franz Fischer and Hans Tropsch developed the thermochemical process that bears their name in 1923 (120).

Evolution developed a biological parallel to the Fischer-Tropsch process billions of year prior to the thermochemical process. This process might even be as old as life itself (9, 99, 319). Modern day bacterial acetogens such as *Clostridium autoethanogenum* and its relatives can grow on syngas while producing useful compounds such as acetate, ethanol, 2,3-butanediol and lactate (14, 87). Employing the biological Fischer-Tropsch process in an industrial setting to convert waste into products can have important advantages in feedstock flexibility and energy use over the thermochemical process (112, 125).

Clostridium autoethanogenum was isolated from rabbit droppings in 1993 (13). In recent years much research has been focused on this bacterium and related species. This has greatly increased our understanding of this organism. However, as with other bacteria, important questions remain unanswered. In this thesis some of those questions have been addressed.

Computer modelling is an important tool to increase our understanding of the metabolism of these organisms. However any computer model depends on the quality data that is available on the organism. To assist our computer modellers the genome annotation was manually improved by a collaboration of all members in our research group working of *C. autoethanogenum* (170). Manual annotation of genomes is laborious and, besides improvements that are currently not possible by automation, might also introduce errors. We improved ~10% of the genome annotation. However while writing this thesis I found a few examples of annotations that could be improved upon even more such as the genes coding for some of the WLP.

As in any bacterial genome, many genes have not been assigned a function. Thomas Millat, one of the computer modellers found some indications that carbonic anhydrases (CAs) could influence certain processes in his model. Therefore he wanted to know if genes coding for CAs were present in the genome of *C. autoethanogenum.* None were annotated and answering this question was not possible with a straightforward BLAST search of the genome.

Chapter 3 describes the finding and characterisation of one previously unannotated carbonic anhydrases that is present in *C. autoethanogenum.* This CA (Caut-bCA) was identified as a member of the most diverse class of CAs, the β-CA class (244). It was significantly dissimilar to other members of this class and did not easily fit any of the previously identified sub-classes of the β-CA class. A diverse group of hypothetical genes in a wide range of bacteria encode proteins that were similar to Caut-bCA. Together these CAs were designated the F-clade of the β-CA class. Clade A-D were previously assigned (235) and the E-clade is the proposed name for a carboxydosome specific group of CAs that were once designated ε-class before they were recognised as β-CAs.

Caut-bCA was purified and biochemically characterised using a CA-assay that was developed for a 96-well plate reader with automated injection. Although the primary structure of the enzyme is dissimilar to other β-CAs the values for the enzyme kinetics as revealed by the assay were within the previous found range for other β-CAs.

For further characterisation protein was purified and handed over to people at the Diamond Light Source in Didcot, Oxfordshire, for X-ray crystallography. The obtained crystals proofed unstable during analysis, but some preliminary data was gathered. New crystal growth has been observed recently which is promising for the future progress of this research.

The protein purification process influenced the activity of the Caut-bCA. Originally a N-terminal His tag was employed. Although protein yields were reasonable, activity was highly variable between several purification attempts. Only one out of nine attempts to purify lead to reasonable active protein. In contrast every purification with the C-terminal Strep-tag yielded active protein. One explanation for this is the effect of a large metal binding his-tag close to the metal binding active site. Another explanation might be the inhibitory effect of compounds involved in the purification process. A range of substances are known to inhibit CAs (240). The inhibitory effect of physiological relevant compounds on the activity of Caut-bCA has not been studied. This might be a valuable direction for future work.

Chapter 4 describes the characterisation of a ClosTron knockout mutant of the Caut-bCA gene. Initially no phenotype for this mutant was found. However, some differences in the metabolism of the mutant

compared to WT were detected using LC-MS. Bioreactor cultures would only start to grow after addition of CO_2 to the gas feed mix. Furthermore the mutant was slightly more sensitive than WT at low pH. These findings inspired further growth experiments in batch cultures, in which more care was taken to not include CO_2 in the media. The mutant was unable to grow at the lower end of the pH growth optimum (of WT) under these conditions. This growth experiment and its replication was the final lab work performed chronologically for this PhD. Complementation of the mutant with a CA gene was not performed and is important future work.

Chapter 5 describes research into the effects of phosphate limitation on the metabolism of *C. autoethanogenum*. In continuous bioreactor cultures the production of ethanol, 2,3-butanediol, CO_2 was significantly higher while biomass and acetate levels were significantly lower at phosphate limiting condition. Metabolomic comparisons between the phosphate and carbon limited steady states revealed higher levels of branched chain amino acids and TCA intermediates such as malate, under phosphate limited culture conditions. This can be explained by redox balancing by redirection of the reducing equivalents from biomass formation toward other redox reaction such as those that produce ethanol, 2,3-butanediol and H_2. This study was the first study of *C. autoethanogenum* that used predefined nutrient limitation at steady state. The genome scale modelling performed in our research group can be refined using the results of these studies. Advisable future direction of this line of research is to further vary the CO gas flow under phosphate limiting conditions. Results of previous studies that varied head space pressure, agitation or gas flow (137, 308, 309) might be partially explained by a switch from carbon limitation being dominant to another nutrient limitation becoming dominant. By working at predefined non-carbon nutrient limitation a better understanding of what happens at to the metabolism at increased CO supply might be established. One shortcoming of this study was the relative short time the steady states lasted which was a trade off to the goal of running multiple steady states at variable conditions in one bioreactor run.

Prior to the bioreactor cultures, pilot batch experiments were performed to establish the range of phosphate concentrations where limitation could be expected. *C. autoethanogenum* was grown in media with a series of phosphate concentrations and fructose, xylose, rhamnose or pyruvate as carbon sources. This resulted in some surprising findings amongst which was the discovery of 1,2 propanediol and 1-propanol as native products of *C. autoethanogenum* when rhamnose was used as substrate, which sparked further investigation in Chapter 6.

Chapter 6 discusses some further growth experiments using fructose, xylose, rhamnose and pyruvate as carbon sources and specifically the effect of headspace composition on the product spectrum of rhamnose grown cultures. It was found that 1,2-propanediol is formed first from rhamnose which is then reduced to 1-propanol. In a CO headpace most of the 1,2-propanediol is further reduced to 1-propanol. For all steps in the pathway toward 1,2-propanediol from rhamnose, putative genes were identified, however, for the further reduction towards 1-propanol, no likely genes were identified. Further research and metabolic engineering might lead to ways to produce 1,2-propandiol and 1-propanol from CO and make its production economically attractive, unlike the production from the expensive rhamnose as carbon source.

Chapter 7 discusses the creation of a Δ*pyrE* strain that was subsequently used to create a clean in frame Δ*alsS* strain of *C. autoethanogenum.* This was the first in-frame deletion created in this background strain and it was an important proof of concept for the use of this technique in *C. autoethanogenum.*

The *alsS* gene encodes an acetolactate synthase, a type of enzyme of which *C. autoethanogenum* possesses two more versions. This redundancy might be the reason why this mutant is one of the few successfully made with this technique. For essential genes the technique might not be suitable. Growth experiments tentatively showed influence of amino acid availability on growth. This research was not further pursued due to restrictions on time. Originally the intention to was to eliminate 2,3-butanediol production to steer carbon flux and redox potential towards ethanol. However this is not a simple task. The ALS step has high redundancy with a total of 3 genes coding for ALS. Recently a *C. autoethanogenum* mutant of acetolactate decarboxylase (ALDC) that catalyses the next step in the pathway from pyruvate to 2,3-butanediol, was produced in our research group. It would be interesting to see if this mutation totally abolishes 2,3-butanediol production. Even though there is just a single gene encoding ALCD, the reaction is known to happen spontaneously (320). The final step again would need a knock out of at least two genes. If only this last step would be eliminated 2,3-butanediol would be abolished and acetoin would be produced. Although this would reduce NAD(P)H consumption in the pathway, the carbon flux would likely not be affected significantly.

Chapter 8 finally, discusses an assessment of a promoter library. This assessment has proven to be useful for other researchers in our group who engineer the metabolism on the *C. autoethanogenum* and

C. ljungdahlii (personal communication Pete Rowe and Florence J. Annan, University of Nothingham) and will likely continue to benefit researchers currently working on this organism.

The work presented in this thesis has expanded the knowledge on *C. autoethanogenum*. We now know that this organism harbours an active carbonic anhydrase of a new sub-class of the β-class that is likely important at lower pH and lower CO_2 concentrations. We learned that phosphate limitation can steer the production from acetate towards ethanol and 2,3-butanediol. Two previously not described native products, 1,2-propanediol and 1-propanol have been discovered and found to be influenced by the headspace composition. In frame deletion was demonstrated and a promoter library tested.

These finding are just a small proportion of the recent developments in the rapidly expanding field of industrial relevant acetogens. Future direction for industrial and environmental perspective should include optimising total carbon use of the syngas. Although we can steer the metabolism towards ethanol production this also increases CO_2 production. At the moment a significant proportion of the CO input is lost as CO_2. Since acetogens can consume CO_2 if enough reduction power is provided it should be possible to engineer the process to fully consume all carbon components of the syngas.

The industrial acetogens are coming of age as biotechnological tools for converting waste to products. The promise they hold is one of a clean, carbon neutral, biological based future for production of small organic compound production.

To paraphrase Charles Darwin: “There is grandeur in this view of life, having been originally breathed into life by H_2 and CO_2 at alkaline hydrothermal vents, from simple beginnings endless forms have been, and are being, evolved.” Of these forms, some, acetogens, methanogens, have retained the primordial metabolic properties to use H_2, CO_2 and CO while a different specific form, humans, created a CO_2 overproduction problem for itself. Using and engineering the acetogens and methanogens for their special metabolic properties to build us a better future does not only make, scientific, economic and environmental sense but is, I feel, also somewhat poetic.

10 References

1. Martin WF. 2011. Early evolution without a tree of life. Biol Direct 6:36.
2. Arrhenius S. 1907. Das Werden der Welten. Salzwasser Verlag.
3. Drake HL, Gössner AS, Daniel SL. 2008. Old acetogens, new light. Ann N Y Acad Sci 1125:100–28.
4. Wieringa KT. 1936. Over het verdwijnen van waterstof en koolzuur onder anaerobe voorwaarden. Antonie Van Leeuwenhoek 3:263–273.
5. Beijerinck M, Delden A Van. 1903. Über eine farblose Bakterie, deren Kohlenstoffnahrung aus der atmosphärischen Luft herrührt. Cent Bakteriol ….
6. Söhngen NLNL. 1906. Het onstaan en verdwijnen van waterstof en methaan onder den invloed van organisch leven. Dissertation.
7. Lane N, Allen JF, Martin W. 2010. How did LUCA make a living? Chemiosmosis in the origin of life. Bioessays 32:271–80.
8. Weiss MC, Sousa FL, Mrnjavac N, Neukirchen S, Roettger M, Nelson-Sathi S, Martin WF. 2016. The physiology and habitat of the last universal common ancestor. Nat Microbiol 1:16116.
9. Sojo V, Herschy B, Whicher A, Camprubí E, Lane N. The Origin of Life in Alkaline Hydrothermal Vents.
10. Lever MA. 2011. Acetogenesis in the energy-starved deep biosphere - a paradox? Front Microbiol 2:284.
11. Drake HL, Küsel K, Matthies C. 2002. Ecological consequences of the phylogenetic and physiological diversities of acetogens. Antonie Van Leeuwenhoek 81:203–213.
12. Müller V, Frerichs J. 2013. Acetogenic BacteriaeLS. John Wiley & Sons, Ltd, Chichester, UK.
13. Abrini J, Naveau H, Nyns E-J. 1994. Clostridium autoethanogenum, sp. nov., an anaerobic bacterium that produces ethanol from carbon monoxide. Arch Microbiol 161:345–351.
14. Liew F, Martin ME, Tappel RC, Heijstra BD, Mihalcea C, Köpke M. 2016. Gas Fermentation—A Flexible Platform for Commercial Scale Production of Low-Carbon-Fuels and Chemicals from Waste and Renewable Feedstocks. Front Microbiol 7:694.
15. Molitor B, Richter H, Martin ME, Jensen RO, Juminaga A, Mihalcea C, Angenent LT. 2016. Carbon recovery by fermentation of CO-rich off gases - Turning steel mills into biorefineries. Bioresour Technol.
16. Redl S, Diender M, Jensen TØ, Sousa DZ, Nielsen AT. 2016. Exploiting the potential of gas fermentation. Ind Crops Prod.
17. Claassens NJ, Sousa DZ, P Martins dos Santos VA, de Vos WM, van der Oost J, dos Santos VAPM, de Vos WM, van der Oost J. 2016. Harnessing the power of microbial autotrophy. Nat Rev Microbiol 14:692–706.
18. Northon K. 2017. NASA, NOAA Data Show 2016 Warmest Year on Record Globally.
19. Pachauri RK, Meyer L.A. 2014. IPCC 2014IPCC 5th Assessment Synthesis Report. Geneva.
20. International Energy Agency (IEA). 2016. Key world energy trends - excerpt from: world energy balancesIEA.
21. García-Segura T, Yepes V, Alcalá J. 2014. Life cycle greenhouse gas emissions of blended cement concrete including carbonation and durability. Int J Life Cycle Assess 19:3–12.
22. Unfccc. Adoptions of the Paris Agreement - Paris Agreement text English.
23. IPCC. 1992. Climate change 1992: The 1990 and 1992 IPCC Assessment Reports. Overview and Policymaker Sumaries and 1992 IPCC suplement.
24. United Nations. 1998. Kyoto Protocol to the United Nations Framework Convention on Climate ChangeReview of European Community and International Environmental Law.
25. Gerland P, Raftery AE, Ševčíková H, Li N, Gu D, Spoorenberg T, Alkema L, Fosdick BK, Chunn J, Lalic N, Bay G, Buettner T, Heilig GK, Wilmoth J. 2014. World population stabilization unlikely this century.

Science (80-) 346.

26. United Nations Development Programme. 2000. World Energy Assessment. Energy and the challenge of SustainabilityWorld Energy Assessment. United Nations Pubns, New York.

27. Kandaramath Hari T, Yaakob Z, Binitha NN. 2015. Aviation biofuel from renewable resources: Routes, opportunities and challenges. Renew Sustain Energy Rev 42:1234–1244.

28. Contestabile M, Offer GJ, Slade R, Jaeger F, Thoennes M. 2011. Battery electric vehicles, hydrogen fuel cells and biofuels. Which will be the winner? Energy Environ Sci 4:3754.

29. Wrigley EA. 2013. Energy and the English Industrial Revolution. Philos Trans R Soc London A Math Phys Eng Sci 371.

30. Inderwildi OR, King DA. 2009. Quo vadis biofuels? Energy Environ Sci 2:343.

31. Afiff S, Wilkenson J, Carriquiry M, Jumbe C, Searchinger T. 2013. Biofuels and food security. A report by the High Level Panel of Experts on Food Security and Nutrition of the Committee on World Food Security.

32. Dutta K, Daverey A, Lin J-G. 2014. Evolution retrospective for alternative fuels: First to fourth generation. Renew Energy 69:114–122.

33. Aro E-M. 2016. From first generation biofuels to advanced solar biofuels. Ambio 45:24–31.

34. Eric Nybo S, Khan N, Woolston BM, Curtis WR. 2015. Metabolic engineering in chemolithoautotrophic hosts for the production of fuels and chemicals. Metab Eng 30:105–120.

35. Hanson RS, Hanson TE. 1996. Methanotrophic bacteria. Microbiol Rev 60:439–71.

36. Imported from http://www.biofuelsdigest.com/bdigest/2015/07/30/the-three-microb-eteers-methanogens-methanotrophs-acetogens-and-knallgas-bacteria/.

37. Valentine DL, Reeburgh WS. 2000. New perspectives on anaerobic methane oxidation. Environ Microbiol 2:477–484.

38. Mueller TJ, Grisewood MJ, Nazem-Bokaee H, Gopalakrishnan S, Ferry JG, Wood TK, Maranas CD. 2015. Methane oxidation by anaerobic archaea for conversion to liquid fuels. J Ind Microbiol Biotechnol 42:391–401.

39. Vela JD, Stadler LB, Martin KJ, Raskin L, Bott CB, Love NG. Prospects for Biological Nitrogen Removal from Anaerobic Effluents during Mainstream Wastewater Treatment.

40. Berg IA. 2011. Ecological aspects of the distribution of different autotrophic CO2 fixation pathways. Appl Environ Microbiol 77:1925–36.

41. Saini R, Kapoor R, Kumar R, Siddiqi TO, Kumar A. 2011. CO2 utilizing microbes - A comprehensive review. Biotechnol Adv.

42. Wijffels RH, Kruse O, Hellingwerf KJ. 2013. Potential of industrial biotechnology with cyanobacteria and eukaryotic microalgae. Curr Opin Biotechnol 24:405–13.

43. Ugwu CUU, Aoyagi H, Uchiyama H. 2008. Photobioreactors for mass cultivation of algae. Bioresource Technology.

44. Pohlmann A, Fricke WF, Reinecke F, Kusian B, Liesegang H, Cramm R, Eitinger T, Ewering C, Pötter M, Schwartz E, Strittmatter A, Voss I, Gottschalk G, Steinbüchel A, Friedrich B, Bowien B. 2006. Genome sequence of the bioplastic-producing "Knallgas" bacterium Ralstonia eutropha H16. Nat Biotechnol 24:1257–62.

45. Müller J, MacEachran D, Burd H, Sathitsuksanoh N, Bi C, Yeh Y-C, Lee TS, Hillson NJ, Chhabra SR, Singer SW, Beller HR. 2013. Engineering of Ralstonia eutropha H16 for autotrophic and heterotrophic production of methyl ketones. Appl Environ Microbiol 79:4433–9.

46. Lu J, Brigham CJ, Gai CS, Sinskey AJ. 2012. Studies on the production of branched-chain alcohols in engineered Ralstonia eutropha. Appl Microbiol Biotechnol 96:283–297.

47. Thauer RK, Kaster A-K, Seedorf H, Buckel W, Hedderich R. 2008. Methanogenic archaea: ecologically relevant differences in energy conservation. Nat Rev Microbiol 6:579–591.

48. Woese CR, Fox GE. 1977. Phylogenetic structure of the prokaryotic domain: the primary kingdoms. Proc Natl Acad Sci U S A 74:5088–90.

49. Mata-Alvarez J, Mac S, Llabr P. Anaerobic digestion of organic solid wastes. An overview of research achievements and perspectives.

50. Trelys. http://www.trelystech.com/

51. Electrochaea GmbH - Power-to-Gas Energy Storage | Technology. http://www.electrochaea.com

52. Schuchmann K, Müller V. 2016. Energetics and Application of Heterotrophy in Acetogenic Bacteria. Appl Environ Microbiol 82:4056–69.

53. Oelgeschläger E, Rother M. 2008. Carbon monoxide-dependent energy metabolism in anaerobic bacteria and archaea. Arch Microbiol 190:257–69.

54. Rother M, Metcalf WW. 2004. Anaerobic growth of Methanosarcina acetivorans C2A on carbon monoxide: an unusual way of life for a methanogenic archaeon. Proc Natl Acad Sci U S A 101:16929–34.

55. Henstra AM, Dijkema C, Stams AJM. 2007. *Archaeoglobus fulgidus* couples CO oxidation to sulfate reduction and acetogenesis with transient formate accumulation. Environ Microbiol 9:1836–1841.

56. Kerby RL, Ludden PW, Roberts GP. 1995. Carbon monoxide-dependent growth of Rhodospirillum rubrum. J Bacteriol 177:2241–4.

57. Svetlichny VA, Sokolova TG, Gerhardt M, Ringpfeil M, Kostrikina NA, Zavarzin GA. 1991. Carboxydothermus hydrogenoformans gen. nov., sp. nov., a CO-utilizing Thermophilic Anaerobic Bacterium from Hydrothermal Environments of Kunashir Island. Syst Appl Microbiol 14:254–260.

58. Do YS, Smeenk J, Broer KM, Kisting CJ, Brown R, Heindel TJ, Bobik TA, DiSpirito AA. 2007. Growth ofRhodospirillum rubrum on synthesis gas: Conversion of CO to H2 and poly-β-hydroxyalkanoate. Biotechnol Bioeng 97:279–286.

59. Wu M, Ren Q, Durkin AS, Daugherty SC, Brinkac LM, Dodson RJ, Madupu R, Sullivan SA, Kolonay JF, Haft DH, Nelson WC, Tallon LJ, Jones KM, Ulrich LE, Gonzalez JM, Zhulin IB, Robb FT, Eisen JA. 2005. Life in hot carbon monoxide: the complete genome sequence of Carboxydothermus hydrogenoformans Z-2901. PLoS Genet 1:e65.

60. Wang S, Huang H, Kahnt J, Mueller AP, Köpke M, Thauer RK. 2013. NADP-specific electron-bifurcating [FeFe]-hydrogenase in a functional complex with formate dehydrogenase in Clostridium autoethanogenum grown on CO. J Bacteriol 195:4373–86.

61. Dürre P, Eikmanns BJ. 2015. C1-carbon sources for chemical and fuel production by microbial gas fermentationCurrent Opinion in Biotechnology.

62. Diender M, Stams AJM, Sousa DZ. 2016. Production of medium-chain fatty acids and higher alcohols by a synthetic co-culture grown on carbon monoxide or syngas. Biotechnol Biofuels 9:82.

63. Richter H, Molitor B, Diender M, Sousa DZ, Angenent LT. 2016. A Narrow pH Range Supports Butanol, Hexanol, and Octanol Production from Syngas in a Continuous Co-culture of Clostridium ljungdahlii and Clostridium kluyveri with In-Line Product Extraction. Front Microbiol 7:1773.

64. Liu K, Atiyeh HK, Stevenson BS, Tanner RS, Wilkins MR, Huhnke RL. 2014. Continuous syngas fermentation for the production of ethanol, n-propanol and n-butanol. Bioresour Technol 151:69–77.

65. Liu K, Atiyeh HK, Stevenson BS, Tanner RS, Wilkins MR, Huhnke RL. 2014. Mixed culture syngas fermentation and conversion of carboxylic acids into alcohols. Bioresour Technol 152:337–346.

66. Hu P, Chakraborty S, Kumar A, Woolston B, Liu H, Emerson D, Stephanopoulos G. 2016. Integrated bioprocess for conversion of gaseous substrates to liquids. Proc Natl Acad Sci U S A 113:3773–8.

67. Gildemyn S, Molitor B, Usack JG, Nguyen M, Rabaey K, Angenent LT. 2017. Upgrading syngas fermentation effluent using Clostridium kluyveri in a continuous fermentation. Biotechnol Biofuels 10:83.

68. Fast AG, Schmidt ED, Jones SW, Tracy BP. 2015. Acetogenic mixotrophy: NOVEL options for yield improvement in biofuels and biochemicals production. Curr Opin Biotechnol.

69. Jones SW, Fast AG, Carlson ED, Wiedel CA, Au J, Antoniewicz MR, Papoutsakis ET, Tracy BP. 2016. CO2 fixation by anaerobic non-photosynthetic mixotrophy for improved carbon conversion. Nat Commun 7:12800.

70. Perez JM, Richter H, Loftus SE, Angenent LT. 2013. Biocatalytic reduction of short-chain carboxylic acids into their corresponding alcohols with syngas fermentation. Biotechnol Bioeng 110:1066–77.

71. Fischer F, Lieske R, Winzer K. 1931. Die umsetzungen des kohlenoxyds. Biochem Z.

72. Braun M, Mayer F, Gottschalk G. 1981. Clostridium aceticum (Wieringa), a microorganism producing acetic acid from molecular hydrogen and carbon dioxide. Arch Microbiol 128:288–293.

73. Fontaine FE, Peterson WH, McCoy E, Johnson MJ, Ritter GJ. 1942. A New Type of Glucose Fermentation by Clostridium thermoaceticum. J Bacteriol 43:701–15.

74. Ragsdale SW, Pierce E. 2008. Acetogenesis and the Wood–Ljungdahl pathway of CO2 fixation. Biochim Biophys Acta 1784:1873–1898.

75. Chinn DMS. 2011. Influence of Carbon Source Pre-Adaptation on Clostridium ljungdahlii Growth and Product Formation. J Bioprocess Biotech.

76. Wood H. 1986. The acetyl-CoA pathway of autotrophic growth. FEMS Microbiol Lett 39:345–362.

77. Kerby R, Zeikus JG. 1983. Growth ofClostridium thermoaceticum on H2/CO2 or CO as energy source. Curr Microbiol 8:27–30.

78. Kusel K, Dorsch T, Acker G, Stackebrandt E, Drake HL. 2000. Clostridium scatologenes strain SL1 isolated as an acetogenic bacterium from acidic sediments. Int J Syst Evol Microbiol 50:537–546.

79. Köpke M, Straub M, Dürre P. 2013. Clostridium difficile is an autotrophic bacterial pathogen. PLoS One 8:e62157.

80. Buschhorn H, Dürre P, Gottschalk G. 1989. Production and Utilization of Ethanol by the Homoacetogen Acetobacterium woodii. Appl Environ Microbiol 55:1835–40.

81. Barik S, Prieto S, Harrison SB, Clausen EC, Gaddy JL. 1988. Biological production of alcohols from coal through indirect liquefaction. Appl Biochem Biotechnol 18:363–378.

82. Vega JL, Prieto S, Elmore BB, Clausen EC, Gaddy JL. 1989. The Biological production of ethanol from synthesis gas. Appl Biochem Biotechnol 20–21:781–797.

83. Klasson KT, Ackerson MD, Clausen EC, Gaddy JL. 1991. Bioreactor design for synthesis gas fermentations. Fuel 70:605–614.

84. Klasson KT, Ackerson MD, Clausen EC, Gaddy JL. 1993. Biological conversion of coal and coal-derived synthesis gas. Fuel 72:1673–1678.

85. Liou JS-C, Balkwill DL, Drake GR, Tanner RS. 2005. Clostridium carboxidivorans sp. nov., a solvent-producing clostridium isolated from an agricultural settling lagoon, and reclassification of the acetogen Clostridium scatologenes strain SL1 as Clostridium drakei sp. nov. Int J Syst Evol Microbiol 55:2085–91.

86. Bengelsdorf FR, Poehlein A, Linder S, Erz C, Hummel T, Hoffmeister S, Daniel R, Dürre P. 2016. Industrial Acetogenic Biocatalysts: A Comparative Metabolic and Genomic Analysis. Front Microbiol 7:1036.

87. Köpke M, Mihalcea C, Liew F, Tizard JH, Ali MS, Conolly JJ, Al-Sinawi B, Simpson SD. 2011. 2,3-butanediol production by acetogenic bacteria, an alternative route to chemical synthesis, using industrial waste gas. Appl Environ Microbiol 77:5467–75.

88. Diender M, Stams AJM, Sousa DZ. 2015. Pathways and Bioenergetics of Anaerobic Carbon Monoxide Fermentation. Front Microbiol 6:1275.

89. Schuchmann K, Müller V. 2014. Autotrophy at the thermodynamic limit of life: a model for energy conservation in acetogenic bacteria. Nat Rev Microbiol 12:809–821.

90. Groher A, Weuster-Botz D. 2016. Comparative reaction engineering analysis of different acetogenic bacteria for gas fermentation. J Biotechnol 228:82–94.

91. Schiel-Bengelsdorf B, Dürre P. 2012. Pathway engineering and synthetic biology using acetogens. FEBS Lett 586:2191–8.

92. Seedorf H, Fricke WF, Veith B, Brüggemann H, Liesegang H, Strittmatter A, Miethke M, Buckel W, Hinderberger J, Li F, Hagemeier C, Thauer RK, Gottschalk G. 2008. The genome of Clostridium kluyveri, a strict anaerobe with unique metabolic features. Proc Natl Acad Sci U S A 105:2128–33.

93. Lee J, Jang Y-S, Han M-J, Kim JY, Lee SY. 2016. Deciphering Clostridium tyrobutyricum Metabolism Based on the Whole-Genome Sequence and Proteome Analyses. MBio 7:e00743-16.

94. Poehlein A, Cebulla M, Ilg MM, Bengelsdorf FR, Schiel-Bengelsdorf B, Whited G, Andreesen JR, Gottschalk G, Daniel R, Dürre P. 2015. The Complete Genome Sequence of Clostridium aceticum: a Missing Link between Rnf- and Cytochrome-Containing Autotrophic Acetogens. MBio 6:e01168-15.

95. Euzeby JP. 1997. List of Bacterial Names with Standing in Nomenclature: a Folder Available on the Internet. Int J Syst Bacteriol 590–592.

96. Stackebrandt E, Kramer I, Swiderski J, Hippe H. 1999. Phylogenetic basis for a taxonomic dissection of the genus Clostridium. FEMS Immunol Med Microbiol 24:253–258.

97. Collins MD, Lawson PA, Wilems A, Cordoba, Fernandez-Garayzabal J, Garcia P, Cai J, Hippe H, Farrow JAE. 1994. The Phylogeny of the Genus Clostridium: Proposal of Five New Genera and Eleven New Species Combinations. Int J Syst Bacteriol 44:812–826.

98. Kalia VC, Mukherjee T, Bhushan A, Joshi J, Shankar P, Huma N. 2011. Analysis of the unexplored features of rrs (16S rDNA) of the Genus Clostridium. BMC Genomics 12:18.

99. Lane N. 2015. The Vital Question - Why Is Life the Way It Is.

100. Borrel G, Adam PS, Gribaldo S, RK. T, BJ. B. 2016. Methanogenesis and the Wood?Ljungdahl Pathway: An Ancient, Versatile, and Fragile Association. Genome Biol Evol 8:1706–1711.

101. Ragsdale SW. 2008. Enzymology of the wood-Ljungdahl pathway of acetogenesis. Ann N Y Acad Sci 1125:129–36.

102. Matson EG, Gora KG, Leadbetter JR. 2011. Anaerobic carbon monoxide dehydrogenase diversity in the homoacetogenic hindgut microbial communities of lower termites and the wood roach. PLoS One 6:e19316.

103. Thauer RK, Fuchs G, Kauefer B, Schnittker U. 1974. Carbon-Monoxide Oxidation in Cell-Free Extracts of Clostridium pasteurianum. Eur J Biochem 45:343–349.

104. Daniel SL, Hsu T, Dean SI, Drake HL. 1990. Characterization of the H2- and CO-dependent chemolithotrophic potentials of the acetogens Clostridium thermoaceticum and Acetogenium kivui. J Bacteriol 172:4464–71.

105. Al-Hinai MA, Fast AG, Indurthi D, Papoutsakis ET. 2012. Installing the Wood-Ljungdahl (WL) Pathway in Clostridium acetobutylicum. Abstr B Clostridium XII Conf Nottingham.

106. Loke HK, Bennett GN, Lindahl PA. 2000. Active acetyl-CoA synthase from Clostridium thermoaceticum obtained by cloning and heterologous expression of acsAB in Escherichia coli. Proc Natl Acad Sci U S A 97:12530–5.

107. Carlson ED, Papoutsakis ET. 2017. Heterologous Expression of the Clostridium carboxidivorans CO Dehydrogenase Alone or Together with the Acetyl Coenzyme A Synthase Enables both Reduction of CO2 and Oxidation of CO by Clostridium acetobutylicum. Appl Environ Microbiol 83:e00829-17.

108. Techtmann SM, Colman AS, Robb FT. 2009. “That which does not kill us only makes us stronger”: the role of carbon monoxide in thermophilic microbial consortia. Environ Microbiol 11:1027–37.

109. Schink B. 1997. Energetics of syntrophic cooperation in methanogenic degradation. Microbiol Mol Biol Rev 61:262–80.

110. Krabben P. 2014. Acetone production during the First World War | Microbiology Society. Microbiol Today.

111. Sauer M. 2016. Industrial production of acetone and butanol by fermentation-100 years later. FEMS Microbiol Lett 363.

112. Daniell J, Köpke M, Simpson S. 2012. Commercial Biomass Syngas Fermentation. Energies 5:5372–5417.

113. Lane J. 2016. Sinatra Bio: Ol’ Brew Eyes is Back : Biofuels Digest. Biofuelsdigest.

114. Sapp M. 2016. INEOS Bio selling 8 MGY demo plant in Florida : Biofuels Digest. Biofuel Dig.

115. LanzaTech. http://www.lanzatech.com/

116. Yasin M, Jeong Y, Park S, Jeong J, Lee EY, Lovitt RW, Kim BH, Lee J, Chang IS. 2015. Microbial synthesis

gas utilization and ways to resolve kinetic and mass-transfer limitations. Bioresour Technol 177:361–74.

117. Speight JG. 2007. Natural Gas : a Basic Handbook. Elsevier Science.

118. Falkus ME. 1967. The British Gas Industry before 1850. Econ Hist Rev 20:494.

119. Nanda S, Dalai AK, Berruti F, Kozinski JA. 2016. Biochar as an Exceptional Bioresource for Energy, Agronomy, Carbon Sequestration, Activated Carbon and Specialty Materials. Waste and Biomass Valorization 7:201–235.

120. Fischer F, Tropsch H. 1923. The preparation of synthetic oil mixtures (synthol) from carbon monoxide and hydrogen. Brennstoff-Chem.

121. Del Alamo G, Kempegowda RS, Skreiberg Ø, Khalil R. 2017. Decentralized Production of Fischer–Tropsch Biocrude via Coprocessing of Woody Biomass and Wet Organic Waste in Entrained Flow Gasification: Techno-Economic Analysis. Energy & Fuels 31:6089–6108.

122. de Klerk A, Li Y-W, Zennaro R. 2013. Fischer-Tropsch Technology, p. 53–79. *In* Greener Fischer-Tropsch Processes for Fuels and Feedstocks. Wiley-VCH Verlag GmbH & Co. KGaA, Weinheim, Germany.

123. Klasson KT, Ackerson MD, Clausen EC, Gaddy JL. 1992. Bioconversion of synthesis gas into liquid or gaseous fuels. Enzyme Microb Technol 14:602–608.

124. Sipma J, Henstra AM, Parshina SN, Lens PNL, Lettinga G, Stams AJM. 2008. Microbial CO Conversions with Applications in Synthesis Gas Purification and Bio-Desulfurization.

125. Fung Min Liew MK and SDS. 2013. Liquid, Gaseous and Solid Biofuels - Conversion Techniques. InTech.

126. Bredwell MD, Srivastava P, Worden RM. 1999. Reactor design issues for synthesis-gas fermentations. Biotechnol Prog 15:834–844.

127. The Science and Technology Committee of the House of Lords. 2014. Waste or resource? Stimulating a bioeconomy.

128. Lane J. 2017. Shazzan!: Turning Urban Trash into Treasure Island, the LanzaTech, Sekisui Chemicals story : Biofuels Digest.

129. Tremblay P-L, Angenent LT, Zhang T. 2017. Extracellular Electron Uptake: Among Autotrophs and Mediated by Surfaces. Trends Biotechnol 35:360–371.

130. Tremblay P-L, Zhang T. 2015. Electrifying microbes for the production of chemicals. Front Microbiol 6:201.

131. Butler CS, Lovley DR. 2016. How to Sustainably Feed a Microbe: Strategies for Biological Production of Carbon-Based Commodities with Renewable Electricity. Front Microbiol 7:1879.

132. Blankenship RE, Tiede DM, Barber J, Brudvig GW, Fleming G, Ghirardi M, Gunner MR, Junge W, Kramer DM, Melis A, Moore TA, Moser CC, Nocera DG, Nozik AJ, Ort DR, Parson WW, Prince RC, Sayre RT. 2011. Comparing Photosynthetic and Photovoltaic Efficiencies and Recognizing the Potential for Improvement. Science (80-) 332.

133. Lovley DR, Nevin KP. 2013. Electrobiocommodities: powering microbial production of fuels and commodity chemicals from carbon dioxide with electricity. Curr Opin Biotechnol 24:385–90.

134. Hohmann-Marriott MF, Blankenship RE. 2011. Evolution of Photosynthesis. Annu Rev Plant Biol 62:515–548.

135. Drake HL, Daniel SL. 2004. Physiology of the thermophilic acetogen Moorella thermoacetica. Res Microbiol 155:869–883.

136. Marcellin E, Behrendorff JB, Nagaraju S, DeTissera S, Segovia S, Palfreyman R, Daniell J, Licona-Cassani C, Quek L, Speight R, Hodson MP, Simpson SD, Mitchell WP, Köpke M, Nielsen LK. 2016. Low carbon fuels and commodity chemicals from waste gases – Systematic approach to understand energy metabolism in a model acetogen. Green Chem.

137. Valgepea K, de Souza Pinto Lemgruber R, Meaghan K, Palfreyman RW, Abdalla T, Heijstra BD, Behrendorff JB, Tappel R, Köpke M, Simpson SD, Nielsen LK, Marcellin E. 2017. Maintenance of ATP Homeostasis Triggers Metabolic Shifts in Gas-Fermenting Acetogens. Cell Syst 196:3949–3963.

138. Nagarajan H, Sahin M, Nogales J, Latif H, Lovley DR, Ebrahim A, Zengler K. 2013. Characterizing acetogenic metabolism using a genome-scale metabolic reconstruction of Clostridium ljungdahlii. Microb Cell Fact 12:118.

139. Tan Y, Liu J, Chen X, Zheng H, Li F. 2013. RNA-seq-based comparative transcriptome analysis of the syngas-utilizing bacterium Clostridium ljungdahlii DSM 13528 grown autotrophically and heterotrophically. Mol Biosyst 9:2775–84.

140. Richter H, Molitor B, Wei H, Chen W, Aristilde L, Angenent LT. 2016. Ethanol production in syngas-fermenting Clostridium ljungdahlii is controlled by thermodynamics rather than by enzyme expression. Energy Environ Sci 9:2392–2399.

141. Li L, Hsu A, Moore PK. 2009. Actions and interactions of nitric oxide, carbon monoxide and hydrogen sulphide in the cardiovascular system and in inflammation — a tale of three gases! Pharmacol Ther 123:386–400.

142. Bertsch J, Müller V. 2015. Bioenergetic constraints for conversion of syngas to biofuels in acetogenic bacteria. Biotechnol Biofuels 8:210.

143. Hu P, Bowen SH, Lewis RS. 2011. A thermodynamic analysis of electron production during syngas fermentation. Bioresour Technol 102:8071–8076.

144. Lorimer JW, Clever HL, Young CL, Cargill RW, Battino R, Bo S, Wiesenburg DA. 1980. Carbon Monoxide. Solubility Data Ser 43:329.

145. Maharajh DM, Walkley J. 1973. Thermodynamic solubility: properties of gas mixtures. Part 1.—Two component gas mixtures in water at 25°C. J Chem Soc Faraday Trans 1 Phys Chem Condens Phases 69:842.

146. Diamond LW, Akinfiev NN. 2003. Solubility of CO2 in water from −1.5 to 100 °C and from 0.1 to 100 MPa: evaluation of literature data and thermodynamic modelling. Fluid Phase Equilib 208:265–290.

147. Valgepea K, Loi KQ, Behrendorff JB, Lemgruber R de SP, Plan M, Hodson MP, Köpke M, Nielsen LK, Marcellin E. 2017. Arginine deiminase pathway provides ATP and boosts growth of the gas-fermenting acetogen Clostridium autoethanogenum. Metab Eng 41:202–211.

148. Tremblay P-L, Zhang T, Dar SA, Leang C, Lovley DR. 2012. The Rnf complex of Clostridium ljungdahlii is a proton-translocating ferredoxin:NAD+ oxidoreductase essential for autotrophic growth. MBio 4:e00406-12.

149. Köpke M, Held C, Hujer S, Liesegang H, Wiezer A, Wollherr A, Ehrenreich A, Liebl W, Gottschalk G, Dürre P, Kopke M, Held C, Hujer S, Liesegang H, Wiezer A, Wollherr A, Ehrenreich A, Liebl W, Gottschalk G, Durre P. 2010. Clostridium ljungdahlii represents a microbial production platform based on syngas. Proc Natl Acad Sci U S A 107:13087–92.

150. Khan FA, Ansari AA. 2005. Eutrophication: An Ecological Vision. Bot Rev 71:449–482.

151. Cordell D, Drangert J-O, White S. 2009. The story of phosphorus: Global food security and food for thought. Glob Environ Chang 19:292–305.

152. Van Vuuren DP, Bouwman AF, Beusen AHW. 2010. Phosphorus demand for the 1970–2100 period: A scenario analysis of resource depletion. Glob Environ Chang 20:428–439.

153. Tan Y, Liu Z-Y, Liu Z, Li F-L. 2015. Characterization of an acetoin reductase/2,3-butanediol dehydrogenase from Clostridium ljungdahlii DSM 13528. Enzyme Microb Technol 79–80:1–7.

154. Kumar RSS, Ferry JG. 2014. Prokaryotic carbonic anhydrases of Earth's environment. Subcell Biochem 75:77–87.

155. Kletzin A, Adams MWW. 1996. Tungsten in biological systems. FEMS Microbiol Rev 18:5–63.

156. Begley TP, Kinsland C, Strauss E. 2001. The biosynthesis of coenzyme a in bacteria. Vitam Horm 61:157–171.

157. Tong L. 2013. Structure and function of biotindependent carboxylases. Cell Mol Life Sci 70:86391.

158. Furdui C, Ragsdale SW. 2000. The role of pyruvate ferredoxin oxidoreductase in pyruvate synthesis during autotrophic growth by the Wood-Ljungdahl pathway. J Biol Chem 275:28494–9.

159. Simpson SD, Koepke M, Smart KF, Tran LP, Sechrist P. September 2014. System and method for controlling metabolite production in a microbial fermentation.

160. Liew F, Henstra AM, Winzer K, Köpke M, Simpson SD, Minton NP. 2016. Insights into CO2 Fixation Pathway of Clostridium autoethanogenum by Targeted Mutagenesis. MBio 7:e00427-16.

161. Doukov TI, Iverson TM, Seravalli J, Ragsdale SW, Drennan CL. 2002. A Ni-Fe-Cu Center in a Bifunctional Carbon Monoxide Dehydrogenase/ Acetyl-CoA Synthase. Science (80-) 298.

162. Volbeda A, Fontecilla-Camps JC. 2004. Crystallographic evidence for a CO/CO(2) tunnel gating mechanism in the bifunctional carbon monoxide dehydrogenase/acetyl coenzyme A synthase from Moorella thermoacetica. J Biol Inorg Chem 9:525–32.

163. Thauer RK, Jungermann K, Decker K. 1977. Energy conservation in chemotrophic anaerobic bacteria. Bacteriol Rev 41:100–80.

164. Brown SD, Nagaraju S, Utturkar S, De Tissera S, Segovia S, Mitchell W, Land ML, Dassanayake A, Köpke M. 2014. Comparison of single-molecule sequencing and hybrid approaches for finishing the genome of Clostridium autoethanogenum and analysis of CRISPR systems in industrial relevant Clostridia. Biotechnol Biofuels 7:40.

165. Mock J, Zheng Y, Mueller AP, Ly S, Tran L, Segovia S, Nagaraju S, Köpke M, Dürre P, Thauer RK. 2015. Energy conservation associated with ethanol formation from H2 and CO2 in Clostridium autoethanogenum involving electron bifurcation. J Bacteriol 197:2965–2980.

166. Liew F, Henstra AM, Köpke M, Winzer K, Simpson SD, Minton NP. 2017. Metabolic engineering of Clostridium autoethanogenum for selective alcohol production. Metab Eng 40:104–114.

167. Köpke M, Gerth ML, Maddock DJ, Mueller AP, Liew F, Simpson SD, Patrick WM. 2014. Reconstruction of an acetogenic 2,3-butanediol pathway involving a novel NADPH-dependent primary-secondary alcohol dehydrogenase. Appl Environ Microbiol AEM.00301-14-.

168. Buckel W, Thauer RK. 2013. Energy conservation via electron bifurcating ferredoxin reduction and proton/Na(+) translocating ferredoxin oxidation. Biochim Biophys Acta 1827:94–113.

169. Bruno-Barcena JM, Chinn MS, Grunden AM. 2013. Genome Sequence of the Autotrophic Acetogen Clostridium autoethanogenum JA1-1 Strain DSM 10061, a Producer of Ethanol from Carbon Monoxide. Genome Announc 1.

170. Humphreys CM, McLean S, Schatschneider S, Millat T, Henstra AM, Annan FJ, Breitkopf R, Pander B, Piatek P, Rowe P, Wichlacz AT, Woods C, Norman RR, Blom J, Goesman A, Hodgman C, Barrett D, Thomas NR, Winzer K, Minton NP. 2015. Whole genome sequence and manual annotation of Clostridium autoethanogenum, an industrially relevant bacterium. BMC Genomics 16:1085.

171. Utturkar SM, Klingeman DM, Bruno-Barcena JM, Chinn MS, Grunden AM, Köpke M, Brown SD. 2015. Sequence data for Clostridium autoethanogenum using three generations of sequencing technologies. Sci data 2:150014.

172. Leang C, Ueki T, Nevin KP, Lovley DR. 2013. A genetic system for Clostridium ljungdahlii: a chassis for autotrophic production of biocommodities and a model homoacetogen. Appl Environ Microbiol 79:1102–9.

173. Pyne ME, Bruder M, Moo-Young M, Chung DA, Perry Chou C. 2014. Technical guide for genetic advancement of underdeveloped and intractable Clostridium. Biotechnol Adv.

174. Reeves A. 2014. Use of Clostridial Methyltransferases for Generating Novel Strains.

175. Jones DT, Shirley M, Wu X, Keis S. 2000. Bacteriophage infections in the industrial acetone butanol (AB) fermentation process. J Mol Microbiol Biotechnol 2:21–6.

176. Callanan MJ, Klaenhammer TR, Callanan MJ, Klaenhammer TR. 2008. Bacteriophages in IndustryEncyclopedia of Life Sciences. John Wiley & Sons, Ltd, Chichester.

177. Köpke M, Dürre P, Luque R, Campelo J, Clark J. 2011. Biochemical production of biobutanol. 221–257.

178. Koepke M, Liew F. April 2012. Production of butanol from carbon monoxide by a recombinant microorganism.

179. Cartman ST, Minton NP. 2010. A mariner-based transposon system for in vivo random mutagenesis of Clostridium difficile. Appl Environ Microbiol 76:1103–9.

180. Williams DR, Young DI, Young M. 1990. Conjugative plasmid transfer from Escherichia coli to Clostridium acetobutylicum. J Gen Microbiol 136:819–826.

181. Heap JT, Pennington OJ, Cartman ST, Minton NP. 2009. A modular system for Clostridium shuttle plasmids. J Microbiol Methods 78:79–85.

182. Heap JT, Pennington OJ, Cartman ST, Carter GP, Minton NP. 2007. The ClosTron: a universal gene knock-out system for the genus Clostridium. J Microbiol Methods 70:452–64.

183. Ng YK, Ehsaan M, Philip S, Collery MM, Janoir C, Collignon A, Cartman ST, Minton NP. 2013. Expanding the repertoire of gene tools for precise manipulation of the Clostridium difficile genome: allelic exchange using pyrE alleles. PLoS One 8:e56051.

184. Heap JT, Ehsaan M, Cooksley CM, Ng Y-K, Cartman ST, Winzer K, Minton NP. 2012. Integration of DNA into bacterial chromosomes from plasmids without a counter-selection marker. Nucleic Acids Res 40:e59.

185. Perutka J, Wang W, Goerlitz D, Lambowitz AM. 2004. Use of Computer-designed Group II Introns to Disrupt Escherichia coli DExH/D-box Protein and DNA Helicase Genes. J Mol Biol 336:421–439.

186. Heap JT, Kuehne SA, Ehsaan M, Cartman ST, Cooksley CM, Scott JC, Minton NP. 2010. The ClosTron: Mutagenesis in Clostridium refined and streamlined. J Microbiol Methods 80:49–55.

187. Kuehne SA, Minton NP. 2012. ClosTron-mediated engineering of Clostridium. Bioengineered 3:247–54.

188. Wellington M, Rustchenko E. 2005. 5-Fluoro-orotic acid induces chromosome alterations in Candida albicans. Yeast 22:57–70.

189. Nagaraju S, Davies NK, Walker DJF, K?pke M, Simpson SD. 2016. Genome editing of Clostridium autoethanogenum using CRISPR/Cas9. Biotechnol Biofuels 9:219.

190. Huang H, Chai C, Li N, Rowe P, Minton NP, Yang S, Jiang W, Gu Y. CRISPR/Cas9-Based Efficient Genome Editing in Clostridium ljungdahlii, an Autotrophic Gas-Fermenting Bacterium.

191. Guo Y, Xu J, Zhang Y, Xu H, Yuan Z, Li D. 2010. Medium optimization for ethanol production with Clostridium autoethanogenum with carbon monoxide as sole carbon source. Bioresour Technol 101:8784–8789.

192. Abubackar HN, Veiga MC, Kennes C. 2012. Biological conversion of carbon monoxide to ethanol: Effect of pH, gas pressure, reducing agent and yeast extract. Bioresour Technol 114:518–522.

193. Cotter JL, Chinn MS, Grunden AM. 2009. Ethanol and acetate production by Clostridium ljungdahlii and Clostridium autoethanogenum using resting cells. Bioprocess Biosyst Eng 32:369–80.

194. Abubackar HN, Bengelsdorf FR, Dürre P, Veiga MC, Kennes C. 2016. Improved operating strategy for continuous fermentation of carbon monoxide to fuel-ethanol by clostridia. Appl Energy 169:210–217.

195. Esvelt KM, Wang HH. 2013. Genome-scale engineering for systems and synthetic biology. Mol Syst Biol 9:641.

196. Thorn GJ, King JR, Jabbari S. 2013. pH-induced gene regulation of solvent production by Clostridium acetobutylicum in continuous culture: Parameter estimation and sporulation modelling. Math Biosci 241:149–166.

197. Kim TY, Sohn SB, Kim Y Bin, Kim WJ, Lee SY. 2012. Recent advances in reconstruction and applications of genome-scale metabolic models. Curr Opin Biotechnol 23:617–23.

198. Branco dos Santos F, de Vos WM, Teusink B. 2013. Towards metagenome-scale models for industrial applications--the case of Lactic Acid Bacteria. Curr Opin Biotechnol 24:200–6.

199. Poolman MG. 2006. ScrumPy: metabolic modelling with Python. Syst Biol (Stevenage) 153:375–8.

200. Okonechnikov K, Golosova O, Fursov M, UGENE team the U. 2012. Unipro UGENE: a unified bioinformatics toolkit. Bioinformatics 28:1166–7.

201. Edgar RC. 2004. MUSCLE: multiple sequence alignment with high accuracy and high throughput. Nucleic Acids Res 32:1792–7.

202. Kumar S, Stecher G, Tamura K. 2016. MEGA7: Molecular Evolutionary Genetics Analysis Version 7.0 for Bigger Datasets. Mol Biol Evol 33:1870–4.

203. Waterhouse AM, Procter JB, Martin DMA, Clamp M, Barton GJ. 2009. Jalview Version 2--a multiple

sequence alignment editor and analysis workbench. Bioinformatics 25:1189–91.

204. Ronquist F, Teslenko M, van der Mark P, Ayres DL, Darling A, Höhna S, Larget B, Liu L, Suchard MA, Huelsenbeck JP. 2012. MrBayes 3.2: efficient Bayesian phylogenetic inference and model choice across a large model space. Syst Biol 61:539–42.

205. Darriba D, Taboada GL, Doallo R, Posada D. 2011. ProtTest 3: fast selection of best-fit models of protein evolution. Bioinformatics 27:1164–5.

206. Rambaut A. 2014. Figtree, a graphical viewer of phylogenetic trees.

207. Kelley LA, Mezulis S, Yates CM, Wass MN, Sternberg MJE. 2015. The Phyre2 web portal for protein modeling, prediction and analysis. Nat Protoc 10:845–858.

208. Kelley LA, Sternberg MJE. 2009. Protein structure prediction on the Web: a case study using the Phyre server. Nat Protoc 4:363–71.

209. Guex N, Peitsch MC. 1997. SWISS-MODEL and the Swiss-Pdb Viewer: An environment for comparative protein modeling. Electrophoresis 18:2714–2723.

210. Gasteiger E, Hoogland C, Gattiker A, Duvaud S, Wilkins MR, Appel RD, Bairoch A. 2005. Protein Identification and Analysis Tools in the ExPASy Server. John M Walk Proteomics Protoc Handbook, Humana Press (2005). Humana Press, Totowa, NJ.

211. Boratyn GM, Camacho C, Cooper PS, Coulouris G, Fong A, Ma N, Madden TL, Matten WT, McGinnis SD, Merezhuk Y, Raytselis Y, Sayers EW, Tao T, Ye J, Zaretskaya I. 2013. BLAST: a more efficient report with usability improvements. Nucleic Acids Res 41:W29-33.

212. Altschul SF, Madden TL, Schäffer AA, Zhang J, Zhang Z, Miller W, Lipman DJ. 1997. Gapped BLAST and PSI-BLAST: a new generation of protein database search programs. Nucleic Acids Res 25:3389–402.

213. Sayers EW, Barrett T, Benson DA, Bolton E, Bryant SH, Canese K, Chetvernin V, Church DM, Dicuccio M, Federhen S, Feolo M, Fingerman IM, Geer LY, Helmberg W, Kapustin Y, Krasnov S, Landsman D, Lipman DJ, Lu Z, Madden TL, Madej T, Maglott DR, Marchler-Bauer A, Miller V, Karsch-Mizrachi I, Ostell J, Panchenko A, Phan L, Pruitt KD, Schuler GD, Sequeira E, Sherry ST, Shumway M, Sirotkin K, Slotta D, Souvorov A, Starchenko G, Tatusova TA, Wagner L, Wang Y, Wilbur WJ, Yaschenko E, Ye J. 2012. Database resources of the National Center for Biotechnology Information. Nucleic Acids Res 40:D13-25.

214. Marchler-Bauer A, Anderson JB, Cherukuri PF, DeWeese-Scott C, Geer LY, Gwadz M, He S, Hurwitz DI, Jackson JD, Ke Z, Lanczycki CJ, Liebert CA, Liu C, Lu F, Marchler GH, Mullokandov M, Shoemaker BA, Simonyan V, Song JS, Thiessen PA, Yamashita RA, Yin JJ, Zhang D, Bryant SH. 2005. CDD: a Conserved Domain Database for protein classification. Nucleic Acids Res 33:D192-6.

215. Xia J, Sinelnikov I V., Han B, Wishart DS, H.P. B, D. R, T. N, J. R, J. K, B. A. 2015. MetaboAnalyst 3.0—making metabolomics more meaningful. Nucleic Acids Res 43:W251–W257.

216. Mihalcea CD, Mon Yee Fung J, Al-Sinawi B, Tran LP. 2011. Optimised Fermentation Media.

217. Bertani G. 1951. Studies on lysogenesis. I. The mode of phage liberation by lysogenic Escherichia coli. J Bacteriol 62:293–300.

218. Tanner RS, Miller LM, Yang D. 1993. Clostridium ljungdahlii sp-Nov, an Acetogenic Species in Clostridial Ribosomal-RNA Homology Group-I. Int J Syst Bacteriol 43:232–236.

219. Hanahan D. 1986. Biologically pure Escherichia coli cell line which is a DeoR- mutant and which is more efficient with foreign plasmids than DeoR+ Escherichia coli cell lines, Processes for obtaining these cell lies, methods of use and transformants there of.

220. Merlin C, Masters M, McAteer S, Coulson A. 2003. Why Is Carbonic Anhydrase Essential to Escherichia coli? J Bacteriol 185:6415–6424.

221. Ungerman AJ, Heindel TJ. 2008. Carbon Monoxide Mass Transfer for Syngas Fermentation in a Stirred Tank Reactor with Dual Impeller Configurations. Biotechnol Prog 23:613–620.

222. Cotter JL, Chinn MS, Grunden AM. 2009. Influence of process parameters on growth of Clostridium ljungdahlii and Clostridium autoethanogenum on synthesis gas. Enzyme Microb Technol 44:281–288.

223. Papoutsakis ET. 1984. Equations and calculations for fermentations of butyric acid bacteria.

Biotechnol Bioeng 26:174–187.

224. Fast AG, Papoutsakis ET. 2012. Stoichiometric and energetic analyses of non-photosynthetic CO2-fixation pathways to support synthetic biology strategies for production of fuels and chemicals. Curr Opin Chem Eng 1:380–395.

225. Grosz R, Stephanopoulos G. 1983. Statistical mechanical estimation of the free energy of formation ofE. coli biomass for use with macroscopic bioreactor balances. Biotechnol Bioeng 25:2149–2163.

226. Saiki RK, Gelfand DH, Stoffel S, Scharf SJ, Higuchi R, Horn GT, Mullis KB, Erlich HA. Primer-Directed Enzymatic Amplification of DNA with a Thermostable DNA Polymerase. Science (80-) 239:487–491.

227. Mullis KB, Faloona FA. 1987. [21] Specific synthesis of DNA in vitro via a polymerase-catalyzed chain reaction, p. 335–350. *In* .

228. Ho SN, Hunt HD, Horton RM, Pullen JK, Pease LR. 1989. Site-directed mutagenesis by overlap extension using the polymerase chain reaction. Gene 77:51–59.

229. Bryksin A, Matsumura I. BioTechniques - Overlap extension PCR cloning: a simple and reliable way to create recombinant plasmids.

230. Sanger F, Nicklen S, Coulson AR. 1977. Biochemistry DNA sequencing with chain-terminating inhibitors (DNA polymerase/nucleotide sequences/bacteriophage 4X174) 74:5463–5467.

231. Laemmli UK. 1970. Cleavage of Structural Proteins during the Assembly of the Head of Bacteriophage T4. Nature 227:680–685.

232. Bradford MM. 1976. A rapid and sensitive method for the quantitation of microgram quantities of protein utilizing the principle of protein-dye binding. Anal Biochem 72:248–254.

233. Zhang T, Creek DJ, Barrett MP, Blackburn G, Watson DG. 2012. Evaluation of Coupling Reversed Phase, Aqueous Normal Phase, and Hydrophilic Interaction Liquid Chromatography with Orbitrap Mass Spectrometry for Metabolomic Studies of Human Urine. Anal Chem 84:1994–2001.

234. Creek DJ, Chokkathukalam A, Jankevics A, Burgess KE V., Breitling R, Barrett MP. 2012. Stable Isotope-Assisted Metabolomics for Network-Wide Metabolic Pathway Elucidation. Anal Chem 84:8442–8447.

235. Smith KS, Ferry JG. 2000. Prokaryotic carbonic anhydrases. FEMS Microbiol Rev 24:335–366.

236. Hawkins AS, McTernan PM, Lian H, Kelly RM, Adams MWW, Toone E, de Winde H, Steffan RJ, Ramos JL. 2013. Biological conversion of carbon dioxide and hydrogen into liquid fuels and industrial chemicals. Curr Opin Biotechnol 24:376–384.

237. Lian H, Zeldes BM, Lipscomb GL, Hawkins AB, Han Y, Loder AJ, Nishiyama D, Adams MWW, Kelly RM. 2016. Ancillary contributions of heterologous biotin protein ligase and carbonic anhydrase for CO_2 incorporation into 3-hydroxypropionate by metabolically engineered Pyrococcus furiosus. Biotechnol Bioeng 113:2652–2660.

238. Del Prete S, Vullo D, Fisher GM, Andrews KT, Poulsen S-A, Capasso C, Supuran CT. 2014. Discovery of a new family of carbonic anhydrases in the malaria pathogen Plasmodium falciparum--the η-carbonic anhydrases. Bioorg Med Chem Lett 24:4389–96.

239. Sawaya MR, Cannon GC, Heinhorst S, Tanaka S, Williams EB, Yeates TO, Kerfeld CA. 2006. The structure of beta-carbonic anhydrase from the carboxysomal shell reveals a distinct subclass with one active site for the price of two. J Biol Chem 281:7546–55.

240. Supuran CT. 2016. Structure and function of carbonic anhydrases. Biochem J 473:2023–2032.

241. Ferry JG. 2010. The gamma class of carbonic anhydrases. Biochim Biophys Acta 1804:374–81.

242. Capasso C, Supuran CT. 2015. An overview of the alpha-, beta- and gamma-carbonic anhydrases from Bacteria: can bacterial carbonic anhydrases shed new light on evolution of bacteria? J Enzyme Inhib Med Chem 30:325–32.

243. Hewett-Emmett D, Tashian RE. 1996. Functional diversity, conservation, and convergence in the evolution of the alpha-, beta-, and gamma-carbonic anhydrase gene families. Mol Phylogenet Evol 5:50–77.

244. Rowlett RS. 2010. Structure and catalytic mechanism of the beta-carbonic anhydrases. Biochim Biophys Acta 1804:362–73.

245. Lindskog S. 1997. Structure and mechanism of carbonic anhydrase. Pharmacol Ther 74:1–20.

246. Ueda K, Tagami Y, Kamihara Y, Shiratori H, Takano H, Beppu T. 2008. Isolation of bacteria whose growth is dependent on high levels of CO2 and implications of their potential diversity. Appl Environ Microbiol 74:4535–8.

247. Ueda K, Nishida H, Beppu T. 2012. Dispensabilities of carbonic anhydrase in proteobacteria. Int J Evol Biol 2012:324549.

248. Al-Haideri H, White M, Kelly DJ. 2010. Major contribution of the type II beta carbonic anhydrase CanB (Cj0237) to the capnophilic growth phenotype of Campylobacter jejuni.

249. Kumar RSS, Hendrick W, Correll JB, Patterson AD, Melville SB, Ferry JG. 2013. Biochemistry and physiology of the β class carbonic anhydrase (Cpb) from Clostridium perfringens strain 13. J Bacteriol 195:2262–9.

250. Kusian B, Sültemeyer D, Bowien B. 2002. Carbonic anhydrase is essential for growth of Ralstonia eutropha at ambient CO(2) concentrations. J Bacteriol 184:5018–26.

251. Guilloton MB, Lamblin AF, Kozliak EI, Gerami-Nejad M, Tu C, Silverman D, Anderson PM, Fuchs JA. 1993. A physiological role for cyanate-induced carbonic anhydrase in Escherichia coli. J Bacteriol 175:1443–51.

252. Braus-Stromeyer S, Schnappauf G, Braus G, Gossner A, Drake H. 1997. Carbonic anhydrase in Acetobacterium woodii and other acetogenic bacteria. J Bacteriol 179:7197–7200.

253. Gai CS, Lu J, Brigham CJ, Bernardi AC, Sinskey AJ. 2014. Insights into bacterial CO2 metabolism revealed by the characterization of four carbonic anhydrases in Ralstonia eutropha H16. AMB Express 4:2.

254. Wilbur KM, Anderson NG. 1948. Electrometric and colorimetric determination of carbonic anhydrase. J Biol Chem 176:147–54.

255. Sundaram V, Rumbolo P, Grubb J, Strisciuglio P, Sly WS. 1986. Carbonic anhydrase II deficiency: diagnosis and carrier detection using differential enzyme inhibition and inactivation. Am J Hum Genet 38:125–36.

256. Fasseas MK, Tsikou D, Flemetakis E, Katinakis P. 2011. Molecular and biochemical analysis of the α class carbonic anhydrases in Caenorhabditis elegans. Mol Biol Rep 38:1777–85.

257. Michaelis L, Menten ML. 1913. Die Kinetik der Invertinwirkung. Biochem Z 49:333–369.

258. Smith KS, Ingram-Smith C, Ferry JG. 2002. Roles of the Conserved Aspartate and Arginine in the Catalytic Mechanism of an Archaeal -Class Carbonic Anhydrase. J Bacteriol 184:4240–4245.

259. Kaur S, Mishra MN, Tripathi AK. 2010. Gene encoding gamma-carbonic anhydrase is cotranscribed with argC and induced in response to stationary phase and high CO2 in Azospirillum brasilense Sp7. BMC Microbiol 10:184.

260. Martin V, Villarreal F, Miras I, Navaza A, Haouz A, González-Lebrero RM, Kaufman SB, Zabaleta E. 2009. Recombinant plant gamma carbonic anhydrase homotrimers bind inorganic carbon. FEBS Lett 583:3425–3430.

261. Kernohan JC. 1964. The activity of bovine carbonic anhydrase in imidazole buffers. Biochim Biophys Acta - Spec Sect Enzymol Subj 81:346–356.

262. Iqbal S, Nisar-ur-Rahman, Iqbal J. 2014. A capillary electrophoresis-based enzyme assay for kinetics and inhibition studies of carbonic anhydrase. Anal Biochem 444:16–21.

263. Hochuli E, Bannwarth W, Döbeli H, Gentz R, Stüber D. 1988. Genetic Approach to Facilitate Purification of Recombinant Proteins with a Novel Metal Chelate Adsorbent. Bio/Technology 6:1321–1325.

264. Schmidt TG, Skerra A. 2007. The Strep-tag system for one-step purification and high-affinity detection or capturing of proteins. Nat Protoc 2:1528–1535.

265. Covarrubias AS, Bergfors T, Jones TA, Högbom M. 2006. Structural mechanics of the pH-dependent activity of beta-carbonic anhydrase from Mycobacterium tuberculosis. J Biol Chem 281:4993–9.

266. Kisiel W, Graf G. 1972. Purification and characterization of carbonic anhydrase from Pisum sativum. Phytochemistry 11:113–117.

267. Johanson I -M, Forsman C. 1993. Kinetic studies of pea carbonic anhydrase. Eur J Biochem 218:439–446.

268. Innocenti A, Mühlschlegel FA, Hall RA, Steegborn C, Scozzafava A, Supuran CT. 2008. Carbonic anhydrase inhibitors: Inhibition of the β-class enzymes from the fungal pathogens Candida albicans and Cryptococcus neoformans with simple anionsBioorganic & Medicinal Chemistry Letters.

269. Syrjänen L, Tolvanen M, Hilvo M, Olatubosun A, Innocenti A, Scozzafava A, Leppiniemi J, Niederhauser B, Hytönen VP, Gorr TA, Parkkila S, Supuran CT. 2010. Characterization of the first beta-class carbonic anhydrase from an arthropod (Drosophila melanogaster) and phylogenetic analysis of beta-class carbonic anhydrases in invertebrates. BMC Biochem 11:28.

270. Smith KS, Ferry JG. 1999. A plant-type (beta-class) carbonic anhydrase in the thermophilic methanoarchaeon Methanobacterium thermoautotrophicum. J Bacteriol 181:6247–53.

271. Heinhorst S, Williams EB, Cai F, Murin CD, Shively JM, Cannon GC. 2006. Characterization of the carboxysomal carbonic anhydrase CsoSCA from Halothiobacillus neapolitanus. J Bacteriol 188:8087–94.

272. Nishimori I, Minakuchi T, Vullo D, Scozzafava A, Supuran CT. 2011. Inhibition studies of the β-carbonic anhydrases from the bacterial pathogen Salmonella enterica serovar Typhimurium with sulfonamides and sulfamates. Bioorg Med Chem 19:5023–30.

273. Gill SR, Fedorka-Cray PJ, Tweten RK, Sleeper BP. 1984. Purification and properties of the carbonic anhydrase of Rhodospirillum rubrum. Arch Microbiol 138:113–118.

274. Smith KS, Jakubzick C, Whittam TS, Ferry JG. 1999. Carbonic anhydrase is an ancient enzyme widespread in prokaryotes. Proc Natl Acad Sci 96:15184–15189.

275. Zimmerman SA, Tomb J-F, Ferry JG. 2010. Characterization of CamH from Methanosarcina thermophila, founding member of a subclass of the {gamma} class of carbonic anhydrases. J Bacteriol 192:1353–60.

276. Dirken MN, Mook HW. 1931. The rate of gas exchange between blood cells and serum. J Physiol 73:349–60.

277. Meldrum NU, Roughton FJW. 1933. Carbonic anhydrase. Its preparation and properties. J Physiol 80:113–142.

278. Supuran CT, Scozzafava A. 2007. Carbonic anhydrases as targets for medicinal chemistry. Bioorg Med Chem 15:4336–50.

279. Moroney J V., Bartlett SG, Samuelsson G. 2001. Carbonic anhydrases in plants and algae. Plant, Cell Environ 24:141–153.

280. Moroney J V, Ma Y, Frey WD, Fusilier KA, Pham TT, Simms TA, DiMario RJ, Yang J, Mukherjee B. 2011. The carbonic anhydrase isoforms of Chlamydomonas reinhardtii: intracellular location, expression, and physiological roles. Photosynth Res 109:133–49.

281. Cannon GC, Heinhorst S, Kerfeld CA. 2010. Carboxysomal carbonic anhydrases: Structure and role in microbial CO2 fixation. Biochim Biophys Acta 1804:382–92.

282. Supuran CT, Ferry JG. 2013. Carbonic anhydrases of anaerobic microbes. Bioorg Med Chem 21:1392–1395.

283. Sachs G, Weeks DL, Wen Y, Marcus EA, Scott DR, Melchers K. 2005. Acid Acclimation by Helicobacter pylori. Physiology 20.

284. LWOFF A, MONOD J. 1946. Carbonic anhydride as an indispensable substance for micro-organisms. Biosynthesis of dicarboxylic acids. Compte Rendu l'Academie des Sci 222:696–697.

285. Gladstone GP, Fildes P, Richardson GM. 1935. Carbon Dioxide as an Essential Factor in the Growth of Bacteria. Br J Exp Pathol 16:335.

286. Coyne FP. 1932. The effect of carbon dioxide on bacterial growth with special reference to the preservation of fish. Part I. J Soc Chem Ind. Royal Society.

287. Ajl SJ. 1949. The function of carbon dioxide in the metabolism of heterotrophic cells.

288. Mohammadi M, Mohamed AR, Najafpour GD, Younesi H, Uzir MH. 2014. Kinetic studies on fermentative production of biofuel from synthesis gas using clostridium ljungdahlii. Sci World J

2014:910590.

289. Marr AG. 1991. Growth rate of Escherichia coli. Microbiol Rev 55:316–33.

290. Szilard L. 1972. The collected works of Leo Szilard. MIT Press.

291. Khatipov E, Miyake M, Miyake J, Asada Y, C. B, R.W. L, H.G. S. 1998. Accumulation of poly-Î²-hydroxybutyrate by *Rhodobacter sphaeroides* on various carbon and nitrogen substrates. FEMS Microbiol Lett 162:39–45.

292. Shang L, Jiang M, Chang HN. 2003. Poly(3-hydroxybutyrate) synthesis in fed-batch culture of Ralstonia eutropha with phosphate limitation under different glucose concentrations. Biotechnol Lett 25:1415–1419.

293. Ryu HW, Hahn SK, Chang YK, Chang HN. Production of Poly(3-hydroxybutyrate) by High Cell Density Fed-Batch Culture of Alcaligenes eutrophus with Phosphate Limitation.

294. Gottschal JC, Morris JG. 1982. Continuous production of acetone and butanol by Clostridium acetobutylicum growing in turbidostat culture. Biotechnol Lett 4:477–482.

295. Tran-Din K, Gottschalk G. 1985. Formation of d(-)-1,2-propanediol and d(-)-lactate from glucose by Clostridium sphenoides under phosphate limitation. Arch Microbiol 142:87–92.

296. Gao J, Atiyeh HK, Phillips JR, Wilkins MR, Huhnke RL. 2013. Development of low cost medium for ethanol production from syngas by Clostridium ragsdalei. Bioresour Technol 147:508–15.

297. Saxena J, Tanner RS. 2012. Optimization of a corn steep medium for production of ethanol from synthesis gas fermentation by Clostridium ragsdalei. World J Microbiol Biotechnol 28:1553–1561.

298. Saxena J, Tanner RS. 2011. Effect of trace metals on ethanol production from synthesis gas by the ethanologenic acetogen, Clostridium ragsdalei. J Ind Microbiol Biotechnol 38:513–21.

299. Phillips JR, Atiyeh HK, Tanner RS, Torres JR, Saxena J, Wilkins MR, Huhnke RL. 2015. Butanol and hexanol production in Clostridium carboxidivorans syngas fermentation: Medium development and culture techniques. Bioresour Technol 190:114–121.

300. Zinn M, Witholt B, Egli T. 2004. Dual nutrient limited growth: models, experimental observations, and applications. J Biotechnol 113:263–279.

301. Baldomà L, Aguilar J. 1988. Metabolism of L-fucose and L-rhamnose in Escherichia coli: aerobic-anaerobic regulation of L-lactaldehyde dissimilation. J Bacteriol 170:416–421.

302. Petit E, LaTouf WG, Coppi M V, Warnick TA, Currie D, Romashko I, Deshpande S, Haas K, Alvelo-Maurosa JG, Wardman C, Schnell DJ, Leschine SB, Blanchard JL. 2013. Involvement of a bacterial microcompartment in the metabolism of fucose and rhamnose by Clostridium phytofermentans. PLoS One 8:e54337.

303. Tocheva EI, Matson EG, Cheng SN, Chen WG, Leadbetter JR, Jensen GJ. 2014. Structure and expression of propanediol utilization microcompartments in Acetonema longum. J Bacteriol 196:1651–1658.

304. Lee SY, Kim HU. 2015. Systems strategies for developing industrial microbial strains. Nat Biotechnol 33:1061–1072.

305. Ali S, Mushtaq J, Nazir F, Sarfraz H. PRODUCTION AND PROCESSING OF SINGLE CELL PROTEIN (SCP) -A REVIEW. Eur J Pharm Med Res 86.

306. Giec A, Skupin J. 1988. Single cell protein as food and feed. Mol Nutr Food Res 32:219–229.

307. Hurst KM, Lewis RS. 2010. Carbon monoxide partial pressure effects on the metabolic process of syngas fermentation. Biochem Eng J 48:159–165.

308. Younesi H, Najafpour G, Mohamed AR. 2005. Ethanol and acetate production from synthesis gas via fermentation processes using anaerobic bacterium, Clostridium ljungdahlii. Biochem Eng J 27:110–119.

309. Najafpour G, Younesi H. 2006. Ethanol and acetate synthesis from waste gas using batch culture of Clostridium ljungdahlii. Enzyme Microb Technol 38:223–228.

310. Eldwards JD, Pickering SF. 1920. PERMEABILITY OF RUBBER TO GASES. Sci Pap Bur Stand no. 387.

311. Bennett GN, San K-Y. MINI-REVIEW Microbial formation, biotechnological production and applications of 1,2-propanediol.

312. Maestri O, Joset F. 2000. Regulation by external pH and stationary growth phase of the acetolactate synthase from *Synechocystis* PCC6803. Mol Microbiol 37:828–838.

313. Holtzclaw WD, Chapman LF. 1975. Degradative acetolactate synthase of Bacillus subtilis: purification and properties. J Bacteriol 121:917–22.

314. Girbal L, Mortier-Barriere I, Raynaud F, Rouanet C, Croux C, Soucaille P. 2003. Development of a Sensitive Gene Expression Reporter System and an Inducible Promoter-Repressor System for Clostridium acetobutylicum. Appl Environ Microbiol 69:4985–4988.

315. Pennington OJ. 2006. THE DEVELOPMENT OF MOLECULAR TOOLS FOR THE EXPRESSION OF PRODRUG CONVERTING ENZYMES IN CLOSTRIDIUM SPOROGENES. PhD-thesis Univ Nottingham.

316. Csörgo B, Fehér T, Tímár E, Blattner FR, Pósfai G. 2012. Low-mutation-rate, reduced-genome Escherichia coli: an improved host for faithful maintenance of engineered genetic constructs. Microb Cell Fact 11:11.

317. Darwin C. 1859. On the origin of the species by natural selection.

318. Latif H, Zeidan AA, Nielsen AT, Zengler K. 2014. Trash to treasure: production of biofuels and commodity chemicals via syngas fermenting microorganisms. Curr Opin Biotechnol 27:79–87.

319. Sousa FL, Thiergart T, Landan G, Nelson-Sathi S, Pereira IAC, Allen JF, Lane N, Martin WF. 2013. Early bioenergetic evolution. Philos Trans R Soc Lond B Biol Sci 368:20130088.

320. Monnet C, Nardi M, Hols P, Gulea M, Corrieu G, Monnet V. 2003. Regulation of branched-chain amino acid biosynthesis by α-acetolactate decarboxylase in *Streptococcus thermophilus*. Lett Appl Microbiol 36:399–405.

11 Appendix

Figure 11-1 Alignment of 160 β-CA sequences

An astract of this alignment is been shown in figure 3.4. This alignment supports the 6-clade (A-F) clustering as proposed in chapter 3.

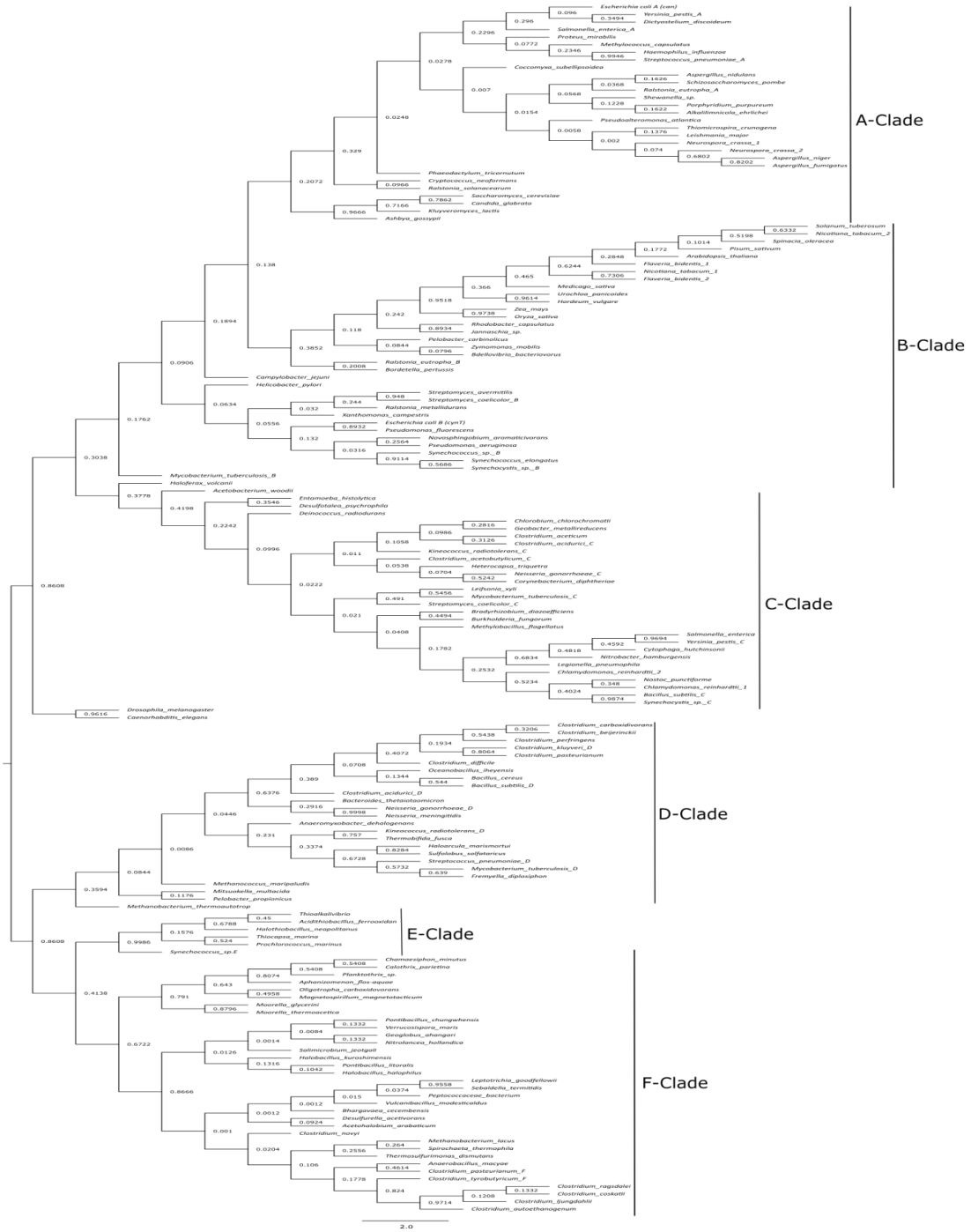

Figure 11-2 Tree diagram of 160 protein sequence constructed using maximum likelihood with LG model with invariant gamma distributed sites in MEGA7.0.

Depicted tree is consensus tree of 5000 bootstrap replicates, values are bootstrap values. Tree is edited for clarity using Figtree and Inktscape. Midpoint rooting and rotations have been applied to get clades in clear and alphabetical order top to bottom.

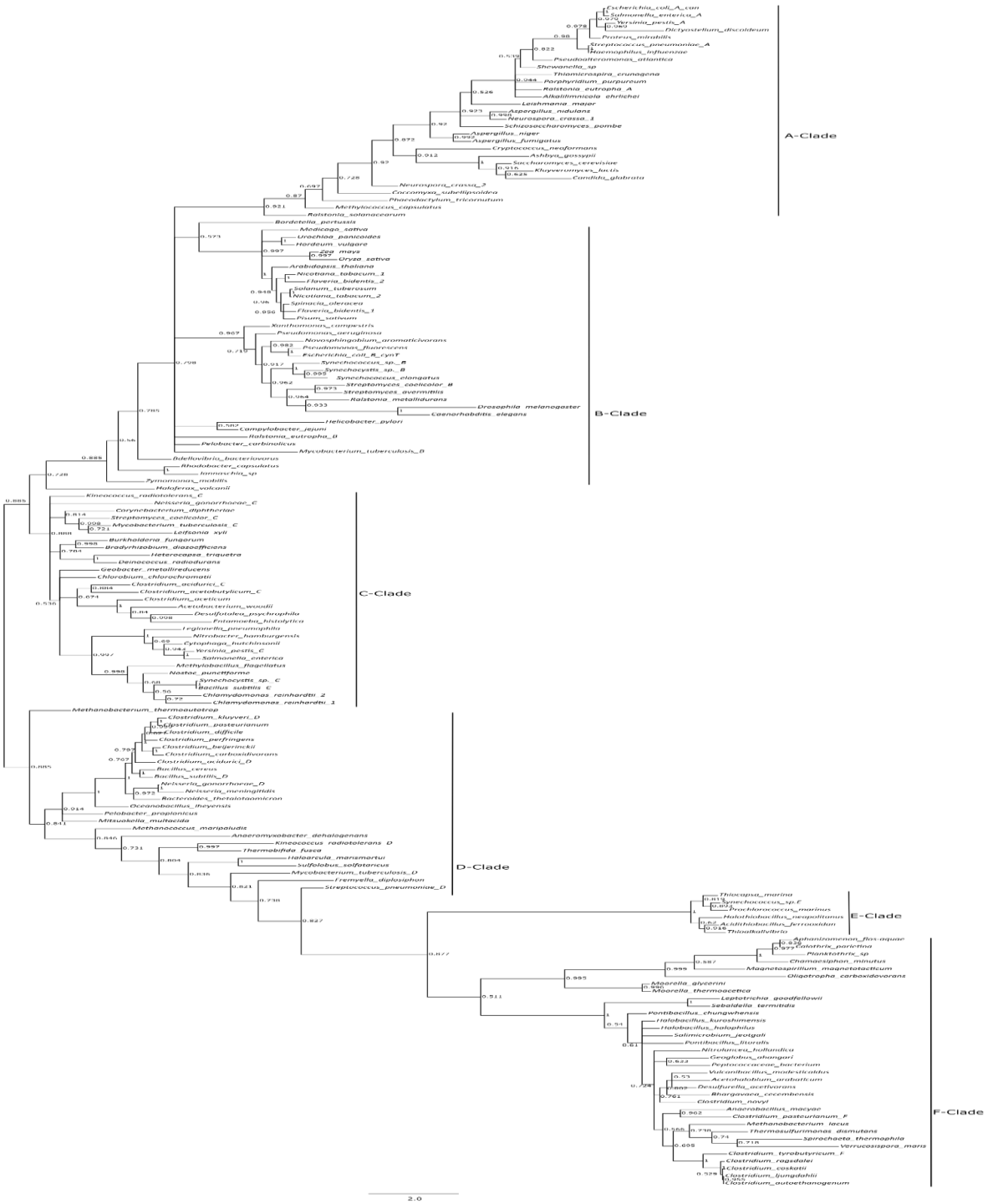

Figure 11-3 Phylogentic tree of 160 protein sequences.

This tree is constructed using Bayesian analysis with LG model with gamma distributed with invariant sites in MrBayes. Depicted tree is consensus tree 5 x 10^6 generations of 4 replicates, probability values are depicted. Average standard deviation of split frequencies reached 0.04 after 3x10^6 generations after which this number stabilised. The tree is edited for clarity using Figtree and Inktscape. Rotations have been applied to get clades in clear and alphabetical order top to bottom

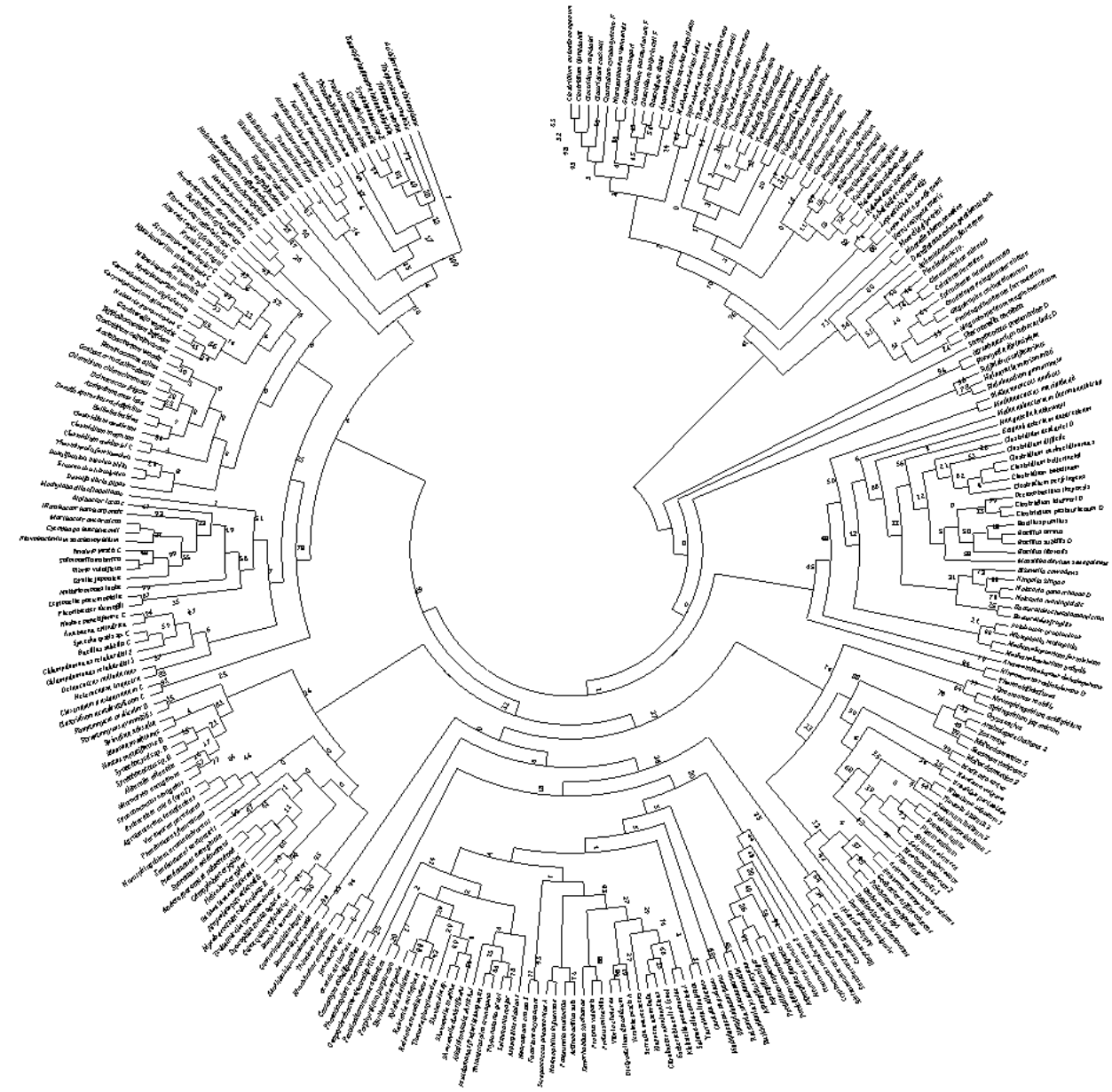

Figure 11-4 Consensus tree diagram of 287 protein sequence constructed using maximum likelihood.
With LG model with invariant gamma distributed sites in MEGA7.0. Depicted tree is consensus tree of 500 bootstrap replicates, values are bootstrap values. Rotations have been applied to put clades in clear order.

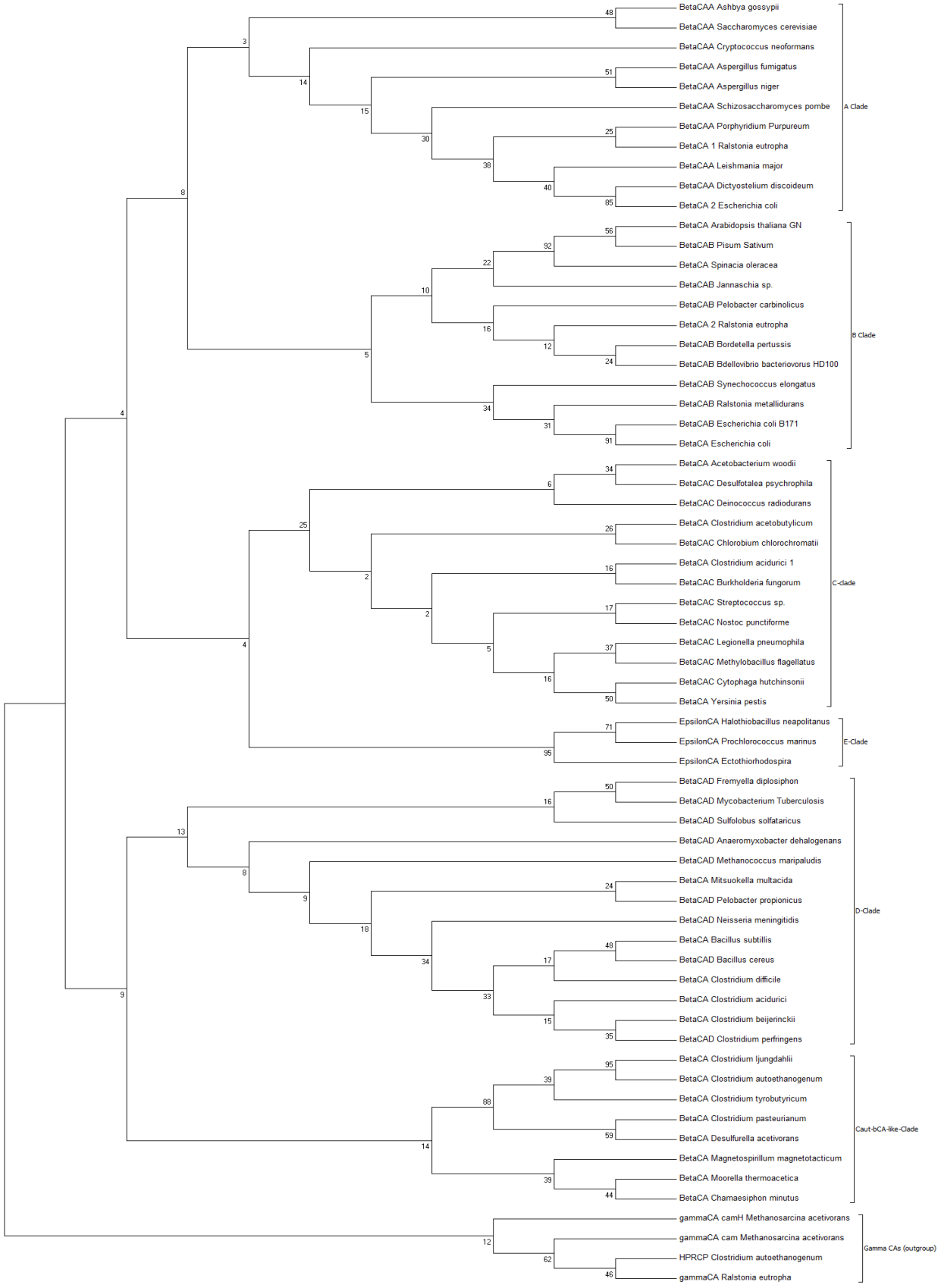

Figure 11-5 Phylogenetic tree constructed with MEGA6.0 maximum likelihood jtt model and bootstrap.
Values on the branches are bootstrap 100 values. Subclades are marked. This analysis shows that the Caut-βCA-like CAs form a distinct subclade of the βCAs.

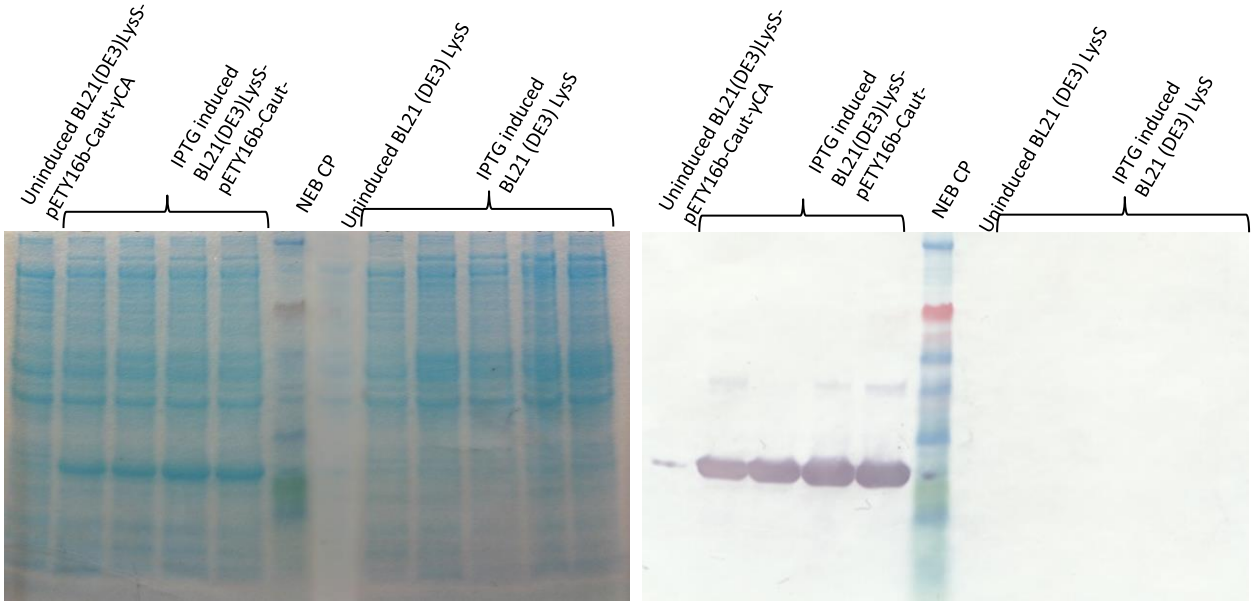

Figure 11-6 SDS-page and Western blot of His-taged Caut-gCA.

Left picture is the SDS-PAGE (4%-12% Bis-Tris) of IPTG induced (0.1 mM, 1mM, 10 mM and 50 mM IPTG from left to right) IBL21(DE3)LysS-pETY16b-Caut-gCA cell lysates and BL21(DE3)LysS that does not carry any additional plasmid. The picture on the left represents a Western blot of a SDS-PAGE gel that was loaded in similar fashion. The NEB Color plus ladder used as a reference band sizes are 230, 150, 100, 80, 60, 50, 40, 30, 25, 20, 15, 10 kDa. The expected size of Caut-TgCA-His protein was 21 kDa while observed band was ~ 25 kDa. The Western blot was immunolabeled with anti-His-tag antibodies and it shows that the pETY16b-Caut-γCA carrying cells produce negligible amounts of His-taged protein when not induced and fair amounts of this protein when induced with IPTG. The BL21(DE3)LysS cells showed no background production of proteins that could be immunnolabelled with the anti-His-tag anti-bodies.

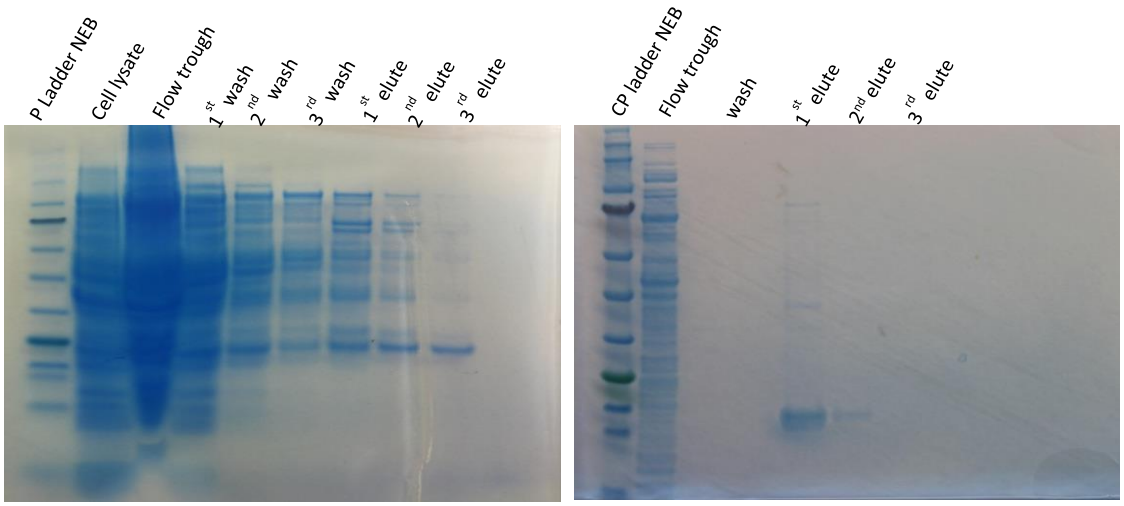

Figure 11-7 SDS-PAGE of Ni-NTAspin column purification.

Picture on the left depicts SDS-PAGE of Ni-NTAspin column purification of the Caut-γCA protein with a wash that was not stringent enough (20mM imidazole) the third elution step yielded fairly pure protein. The NEB protein ladder ladder used as a reference band sizes are 190, 135, 100, 75, 58, 46, 32, 25, 20, 17, 11 kDa. The expected and observed size of the purified Caut-gCA-his is ~21 kDa The picture on the right shows a SDS-PAGE of a 1 ml HisTrap Ni-NTA column purification of the Caut-βCA-protein. The NEB Color plus ladder used as a reference band sizes are 230, 150, 100, 80, 60, 50, 40, 30, 25, 20, 15, 10 kDa. The expected and observed size of the purified Caut-bCA-his is ~17 kDa The wash step was done with 15 ml 40 mM imidazole buffer. The first 2 ml of this wash was lost and apparently contained most of the washed off protein further protein was to dilute to see on this PAGE.

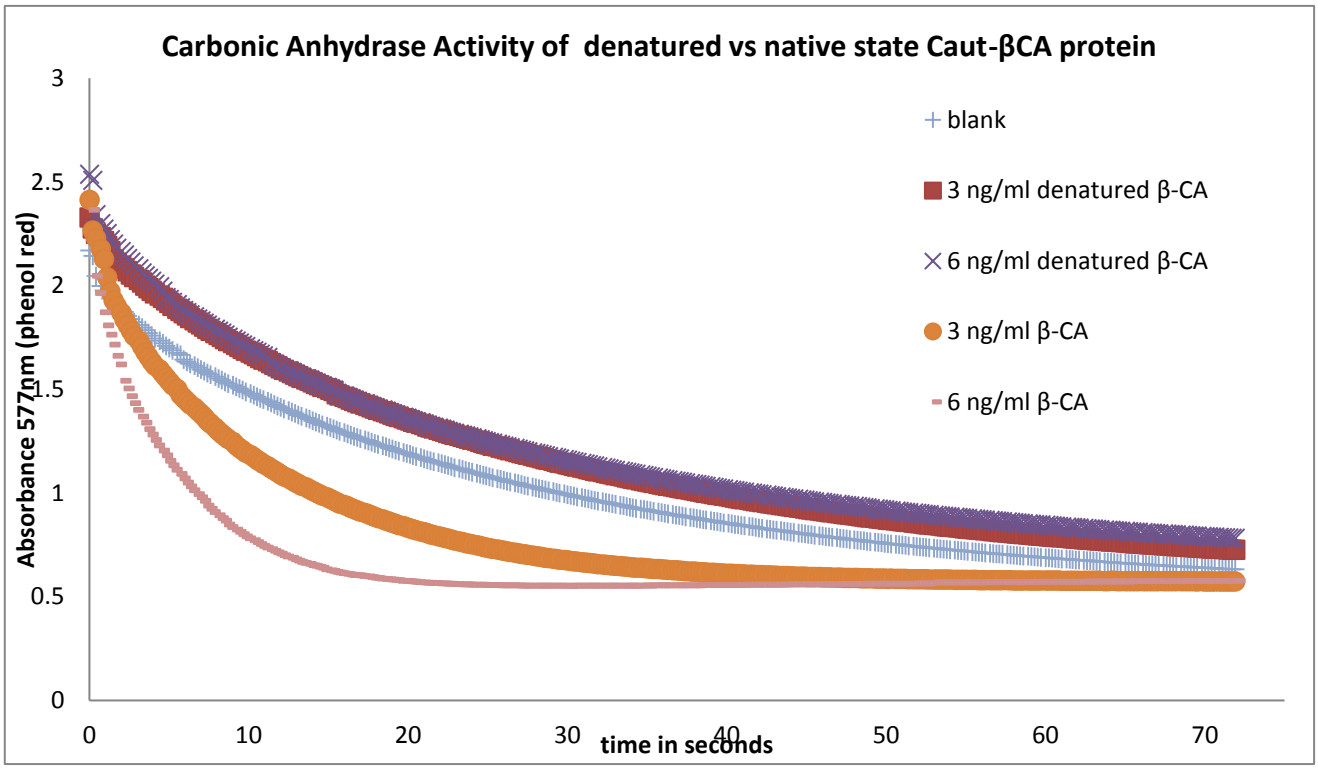

Figure 11-8 shows the effect of denaturing the Caut-βCA protein.

Two reactions with 3 ng ml^{-1} and 6 ng ml^{-1} denatured protein show clearly reduced reaction speeds compared with the native proteins in the same concentrations.

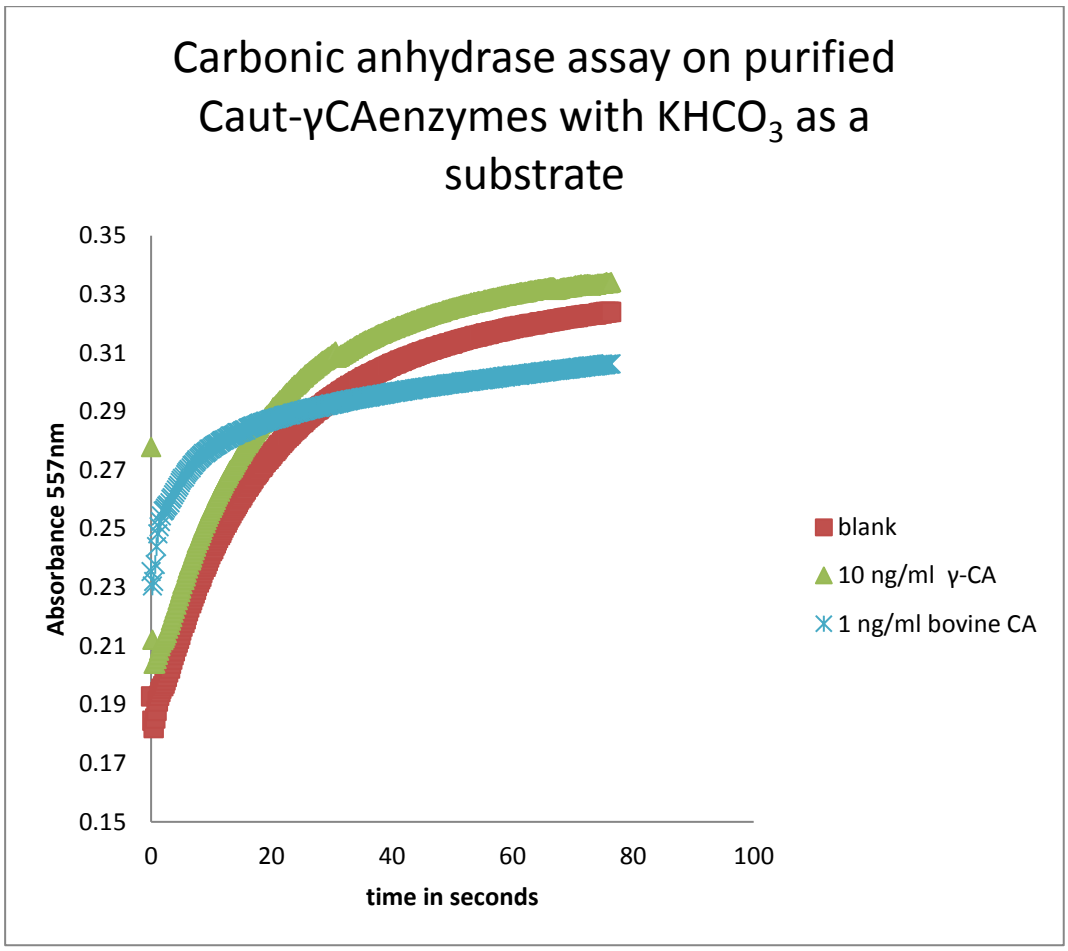

Figure 11-9 Caut-γCA CA assayed with bicarbonate.

Results of the CA assays with bicarbonate as substrate for a fairly high concentration (10 µl of undiluted purification mixture) of heterologous expressed and purified Caut-γCA. No effect of this protein on the carbon dioxide hydration reaction was established. Here a positive control (bovine CA) is included.

Table 11-1 Table of top 20 most differentiating metabolites of batch grown bCA::CT and WT

m/z	Charge	Identification	Highest
228.9845	ESI-	Diazoxide	WT
277.0928	ESI-	Isovalerylglucuronide	WT
133.0869	ESI-	Diethylene glycol monoethyl ether/Polypropylene glycol	WT
271.0138	ESI-	Brassinin (M+Cl)	WT
225.0438	ESI-	No possible identification	WT
239.0417	ESI-	3-Methylthiopropionic acid	WT
215.0561	ESI-	Methylglyoxal Pyruvaldehyde Acrylic acid Malondialdehyde 1-Isopropyl citrate 2-Isopropyl citrate	WT
496.2684	ESI-	[PS(16:0)] 1-hexadecanoyl-sn-glycero-3-phosphoserine	WT
189.0226	ESI-	(+)-1-methylpropyl 3-(methylthio)-2-Propenyl disulphide 3-methyl-5-pentyl-1,2,4-trithiolane	WT
117.0556	ESI-	3-Hydroxyvaleric acid 3-Hydroxyisovaleric acid 2-Methyl-3-hydroxybutyric acid 2-Hydroxy-2-methylbutyric acid 3-Hydroxy-2-methyl-[R-(R,S)]-butanoic acid Erythronilic acid 3-Hydroxy-2-methyl-[S-(R,R)]-butanoic acid Ethyl lactate 2-Hydroxyvaleric acid Diethyl carbonate 4-Hydroxyisovaleric acid 2-Ethylhydracrylic acid Methyl 3-hydroxybutyrate 2-Hydroxy-3-methylbutyric acid 1-Deoxy-D-ribitol 2-Deoxy-D-ribitol 2-Methylerythritol 3-Deoxy-D-arabinitol	mutant
110.9579	ESI-	No possible identification	mutant
281.1031	ESI-	4-methyoxybenzyl glucoside 2-(3-hydroxyphenyl)ethanol 1'-glucoside 3-Hydroxynevirapine 12-Hydroxynevirapine 2-Hydroxynevirapine 8-Hydroxynevirapine	WT
181.0506	ESI-	Methylphoracetophenone 3-(3-hydroxypropanoic acid R-3-(4-Hydroxyphenyl)lactate 3-(4-Hydroxyphenyl)lactate Cis-3-(3-carboxyethenyl)-3,5-cyclohexadiene-1,2-diol Dihydrocaffeic acid 3-(2,3-dihydroxyphenyl)propanoate	WT
257.1202	ESI-	Eriojaposide B	mutant
105.0192	ESI-	Glyceric acid D-2,3-Dihydroxypropanoic acid L-Glyceric acid	WT
167.0373	ESI+	No possible identification	mutant

498.2826	ESI+	2-14:0-lysoPG 1-acyl-sn-glycero-3-phosphoglycerol (n-C14:0) [PG(14:0)] 1-tetradecanoyl-sn-glycero-3-phospho-(1'-sn-glycerol) PG(14:0/0:0) [PS(16:0)] 1-hexadecanoyl-sn-glycero-3-phosphoserine Candoxatril	WT
297.148	ESI+	GA40 Gibberellin A4 Gibberellin A20 Gibberellin A51 5-[(4-Hydroxypheny)ethenyl]-2-(3-methyl-1-butenyl)-1,3-benzenediol (R)-Marmin Menadiol dibutyrate Parakmerin A Gibberellin A61 Gibberellin A51 Gibberellin A45 Cryptotanshinone Gibberellin A120 Gibberellin A70 (E)-Arachidin II 7-[(6-Hydroxy-3,7-dimethyl-2,7-octadienyl)oxy]-2H-1-benzopyran-2-one exo-Dehydrochalepin	WT
252.1229	ESI+	6-(4-methyl-2-oxopentyl)-4-hydroxy-2-pyrone Multifidol 3-Methyl-1-(2,4,6-trihydroxyphenyl)butan-1-one Ac-Tyr-OEt Sinapyl alcohol Bancroftinone Sinapyl alcohol 2-Methoxy-3-(4-methoxyphenyl)propanoic acid 2'-Hydroxy-4',6'-dimethoxy-3'-methylacetophenone 3,4-Dihydroxyphenylvaleric acid 5-(3',5')-Dihydroxyphenyl-gamma-valerolactone 2-Methoxy-4-(4-methyl-1,3-dioxolan-2-yl)phenol 3-(4-Hydroxy-3-methoxyphenyl)-2-methylpropionic acid 3-Methyl-1-(2,4,6-trihydroxyphenyl)-1-butanone Artemidiol Coixinden B Aloesol 1'-Acetoxychavicol (S)-2,3-Dihydro-6-hydroxy-5-(hydroxyacetyl)-2-isopropenylbenzofuran Methyl(2R*,3S*)-2,3-dihydro-3-hydroxy-2-isopropenyl-5-benzofurancarboxylate 1'-Acetoxychavicol acetate	WT
139.0974	ESI+	L-Arginine D-arginine	WT

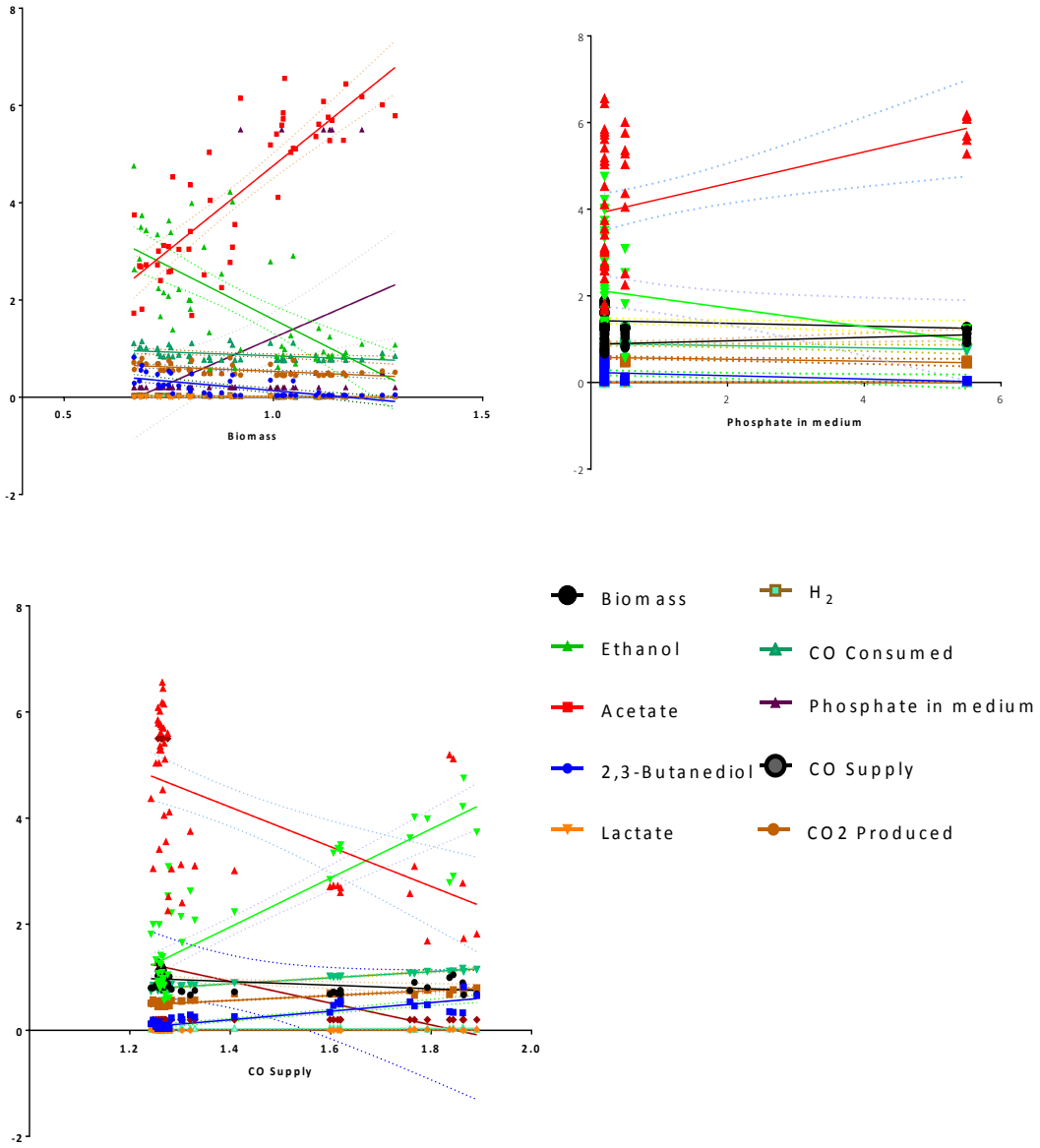

Figure 11-10 Linear regression of PL002 CO supply, phosphate in medium and biomass

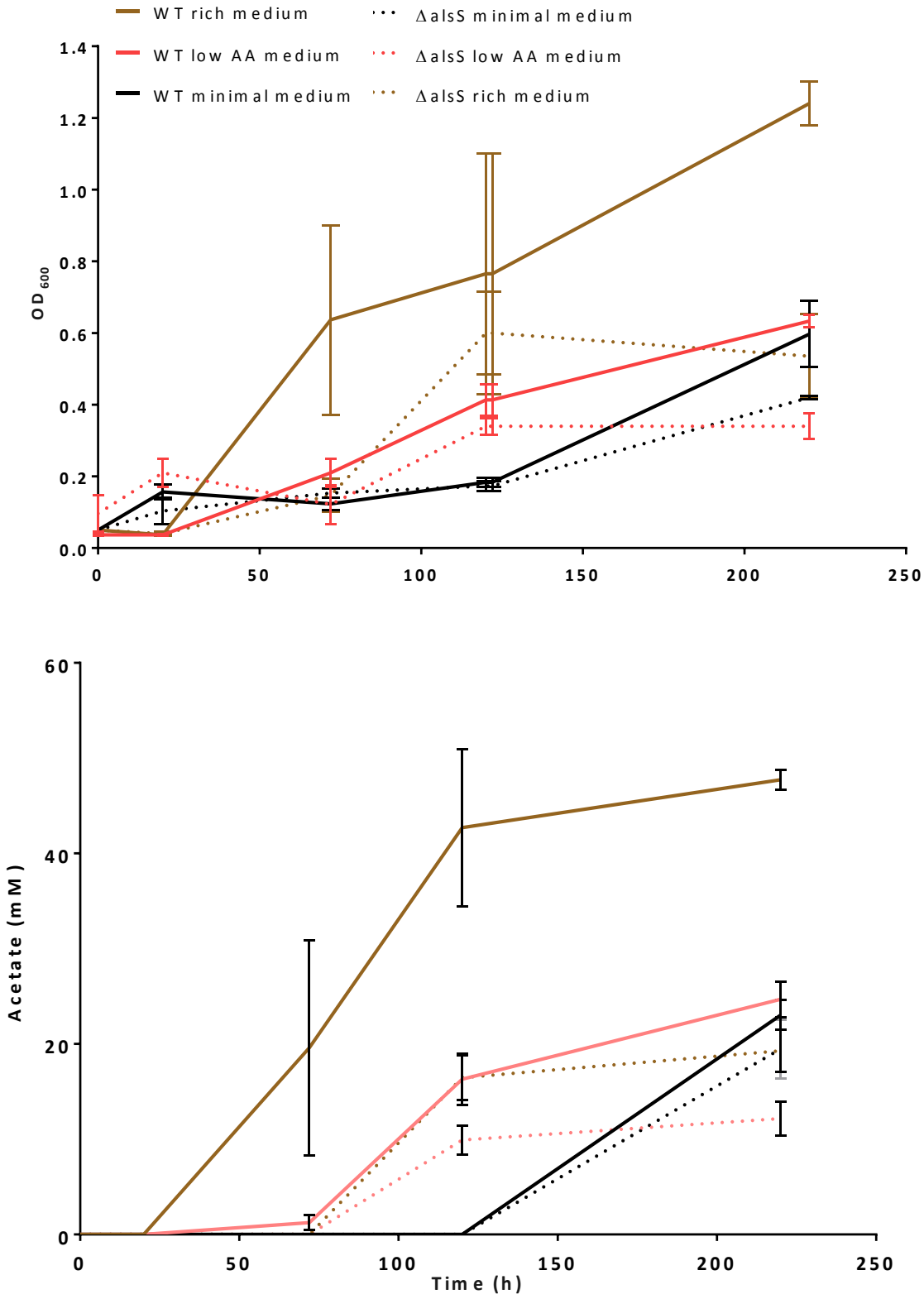

Figure 11-11 Growth of AlsS mutant at three different CAA concentrations.

Top graph shows the headspace pressure and optical density of the cultures. Bottom graph shows the product formation. The *ΔalsS* behaves similar to WT when grown on minimal medium without any added amino acids. WT benefits more from addition of CAA compared to *ΔalsS*.